FROM BIRTH TO BIRTH

A CELL CYCLE CONTROL NETWORK OF *S. cerevisiae*

INAUGURALDISSERTATION

zur Erlangung des akademischen Grades

doctor rerum naturalium

(Dr. *rer. nat.*)

im Fach

Biophysik

eingereicht an der

Lebenswissenschaftlichen Fakultät

der

HUMBOLDT–UNIVERSITÄT ZU BERLIN

von

ULRIKE TATJANA ELISABETH MÜNZNER, M.SC.

Präsidentin der Humboldt–Universität zu Berlin:
Prof. Dr.-Ing. Sabine Kunst

Dekan der Lebenswissenschaftlichen Fakultät
Prof. Dr. Bernhard Grimm

GutacherInnen:
1. Dr. Marcus Krantz
2. Prof. Dr. Dr. *h.c.* Edda Klipp
3. Dr. Matteo Barberis

Tag der mündlichen Prüfung: 14. November 2017

Abstract

The survival of a species depends on the correct transmission of an intact genome from one generation to the next. The cell cycle regulates this process and its correct execution is vital for survival of a species. The cell cycle underlies a strict control mechanism ensuring accurate cell cycle progression, as aberrations in cell cycle progression are often linked to serious defects and diseases such as cancer.

Understanding this regulatory machinery of the cell cycle offers insights into how life functions on a molecular level and also provides for a better understanding of diseases and possible approaches to control them. Cell cycle control is furthermore a complex mechanism and studying it holistically provides for understanding its collective properties. Computational approaches facilitate holistic cell cycle control studies. However, the properties of the cell cycle control network challenge large-scale *in silico* studies with respect to scalability, model execution and parameter estimation.

This thesis presents a mechanistically detailed and executable large-scale reconstruction of the *Saccharomyces cerevisiae* cell cycle control network based on reaction-contingency language. The reconstruction accounts for 229 proteins and consists of three individual cycles corresponding to the macroscopic events of DNA replication, spindle pole body duplication, and bud emergence and growth. The reconstruction translated into a bipartite Boolean model has, using an initial state determined with *a priori* knowledge, a cyclic attractor which reproduces the cyclic behavior of a wildtype yeast cell. The bipartite Boolean model has 2506 nodes and correctly responds to four cell cycle arrest chemicals. Furthermore, the bipartite Boolean model was used in a mutational study where 37 mutants were tested and 32 mutants found to reproduce known phenotypes.

The reconstruction of the cell cycle control network of *S. cerevisiae* demonstrates the power of the reaction-contingency based approach, and paves the way for network extension with regard to the cell cycle machinery itself, and several signal transduction pathways interfering with the cell cycle.

Keywords: *Saccharomyces cerevisiae*, cell cycle control, large-scale network reconstruction, reaction-contingency language, bipartite Boolean modeling

Zusammenfassung

Der Zellzyklus organisiert die Zellteilung, und kontrolliert die Replikation der DNA sowie die Weitergabe des Genoms an die nächste Zellgeneration. Er unterliegt einer strengen Kontrolle auf molekularer Ebene. Diese molekularen Kontrollmechanismen sind für das Überleben eines Organismus essentiell, da Fehler Krankheiten begüngstigen können. Vor allem Krebs ist assoziiert mit Abweichungen im Ablauf des Zellzyklus. Die Aufklärung solcher Kontrollmechanismen auf molekularer Ebene ermöglicht einerseits das Verständnis deren grundlegender Funktionsweise, andererseits können solche Erkenntnisse dazu beitragen, Methoden zu entwickeln um den Zellzyklus steuern zu können. Um die molekularen Abläufe des Zellzyklus in ihrer Gesamtheit besser zu verstehen, eignen sich computergestützte Analysen.

Beim Zellzyklus handelt es sich um einen Signaltransduktionsweg. Die Eigenschaften dieser Prozesse stellen Rekonstruktion und Übersetzung in digital lesbare Formate vor besondere Herausforderungen in Bezug auf Skalierbarkeit, Simulierbarkeit und Parameterschätzung.

Diese Studie präsentiert eine großskalige Netzwerkrekonstruktion des Zellzyklus des Modellorganismus *Saccharomyces cerevisiae*. Hierfür wurde die *reaction-contingency* Sprache benutzt, die sowohl eine mechanistisch detaillierte Rekonstruktion auf molekularer Ebene zulässt, als auch deren Übersetzung in ein bipartites Boolesches Modell.

Für das Boolesche Modell mit 2506 Knoten konnte ein zyklischer Attraktor bestimmt werden, der das Verhalten einer sich teilenden Hefezelle darstellt. Das Boolesche Modell reproduziert zudem das erwartete phänotypische Verhalten bei Aktivierung von vier Zellzyklusinhibitoren, und in 32 von 37 getesteten Mutanten.

Die Rekonstruktion des Zellzyklus der Hefe kann in Folgestudien genutzt werden, um Signaltransduktionswege zu integrieren, die mit dem Zellzyklus interferieren, deren Schnittstellen aufzuzeigen, und dem Ziel, die molekularen Mechanismen einer ganzen Zelle abzubilden, näher zu kommen. Diese Studie zeigt zudem, dass eine auf *reaction-contingency* Sprache basierte Rekonstruktion geeignet ist, um ein biologisches Netzwerk konsistent mit empirischer Daten darzustellen, und gleichzeitig durch Simulation die Funktionalität des Netzwerkes zu überprüfen.

Schlagwörter: *Saccharomyces cerevisiae*, Zellzyklus, großskalige Netzwerkrekonstruktion, *reaction-contingency* Sprache, bipartites Boolesches Modell

Contents

1

Introduction

Kirk: No sign of present life?
Spock: Instrument readings indicate life form but of a highly unusual and intermittent nature. They have no discernible form or location. A most puzzling phenomenon, Captain.

(Star Trek, Wink of an eye)

WHILE EXTRATERRESTRIAL LIFE FORMS frequently occur in science fiction, current space explorations have not uncovered any living objects outside Earth, yet. Until we do so, we have a little more time to concentrate on studying life on Earth. This thesis evolves around the question what we on a molecular level know about the yeast cell division cycle and its regulation, a crucial process which gives rise to what we call life. The first chapter gives a brief overview of this field: The cell division cycle of the model organism baker's yeast, and how we can use network reconstruction to better understand the mechanisms of life.

1.1 Fundamentals of life

One of the missions of the *Curiosity* rover is to detect and analyze potential indicators of present or past life forms on Mars (Gross, 2012). These indicators include organic compounds in the Martian soil and rocks, as well as potentially biogenic gases in

the Martian atmosphere. While current data from Mars indicates the presence of methane (Webster *et al.*, 2015), which can imply the existence of methanogens, the data analysis can currently not conclusively attribute the methane to biogenic origin. Interestingly, the molecule candidates for potential biosignatures are derived from known byproducts of organisms that inhabit Earth. The candidate list is based on the assumption that Martian life forms could be similar to terrestrial life forms due to geophysical similarities between Earth and Mars (Chang, 1988). This assumption leads to further implications on the general search for life outside Earth: How does our definition of life influence the search for life on other planets? Would alien life forms elicit similar properties to terrestrial life forms on a planet dissimilar to Earth? If they would not, how would we be able to distinguish alien life from non–living matter? As this thesis evolves around living organisms on Earth, currently our only example of biological matter, terrestrial life shall be the focus here.

Firstly, what is life? This question has a long history and finding a definition of life is an ongoing debate in the scientific community (Benner (2010), Tsokolov (2009)). One difficulty in finding a consensus definition for life originates from the argument that any definition of life is arbitrary and thus, renders a scientific definition challenging (Tessera, 2011). Instead, the different existing definitions can be viewed as attributes or features describing life. It was also pointed out that some definitions render individual representants of life as dead. This confusion stems from the linguistic imprecision between life and alive. Due to the difficulty in finding a definition for life, the status of viruses remains unclear.

Amongst the different efforts to define life, the *Seven pillars of life* (Koshland, 2002) offer a detailed characterization of the principles representing life. According to Koshland's definition, seven principles suffice to characterize life: A program, improvisation, confinement, energy, regeneration, adaptability and seclusion. The program contains information about the parts of the system, how they are assembled and interact with each other, and is implemented as DNA. Improvisation refers to the ability to adapt the program to longterm environmental changes, such as climate change. Improvisation can be achieved by small errors such as mutations in the program. Some of these mutations are reproducible and even desirable to permit improvisation. Confinement to a finite volume is the next principle of life, as living objects even on the smallest scale are encompassed by a covering layer, a membrane. Confinement enables the program to execute in a protective environment where certain chemical conditions can be maintained. Confinement also provides an environment where metabolic reactions can take place. Energy is a fundamental requirement for the processes of life to be carried out. Regeneration refers to the compensation of losses during energy consumption and enables the maintenance of the processes of life. Adaptability is related to improvisation but on a different time scale. Adaptability requires an immediate response to signals, such as nutritional depletion or thermodynamic threats. The seventh principle of life is seclusion. Seclusion refers to the ability to maintain distinct pathways carrying out

distinct functions. The *Seven pillars of life* describe the principles of life for a population of representants of life, as some of these principles cannot be observed in an individual only but are transmitted from one generation to the next and require the interaction between several individuals.

Secondly, how did life evolve? Since matter consists of atoms, so does life. However, observing the mechanics of atoms, it is difficult to predict life as an emergent property. Life requires the transition from abiotic molecules to the assembly of higher order structures. This is connected to the features confinement and improvisation. The evolution of life thus, created finite structures which contain the ingredients of life and clearly distinguish themselves from non–living matter (Schrum *et al.*, 2010). These structures are known as cells and form the smallest unit of a living being.

The third question, and perhaps the most crucial one in the context of this thesis is, why a discourse and research about life, more precisely about the cell cycle, is important. Studying the cell cycle is crucial for at least two reasons.

Firstly, it offers elemental insights into how life functions on a molecular level. The cell cycle unites many characteristics of life as defined by Koshland: Confinement, as the cell cycle occurs at the smallest unit of confinement characteristic to life, a cell. The cell cycle copies the program, the DNA, and transmits it to the next generation. The copying mechanism of the DNA is prone to small errors which results in mutations, where the reproducible ones permit long-term improvisation. Furthermore, a strict regulatory program protects the maintenance and correct execution of the cell cycle. The program reacts to signals that threat correct cell cycle progression, referred to as adaptability. The cell cycle consumes energy by a mechanism with a well defined order of events and highly specific reactants that carry out those events. Thus, the mechanism is clearly distinct from other mechanisms and an example of seclusion on a cellular level. The cell cycle is a process shared amongst all eukaryotes and has many conserved properties despite the vast diversity amongst living organisms. Prokaryotes have a simplified mechanism for proliferation (for a review see Margolin and Bernander (2004)). The cell cycle is characterized by a series of events that lead to the replication of the genome and its transmission to a new cell. Genomic stability is essential in order to ensure the survival of a species. For this purpose, the cell cycle has implemented certain mechanisms which control its progression. Studying the cell cycle will be crucial to understand these control mechanisms entirely, as they have not been deciphered completely, yet.

Secondly, studying the cell cycle offers a prospect to understand and cure diseases, as errors in the cell cycle machinery are often linked to severe illnesses. Generally, these aberrations may lead to two distinct phenotypes: Uncontrolled proliferation and cell death. Especially cancer is tightly coupled to misregulated cell cycle progression and elevated proliferation (Kolch *et al.*, 2015). In cancer cells, the regulatory control between the cell cycle events is uncoupled, which is often caused by mutations. However, the molecular details of the impairment of cell cycle control remain elusive. Understanding

the cell cycle machinery enables us to understand the mechanisms of disease, and thus, to correct or control misbehavior by developing medical therapies.

Studying the fundamental processes of the cell cycle requires the selection of an appropriate model organism. With a long history of domestication (Gallone *et al.*, 2016), the baker's or budding yeast *Saccharomyces cerevisiae* is an invaluable resource for the fermentation of bread and beverages. In addition to its nutritional contributions, *S. cerevisiae* makes an excellent model organism in cell biology. In fact, early molecular studies on the eukaryotic cell cycle involved *S. cerevisiae*. Pioneering work revealed the genetic control of the cell cycle using *S. cerevisiae*. In particular, studies in the 1970s dissected the genetic interactions associated with the cell cycle (Hartwell *et al.* (1970), Hartwell (1971a), Culotti and Hartwell (1971), Hartwell (1971b), Hartwell *et al.* (1973) Hartwell *et al.* (1974)). Importantly, these studies contributed to the identification of checkpoints that regulate the progression of the cell cycle. The insights from these studies became even more important when studies in other organisms demonstrated how well the cell cycle is conserved mechanistically across eukaryotes ranging from fungi to mammals (Harashima *et al.*, 2013). Accordingly, *S. cerevisiae* became the prime model organism for cell cycle studies. The findings from the yeast model system lay the ground to infer functions from genes in higher eukaryotic organisms. Furthermore, the budding yeast has a relatively small yet sufficiently complex genome. It can easily be manipulated and was the first with a completely deciphered genomic sequence (Goffeau *et al.*, 1996). The functions of protein coding genes are readily available in databases such as the *Saccharomyces* Genome Database (SGD) (`www.yeastgenome.org`, Cherry *et al.* (2011)).

1.2 The yeast cell division cycle

The cell division cycle traverses four phases (Figure 1.1) beginning with the birth of a daughter cell, and finishing with the cell giving birth to its offspring, a new daughter cell. Due to the morphological changes of a dividing yeast cell, this type of reproduction is also called budding. Starting in gap phase 1 (G_1), the daughter cell grows and prepares for the next phase, the synthesis phase (S). The cell replicates its genome during S phase and transits to gap phase 2 (G_2). Finally, the cell cycle culminates in the mitotic exit phase (M), leading to cytokinesis and resetting of the molecular machinery to G_1 conditions (reviewed in Nurse (2000)). Yeast cells occur as haploid or diploid cells and both types undergo this budding pattern.

In addition to the four canonical phases, yeast can reproduce by mating. Haploid yeast cells are of mating type a or α and responsive to pheromone during G_1 phase. When stimulated with pheromone, two haploid yeast cells of opposite mating types form a mating projection or shmoo and grow towards each other. Upon successful mating, the genomes of the two yeast cells recombine to form one diploid cell of mating type a/α. Diploid yeast cells are not responsive to pheromone treatment anymore. However, diploid cells can sporulate in starvational conditions, such as

nitrogen depletion combined with low carbon supply. In starvational conditions, the haploid cell undergoes two phases of meiosis, forming four haploid nuclei that are individually encompassed by a plasma membrane but remain in the mother cell forming an ascus or spore. The four haploid cells occur in pairs of mating types a or α. The cells remain in the ascus and resume cell cycle progression upon favorable changes in the environment.

The yeast life cycle in Figure 1.1 shows the four phases and the morphological changes of a yeast cell (red area). The gray areas show mating (reviewed in Haber (2012)) and sporulation (reviewed in Neiman (2011)) and are not the focus of this thesis.

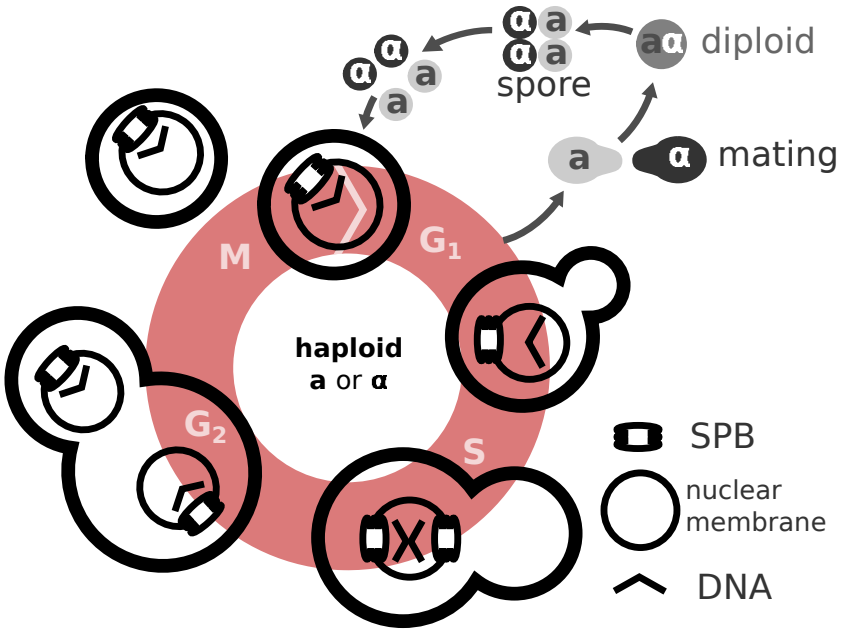

Figure 1.1. *The yeast life cycles.* The three macroscopic events of the cell cycle are shown here: DNA replication, duplication of the spindle pole body, and the growth of a bud. In *S. cerevisiae*, these events are coordinated and synchronized by the kinase Cdc28. At the end of the cycle, the daughter cell separates from the mother. Gray: Mating pathway via shmoo formation and formation of a diploid cell of mating type a/α. The diploid cell can continue to grow and divide or sporulate under starvational conditions. Sporulation leads to the formation of four haploid cells of mating type a or α. The four haploid cells remain in an ascus until conditions permit to resume the cell cycle.

For the survival of a species, it is crucial that cell cycle events progress orderly and ensure transmission of an intact genome to the next generation. For this purpose, several checkpoints have evolved that regulate the main transitions of the cell cycle: the G_1/S transition triggering the initiation of DNA replication, the G_2/M transition marking mitotic entry and the M/G_1 transition, the mitotic exit leading to cytokinesis. The transition from S to G_2 phase has no known regulatory mechanism. In yeast, the cyclin dependent kinase (CDK) Cdc28 orchestrates the cell cycle and is highly involved in the activation and deactivation of the checkpoints. During the course of a cycle, Cdc28 sequentially binds to its regulatory partners, the cyclins Cln1-3 and Clb1-6.

The first checkpoint *Start*, known as the restriction point in mammalian cells, occurs at the onset of the G_1/S transition initiating DNA synthesis. Upstream of the Start checkpoint is Cln3, a cyclin which accumulates during G_1 upon favorable nutritional conditions. Cln3 binds and activates Cdc28 and subsequently two gene clusters controlled by the Mlu1-box binding factor (MBF) and the Swi4-Swi6 cell cycle box binding factor (SBF). Above a certain threshold, Cdc28 activation is sufficient for the cell to initiate Start and the cell irreversibly passes the G_1/S transition and commits to initiate DNA replication. During G_1, a yeast cell is also sensitive to pheromone treatment. Pheromone stabilizes the Start inhibitor Far1.

The initiation of DNA replication activates another checkpoint, the *DNA replication checkpoint* which remains active until DNA replication is completed. DNA replication leads to the formation of two sister chromatids which are connected to each other via cohesin rings. At the centromeric region of the DNA, the kinetochore forms. The kinetochore serves as the docking platform for the microtubules emanating from the spindle pole bodies (spbs) that are required for DNA segregation. DNA segregation is the process of one copy of the DNA being transferred to the daughter cell. The SPBs provide the infrastructure for this process and their regulation is tightly coupled to cell cycle progression. A SPB is a quasicrystalline structure composed of three layers, the outer, inner and central plaque. The SPBs are embedded in the pores of the nuclear membrane. The SPBs polymerize microtubules that connect to the kinetochores of the sister chromatids. Upon correct attachment of the microtubules to the kinetochore, called biorientation, tension is exerted on the DNA. This tension activates the spindle activation checkpoint, leading to DNA segregation and movement of one DNA copy to the daughter cell. At this time, the Cdc20 subunit of the anaphase promoting complex/cyclosome (APC/C) is released. The APC/C is a ubiquitin ligase machinery and responsible for targeted degradation of proteins. Simultaneously to APC/C activation, the Cdc28 antagonist Cdc14 is released, which resets the cell to a G_1/S state. Along with these processes, the plasma membrane becomes polarized and subsequentially forms a bud. Bud emergence and growth is controlled by the *morphogenesis checkpoint*. The protein Swe1 maintains the activity of the checkpoint and is degraded upon correct bud formation.

In addition to these checkpoints that operate in the unperturbed cell cycle, there are a few interfaces to other signal transduction pathways. These pathways monitor the surroundings and halt the cell cycle in circumstances that pose a danger to accurate cell cycle progression. Such signals include nutrient depletion; radiation, inducing DNA damage; hyper– or hypoosmolarity.

1.3 Systems biology of complex systems

The cell cycle involves many components with a complex regulatory layer between them. One approach to study complex processes is to dissect them into smaller parts and study the parts in isolation. This approach is the *reductionist approach* and it

offered tremendous insights into the molecular machineries of living systems. However, dissecting the system into smaller parts makes it difficult to capture its complexity as well as emergent properties on the systems level. The reductionist approach is limited to explain microscopic properties of a system. Explaining macroscopic behavior requires the integration of different types of data into larger and more complex systems.

Biological processes tend to be complex. For example, the study of the isolated biochemical reactions does not explain how these reactions behave in a system. In a system, complex behaviors emerge from the interplay between the simple parts, such as the reactions. How does the cell integrate signals and decide to divide? How can we explain the oscillatory behavior of cell cycle progression? These features emerge on a global level and can typically not be detected or studied with a reductionist approach. The cell cycle is an example of a complex process. The urge to understand the system properties of such processes paved the way for the discipline of systems biology (Kitano, 2002).

1.3.1 *Systems biology*

Systems biology aims at understanding biological systems in a holistic way. This approach combines experimental with theoretical studies and is thus, an integrative and interdisciplinary research area. A systems biology approach requires biological data of the process of interest. This in turn requires expert knowledge of the biological system but also an expertise in experimental techniques. The empirical data must be formalized, which requires mathematical and computational skills, as the mathematical description is typically interrogated computationally. The distinction between mathematical and computational models was debated (Fisher and Henzinger, 2007; Hunt *et al.*, 2008). For clarity, the terms are used here with the following meaning: A mathematical model is an abstraction of biological processes into valid mathematical equations. This abstraction does not necessarily require a digitalization, as equations can be written down on paper. A computational model contains the mathematical information in a format that is computationally executable. The computational formalization makes a variety of tools available to analyze the formulated model. The aim of the computational study is first, to give an accurate description of the empirical knowledge. Second, with the tools available for analysis, the biological system can be tested for many conditions *in silico*. Since the computational cost compared to empirical expenses tends to be low, *in silico* studies enable hypothesis generation and testing in a more efficient way. The systems biology approach involves iterative steps: The computational model can be updated when new data becomes available, and predictions from the model generate hypotheses which can be tested empirically.

1.3.2 *Network reconstruction*

The systems biology approach requires the formalization of the empirical knowledge of a certain biological process into a format that in turn can be used for computational

interrogation. This formalization process is known as *network reconstruction*.

Generally, there are two approaches to perform network reconstruction: *Top-down* and *bottom-up*. The top-down approach uses data of all the components in a system simultaneously. The acquisition of such high-dimensional data sets is dependent on techniques that can measure the whole transcriptome or proteome at once. This kind of data is known as *omics* data and provides high-level information on the constituents of a system. The calculation of the relationships between the components is based on statistical evidence and, depending on the quality of the data, may result in different outcomes. Furthermore, the top-down approach does typically not provide mechanistic insights. The bottom-up approach uses targeted experimental data of the components of the system, which can be directly assembled into models. The data acquisition for bottom-up models requires manual curation but can provide mechanistic understanding of a system.

On a cellular level, there are three different biochemical networks: Signal transduction pathways, gene regulatory networks and metabolic networks. These networks are fundamentally different and thus, require distinct reconstruction approaches.

Metabolic pathways transfer mass and hence, they are called mass transfer networks. Metabolic networks use components from the environment and convert them into components that the cell can use. This process also creates waste products that will be discarded from the cell. The reconstruction of metabolic pathways leading to an executable computational model is based on the bottom-up approach. The community has established a workflow to reconstruct metabolic networks (Thiele and Palsson, 2010). The data acquired from manual curation can then be formulated into a biochemical reaction format that describes the kinetics of each reaction. The reaction kinetics are typically described with ordinary differential equations (ODEs). Due to the properties of a mass transfer network, the ODE based approach scales well with the size of a metabolic network. Indeed, there are many published metabolic reconstructions from different organisms at genome-scale, such as the reconstruction of the prokaryotic organisms *Escherichia coli* (Orth *et al.*, 2011) and *Mycobacterium tuberculosis* (Rienksma *et al.*, 2014); as well as from *S. cerevisiae* (Aung *et al.*, 2013).

Gene regulatory networks alter the activity of genes. While house-keeping genes tend to be constitutively active, other genes are turned on or off depending on incoming signals. The activity of a gene depends on the regulation by transcription factors that bind to a certain control sequence of the DNA. The transcription factors are controlled by signal transduction pathways and alter the transcriptional output of a gene. The activity of a vast number of genes is often measured on a transcriptional level and in a variety of conditions. Based on the information from such top-down measurements, the gene activity can be described and formalized with different approaches. These approaches include ODEs, probabilistic functions and Boolean functions (reviewed in Thompson *et al.* (2015)). The Boolean functions, however, are most widely used.

Signal transduction pathways integrate internal or external signals and typically

require a response of the cell. These signals can be induced by external stresses including nutrient depletion, heat shock, high or low osmolarity, or internal stresses, such as DNA double strand breaks, and they all require an appropriate adaptation of the cell. Signal transduction pathways convey information as opposed to the mass transfer in metabolic networks and hence, are called information transfer networks. The information is encoded in the modifications of proteins, the molecules that transmit the signal. The reconstruction of signal transduction pathways requires a bottom-up approach to yield a mechanistically detailed network. Thus, the reconstruction approach for metabolic pathways can also be applied to signal transduction networks. The formulation of ODEs works well for small signal transduction networks. However, the ODE based approach does not scale well with the size of a network and so far, large-scale reconstructions of signal transduction networks either relied on simplifications, or on other reconstruction approaches that lack mechanistic detail. The next section explains why large-scale reconstruction of signal transduction poses a challenge.

1.3.3 *Properties of signal transduction pathways*

Molecules, most often proteins, convey the information in signal transduction networks. The information is encoded in the specific modification configurations of those molecules. The modification changes in response to signaling events. A single modification, also called *macrostate*, can occur in the form of complexation, posttranslational modification and sometimes conformational changes. Each combination of different macrostates resembles a certain *microstate* that a protein can adopt. Macrostates have binary values, as a modification can either be true or false. This means that a protein with n different modifications can occur in 2^n possible, mutually exclusive microstates. Thus, the full number of states grows exponentially with the number of modifications.

Signaling pathways typically involve many of these modifications and are thus, prone to a property known as combinatorial complexity (Hlavacek *et al.*, 2003). Potentially, each microstate may contribute to a specific reaction in the signal transduction process. Furthermore, microstates are regulated and conditionally active. One molecule can be involved in different cellular responses dependent on its microstate configuration. Signal transduction pathways typically require many of these modifications and even a small network with few components may give rise to a large number of microstates. The fact that signaling pathways elicit these properties also influences the empirical data and knowledge we can obtain from them (Dougherty and Shmulevich, 2012). To summarize, signaling pathways are prone to the combinatorial complexity of the states of the involved proteins. This has an implication on the strategy to reconstruct and model signal transduction networks as well as on the empirical knowledge we can retrieve. These two characteristics render signal transduction network reconstruction a challenge and must be addressed in the development of reconstruction approaches.

1.3.4 *Network reconstruction and the cell cycle*

The properties of signal transduction pathways in combination with the empirical knowledge we can obtain challenge the current approaches for large-scale signal transduction network reconstruction. The systems biology community has developed several approaches to reconstruct signal transduction pathways. Chapter 2 describes and discusses these approaches in more detail. The *reaction-contingency* (rxncon, Tiger *et al.* (2012)) approach was developed to address the challenges associated with large-scale reconstruction of signal transduction networks. The objective of the rxncon approach is to establish an integrated workflow that enables reconstruction, validation and simulation of mechanistically detailed large-scale signal transduction networks. The cell cycle is a signal transduction network, and to capture its full complexity, a large-scale reconstruction is necessary.

1.4 Scope and outline of this thesis

This thesis presents a large-scale, mechanistically detailed and simulatable reconstruction of the control network of the yeast cell cycle. The network captures the components and mechanisms that control cell cycle dependent events such as DNA replication, SPB duplication and cell growth. The reconstruction is formulated in rxncon language and translated into a bipartite Boolean model formalism. In particular, the reconstruction aims to answer the following questions: Is the current knowledge sufficient to link the relevant components of the cell cycle control network mechanistically? Can we reproduce the oscillatory behavior of the cell cycle? Can we identify gaps in the network? Does the reconstructed network reproduce known phenotypes? The reconstruction is based on the rxncon approach. Thus, the thesis furthermore demonstrates the utility of the proposed approach to reconstruct large-scale signal transduction networks.

Chapter 2 discusses the main approaches to reconstruct and to study signal transduction networks computationally, as well as the limitations of these methods with regard to large-scale modeling. The chapter gives an overview of the current advances in cell cycle modeling, and specifically large-scale models.

Chapter 3 explains the rxncon based network reconstruction approach. The chapter introduces the rxncon language, and how a quantitative model can be developed from a network reconstruction in rxncon language.

Chapter 4 describes how I applied the rxncon approach to develop a mechanistically detailed large-scale reconstruction of the *S. cerevisiae* cell cycle control network.

Chapter 5 presents the reconstruction of the cell cycle control network, and Chapter 6 presents the gap-filling process and the validation of the bipartite Boolean model.

Chapter 7 concludes and summarizes the main findings of this work and gives a short look into the future.

2

Computational approaches to signal transduction pathways

SIGNAL TRANSDUCTION PATHWAYS REGULATE fundamental cellular processes. They monitor the cellular environment and implement stimuli in order to adapt the behavior to ensure survival of the cell. Systems biology aims at understanding these regulatory processes in a holistic way. To this end, several approaches have been developed to study signal transduction pathways *in silico*. These approaches typically involve the formalization of the biological process into a mathematical expression. The mathematical expression can then be translated into a format suitable for computational interrogation. This chapter gives an overview of existing methods and models in this field, and highlights their benefits, but also discusses their shortcomings with regard to large-scale signal transduction network reconstruction. Sections 2.1 to 2.3 give an overview of the three most widely used methods to reconstruct and simulate signaling pathways with systems biology approaches. Section 2.4 reviews existing cell cycle models, and discusses their scope with regard to large-scale modeling. Section 2.5 discusses the challenges associated with modeling large-scale signal transduction pathways, and how the currently available methods deal with them. This chapter is based on Münzner *et al.* (2017) and Rother *et al.* (2013).

2.1 Microstate-based models

Biochemical reactions of a signal transduction network are often defined using ODEs, which describe the temporal evolution of species in a network. Species in this context refers to all possible states of all components in the system. Hence, the ODE based approach is microstate-based. An ODE based network requires an expression of the rate of change in terms of a kinetic law, which results in the formulation of an individual ODE for each species. Commonly, the concentration over time is given by an ODE assuming well-mixed compartments, allowing the development of expressions for the number of molecules in a cell or average compartment. In systems where this assumption cannot be justified, partial differential equations (PDEs) are used, which account for the spatial evolution of species. However, here, well-mixed compartments are assumed. Expressing the ODEs of a biochemical network requires the selection of relevant components and how they interact with each other.

A generic ODE for the temporal evolution of species x_i depends on time t, requires parameters p to describe the kinetics, and is given by the following equation:

$$\frac{dx_i}{dt} = f_i(\vec{x}, t, \vec{p}), \tag{2.1}$$

where $\vec{x} = (x_1, \ldots, x_n)$ and $\vec{p} = (p_1, \ldots, p_m)$. Each equation in an ODE system can be refined by specifying a rate law such as mass action or Michaelis–Menten kinetics and thus, the number of parameters m depends on the kinetic laws (Tummler *et al.*, 2014).

ODE based modeling is a widely used approach and has been successfully applied to describe metabolic, gene regulatory networks, and signal transduction networks. The advantages derive from the fact that a biological network formulated in ODEs can describe empirical data quantitatively, dynamically and in mechanistic detail (Klipp *et al.*, 2016).

A model formulated in ODEs can be analyzed with regard to its dynamic properties and with regard to its steady state. The steady state of the system is often calculated to characterize the ODE system by using bifurcation analysis (Klipp *et al.*, 2016). The steady state can be a stable or instable fixpoint, or show oscillatory behavior. The determination of the steady states often requires numerical methods. For dynamic and perturbation analysis, a vast mathematical apparatus is available. However, very detailed information about molecular interactions is needed for model calibration and validation.

As the modelled systems are inherently complex and can be expressed in many different ways, the systems biology community realized the need for standardization with regard to model annotation and tool development (Klipp *et al.*, 2007). Several standards and tools emerged, some of which became widely used. Amongst them several standards for model annotation were developed to facilitate model exchange, and to ensure unambiguous interpretation of the knowledge in the model. Commonly used standards are the Systems Biology Markup Language (SBML) (Hucka *et al.*, 2003),

CellML (Lloyd *et al.*, 2004), BioPAX (Demir *et al.*, 2010), and the Systems Biology Graphical Notation (SBGN) (Le Novere *et al.*, 2009). The COmplex PAthway SImulator (COPASI) (Hoops *et al.*, 2006) provides a graphical interface to both build, simulate, and visualize ODE models. The tool CellDesigner (Funahashi *et al.*, 2008) enables model building graphically. The different tools often support these three standards, and even translation from one format into another one. Model databases such as BioModels (Le Novere *et al.*, 2006) provide infrastructure for storage of and access to ODE models.

There is a plethora of published reconstructions or models of signal transduction pathways formulated as ODE systems. The largest microstate-based reconstructions of signal transduction pathways are the CellDesigner based maps provided by Kitano and colleagues (Oda *et al.* (2005), Oda and Kitano (2006), Caron *et al.* (2010), Kaizu *et al.* (2010), Matsuoka *et al.* (2013), Kawakami *et al.* (2016)). However, these reconstructions are not parametrized, and not executable.

2.2 Logical modeling

Logical, or Boolean models, were introduced in the 1960s to describe gene regulatory networks (Kauffman, 1969). A Boolean network $G(V, F)$ describes qualitatively the dynamic behavior of a biological system. It consists of a set of nodes or vertices $V = \{v_1, v_2, ..., v_n\}$ and Boolean functions or update rules $F = (f_1, f_2, ..., f_m) \subset V \times V$ which describe the edges as relations of the nodes to each other. The nodes typically represent proteins or genes. Each node v_i can adapt two logical values: 1 or 0 (true or false). True refers to a measurable value of a protein or gene, and false to a protein or gene that cannot be measured, or falls below a defined threshold. The functions F between the nodes V employ the basic Boolean operators $\wedge$ (AND), $\vee$ (OR) and $\neg$ (negation). These operators describe the following relations between a pair of nodes v_i and v_j (Table 2.1):

Table 2.1. *Boolean operators.* The truth tables of nodes v_i and v_j for the three Boolean operators (a) Boolean AND; (b) Boolean OR; (c) Boolean negation. 0 refers to false, 1 refers to true.

(a)

v_i	$\wedge$	v_j	Value
0		0	0
0		1	0
1		0	0
1		1	1

(b)

v_i	$\vee$	v_j	Value
0		0	0
0		1	1
1		0	1
1		1	1

(c)

v_i	$\neg v_i$
0	1
1	0

Given a certain set of initial values for each node v_i, the initial state at time point t_x, these update rules or Boolean functions F are applied to each node v_i and result in the state of the system at time point t_{x+1}. A Boolean system will reach a state in which the values for each node either do not change anymore, a *point* or *singleton attractor*, or

reach a state in which the values oscillate, a *cyclic attractor*.

The Boolean update rules can be inferred from transcriptomics data or proteomics data applying a top-down approach and can be updated synchronously or asynchronously. Furthermore, certain Boolean formalisms permit stochastic simulation. The systems biology community has developed modeling environments which facilitate the reconstruction, simulation and analysis of Boolean models, most notably, the BoolNet package for R (Müssel *et al.*, 2010), and the Cytoscape plug-in SimBoolNet (Zheng *et al.*, 2010).

The Boolean formalism is advantageous for modeling signal transduction networks as it ignores the microstates, thereby circumventing the combinatorial explosion. It requires an initial value for each node v_i, but no estimation of parameters. Furthermore, input-output relationships and robustness can easily be assessed in a Boolean system. Despite its use in gene regulatory systems, Boolean approaches have great potential for signal transduction networks. Examples include the mammalian cell cycle (Fauré *et al.*, 2006), somatic cell reprogramming (Flöttmann *et al.*, 2012), and ERBB receptor signaling (Sahin *et al.*, 2009).

2.3 Rule-based modeling

Rule-based modeling was developed to address the combinatorial complexity of signal transduction networks (Hlavacek *et al.*, 2003). In a rule-based model, a rule refers to a biochemical reaction, where the known site dynamics of molecules are defined. These dynamics are specified on the level of available information, explicitly referring to the measured states. Thus, the resolution of data described by a rule ranges from macrostates to microstates, depending on the resolution of available empirical findings. As all microstates typically are not measured in a system, this modeling approach scales with the number of rules, which in turn do not scale with the number of macrostates. Hence, the rule-based approach avoids the combinatorial complexity.

The two most common rule-based languages are κ (Feret *et al.*, 2009) and BNG language (BNGL) (Faeder *et al.* (2009), Harris *et al.* (2016)), recently joined by PySB (Lopez *et al.*, 2013). BioNetGen (BNG) is a modeling environment developed for the simulation of rule-based models (Blinov *et al.*, 2004). The model must be provided in BNGL, developed to formalize rule-based models (Faeder *et al.*, 2009). Equation 2.2 shows a simple rule for the phosphorylation of a protein A at a threonine (T) residue by a kinase K in BNGL. No other sites have been specified.

$$A(T \sim U) + K \longrightarrow A(T \sim P) + K \tag{2.2}$$

The rule-based languages are similar to each other and for κ and BNGL, the community has developed tools, enabling model development, simulation and visualization. A rule-based model can be simulated either deterministically or stochastically. Deterministic simulation requires the translation into an ODE based model, whereas

stochastic simulation is often performed as agent-based. NFsim (Sneddon *et al.*, 2011) is a tool to analyze models formalized in BNGL, provides for agent–based simulation and translation into an ODE based system. RuleMonkey (Colvin *et al.*, 2010) and DYNSTOC (Hlavacek *et al.*, 2008) are tools which provide stochastic simulation environments. Rule-based modeling was successfully applied to model receptor signaling. Several pathways have been reconstructed in rule-based language. Notably, the ERBB receptor (Creamer *et al.*, 2012), T-cell receptor signaling (Chylek *et al.*, 2014), and the insulin signaling pathway (Di Camillo *et al.*, 2016).

2.4 Cell division cycle modeling

The cell cycle is a popular target of the systems biology approach (Csikász-Nagy (2009), extensive review of existing eukaryotic cell cycle models in Ferrell *et al.* (2011)). Many of these models have been formulated as ODE systems and their complexity has tremendously increased over the past decades. One of the early ODE based models is the mitotic oscillator (Goldbeter, 1991). The model consists of a few ODEs and offers a theoretical explanation of the oscillatory activation of cdc2 kinase in the eukaryotic cell cycle. Other ODE based models focus on cell cycle related events and observations, such as cell size homeostasis in dividing cells (Spiesser *et al.*, 2012), cell size at the G_1/S transition (Barberis *et al.*, 2007), or the morphogenesis checkpoint (Ciliberto *et al.*, 2003).

Amongst the different cell cycle models of *S. cerevisiae*, the model published by Chen *et al.* (2004) (Chen model) is one of the largest, simulatable cell cycle control models with an ODE approach. The Chen model consists of in total 40 equations with specified rate laws and fully estimated parameters. The model behavior can quantitatively describe more than 100 tested mutant phenotypes. The Chen model describes a complete cell cycle and can reproduce the oscillatory behavior of its components. Similarly, the model published by Kraikivski *et al.* (2015) (Kraikivski model) consists of 60 ODEs and is fully parametrized. The Chen and Kaikivski models are simulatable and can explain the different mutant phenotypes. However, both model are limited to a small number of components which control the cell cycle. Moreover, both models are simplified in terms of mechanistic detail.

The largest cell cycle reconstruction published so far is the comprehensive molecular interaction map by Kaizu *et al.* (2010), referred to as the Kaizu model hereafter. The Kaizu model accounts for 880 species and is mechanistically highly detailed. The Kaizu model is visualized as SBGN process diagram (SBGN-PD) (Le Novere *et al.*, 2009), and also available in SBML. However, the Kaizu model expressed in SBML has no specified rate laws and hence, is not executable. Due to its comprehensiveness and large-scale scope, the Kaizu model is later used for comparison with the cell cycle control network of this thesis (Section 5.9).

Several cell cycle models have been published in the Boolean formalism. The Boolean models by Li *et al.* (2004), Fauré *et al.* (2009), and Irons (2009) describe a complete cell cycle and consist of 11, 32 and 18 nodes, respectively. The size of these models allows

the identification of the trajectories and attractors of all initial states of the Boolean network. Analysis of the trajectories and attractors reveals network robustness. In the study by Braunewell and Bornholdt (2007), the model by Li *et al.* (2004) was adapted to include noise, which allows to account for biological fluctuations. These models demonstrated the power of Boolean cell cycle modeling with regard to the underlying principles of network structure and vulnerability towards perturbations. However, these Boolean models take a subset of the relevant genes into account and do not account for mechanistic detail.

Thus, cell cycle models formulated as ODE systems quantify the cell cycle system, but cannot mirror the existing empirical knowledge in mechanistic detail, as the combinatorial complexity requires the formulation of kinetic laws for which parameter estimation becomes infeasible. Boolean models avoid the combinatorial complexity and are simulatable, thereby neglecting mechanistic detail.

2.5 Challenges in large-scale modeling approaches

The presented approaches in Sections 2.1 to 2.3 are frequently applied to model signal transduction networks and specifically the cell cycle (Ferrell *et al.*, 2011; Barberis *et al.*, 2017). However, with regard to large-scale signal transduction modeling, these approaches deal differently well with the challenges associated with the reconstruction of especially large signal transduction networks.

ODE based modeling scales with the number of microstates. This is problematic due to the large number of parameters which must be measured or estimated alongside the exponentially expanding number of microstates. Because of the combinatorial complexity, it becomes very difficult to measure all possible microstates and hence, these parameters must be estimated computationally. Often, the resolution of states in an ODE based model is higher than the empirical knowledge, resulting in an inflation of the knowledge represented in the model. Furthermore, the parameter estimation becomes infeasible with network size, hence, large ODE based models can no longer be simulated in a meaningful way.

Boolean models avoid the combinatorial complexity and do not require parametrization except for the definition of an initial state. They reduce their computational costs compared to ODE based models. Boolean models are thus, free from parameter estimation. However, due to the lack of states, the mechanistic detail is not reflected in Boolean models.

The rule-based approach is designed for the reconstruction of signal transduction networks and mirrors the resolution of empirical data. Thus, the number of reactions in a rule-based model scales with the number of macrostates which are considered in the study. Rule-based modeling furthmore enables the description of mechanistic detail. However, validating a rule-based model is difficult, as the information flow in the network cannot be followed easily.

Signal transduction networks are prone to the combinatorial complexity, which poses

a difficulty in assessing empirical knowledge about all possible microstates. These two characteristics play minor roles in models with a narrow scope. However, in large-scale reconstructions, both the combinatorial complexity and the resolution of empirical data pose a challenge. To overcome these challenges, a large-scale reconstruction should address the following criteria (Münzner *et al.*, 2017):

Accuracy The knowledge in the reconstruction format should reflect the available, empirical data.

Comprehensiveness The reconstruction must account for all reactions within the scope of the study.

Scalability The reconstruction language must allow comprehensive, yet accurate network reconstruction.

Machine readability The reconstruction format must be processable and readable *in silico*.

Executability The reconstruction format must comply to a computational format which can be simulated.

Reusability The reconstruction must be stored in a reusable and extendable format.

Functionality The knowledge in the reconstruction format should explain the underlying empirical knowledge.

2.6 Summary

The approaches presented in this chapter have proven to be useful and applicable for the reconstruction of signal transduction networks. Indeed, they brought forward a variety of models that in combination with empirical data offered insights and provided theoretical explanations of how biological processes work. With regard to large-scale modeling, the different approaches deal differently well with the combinatorial complexity of signal transduction networks. ODE modeling is microstate-based and suffers from combinatorial complexity. Boolean modeling ignores the microstates but loses mechanistic detail. The rule-based approach scales well with network size and provides expressiveness for mechanistically detailed models, but renders model validation in terms of information flow difficult.

The special properties of signal transduction networks render the current reconstruction formats challenging in order to accomplish the goal of holistic description and understanding of cellular networks. The rxncon approach was developed to address the criteria required for the reconstruction of large-scale signal transduction networks. The rxncon approach empowers an integrated workflow which enables the reconstruction of a mechanistically detailed, empirically congruent, simulatable and functional signal transduction network. The details of the rxncon workflow are described in Chapter 3.

3

Network reconstruction with rxncon

THE PROPERTIES OF signal transduction networks challenge the computational approaches to mechanistically describe large-scale networks. The reaction–contingency (rxncon) based approach (Tiger *et al.*, 2012) was developed as a formalism that addresses the challenges associated with large-scale signal transduction network reconstruction. Chapter 3 provides the theoretical background of the rxncon language and describes the process of reconstructing a signal transduction network with the rxncon approach. The rxncon approach enables an integrated workflow starting with an initial reconstruction of a biological network and leading to a mechanistically detailed and validated model. Section 3.1 introduces the semantics of the rxncon language. Section 3.2 gives an overview of the workflow, starting with the network reconstruction, and finishing with the creation of a rule-based model. Sections 3.3 to 3.5 describe the different steps in detail. The workflow presented here is a revision of the original rxncon framework (Tiger *et al.*, 2012) and the bipartite Boolean formalism (Flöttmann *et al.*, 2013). The main content in this chapter is based on Romers and Krantz (2017); Romers *et al.*; Thieme *et al.* (2017); Münzner *et al.* (2017). A protocol description of the rxncon workflow is available in Romers *et al.* (*under review*); the potential of the rxncon based method is reviewed in Münzner *et al.* (2017); and the bipartite Boolean formalism is described in Thieme *et al.* (2017).

3.1 The rxncon language

The rxncon language was introduced in Tiger *et al.* (2012) and completely revised in Romers and Krantz (2017). The updated rxncon 2.0 language is described here and used throughout the thesis. The rxncon language describes a biological network based on two types of information: Elemental reactions (*rxn*) which change elemental states of molecules, and the regulatory layer (contingencies, *con*) imposed on these reactions.

An elemental state refers to the macrostate of a molecule and can be defined on different levels of resolution. For example, an elemental state of a protein can be defined on the level of domains for an interaction, and on the level of residues for a modification. The highest level of resolution depends on the property described by the elemental state. For example, a protein which undergoes a binding interaction has a defined elemental state on the resolution of a specific binding domain. The binding interaction cannot be defined on a higher molecular resolution, such as a residue. Similarly, a protein which undergoes a modification reaction has a defined elemental state on the resolution of a specific residue which is modified. The modification cannot occur on a higher level of detail, such as a specific atom, and hence, describes an elemental state of a protein. Two elemental states of the same level of resolution acting on the same instance are mutually exclusive. One of these mutually exclusive states refers to the unmodified or unbound state of a molecule and is called the *neutral state*. For example, a protein which undergoes an interaction has two elemental states on the resolution of the domain which interacts with another molecule. The neutral elemental state of this protein at this domain refers to the protein being unbound on this specific domain. The non-neutral elemental state of this protein at this domain refers to the protein being bound to another molecule on this specific domain. The protein cannot be bound and unbound simultaneously at the same domain and hence, the two elemental states are mutually exclusive. The same protein may have several binding domains and several residues which can undergo a modification. Thus, the number of elemental states of a molecule depends on the number of macrostates which describe a molecule. For example, a protein which interacts with other molecules at a specific domain and undergoes one modification at a specific residue has in total four elemental states: The neutral and non-neutral states of the unbound and bound binding domain; and the neutral state and non-neutral states of the unmodified and modified residue, respectively.

An elemental reaction changes a specific elemental state of a molecule. For example, a protein which participates in an interaction reaction changes the elemental state of the binding domain involved in the reaction. The elemental association reaction of a protein interacting with another molecule changes the neutral elemental state of the unbound domain of the protein to the elemental bound state of the protein domain. The elemental dissociation reaction of a protein consumes the bound elemental state of the protein domain and produces the neutral elemental state which refers to the unbound protein domain. Thus, in an elemental reaction, only one elemental state

of a molecule is changed. Other modifications which the molecule is involved in are ignored. Hence, an elemental reaction describes the change of a macrostate a molecule.

There are two special types of reactions: Synthesis and degradation. They are different from the canonical elemental reactions with regard to the number of elemental states they act upon. The synthesis of a molecule leads to the generation of all neutral elemental states of a molecule. Synthesis thus refers to the *de novo* production of a molecule. Accordingly, the degradation of a molecule can act upon one or more elemental states of a molecule and removes them from the system. Thus, technically, synthesis and degradation can create and consume more than one elemental state of a molecule. This is different from truly elemental reactions, which only change one elemental state of a molecule.

Contingencies describe the regulatory constraints for elemental reactions to occur. Each elemental reaction can thus be regulated based on the presence or absence of another elemental state or a combination of elemental states. The strict distinction between qualitative and regulatory information has two main advantages: First, the elemental reactions correspond to the biochemical reactions which take place in a cell and can be measured and validated *in vitro* and *in vivo*. Similarly, only contingencies which have been measured to influence certain elemental reactions are considered. A network based on rxncon language is thus reconstructed on the same resolution as the available empirical data. Second, the reconstruction is easily extendable as soon as more data becomes available. By the same principle, rxncon models can be conveniently merged to expand the scope of a model.

The rxncon language is the core of the rxncon approach, as a network reconstruction in rxncon language serves as a base for three distinct steps that ultimately result in a quantitative, simulatable, mechanistically detailed model of a signal transduction pathway.

3.2 Workflow overview

The rxncon approach was developed to reconstruct signal transduction pathways and validate, visualize and simulate the reconstruction in an integrated way. The workflow involves three main steps: (i) Initial network reconstruction in rxncon language, (ii) network simulation and validation with a bipartite Boolean model, and (iii) simulation of a quantitative network in rule-based language. Figure 3.1 shows an overview of the three main steps and their respective subtasks. The initial network reconstruction step requires the formalization of the signal transduction pathway into rxncon language. The knowledge stored in rxncon language constitutes the basis for all consecutive steps and is called model base. The reconstruction step proceeds from an initial literature research, network reconstruction, visual validation with a regulatory graph and network refinement in an iterative manner until the visual inspection is satisfactory. The outcome of the visual inspection check is a candidate qualitative network model (QlM). The following validation step involves the translation of the candidate QlM into a bipartite

Boolean formalism. The Boolean model serves as a validation check for the signal transfer in the network, as the input and output relationships in the reconstructed candidate network model can be assessed. While the visual inspection focusses on the connectivity of the components, the simulation of the Boolean network reveals the behavior of the network according to the contingencies. Thus, the Boolean simulation validates the knowledge input with regard to signal transmission and provides for comparison between model expectation and outcome. Upon successful validation of the bipartite Boolean model, the outcome of the second main step is a validated QlM. The validated QlM can then be translated into rule-based language. The rule-based model requires parameter estimation and enables the quantitative analysis of the signal transduction pathway originally annotated in rxncon language.

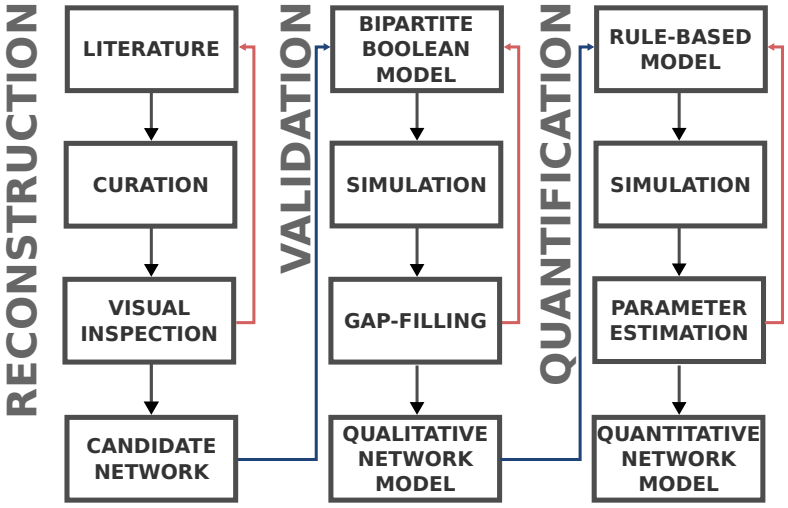

Figure 3.1. *The rxncon workflow.* The three main steps of the rxncon workflow are reconstruction, validation and quantification. Each main step includes several subtasks which are executed iteratively (red). The last step of each main step is the respective outcome and serves as the input for the next main step (blue). Refer to text for details.

The rxncon toolbox (available as GitHub repository at `http://github.com/rxncon/rxncon`) provides the functions for translation from a rxncon model base to the three different formats regulatory graph, bipartite Boolean formalism and rule-based model.

3.3 Reconstructing a candidate network

The reconstruction step occurs iteratively and starts with a definition of scope, literature research and curation. To facilitate the validation of the reconstruction, the network can be visualized as a regulatory graph.

3.3.1 *Literature research and curation*

The first step of the reconstruction is to define the scope of the signal transduction system of interest. Dealing with signaling pathways, this often follows the relationship

between a signal and the cellular response, the input-output relationship. Following the definition of such a relation, a biochemical pathway needs to be identified which mediates the input-output relation. Thus, the next step is literature research and curation to identify the components of the signaling pathway and their mechanistic connection. The literature research includes finding support for the biochemical reactions conveying the signal and formalizing these reactions in rxncon language.

The data is collected in a specially designed table storage format, a derivative of the SBtab format (Lubitz *et al.*, 2016). This table storage format is also called rxncon database and contains four sheets: *ReactionTypeDefinition*, *ModificationTypeDefinition*, *ReactionList* and *ContingencyList*. The two sheets *ReactionTypeDefinition* and *ModificationTypeDefinition* are needed for the internal interpretation and parsing of the rxncon table and contain general information about the reaction types. The *ReactionTypeDefinition* sheet contains the names of the reactions, their abbreviations, information on reaction directionality as well as the molecular resolution for each reaction. This sheet also contains skeleton rules which represent elemental reactions in a format similar to rule-based language. The skeleton rules define how a specific elemental reaction should be interpreted computationally. The *ModificationTypeDefinition* contains the valid modification labels from all reactions. These two lists can be customized to include reactions which are not standard reactions in rxncon. The *ReactionList* and *ContingencyList* contain the information of the signal transduction pathway in rxncon language. The *ReactionList* contains the elemental reactions that are extracted from the literature. Auxiliary columns provide for the inclusion of references and comments, and specification of experiments.

Table 3.1 shows the standard elemental reactions, and which type of biochemical reaction they refer to. Each elemental reaction typically changes only one elemental state of a component. The table shows which elemental states are consumed and produced in each reaction. The reactions which synthesize molecules (synthesis, transcription and translation), and the degradation reaction are exceptions. The synthesizing reactions produce all neutral, elemental states associated with the molecule. The degradation reaction does not produce elemental states, but degrades molecules by removing them from the system, and can act upon several elemental states. The indicated interactions reactions are reversible, and their abbreviations imply association and dissociation reactions. These reactions can also be explicitly expressed by adding a plus sign (+) for association, and a minus sign (-) for dissociation to the reaction type. For example, the explicit association between two proteins, A and B, is expressed with *A_ppi+_B*, and the dissociation with *A_ppi-_B*.

The *ContingencyList* contains the regulatory layer of the elemental reactions. There are five types of contingencies (Table 3.2) which can act on a reaction. The two pairs strict requirement/inhibition and positive/negative influence have different quantitative meaning. A strictly required (or inhibitory) contingency refers to a biochemical context which is absolutely required in order to catalyze (or inhibit) an elemental reaction. A

Table 3.1. *Standard reactions in rxncon.* Interaction reactions are reversible. A,B,C: generic protein names; D: domain; R: residue.

Reaction type	Elemental reaction	Elemental state(s) consumed	Elemental state(s) produced
Protein-protein interaction	A_[D]_ppi_B_[D]	A_[D]-0, B_[D]-0	A_[D]-B_[D]
Intra-protein interaction	A_[D1]_ipi_A_[D2]	A_[D1]-0, A_[D2]-0	A_[D1]-A_[D2]
Protein-gene interaction	A_[D]_BIND_BGene_[D]	A_[D]-0, BGene_[D]-0	A_[D]-BGene_[D]
Interaction	A_[D]_i_B_[D]	A_[D]-0, B_[D]-0	A_[D]-B_[D]
Phosphorylation	B_P+_C_[(R)]	C_[(R)]-{0}	C_[(R)]-{P}
Dephosphorylation	B_P-_C_[(R)]	C_[(R)]-{P}	C_[(R)]-0
Autophosphorylation	A_AP+_A_[(R)]	A_[(R)]-{0}	A_[(R)]-{P}
Phosphotransfer	B_PT_C_[(R)]	B_[(R)]-{P},C_[(R)]-{0}	B_[(R)]-{0},C_[(R)]-{P}
Guanine nucleotide exchange	B_GEF_C_[(R)]	C_[(R)]-{0}	C_[(R)]-{GTP}
GTPase activation	B_GAP_C_[(R)]	C_[(R)]-{GTP}	C_[(R)]-{0}
Ubiquitination	B_Ub+_C_[(R)]	C_[(R)]-{0}	C_[(R)]-{Ub}
Truncation	B_CUT_C_[(R)]	C_[(R)]-{0}	C_[(R)]-{truncated}
Synthesis	A_SYN_B	not applicable	all neutral states of B
Transcription	A_TRSC_B	not applicable	all neutral states of BmRNA
Translation	A_TRSL_B	not applicable	all neutral states of B
Degradation	A_DEG_B	several states of B	not applicable

positive or negative influence of a contingency towards an elemental reaction refers to the rate at which the reaction takes place. A positive influence increases the reaction rate, whereas a negative influence decreases the reaction rate. While the strict requirements are interpreted as absolute, the two types of influences can be interpreted differently in the two computational modeling formalisms, bipartite Boolean and rule-based, which the rxncon database can be exported to. In the bipartite Boolean formalism, the positive and negative influence can either be ignored, or interpreted as strict requirements. In the rule-based format, two different rules are created for one reaction with a positive (or negative) influence. In one rule, the influence is not considered, whereas in the second rule the influence is expressed. This allows to specify different rate laws for the two different rules.

Table 3.2. *Contingencies in rxncon.*

Contingency	Meaning
!	Strict requirement
x	Strict inhibition
K+	Positive influence
K-	Negative influence
0	No influence

In rxncon, it is also possible to explicitly express that an elemental reaction is not influenced in a certain biochemical context by using the o (zero) contingency. In addition to the five standard contingencies, Boolean expressions can be used to express combinations of contingencies that apply to a reaction. The Boolean expressions AND, OR and NOT can be used.

3.3.2 *Visual inspection*

The rxncon toolbox provides the translation of the knowledge stored in the rxncon model base into a directed, bipartite graph, the regulatory graph. The regulatory graph is visualized with Cytoscape (Shannon *et al.*, 2003) using a rxncon tailored property style sheet. The colors used here are adapted to fit the general style of this thesis. Figure 3.2 shows an example of a small network motif in which the gene *SIC1* is transcribed, mediated by either of the transcription factors Ace2 or Swi5. The *SIC1* mRNA transcript is then used for translation, producing the Sic1 protein, which can be phosphorylated by Cdc28.

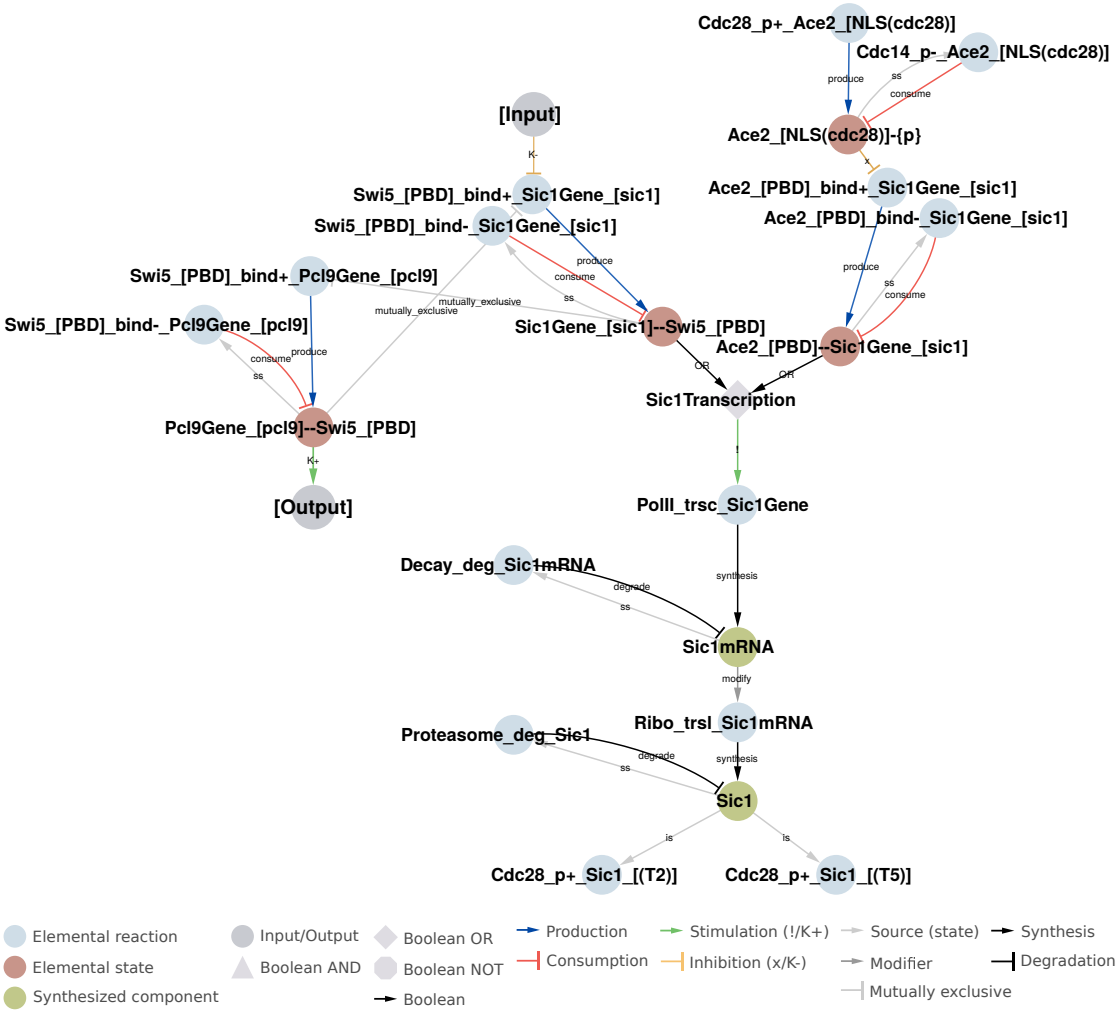

Figure 3.2. *Example of a regulatory graph.* This regulatory graph shows how the rxncon information is visualized. The example shows the regulation of the transcription of the *SIC1* gene, the transcriptional output, and translation into the protein Sic1. Sic1 can then be phosphorylated by Cdc28. In the example, Swi5 also binds the *PCL9* gene. This interaction demonstrates the mutually exclusive binding ability of a single Swi5 molecule.

Each elemental reaction is visualized as a node (lightblue) and connects to another node, corresponding to the elemental state (brownred) which is produced or consumed. In such a node pair, the blue edges with the edge label *produce* indicate that the elemental state is produced by the elemental reaction it is connected to, the red edge with the label *consume* indicates consumption by the elemental reaction it is connected to. The light gray edges with the label *ss* indicate that a specific elemental state is the source state required for the execution of the reaction it points towards. A network defined in the rxncon language can use inputs and outputs (gray nodes) which may refer to properties which cannot be described as elemental states or reactions. Examples of inputs and outputs are turgor, pH value, or temperature sensitivity. In the example, the interaction between Swi5 and the *SIC1* gene, described by the node *Swi5_[PBD]_bind+_Sic1Gene_[sic]* is negatively influenced by such an input, visualized by the node *[Input]*. The negative influence is visualized by the yellow edge with the label *K-*. The elemental state of the gene *PCL9* bound to Swi5, described by the node *Pcl9Gene_[pcl]–Swi5_[PBD]*, positively influences the existence of an output state, visualized by the node *[Output]*. The positive influence contingency is visualized with a green edge and the edge label *K+*.

In the example, *SIC1* gene transcription requires the binding of either of the transcription factors Ace2 or Swi5 to the *SIC1* gene. This is visualized by the gray diamond node *Sic1Transcription*, which is an absolute requirement, indicated by the green edge with the exclamation mark (*!*) label, for the transcription reaction *PolII_TRSC_Sic1Gene* to execute. The *Sic1Transcription* node visualizes a Boolean OR statement. In the example, this node is regulated by two elemental states: Ace2 bound to the *SIC1* gene, visualized by the node *Sic1Gene_[sic]–Swi5_[PBD]*, and Swi5 bound to the *SIC1* gene, visualized by the node *Ace2_[PBD]–Sic1Gene_[sic1]*. Either of these elemental states is required for the transcription reaction to execute. These two elemental states are regulated. For Swi5, binding to the *SIC1* gene is negatively influenced in the presence of the generic *[Input]*. Ace2 binding to the *SIC1* gene is influenced by the phosphorylation status of Ace2. In the example, Ace2 can be phosphorylated by Cdc28 at a generic residue *cdc28*, which is specified to occur in the Ace2 domain *NLS*. This phosphorylation reaction *Cdc28_p+_Ace2_[NLS(cdc28)]* produces the phosphorylated, elemental state of Ace2 at the residue *cdc28* within the *NLS* domain, *Ace2_[NLS(cdc28)]-{p}*. This elemental state, in turn, inhibits Ace2 from interacting with the *SIC1* gene, visualized by the inhibitory contingency edge in yellow and the edge label *x*. The phosphorylation is reversed by the dephosphorylation reaction *Cdc14_p-_Ace2_[NLS(cdc28)]*. In the example, the phosphorylation and dephosphorylation reactions of Ace2 are not regulated.

Upon fulfilment of the transcriptional requirement for the *PolII_TRSC_Sic1Gene* reaction to execute, *SIC1* mRNA is synthesized, indicated by the black edge with the *synthesis* label, creating the green node *Sic1mRNA*. The *SIC1* mRNA transcript is then used as a modifier in the translation reaction *Ribo_trsl_Sic1mRNA*. The mRNA in this reaction does not change its elemental state, but is used as a modifier for the

Ribo_trsl_Sic1mRNA reaction. The translation reaction synthesizes the Sic1 protein, visualized with the green *Sic1* node. Both, the *SIC1* mRNA and Sic1 protein are degraded, visualized by the reaction nodes *Decay_deg_Sic1mRNA* and *Proteasome_deg_Sic1*. The two degradation reactions require the mRNA and protein to be present, respectively, which is indicated by the gray source state edges. The degradational relationship between synthesized components and degradation reaction is visualized with the black edge and the *degrade* label.

Transcription and translation synthesize all neutral elemental states of a component. In the example, the protein Sic1 undergoes phosphorylation by Cdc28 at two different residues, T2 and T5. This is visualized by the reactions *Cdc28_p+_Sic1_[(T2)]* and *Cdc28_p+_Sic1_[(T5)]*. These two reactions create the elemental states *Sic1_[(T2)]-{p}* and *Sic1_[(T5)]-{p}*, respectively. The two corresponding neutral elemental states are *Sic1_[(T2)]-{0}* and *Sic1_[(T5)]-{0}*. These two neutral elemental states are omitted in Figure 3.2, as it is the compact visualization of the regulatory graph. Instead, the green *Sic1* node implies the existence of all neutral elemental states belonging to the component. The implied existence of the neutral elemental states is visualized by the two gray edges with the *is* label, connecting the green *Sic1* component node with the two phosphorylation reaction nodes.

Finally, an elemental state of a component can be involved in several reactions. On a single molecule level, this means that this elemental state cannot be involved in several reactions simultaneously. In Figure 3.2, this is exemplified by Swi5, which binds with its *PBD* domain to the *SIC1* gene or *PCL9* gene. The gray edges with the *mutually_exclusive* indicate that these two reactions cannot be carried out simultaneously by the same Swi5 molecule.

The regulatory graph visualizes the information stored in a rxncon modelbase. As the regulatory graph explicitly shows the regulation between the different components in the rxncon network, it supports the detection of gaps in the information flow during the reconstruction process. The regulatory graph is also used in Chapter 5 to present the cell cycle control network developed in this study.

3.4 Validation with bipartite Boolean modeling

The second part of the rxncon workflow is the translation of the rxncon candidate network into a bipartite Boolean model and its analysis. The bipartite Boolean model is used to qualitatively assess the model dynamics and to reveal gaps. A Boolean model requires an initial state as input but no further parameters for a simulation. As the computational cost of a Boolean simulation is relatively low compared to, for example, ODE systems, the bipartite Boolean model provides a computationally inexpensive way to validate the systems behavior of a rxncon model base.

3.4.1 *Bipartite Boolean formalism*

The translation from rxncon language into the bipartite Boolean formalism is described in detail in Thieme *et al.* (2017). In this bipartite Boolean formalism, the Boolean nodes represent two types of information: Reactions and states corresponding to reaction nodes r_i for $i = 1, \ldots, N$ and state nodes s_j for $j = 1, \ldots, M$, respectively, where N is the total number of elemental reactions and inputs and M is the total number of elemental states and outputs in a rxncon system. Given a certain value for each of these nodes at time point t, the value for time point $t+1$ is returned by a Boolean update rule. The different parts of the Boolean update rule are connected to each other via the Boolean operators $\wedge$ (AND), $\vee$ (OR) and $\neg$ (negation). The Boolean update rules employ a component check $f(\mathrm{Comp}_k(t))$ for $k = 1, \ldots, K$, where K is the total number of elemental states of a certain component. The component check evaluates if any elemental state of a component is true. Furthermore, the Boolean update rules employ a contingency check $g(\mathrm{Cont}_l(t))$ for $l = 1, \ldots, L$, where L is the total number of contingencies that apply to reaction r_i. The contingency check evaluates if all contingencies applying to a reaction are true. For each reaction r_i, there is a set of components denoted by $\mathcal{R}_i^{\mathrm{Comp}}$ and a set of contingencies denoted by $\mathcal{R}_i^{\mathrm{Cont}}$ that apply to this reaction. The value, true or false, of a reaction node r_i at time point $t+1$ is determined by the following equation:

$$r_i(t+1) = \left(\bigwedge_{\mathrm{Comp}_k \in \mathcal{R}_i^{\mathrm{Comp}}} f(\mathrm{Comp}_k(t)) \right) \wedge \left(\bigwedge_{\mathrm{Cont}_l \in \mathcal{R}_i^{\mathrm{Cont}}} g(\mathrm{Cont}_l(t)) \right). \tag{3.1}$$

The value of the Boolean update rule $r_i(t+1)$ for a reaction node r_i returns true if at least one elemental state of every component involved in reaction r_i is true and if all contingencies applying to reaction r_i are true at time point t.

The Boolean update rule for the state node s_j for $t+1$ uses R_S for synthesis reactions, R_D for degradation reactions, R_P for production reactions and R_C for consumption reactions. R_S refers to all synthesis reactions, such as the standard elemental reactions transcription, translation or synthesis. The degradation reaction R_D refers to the elemental degradation reaction. R_P and R_C refer to reaction types that either produce or consume a certain elemental state s_j and are different from the synthesis reaction R_S and degradation reaction R_D with regard to the number of elemental states they can act upon. Synthesis and degradation reactions may act upon several elemental states, whereas production and consumption reactions only act upon one elemental state.

The following equation describes the update rule for state node s_j for $t+1$:

$$\begin{aligned} s_j(t+1) \;=\; & R_S(s_j(t)) \\ & \vee \left(\neg R_D(s_j(t)) \wedge f(\mathrm{Comp}_{h(j)}(t)) \right) \\ & \wedge \left(S_t(R_P(s_j), (s_j)) \wedge \neg R_C(s_j(t)) \right). \end{aligned} \tag{3.2}$$

Equation 3.2 consists of three parts. The first part $R_S(s_j)$ evaluates if the state s_j is synthesized at time point t in at least one synthesis reaction R_S. A state node s_j becomes true as soon as it is synthesized and thus, the synthesis reaction dominates the other two parts of the equation. This is based on the assumption that in a system where a component is simultaneously synthesized and degraded and the component can still be measured, the synthesis dominates the degradation. The second part $\neg R_D(s_j(t)) \wedge f(Comp_{h(j)})$ evaluates if the degradation reaction R_D of the state s_j is false and the component check $Comp_h$ that state s_j belongs to is true. The third part $S_t(R_P(s_j),(s_j)) \wedge \neg R_C(s_j(t)$ is special and should be used with caution. In principle, this part evaluates if a state node s_j is produced by R_P or if the state node s_j is true, and if the consumption reaction R_C for s_j is false. This describes the behavior of a single molecule which has mutually exclusive states on a certain molecular resolution. The trajectory for one elemental state of a molecule oscillates in such a system, turning true and false in an alternating manner. However, on a systems level with many molecules, mutually exclusive states do occur simultaneously. To account for the systems behavior, a smoothing strategy was developed that can evaluate the value for a production reaction R_P and the value for state node s_j at two consecutive time points, t and $t+1$, and thus, the oscillatory behavior vanishes for the trajectory of the whole system. The term $S_t(R_P(s_j),(s_j))$ evaluates one time point without the smoothing strategy, and evaluates two consecutive time points when smoothing is applied.

Figure 3.3 shows the trajectories and attractors of a system with two reactions, a phosphorylation reaction and a dephosphorylation reaction of a protein at residue A, with and without smoothing strategy, respectively. In both systems, the same initial state was used, with the three components, kinase, phosphatase and the neutral elemental state of the protein set to true.

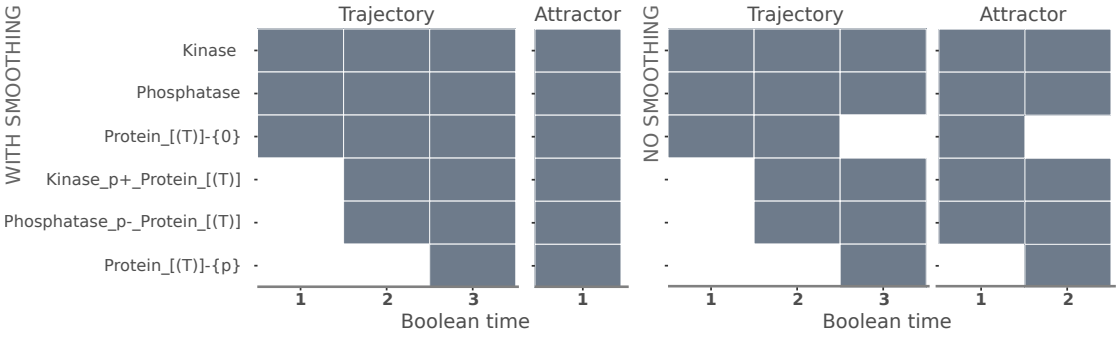

Figure 3.3. *Reaction motif with and without smoothing strategy.* A system with two reactions, phosphorylation and dephosphorylation of a protein at residue A. Left: The smoothing allows both elemental states of the protein to be present simultaneously. The initial state with the three components of the system set to true, the system has a point attractor. Right: Without smoothing, the phosphorylated and unphosphorylated elemental states of the protein cannot occur simultaneously. Using the same initial state as on the left side, the system has an oscillating attractor with period two. Blue: Active states; white: inactive states.

The left side of Figure 3.3 shows the system when smoothing is applied. Both phosphorylated and unphosphorylated protein are present in the system simultaneously.

This system has a point attractor. The right side of Figure 3.3 shows a system without smoothing. Phosphorylated and unphosphorylated states of the protein cannot occur simultaneously. This system has a cyclic attractor.

3.4.2 *Model validation and gap-filling*

The rxncon toolbox provides an automatic translation of a rxncon network into a bipartite Boolean formalism, compliant with the BoolNet format (Müssel *et al.*, 2010). The model files can be created with either of the smoothing strategies. The translation of a rxncon modelbase into a bipartite Boolean model yields three files: The model file containing the Boolean update rules for the reactions and states, where the reactions and states are represented by symbols instead of the full names; a file containing the default initial values for each reaction and state node; and an auxiliary file containing the symbols used in the model file. The model file can be created with either of the smoothing strategies. The standard initial state defines all modified elemental states and all reactions to be false, and all neutral elemental states to be true. The initial values can be changed according to *a priori* knowledge or an initial guess. The simulation of the bipartite Boolean model should reflect the physiological sequence of events in a signal transduction pathway and yield the expected activation or inactivation of a pathway dependent on the input signal. As the order of activation or deactivation can be followed in a simulation, gaps might be detected resulting from the systems behavior of the network. These gaps should be addressed by changing or adding information to the candidate network. The validation step using the Boolean formalism is executed iteratively with model refinement until a satisfactory input-output relation is observed. At this stage, a curated QlM is retrieved which can be used for quantification in the next step.

3.5 A quantitative rule-based model

The export of the curated QlM into a quantitative, rule-based model is the last step in the rxncon workflow (marked as Quantification in Figure 3.1). The rxncon toolbox provides automatic translation from a rxncon model base into a rule-based format compliant with BNGL (Faeder *et al.*, 2009). The rule-based model is the starting point for the quantitative analysis of the reconstructed network. It requires parameter values, such as kinetic constants and initial amounts of the components in the system. The quantification step is not considered in this thesis. A detailed protocol of this step can be found in Romers *et al.* (*under review*).

3.6 Summary

The rxncon approach provides an integrative workflow starting with an initial network reconstruction in rxncon language, ultimately leading to the development of a quantitative model in rule-based language. The rxncon workflow is divided into three main

steps. These steps include iterative model building, as well as model validation via a bipartite Boolean model formalism. The challenges associated with the reconstruction of large-scale signal transduction networks (Section 2.5) are addressed by the rxncon approach in the following way. A rxncon reconstruction scales with the number of elemental reactions and contingencies, hence, the reconstruction scales approximately with the macrostates. This reduces the complexity in the reconstruction process because it avoids the combinatorial complexity, accomplishing *scalability* without the need for reduction. Thus, a rxncon based reconstruction also allows *comprehensiveness*. Furthermore, the elemental reactions and contingencies are added to a model in correspondence with available empirical data. This ensures congruence with empirical data and avoids the description of microstates which lack empirical support, adding to *accuracy*. The reconstruction of a network is performed by including biochemical information and references into a format with a strictly defined structure, enabling *reusability*. The rxncon functionality enables the translation of this electronic format into computational models, addressing *machine readability*. The bipartite Boolean formalism directly translates the information stored in rxncon language into a computationally interrogatable format and provides a default initial state, thereby enabling *executability* without further need for parametrization. The rxncon language provides expressiveness to describe signal transduction processes accurately and with well defined vocabulary, and together with the bipartite Boolean formalism enables analysis of the model behavior in comparison to the observed *in vivo* behavior. This analysis permits model improvement until network *functionality* is accomplished. The rxncon approach has been successfully applied to the reconstruction of the yeast MAPK pathways (Tiger *et al.*, 2012), the yeast Snf1/AMPK pathway (Lubitz *et al.*, 2015), and the yeast pheromone pathway (Thieme *et al.*, 2017).

4

Reconstruction and analysis of the cell cycle control network

CHAPTER 4 DESCRIBES THE PROCESS of the reconstruction and analysis of the yeast cell cycle control network. The procedure follows the network reconstruction workflow described in Chapter 3 and covers the network reconstruction and validation steps (Sections 4.1 to 4.3). The aim of the reconstruction is to provide a mechanistically detailed, qualitative network model of the *S. cerevisiae* cell cycle control network, which can later be used for quantitative rule-based modeling. The genes and proteins used in the model follow the standard name convention according to the SGD (Cherry *et al.*, 2011). The functions of the rxncon toolbox used here are provided in the rxncon repository at GitHub (`https://github.com/rxncon/rxncon`)[1]. The cell cycle control network was then compared to the largest cell cycle control network reconstruction, the Kaizu model (Kaizu *et al.*, 2010). The comparison required the translation of the Kaizu model into rxncon language as described in Section 4.4.

4.1 Literature research and visual inspection

The first part of the reconstruction aims at providing a candidate QlM which captures the processes involved in control of the cell cycle in *S. cerevisiae*. The candidate QlM was constructed from iterative literature research, annotation of the information in

[1] Using the version with the commit id 414c9c784a167dc5b04b5d4303f5d5116c0f55ed.

the rxncon language and format; and visual inspection with a regulatory graph. The literature research was initially based on review papers which provide an overview of the different aspects of the yeast cell cycle. A tentative sketch of the cell cycle events was then developed, describing the three main transitions G_1/S, G_2/M and M/G_1. For each transition, macroscopic processes which are required for each transition to execute were defined. These macroscopic processes cannot be described on the level of elemental biochemical reactions and, thus, new reaction types were added to the rxncon format. The macroscopic reactions are presented in Section 5.5. Next, empirical knowledge about the biochemical reactions regulating these macroscopic events was collected. Two types of information were gathered: Biochemical reaction knowledge representing elemental reactions, and mechanistic information providing the regulatory context of these reactions. This information was assembled into a model base in rxncon language. Primary literature was then used to substantiate and refine network topology and the regulatory layer of the network. The knowledge from the rxncon data base was exported to a regulatory graph with the *rxncon2regulatorygraph* function provided by the rxncon toolbox. The connectivity of the components in the regulatory graph was visually analyzed using Cytoscape (version 3.4.0) (Shannon *et al.*, 2003). To reduce complexity in the regulatory graphs, the edges indicating mutually exclusive states were omitted. Furthermore, the neutral elemental states are not shown explicitly. Instead, component nodes are used.

For missing connections revealed by visual inspection, more information was gathered from the literature and added to the model base. For missing connections lacking support in the literature, hypothetical links were added and marked as hypotheses in the rxncon database.

Literature research, model base extension and visual inspection were iteratively performed until the following criteria were fulfilled:

1. Is there a mechanistic link between the components regulating the macroscopic reactions?
2. Do all physiologically relevant reactions included in the network have antagonizing reactions?
3. Are all relevant components required for cell cycle control included and, when applicable, connected to the control network?

The candidate QlM resulting from this step was used for model validation and gap-filling in the next step.

4.2 Gap-filling with Boolean modeling

The candidate QlM was exported to the bipartite Boolean formalism using the *rxncon2boolean* function of the rxncon tool and with the option to ignore quantitative (K+

and K-) contingencies. All simulations of the bipartite Boolean model were performed in R (R Core Team (2013), version 3.4.0) using the BoolNet package (Müssel *et al.*, 2010).

The macroscopic states resulting from the macroscopic reactions describe mutually exclusive states of the cell. To account for this in the Boolean model, two versions were created, one with and the other one without the smoothing strategy. The update functions of the macroscopic states in the smoothed model were then substituted with the ones in the non-smoothed model, producing a hybrid model.

The first goal of the gap-filling process is to analyze if the Boolean model can reproduce the wildtype behavior corresponding to the physiological G_1 state in the absence of nutrients. This analysis required two actions: The adaptation of the default initial state provided by the model export; and the simulation of the candidate QlM, analysis of its behavior and adaptation of the model. In the default initial state vector provided from the model, all neutral elemental states are set to true, and all non-neutral states, input-output states as well as the reactions are set to false. The default initial state vector was modified according to *a priori* knowledge corresponding to the early G_1 phase by setting all gene clusters and their products to false. The simulation to define the G_1 state was performed without nutrient availability, which corresponds to a cell which cannot pass the G_1 state. The simulation trajectories were analyzed with regard to the expected wildtype behavior. Observations which were not in accordance with wildtype behavior were identified and the candidate QlM adapted accordingly. Gap-filling step 1 and model adaptation in combination with refinement of the initial state resulted in the identification of a point attractor which was considered the G_1 state in a yeast cell without nutrients.

Next, this point attractor with nutrients set to true was used as initial state and the model retrieved from step 1 was simulated again in a second gap-filling step. For each simulation, the flow of activation of the gene clusters and macroscopic states was observed. The model was gap-filled iteratively until the physiological order of activation was reflected in the simulation of the model. Gap-filling step 2 led to the identification of a cyclic attractor. For each observation according to the gap-filling steps 1 and 2, the candidate QlM was changed and used for export to a new bipartite Boolean model. The two gap-filling steps yielded a model that reflects the physiological behavior of the yeast cell cycle. This validated model was then analyzed in order to investigate phenotypes resulting from knockout experiments. The qualitative network model in rxncon language retrieved after the gap-filling process is presented in detail in Chapter 5. The gap-filling process as well as the analysis of the bipartite Boolean model is presented in Chapter 6. The rxncon database can be found in Section A.1.

4.3 Model analysis

The bipartite Boolean model retrieved after the gap-filling process was further analyzed. This analysis included three types of *in silico* experiments: Cell cycle arrest by setting cell cycle arrest agents to true; knockout experiments by deactivating selected genes

or proteins; and residue substitution experiments by deactivating selected protein residues. Cell cycle arrest was tested with pheromone, nocodazole, hydroxyurea (HU), and latrunculin A (LatA). The knockout analysis was performed by setting the genes or, where applicable, the proteins to false in the initial state, and observe the model behavior. The residue substitution analysis was performed for alanine substitutions. To this end, the phosphorylated states of the considered proteins were set to false in the initial state, and the corresponding phosphorylation reactions were deactivated in the bipartite Boolean model. All simulations were performed with the nutrient input set to true.

4.4 Model comparison

To investigate the scope of the control network, the cell cycle control network was compared to the Kaizu model (Kaizu *et al.*, 2010), which is the largest cell cycle control network reconstruction known today. The Kaizu model is annotated in SBGN–PD language and to perform a comparison, the Kaizu model was manually translated into rxncon language. The SBGN–PD is an explicit, visual format showing all microstates of a network. However, in the Kaizu model, some simplifications were applied resulting in the omission of microstates. Hence, not all reactions in the Kaizu model directly translate to elemental reactions. To account for this in the translation, it was assumed that a reaction which changed more than one state of a component in the Kaizu model, was dissected into several elemental reactions describing the change of each state individually. In addition, in some cases, the Kaizu model used several modifiers in a reaction at once. The true modifiers were identified in these cases and for each modifier, one elemental reaction was added. Additional empirical information was gathered in ambiguous cases. Furthermore, the Kaizu model contains protein complexes where the topology is not explicitly defined. For these complexes, a linear structure was assumed and accounted for by adding protein-protein interaction reactions. The Kaizu model takes transport reactions into account. Spatial information cannot be expressed explicitly in rxncon language and hence, these transport reactions were not considered in the translation.

The translation of the Kaizu model resulted in a list of elemental reactions (Table A.6). From these reactions, the protein names were filtered and used for comparison to the cell cycle control network. Before comparison, certain proteins of the Kaizu model were filtered out as they were considered to be out of scope for the cell cycle control network. The proteins not considered in the comparison belong to signal transduction pathways and metabolic processes, interfering with the cell cycle. The proteins used in the comparison, and the ones which were not considered in the comparison, are listed in Table A.1, and the comparison is presented in Section 5.1.

5

The cell cycle control network

THIS CHAPTER PRESENTS THE qualitative network model of the cell cycle control machinery of *S. cerevisiae*. The qualitative network model is the outcome of the reconstruction and validation steps according to the rxncon workflow in Section 3.2 and is referred to as cell cycle control network (CC-CNW) hereafter. The CC-CNW is stored in the rxncon language as a model base. Here, the regulatory graph corresponding to the knowledge in the rxncon model base is presented. Section 5.1 gives an overview of the structure and the different parts of the CC-CNW: The transcriptional layer, the CDK module accounting for regulation of Cdc28 and Pho85, regulation of the CDK antagonist Cdc14, the degradation machinery, and the three macroscopic cycles describing DNA replication, SPB duplication and bud growth. Sections 5.2 to 5.4 present the regulatory layers of the CC-CNW including the transcriptional machinery, the CDK and Cdc14 module, and the degradation machinery. Sections 5.5 to 5.8 describe the macroscopic cycles and their regulation. Section 5.9 presents the results from the comparison of the CC-CNW to the Kaizu model. Section 5.10 summarizes and discusses the results from this chapter.

5.1 The rxncon reconstruction

The yeast CC-CNW consists of 1246 elemental reactions and 801 contingencies accounting for 229 proteins. The proteins are listed in Table A.1. The rxncon model base of the CC-CNW is shown in three tables: Table A.2 lists all the Boolean contingency statements

used in the model, Table A.3 lists all outputs and contingencies, and Table A.4 contains all elemental reactions and contingencies. These three tables together form the rxncon model base, or QlM, of the CC-CNW.

Figure 5.1 shows the bird's-eye view of the regulatory graph of the CC-CNW. The regulatory graph consists of in total 1971 nodes and 3136 edges. In this graph, the neutral elemental states are not shown explicitly to reduce complexity. The different layers of the CC-CNW are marked on the left side. The layout of the graph follows approximately the time progression of the cell cycle from left to right. The CC-CNW accounts for six gene regulatory clusters and their regulation. The CC-CNW furthermore accounts for the CDKs Cdc28 and Pho85 and their regulation. The CC-CNW accounts for the CDK antagonist Cdc14 and its regulation. The CC-CNW accounts for the three macroscopic processes which are essential during the course of a cell cycle: DNA replication, SPB duplication and bud growth. The fully detailed regulatory graph of the CC-CNW does not fit on a single page in this thesis. Instead, the subsequent sections show the different motifs of the CC-CNW in isolation and describe how they are regulated. Some nodes in these motifs are regulated by incoming edges which are not explicitly shown. The labels of these nodes are marked in green and the regulation of the incoming edges is explained in the text.

The CC-CNW is based on two global hypotheses. First, physiologically relevant and regulated phosphorylation reactions are antagonized by dephosphorylation reactions. The CC-CNW accounts for several physiologically relevant phosphorylation reactions, hence, the resulting phosphorylated states must be antagonized. For phosphorylated proteins without empirically tested phosphatases, a hypothetical phosphatase was included and named after the protein with the additional letters *PPT*. In addition, it is hypothesized that all Cdc28- and Pho85-mediated phosphorylation reactions, where dephosphorylation of the substrates was not explicitly demonstrated, are antagonized by the phosphatase Cdc14. Cdc14 as an antagonist for Cdc28 substrates is based on Visintin *et al.* (1998), and the analogous case for Pho85 is based on substrate similarity between Pho85 and Cdc28 (Huang *et al.*, 2007). Second, mRNA transcripts are turned over by decay. Regulated gene clusters are only active during a certain period of the cell cycle. Hence, this must be reflected in the presence of their mRNA products which are supposedly only present during gene activation. To counteract mRNA transcripts, decay reactions were implemented, reflecting the deactivation of the genes, based on Das *et al.* (2017).

The rxncon language lacks expressiveness for spatial information, but cell cycle processes have spatial regulation. Hence, in the CC-CNW, effects of spatial regulation are implemented indirectly. The CC-CNW accounts for spatial effects by making modifications or interactions dependent on their implicit localization. For example, a protein which is phosphorylated at a residue within a nuclear localization sequence may have a regulated nucleo-cytoplasmic localization. Such a protein can then be inhibited to react with other proteins, depending on the modification and localization

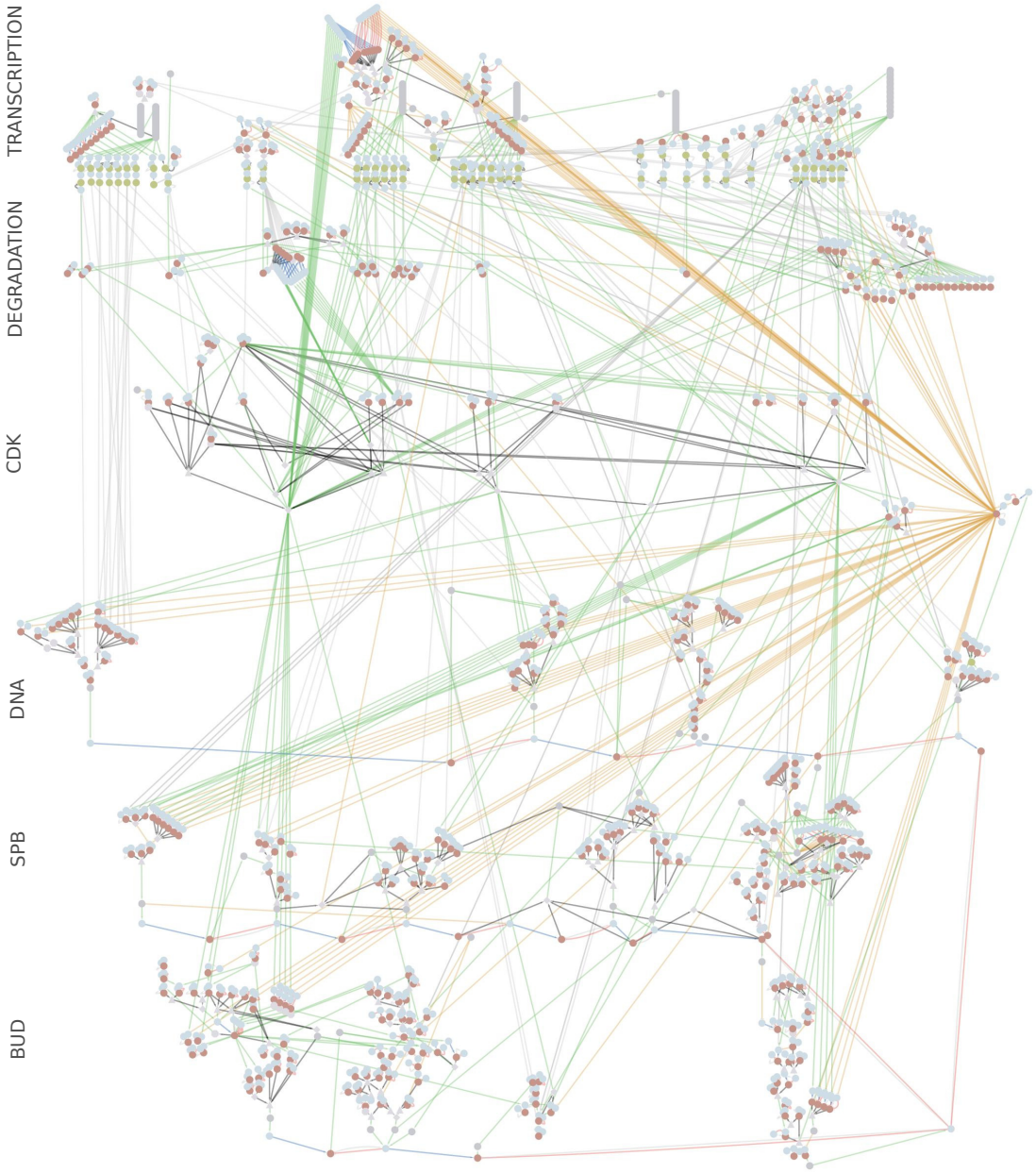

Figure 5.1. *Bird's-eye view of the CC-CNW.* From top to down, the different layers of the network include a transcriptional machinery with six regulated clusters, a degradation machinery, the regulation of the CDK Cdc28, and the three macroscopic cycles DNA replication, SPB duplication and bud growth. From left to right, the order of appearance follows approximately cell cycle progression from G_1 to M phase.

of the potential interaction partner. To restrict certain spatially regulated proteins, their elemental states representing an implicit localization are then either required or inhibitory for reactions with an implicit localization. It is assumed that transcription takes place in the nucleus and that certain membrane bound proteins cannot freely

interact with proteins assumed to be localized to the nucleus.

Furthermore, protein domain names without established names in the literature were given trivial names in the CC-CNW. Similarly, for protein residues without empirical specification, trivial residue names were given.

5.2 Transcriptional clusters

The CC-CNW accounts for six gene regulatory clusters and six unregulated genes. Table 5.1 gives an overview of the clusters and the genes considered in this study. Here, the clusters are named according to their activating transcription factors. The considered genes are a subset of the complete number of genes controlled by these clusters (Spellman *et al.*, 1998), and were selected based on their role in cell cycle control and execution. Gene cluster implementation and regulation is described in this section. Each gene regulatory cluster uses a transcriptional delay implemented as a cascade of twenty input-output nodes. Additionally, the Mcm1 cluster uses an equilibrium delay. These delays are the outcome of the gap-filling steps and explained in Section 6.1. The clusters are presented according to their order of activation during cell cycle progression with the Mcm1 cluster being active during early G_1 phase (Spellman *et al.*, 1998).

Table 5.1. *Transcriptional clusters.* The CC-CNW accounts for six gene regulatory clusters named after their activating transcription factors. Additionally, the CC-CNW accounts for six genes without regulation. SBF: Swi4, Swi6. MBF: Swi6, Mbp1. Fkh2: Fkh2, Mcm1, Ndd1. *repressors; **regulated by SBF or MBF.

Mcm1	SBF	MBF	Hcm1	Fkh2	Ace2Swi5	Unregulated
CDC6	*CLN1*	*ACM1*	*CIN8*	*ACE2*	*PCL9*	*ASE1*
CLN3	*CLN2*	*CLB5*	*FKH1*	*CDC20*	*SIC1*	*CLB4*
MCM2	*HCM1***	*CLB6*	*FKH2*	*CDC5*		*DBF4*
MCM3	*PCL1*	*HCM1***	*NDD1*	*CLB1*		*FAR1*
MCM4	*PCL2*	*NRM1**	*YHP1**	*CLB2*		*KIP1*
MCM5	*SWE1*	*PDS1*		*CLB3*		*MPS1*
MCM6	*YOX1**	*RAD53*		*SWI5*		
MCM7		*SCC1*				
SWI4		*SPC42*				

The transcriptional clusters account for synthesis of mRNA and translation into the corresponding proteins. Transcription is realized by RNA polymerase II, abbreviated with *PolII* in the CC-CNW. Translation reactions are realized by ribosomes, abbreviated with *Ribo*. The activity of each cluster is regulated, hence, the activation and deactivation must be reflected in the presence of the transcriptional output. To account for this, mRNA transcripts are antagonized with a degradational decay reaction in the CC-CNW according to the second hypothesis stated in Section 5.1.

5.2.1 *Mcm1*

The genes considered in the Mcm1 cluster (Figure 5.2) are *MCM2–7* and *CDC6* (Pramila *et al.*, 2002), later used in the DNA replication process (Section 5.6), and *SWI4* (Pramila *et al.*, 2002), a transcription factor regulating the SBF cluster. Importantly, Mcm1 also transcribes *CLN3* (Pramila *et al.*, 2002). Cln3 is the first Cdc28 cyclin appearing during the cell cycle and its translation depends on nutrient availability (Barbet *et al.*, 1996). Thus, in early G_1, the cell cycle machinery integrates environmental information and assesses whether or not to commit to cell cycle progression. The CC-CNW accounts for this with the input *[NutrientAvailabilityCheck]* as a requirement for the activation of Cln3 translation. The activation of the Mcm1 cluster in the presence of nutrients leads to Cln3 expression which in turn induces the activation of the two subsequent clusters regulated by SBF and MBF. Degradation of Cdc6 and Cln3 is regulated via the Skp, Cullin, F-box containing complex (SCF) (Perkins *et al.*, 2001; Landry *et al.*, 2012), and presented in Section 5.3.

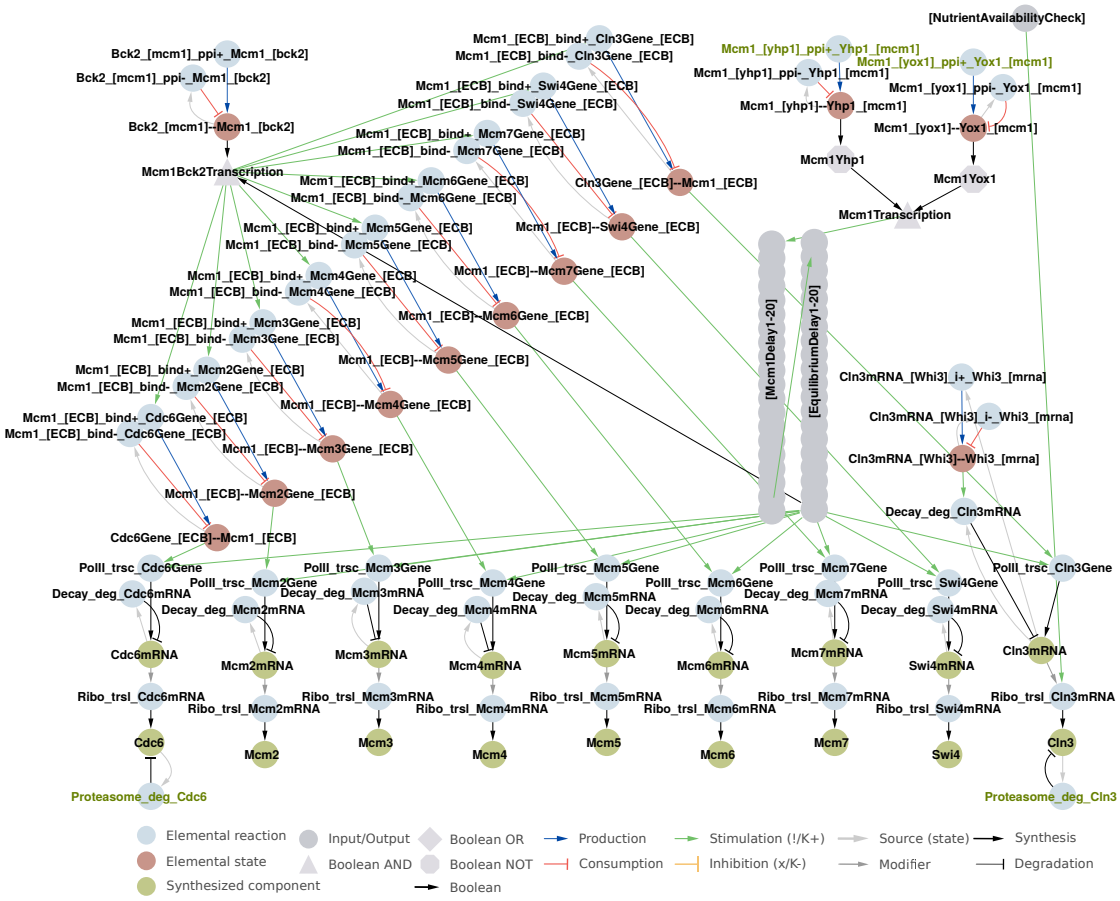

Figure 5.2. *Mcm1 regulated genes.* The Mcm1 cluster mediates activation of *MCM2–7, CDC6, CLN3 and SWI4.* The Mcm1 cluster is negatively regulated by Yox1 and Yhp1. *YOX1* is regulated by MBF, *YHP1* is regulated by Hcm1.

Bck2 has a positive influence on Mcm1 transcription (Bastajian *et al.*, 2013), which is accounted for in the CC-CNW with a positive influence of the Bck2–Mcm1 dimer on the activity of the Mcm1 cluster. Mcm1 cluster activity is negatively regulated by interaction of Mcm1 with either Yhp1 or Yox1 (Pramila *et al.*, 2002). This is reflected in the conditions for Mcm1 transcription and implemented in the *Mcm1Transcription* node.

5.2.2 *SBF*

The SBF cluster (Figure 5.3) accounts for the activation of *SWE1*, *CLN1*, *CLN2*, *YOX1*, *PCL1* and *PCL2* (Nasmyth and Dirick, 1991; Cho *et al.*, 1998; Sia *et al.*, 1996; Haase and Wittenberg, 2014), which are considered in this study. Cln1,2 and Pcl1,2 are cyclins required for activity of their associated CDKs Cdc28 and Pho85, respectively. The transcriptional repressor Yox1 inhibits the upstream Mcm1 cluster. Swe1 is later used in the morphogenesis checkpoint (Section 5.8). SBF is a Swi4–Swi6 dimer, controlling Swi4/Swi6 cell cycle box (SCB) promoter elements. Its activity is by default inhibited by Whi5 and the histone deacetylases (HDACs) Hos3 and Rpd3 (Wagner *et al.*, 2009), accounted for in the CC-CNW by the inhibitory effect of Whi5 bound to Swi6, and additionally, the recruitment of Hos3 and Rpd3 to Whi5. The inhibition by Whi5 is counteracted by Cdc28–Cln1,2,3 phosphorylation. Phosphorylated Whi5 dissociates from SCB promoters (Wagner *et al.*, 2009). Furthermore, one of two combinations of Whi5 phosphorylation (*Whi5Comb1* and *Whi5Comb2* in the CC-CNW) forces dissociation of the inhibitory HDACs (Wagner *et al.*, 2009), which is accounted for in the CC-CNW by the explicit definition of these Whi5 phosphorylation combinations and the inhibitory role of their output *Whi5PhosCombinations*. The same study also reported that hyper-phosphorylation of Whi5, represented as *Whi5HyperPhos*, and Swi6 phosphorylation at four residues, represented as *Swi6Phosphorylation*, forces Whi5 dissociation from Swi6, combined in the node *Whi5HyperPhosOrSwi6Phosphorylation*. These conditions together with SBF, combined in the *SBF* node, and Swi4 bound to SCB promoters, allow transcription of the SBF cluster.

CDK Pho85 has a partially redundant role in the activation of SBF, accounted for in the CC-CNW by a negative influence of phosphorylated Whi5 towards its interaction with the HDACs. This phosphorylation is mediated by Pho85 interacting with either Pcl1 or Pcl9 (Huang *et al.*, 2009). However, the exact mechanism has not been demonstrated. It is tempting to speculate that Pho85 and Cdc28 share the same Whi5 targets, as a Whi5 mutant with 12 CDK-site alanine substitutions is not viable (Wagner *et al.*, 2009). Since less is known about Pho85 regulation, the effect of its phosphorylation of Whi5 on Whi5 interactions with the HDACs was implemented as a negative influence instead of a strict inhibition. *CLN1,2* and *PCL1* are activated by SBF and contribute to Whi5 phosphorylation, constituting a positive feedback loop. Deactivation of the SBF cluster first occurs after DNA replication is finished and Clb1,2 activity rises due to activation of the cluster controlled by Fkh2, Ndd1 and Mcm1. Cdc28–Clb1,2-mediated phosphorylation of Swi4 inhibits Swi4 promoter association (Koch *et al.*, 1996). SBF has

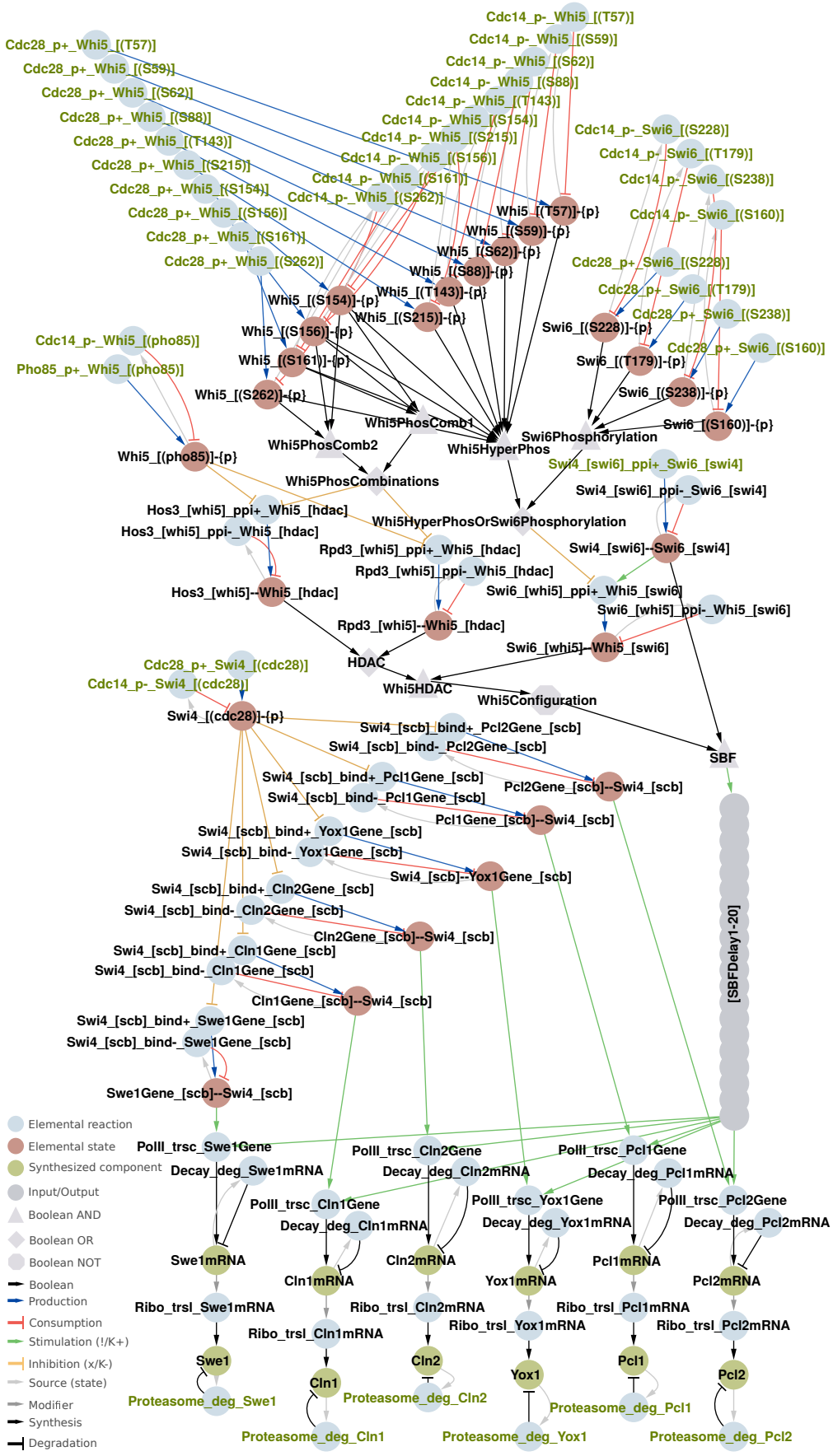

Figure 5.3. *SBF regulated genes.* SBF regulates the activation of *SWE1, CLN1, CLN2, YOX1, PCL1* and *PCL2*, which are considered here. SBF activity is repressed by Whi5 and activated by Cdc28–Cln1-3 and Pho85–Pcl1,9. Subsequent activation of Clb1,2 and Yox1 contributes to the deactivation of the cluster.

an indirect autoinhibitory feedback loop by antagonizing the upstream Mcm1 cluster via Yox1. Furthermore, the G_1 cyclins Cln1,2,3 are degraded and their phosphorylations of Whi5 and Swi6 antagonized by Cdc14 at a later stage in the cell cycle, which is accounted for in the CC-CNW. Proteins regulated by this cluster are turned over as described in Section 5.3.

5.2.3 *MBF*

The MBF regulated genes *ACM1, SPC42, CLB5, CLB6, RAD53, NRM1, SCC1* and *PDS1* (Ostapenko *et al.*, 2008; Enserink and Kolodner, 2010; MacIsaac *et al.*, 2006; Zheng *et al.*, 1993) are considered in this study (Figure 5.4). Their protein products are turned over in a regulated manner (Section 5.3). The cyclins Clb5 and Clb6 are required for initiation of DNA replication, while Rad53 monitors ongoing DNA replication (Section 5.6). Scc1 and Pds1 are involved in cohesin loading (Marston, 2014) during the chromosome cycle (Section 5.6). Acm1 is a pseudosubstrate inhibitor of the APC/C (Dial *et al.*, 2007) and responsible for the inhibition of premature APC activation (Section 5.3). The protein Spc42 is an integral part of the SPB and used in the SPB replication cycle (Section 5.7).

Activation of MBF regulated genes occurs slightly after SBF activation and requires binding of the Mbp1–Swi6 (MBF) dimer to Mlu1 cell cycle box (MCB) promoter elements (Koch *et al.*, 1993). The CC-CNW accounts for MBF activation, represented in the node *MBF*, in the following way: MBF interacting with MCB promoters requires Cdc28–Cln1,2,3-mediated phosphorylation of Swi6 (*Swi6Phosphorylation*). Nrm1 inhibits MBF formation by binding to Swi6 (de Bruin *et al.*, 2006). Additionally, the CC-CNW accounts for the positive influence of Stb1 binding to Swi6 and enhancing transcription (de Bruin *et al.*, 2008). Stb1 phosphorylation by Cdc28 negatively influences MBF activity by reducing its affinity to Swi6 (Costanzo *et al.*, 2003).

Nrm1 inhibition is counteracted by the kinase Rad53, which in turn phosphorylates Nrm1 and inhibits association of Nrm1 to Swi6 (Travesa *et al.*, 2012, 2013), accounted for in the CC-CNW. Rad53 activity depends on ongoing DNA replication as described in Section 5.6. Only after DNA replication is finished, Rad53 is inactivated, resulting in the dephosphorylation of Nrm1, which can then bind to Swi6 and inhibit MBF activity (de Bruin *et al.*, 2006).

The exact mechanism of MBF activation is disputed (Enserink and Kolodner, 2010). In the CC-CNW, unregulated binding of the transcription factor MBF to MCB target promoters renders the MBF cluster constitutively active, which is not desired. Literature research did not provide a fully conclusive mechanism of MBF regulation. Instead, a hypothetical requirement of Swi6 phosphorylation mediated by Cdc28 and Cln1-3 was implemented based on the study by Palumbo *et al.* (2016). This model hypothesis was introduced during the gap-filling process (Section 6.1.1), based on the study by Palumbo *et al.* (2016). This hypothesis solves a technical problem, as the corresponding bipartite Boolean model requires absolute statements to convey signals. This link, however, cannot be a strict requirement as a Swi6 mutant with four alanine-substituted Cdc28

residues is viable (Wagner *et al.*, 2009) and hence, can bypass MBF activation. Thus, the mechanistic regulation of MBF activation requires more experimental attention.

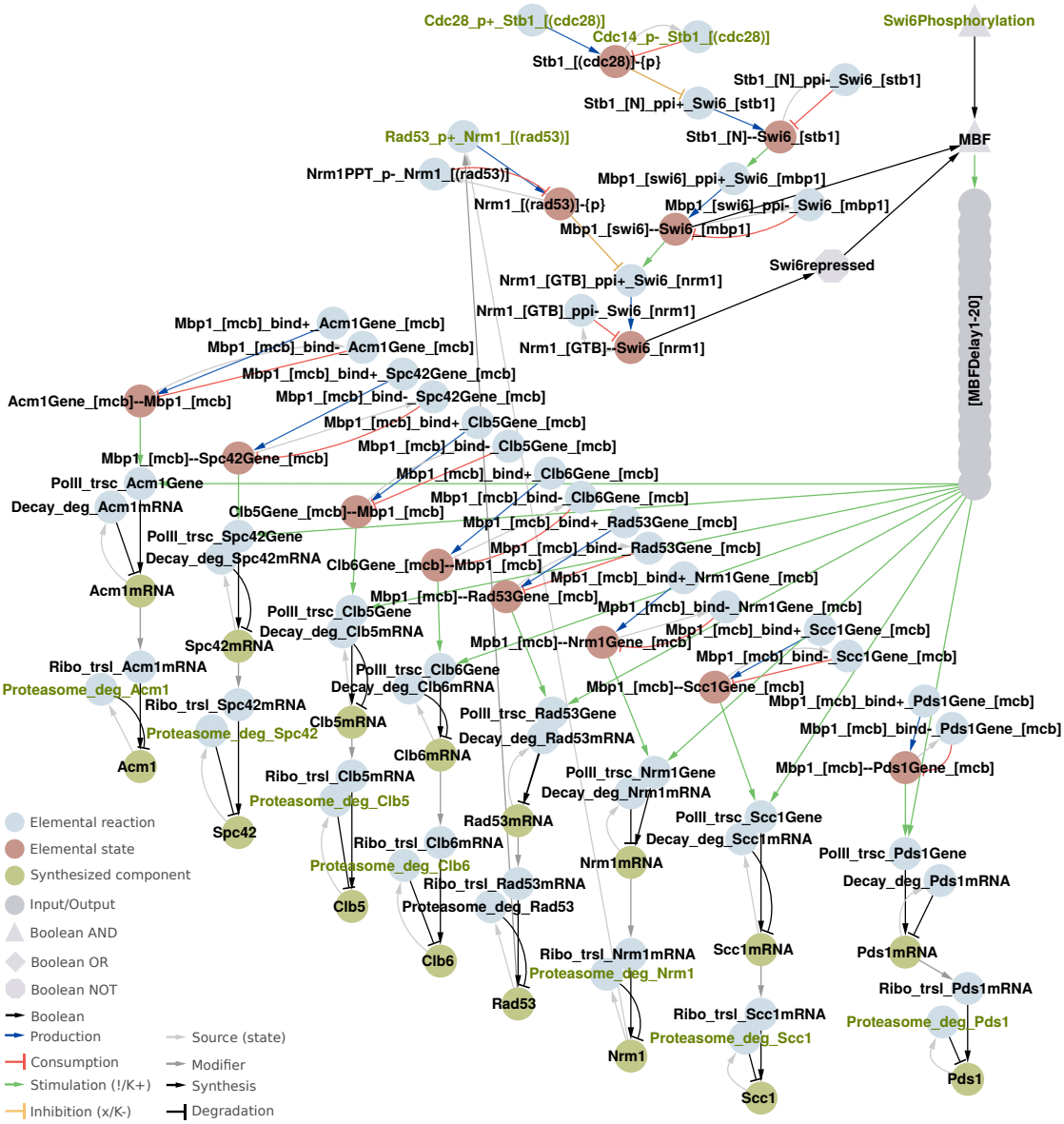

Figure 5.4. *MBF regulated genes.* MBF activates the transcription of *ACM1, SPC42, CLB5, CLB6, RAD53, NRM1, SCC1* and *PDS1*, which are considered here. MBF activation is positively regulated via Swi6, based on a model hypothesis. MBF activity is maintained while DNA replication is ongoing, accomplished by Rad53 dependent phosphorylation of the repressor Nrm1. Rad53 is deactivated after DNA replication has finished, rendering Nrm1 unphosphorylated, enabling it to bind Swi6, resulting in the deactivation of the MBF cluster.

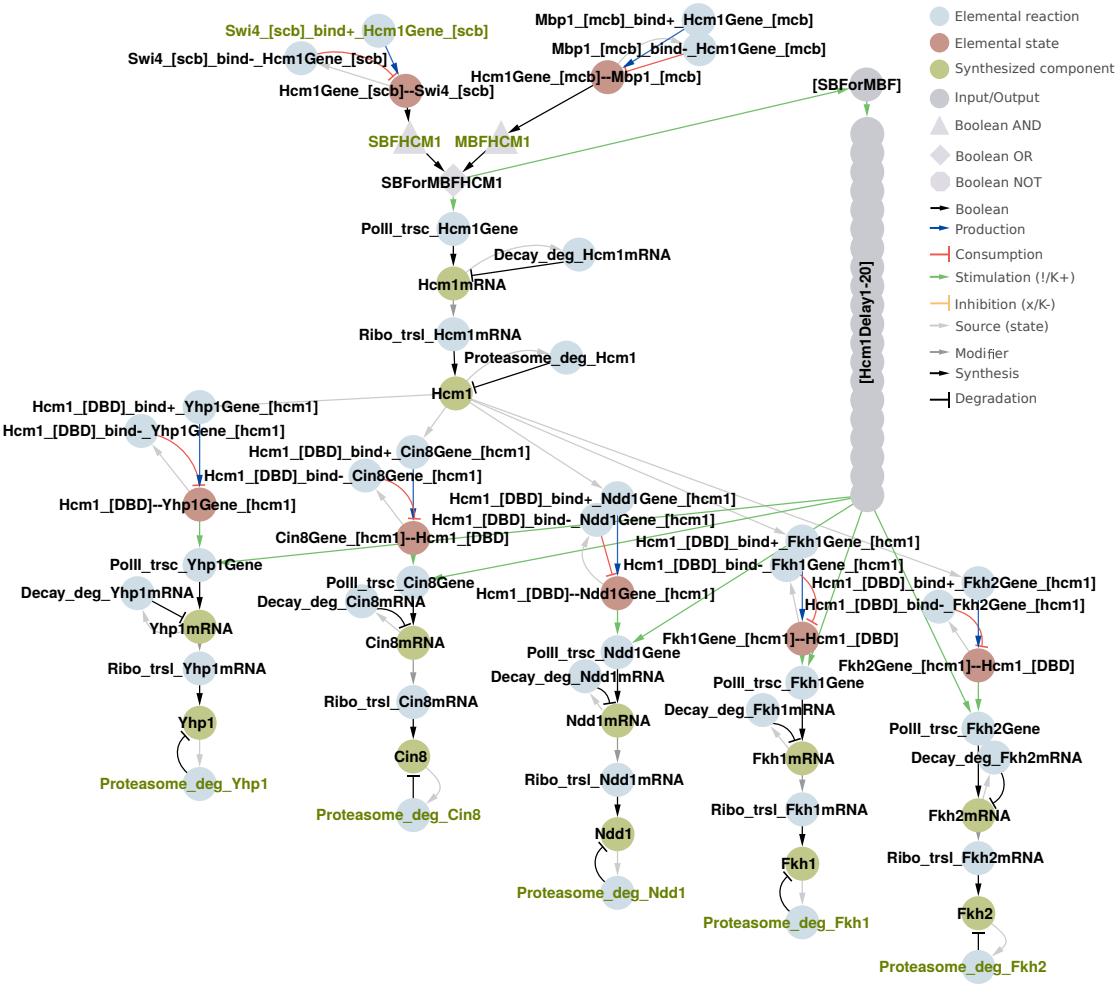

Figure 5.5. *Hcm1 regulated genes.* Hcm1 activates the transcription of *YHP1, CIN8, NDD1, FKH1* and *FKH2*. *HCM1* is regulated via SBF or MBF. The Hcm1 cluster is indirectly negatively regulated by transcription of the repressor Yhp1, which targets the upstream Mcm1 cluster.

5.2.4 *Hcm1*

The Hcm1 cluster (Figure 5.5) is regulated by the transcription factor Hcm1 and *HCM1* in turn is transcribed by either SBF or MBF (Horak *et al.*, 2002; Bean *et al.*, 2005), implemented with the *SBForMBFHCM1* node. Hcm1 regulated genes considered in this study are *YHP1, CIN8, NDD1, FKH1* and *FKH2* (Pramila *et al.*, 2006). Yhp1 is a transcriptional repressor of the upstream Mcm1 regulated cluster and thus, Yhp1 contributes indirectly to the deactivation of the Hcm1 cluster. The Hcm1 cluster activates the transcription factors Fkh2 and Ndd1, required for the upregulation of genes controlled by Fkh2, Ndd1, and Mcm1. Hcm1 also transcribes *CIN8*, which is translated into a kinesin motor protein (Hildebrandt *et al.*, 2006) and required for proper SPB separation (Section 5.7.3). The protein products of the genes considered in the

Hcm1 cluster are regulated by turnover as described in Section 5.3.

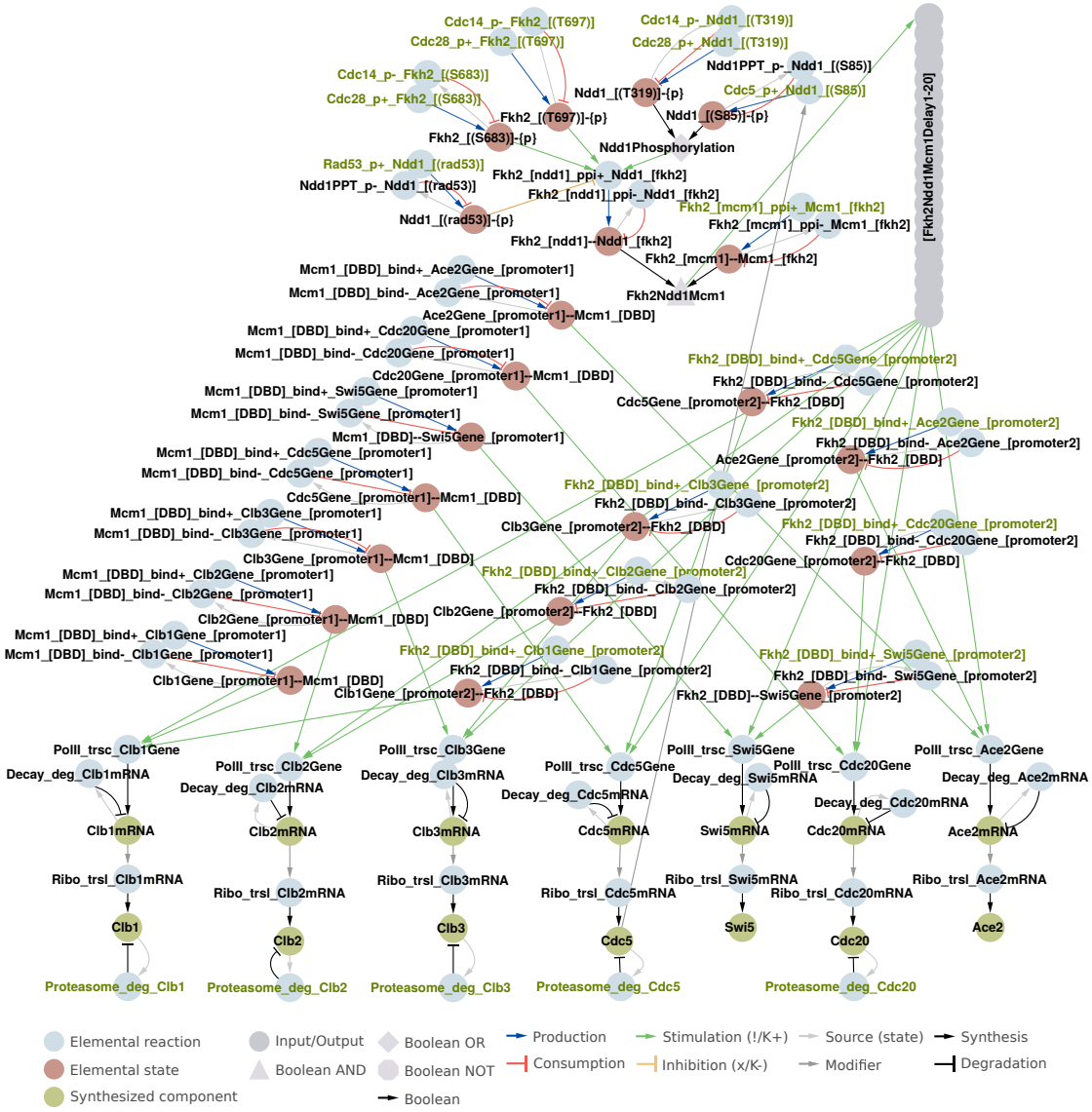

Figure 5.6. *Fkh2Ndd1Mcm1 regulated genes.* The CC-CNW accounts for the transcription of *CLB1, CLB2, CLB3, CDC5, SWI5, CDC20* and *ACE2*, which are upregulated by the transcription factors Fkh2, Ndd1 and Mcm1. The Fkh2Ndd1Mcm1 cluster is positively influenced by the Hcm1 dependent transcription of *NDD1* and *FKH1*, and involvement of the kinases Cdc28 and Cdc5. The Rad53 kinase inhibits Fkh2Ndd1Mcm1 mediated transcription until DNA replication has finished.

5.2.5 *Fkh2, Ndd1, Mcm1*

The genes regulated by Fkh2, Ndd1, and Mcm1 (Figure 5.6) considered in this study are the cyclins *CLB1,2,3*, the kinase *CDC5*, the APC/C regulatory subunit *CDC20*, and the transcription factors *ACE2* and *SWI5* (Simon *et al.*, 2001; Haase and Wittenberg, 2014). Here, the cluster is referred to as Fkh2Ndd1Mcm1 cluster. Clb1,2 are later used

for Cdc28 kinase activity to promote the G_2/M transition. Cdc5 is a kinase involved in several processes, such as Cdc14 activation (Section 5.4) and bud morphology (Section 5.8).

Swi5 and Ace2 are transcription factors and described in the next cluster. Cdc20 is a regulatory subunit of the APC/C and described in Subsection 5.3.1. Fkh2Ndd1Mcm1 cluster activation in the CC-CNW requires binding of the transcription factors Fkh2 and Mcm1 to promoter elements, and the binding of Ndd1 to Fkh2, based on Haase and Wittenberg (2014). The formation of the protein trimer Ndd1–Fkh2–Mcm1, represented in the *Fkh2Ndd1Mcm1* node, is regulated by Cdc28-mediated phosphorylation of Fkh2 and Ndd1 (Pic-Taylor *et al.*, 2004; Darieva *et al.*, 2006). Fkh2 phosphorylation by Cdc28–Clb1,2,5,6 at residues S683 and T697 is implemented as a strict requirement for the interaction between Fkh2 and Ndd1. The strict requirement is an outcome from the gap-filling process (Section 6.1), and was previously implemented as a positive influence. Fkh2 phosphorylation by Cdc28 as implemented in the CC-CNW requires Clb1,2,5 or Clb6 (Pic-Taylor *et al.*, 2004). Phosphorylation of Ndd1 by Cdc28–Clb1,2 (Reynolds *et al.*, 2003) or Cdc5 (Darieva *et al.*, 2006) has a positive influence on Fkh2Ndd1Mcm1 transcriptional regulation. Thus, the transcriptional output of the Fkh2Ndd1Mcm1 has a positive feedback loop via Clb1,2 (Reynolds *et al.*, 2003). Fkh2 and Ndd1 are positively regulated via the Hcm1 cluster.

Similar to MBF regulation, Fkh2Ndd1Mcm1 cluster activation depends on the status of DNA replication. The phosphorylation of Ndd1 by Rad53 inhibits the association between Fkh2 and Ndd1 (Yelamanchi *et al.*, 2014). Upon termination of DNA replication, Rad53 is deactivated, Ndd1 becomes dephosphorylated at the Rad53 modified residue(s) and can bind Fkh2, which ultimately results in transcriptional activation of Fkh2Ndd1Mcm1 regulated genes. Activation of the Fkh2Ndd1Mcm1 cluster thus occurs after S phase and by activating Clb1,2, it contributes to progression from G_2 to M phase. Deactivation of the Fkh2Ndd1Mcm1 cluster is furthermore regulated by downregulation of Fkh2 and Ndd1, as well as the dephosphorylation of Fkh2 and Ndd1 towards the end of the cell cycle when Cdc14 is active. The proteins activated by the Fkh2Ndd1Mcm1 cluster, except Ace2 and Swi5, are turned over in a regulated manner as described in Section 5.3.

5.2.6 *Ace2 and Swi5*

Ace2 and Swi5 redundantly transcribe *PCL9* (Tennyson *et al.*, 1998) and *SIC1* (Enserink and Kolodner, 2010) (Figure 5.7). Both transcription factors are positively regulated by the Fkh2Ndd1Mcm1 cluster. The CC-CNW accounts for Ace2 and Swi5 downregulation by Cdc28-mediated phosphorylation, which results in nuclear exclusion, rendering Ace2 and Swi5 inaccessible for DNA binding (Sbia *et al.*, 2008). In addition to its nucleo-cytoplasmic regulation, Ace2 localizes to the daughter nucleus, where it induces daughter-specific transcriptional programs (Colman-Lerner *et al.*, 2001). Here, the distinction between mother and daughter nucleus is omitted, as the expressiveness of the

rxncon language does not permit a distinction between between these compartments.

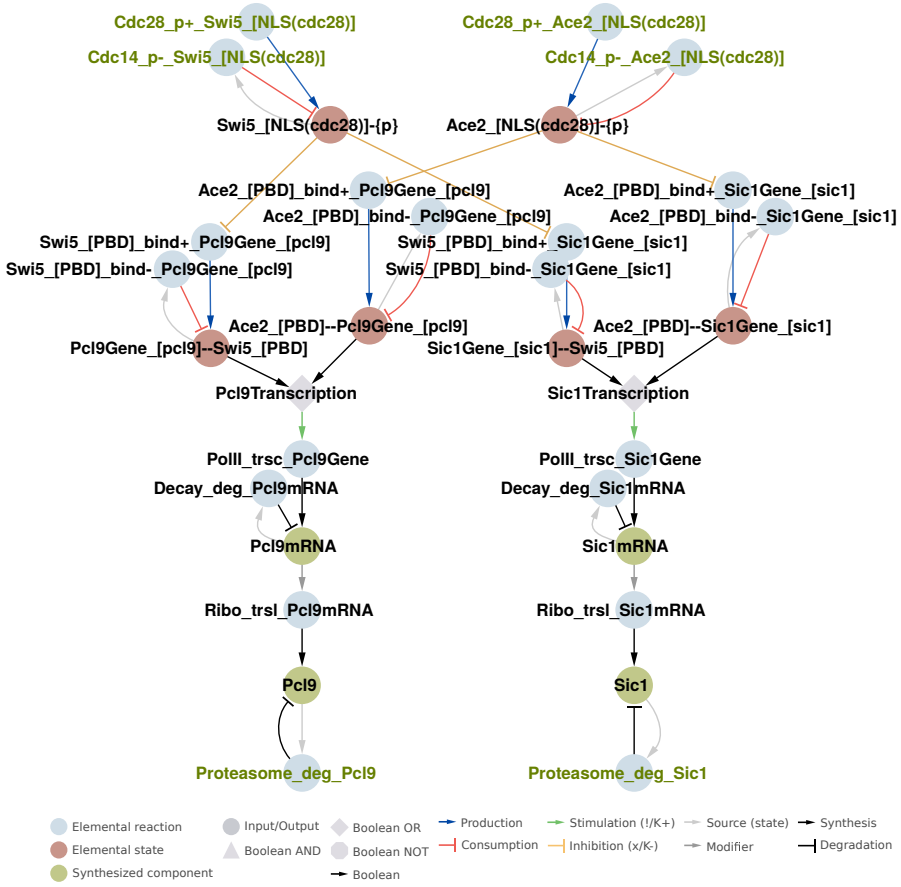

Figure 5.7. *Ace2/Swi5 regulated genes.* The transcription factors Ace2 and Swi5 redundantly regulate the genes *PCL9* and *SIC1*, which are considered here. Both transcription factors are spatially regulated via a nuclear localization sequence (NLS). Cdc28-mediated phosphorylation of the NLS excludes both transcription factors from the nucleus, thereby inhibiting them from DNA binding. Cdc14 dephosphorylates Ace2 and Swi5, which enables them to bind to their target genes.

5.2.7 *Unregulated genes*

In addition to the described clusters and genes, the CC-CNW also accounts for the transcription of the genes *ASE1*, *CLB4*, *DBF4*, *FAR1*, *KIP1* and *MPS1* (Figure A.1). With the exception of Far1, no conclusive support could be found which demonstrates how these genes are regulated. However, these genes are involved in several cell cycle processes and potentially transcriptionally regulated. Hence, their transcriptional reactions are included in the model and can later be linked to a regulatory mechanism.

5.3 Regulated degradation

The gene products of the clusters described in Section 5.2 require turnover in order to reflect transcriptional and translational deregulation. The CC-CNW accounts for

regulated degradation via the ubiquitin ligation machineries APC/C and the SCF. Table 5.2 lists their targets accounted for in this study.

Table 5.2. *Ubiquitin-mediated degradation targets.* *Proteins degraded by several machineries.

APC/C–Cdh1	APC/C–Cdc20	SCF–Cdc4	SCF–Grr1	SCF–Met30	Dma1
Ase1	Acm1	Cdc6	Cln1*	Swe1	Pcl1
Cdc20	Clb2*	Clb6	Cln2		Pcl2
Cdc5	Clb5*	Cln1*	Cln3*		Pcl9
Cin8	Dbf4	Cln3*	Ndd1		
Clb1	Kip1	Far1			
Clb2*	Pds1	Sic1			
Clb3					
Clb4					
Clb5*					
Fkh1					
Fkh2					
Mps1					
Nrm1					
Yhp1					
Yox1					

5.3.1 *The APC/C machinery*

The APC/C is a multimeric complex (Schreiber *et al.*, 2011) and requires binding to a regulatory subunit, Cdc20 or Cdh1 (Figure 5.8). The APC/C has an additional regulatory subunit, Ama1, which is omitted here due to its function during meiosis (Finley *et al.*, 2012), falling outside the scope of this study. Although structural insights into APC/C topology have been reported (Schreiber *et al.*, 2011), the information on the level of elemental reactions and contingencies necessary to describe APC/C assembly, topology, and regulation, is sparse. Thus, in the CC-CNW, the APC/C is implemented as one component APC, symbolizing the complete multimeric APC/C. APC/C promotes progression through anaphase and its activity is tightly regulated, which is required to prevent premature cell cycle progression. The CC-CNW accounts for APC/C regulation and the two regulatory subunits Cdc20 and Cdh1 in the following way: Active APC/C-Cdh1 is combined in the node *APCCdh1Active*. Its activity is inhibited via pseudosubstrate binding of either of the two dimers Acm1–Bmh1 or Acm1–Bmh2 to Cdh1, blocking the substrate binding domain of Cdh1 (Heusden *et al.*, 1995; Dial *et al.*, 2007). This inhibition is combined in the *CAB* node (Cdh1, Acm1, Bmh1 complex). Acm1 is activated by MBF and phosphorylation by Cdc28–Cln1,2,3 during G_1 phase, combined in the *Acm1Phosphorylation* node, negatively influences ubiquitination of Acm1. The contribution of each Acm1 phosphorylation was not entirely determined (Ostapenko *et al.*, 2008). This renders APC/C-Cdh1 inactive until Cdc28-mediated phosphorylations are reversed by Cdc14 towards the end of

the cell cycle, resulting in Acm1 downregulation by APC–Cdc20 (Enquist-Newman *et al.*, 2008). Additionally, APC/C-Cdh1 activity is regulated by Cdc28–Clb1,2, which phosphorylates Cdh1 and inhibits APC/C-Cdh1 activity. This inhibition is lifted by Cdc14-mediated dephosphorylation of Cdh1, allowing association between APC/C and Cdh1. APC/C-Cdc20 is kept inactive as long as Cdc20 is bound to Mad2, inhibiting its interaction with the APC/C. This interaction is regulated via a mechanism monitoring correct spindle alignment as described in Section 5.7. Cdc20 itself is regulated by the Fkh2Ndd1Mcm1 cluster. APC/C substrates accounted for here have transcriptional regulation. The securin Pds1 is phosphorylated by Cdc28–Cln1,2,3 (Agarwal and Cohen-Fix, 2002; Kõivomägi *et al.*, 2011), inhibiting its APC/C recognition (Holt *et al.*, 2008). Only after Cdc14 activation towards the end of the cell cycle, Pds1 is dephosphorylated and becomes susceptible for APC/C degradation. Pds1 regulation is described in Section 5.6. Mps1 phosphorylation has a negative influence on APC/C recognition (Enserink and Kolodner, 2010), accounted for in the model. All ubiquitinated APC/C substrates are degraded by the proteasome.

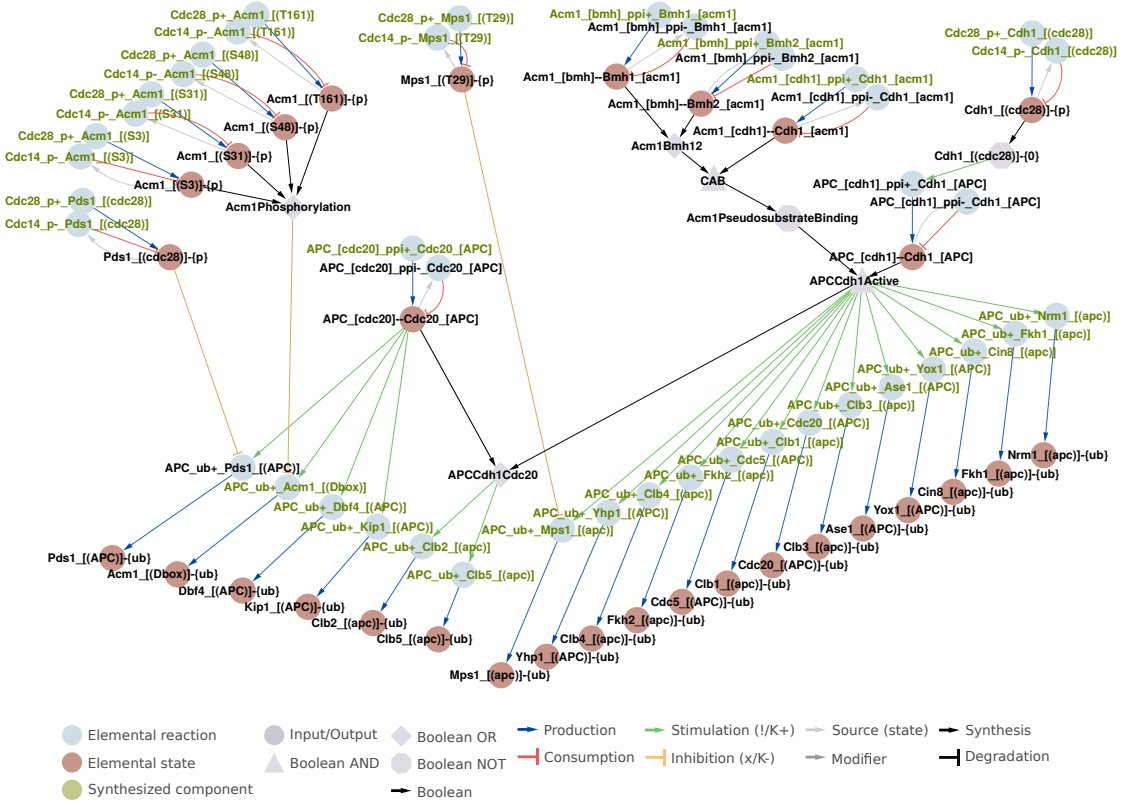

Figure 5.8. *APC/C-mediated degradation.* The CC-CNW accounts for the APC/C regulatory subunits Cdc20 and Cdh1 and the substrates listed in Table 5.2. APC/C–Cdh1 activity is inhibited by pseudosubstrate binding via Acm1, and furthermore by Cdc28-mediated phosphorylation. The phosphorylation is antagonized by Cdc14 towards the end of the cell cycle. APC/C-Cdc20 activity depends on the spindle assembly checkpoint (SAC) as described in Section 5.7 and shown in Figure 5.22.

5.3.2 *The SCF machinery*

The CC-CNW accounts for the four SCF subunits Cdc53, Cdc34, Cdc53 and Skp1 which form the core ligase complex (Seol *et al.*, 1999), combined in the *SCF* node (Figure 5.9).

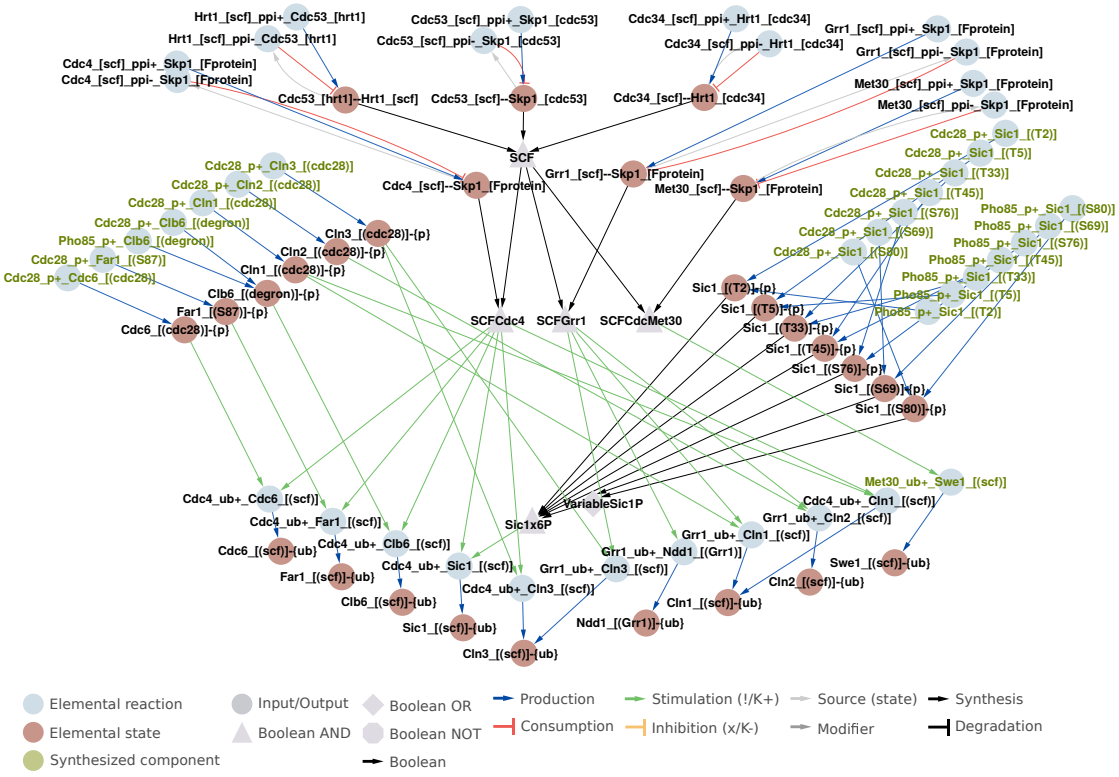

Figure 5.9. *SCF-mediated degradation.* The CC-CNW accounts for the SCF and the three F-box proteins Cdc4, Grr1 and Met30, which enable SCF substrate specificity. The SCF substrates considered here (Table 5.2) require phosphorylation for SCF recognition.

SCF activity requires binding to an F-box protein to enable substrate specificity. The CC-CNW accounts for the F-box proteins Cdc4, Grr1 and Met30, combined in the nodes *SCFCdc4*, *SCFGrr1* and *SCFMet30*. Additionally, the CC-CNW accounts for ubiquitin ligase recognition by requiring substrate phosphorylation prior to ubiquitination. The SCF substrate Swe1 inhibits Cdc28–Clb1,2 activity (Section 5.4) to prevent premature cell cycle progression. Hence, Swe1 degradation is regulated to time this inhibition. The CC-CNW takes two regulatory mechanisms for Swe1 degradation into account. First, Swe1 monitors bud morphology. Only after formation of a bud, Swe1 is phosphorylated (Section 5.8) and primed for degradation. Second, Swe1 has a role in the DNA replication checkpoint (Section 5.6), during which it becomes phosphorylated by Mec1 (Palou *et al.*, 2015). This phosphorylation is hypothesized to stabilize Swe1, as based on Palou *et al.* (2015). Sic1, another SCF substrate, inhibits Cdc28–Clb1,2,5,6 (Section 5.4) and requires phosphorylation by Cdc28–Cln1,2,3 or Pho85–Pcl1 for SCF recognition

(Nash *et al.*, 2001; Nishizawa *et al.*, 1998). The CC-CNW accounts for the contribution of the phosphorylation of different Sic1 residues as reported by Nash *et al.* (2001), implemented by the nodes *VariableSic1P* and *Sic1x6P*. These Sic1 phosphorylations at Cdc28 sites are hypothesized to be equivalent for Pho85 phosphorylation (Nishizawa *et al.*, 1998), with the same degradational consequences for Sic1.

The CC-CNW accounts for Pcl1,2 and Pcl9 turnover (Figure 5.10) via the Dma1 ubiquitin ligase. This is based on the report by Hernández-Ortega *et al.* (2013), in which Pcl1 degradation was tested. In the CC-CNW, it is hypothesized that Pcl2 and Pcl9 are turned over in a similar way due to similarity between Pcl1,2,9. Dma1 recognition furthermore requires prior phosphorylation by Pho85. This requirement was tested with Pcl1 (Hernández-Ortega *et al.*, 2013), and similarly, hypothesized here, to be equivalent for recognition of Pcl2 and Pcl9 by Dma1.

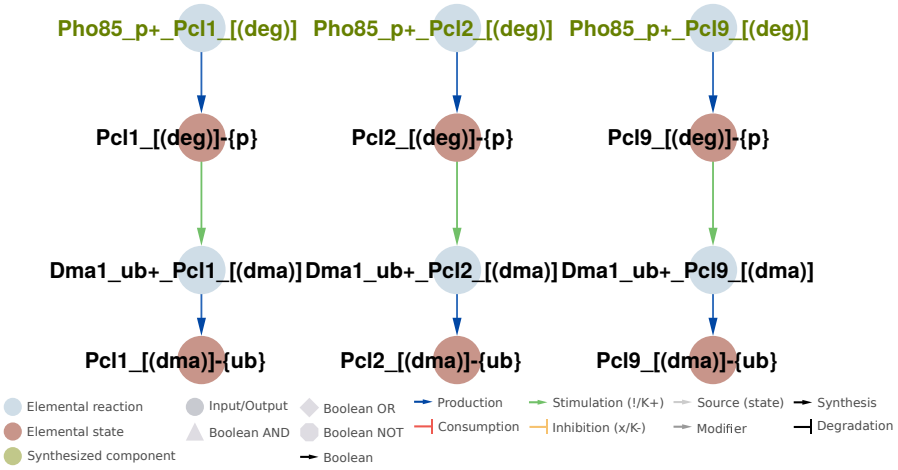

Figure 5.10. *Dma1-mediated degradation.* The accounts CC-CNW for regulated degradation of Pcl1, Pcl2 and Pcl9 by Dma1-mediated ubiquitination. Dma1 recognition requires substrate phosphorylation.

5.4 The CDK module

The CC-CNW accounts for the essential CDK Cdc28 and the partially redundant CDK Pho85, and how they are regulated (Section 5.4.1). The CC-CNW also accounts for the regulation of the CDK antagonist Cdc14, which becomes active towards the end of the cell cycle (Section 5.4.2).

5.4.1 *Cdc28 and Pho85*

Tables 5.3 and 5.4 show an overview of the CDK-cyclin pairs and their substrates considered in the CC-CNW. The upper part of Figure 5.11 shows the upstream regulation of Cdc28 kinase activity and how binding to its different cyclins is regulated, as accounted for in the CC-CNW. Cdc28 activity depends on phosphorylation by Cak1 on residue T169, serving as a prerequisite for cyclin binding (Ross *et al.*, 2000), and

implemented as a strict requirement in the CC-CNW. Cyclin binding to Cdc28 ensures substrate specificity. The different Cdc28-cyclin pairs promote different processes during the cell cycle and are differentially regulated, ensuring their temporally restricted activation. The CC-CNW accounts for Cdc28–cyclin regulation in the following way: Activation of the G_1 cyclins Cln1,2,3 requires Cks1 binding to Cdc28 (Reynard *et al.*, 2000). Furthermore, Cln3 associates with the chaperone Ydj1. Ydj1 regulates Cln3 stability via phosphorylation (omitted here) and localization (Yaglom *et al.*, 1996). Ydj1 itself requires activation via Ssa1 or Ssa2, combined in the *ActiveYdj1* node. Ssa1 is also a Cdc28 substrate (Truman *et al.*, 2012), but the physiological relevance of its phosphorylation remains unclear.

Table 5.3. *Cdc28 substrates.* These Cdc28-cyclin pairs and their substrates are accounted for in the CC-CNW. *only Cln1,2.

Cln1,2,3	Clb1,2	Clb5,6
Acm1	Ace2	Cdc6
Bem2	Cdc5	Clb6
Bem3	Cdh1	Dbf4
Boi1	Chs2	Fin1
Boi2	Fkh2	Fkh2
Cdc24	Lte1	Kar9
Cln1	Mcm3	Orc2
Cln2	Ndd1	Orc6
Cln3	Net1	Sld2
Far1	Sfi1	Sld3
Mps1	Smc4	Spc110
Pds1	Spc110	Ssa1
Rga1	Swe1	Tgl4
Rga2	Swi4	
Sic1*	Swi5	
Spc42	Tub4	
Stb1		
Swi6		
Tus1		
Whi5		

Table 5.4. *Pho85 substrates.* These Pho85-cyclin pairs and their substrates are accounted for in the CC-CNW.

Pcl1	Pcl2	Pcl1,9	Pcl1,2,9
Sic1	Ssa1	Whi5	Clb6
			Pcl1
			Pcl2
			Pcl9

The CC-CNW accounts for pheromone sensitivity, accomplished by the inhibition of Cdc28 dissociation from Far1 in the presence of *[Pheromone]*, inhibiting the formation of Cdc28–Cln1,2,3 (Peter and Herskowitz, 1994). In this way, Cdc28–Far1 accomplishes pheromone sensitivity during G_1 phase. Pheromone sensitivity has been studied in detail (reviewed in Haber (2012)), but is simplified here, as pheromone signaling is not part of the core cell cycle control network. The requirements for Cdc28–Cln1,2,3 activity are combined in their respective nodes *Cdc28Cln1*, *Cdc28Cln2* and *Cdc28Cln3*. *CLN3* is

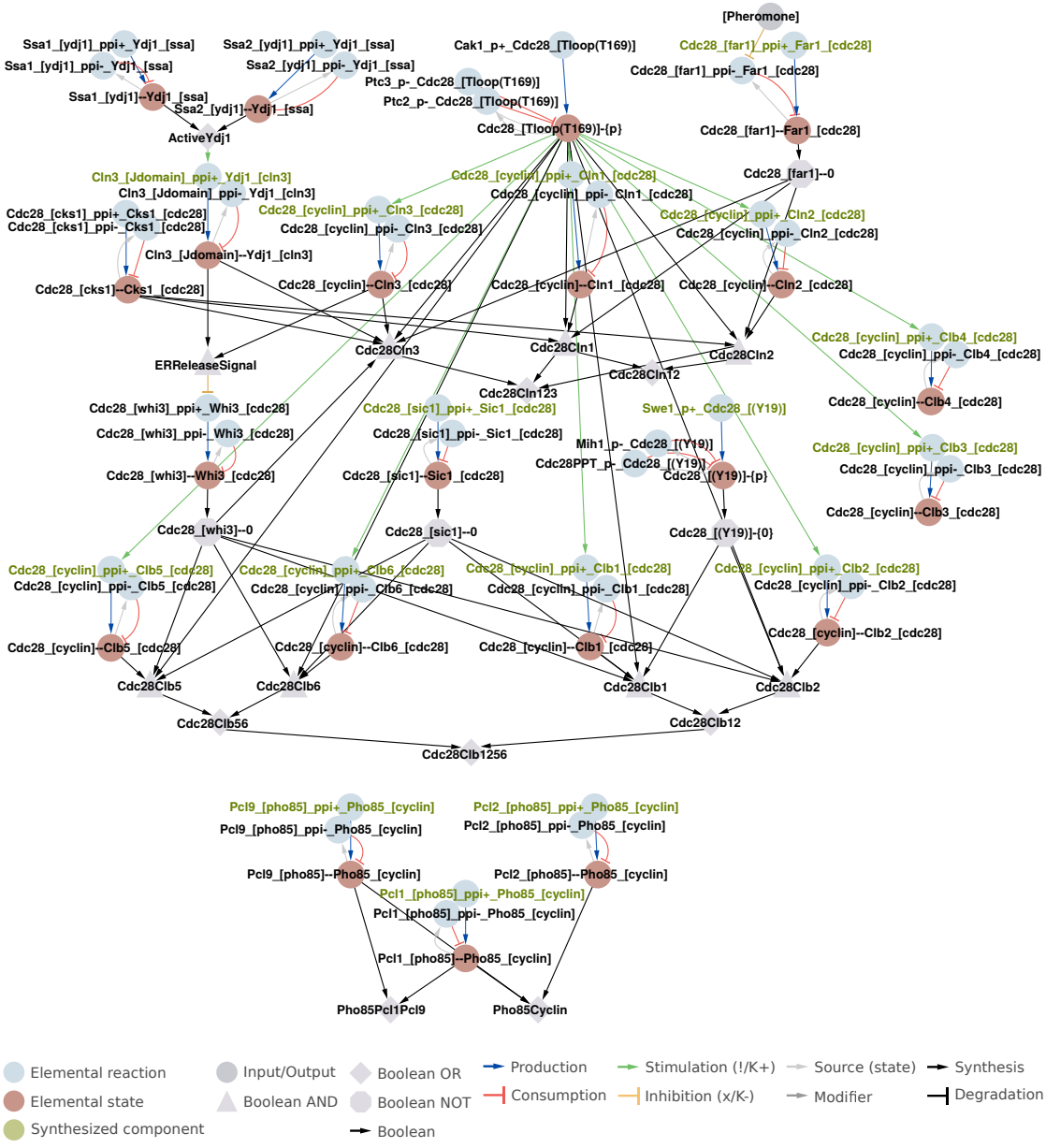

Figure 5.11. *CDK regulation.* Top: Cdc28 kinase activity depends on phosphorylation by Cak1. Cdc28 substrate specificity is enabled by binding to one of six cyclins (Cln1–3, Clb1–6). Differential regulation of these Cdc28–cyclin pairs is shown. Bottom: Regulation of the CDK Pho85 is shown and binding to its cyclins Pcl1,2 and Pcl9.

transcriptionally regulated by Mcm1, *CLN1,2* are transcriptionally regulated by SBF (Section 5.2.2). Protein degradation is regulated by SCF (Section 5.3.2). Furthermore, the CC-CNW accounts for Cdc28 regulation by Whi3, which binds and regulates the localization of Cdc28. Whi3 restricts Cdc28 to the cytoplasm (Wang *et al.*, 2004). The interaction between Cln3 and Ydj1 and Cdc28 together relieves the interaction between

Cdc28 and Whi3, combined in the *ERReleaseSignal*, a hypothesis based on Yaglom *et al.* (1996).

Activity of the Cdc28–cyclin pairs is inhibited by CDK inhibitors (CDKIs). The CC-CNW accounts for the CDKI Sic1, which inhibits activity of Cdc28–Clb1,2 and Cdc28–Clb5,6 (Mendenhall and Hodge, 1998). Sic1 is antagonized by phosphorylation by Cdc28–Cln1,2,3, and Pho85–Pcl1, which primes it for regulated degradation (Nash *et al.*, 2001). In the CC-CNW, Sic1 phosphorylation is mediated only by Cdc28–Cln1,2, which is one outcome of the gap-filling process (Section 6.1). Cdc28–Clb1,2 is additionally inhibited by phosphorylation of Cdc28 on residue Y19 by Swe1. Swe1 monitors bud emergence (Section 5.8.3) and is degraded when a bud has formed, preventing premature cell cycle progression. There is functional redundancy between the Cdc28 cyclins, as reviewed and discussed by Mendenhall and Hodge (1998). In general, the cyclins can compensate for each other pairwise. These functional redundancies are supported by observations of single and multiple mutant phenotypes. The G_1 cyclins Cln1, Cln2 and Cln3 have redundant functions, and a triple deletion is lethal (Richardson *et al.*, 1989). Similarly, the cyclin pair Clb1 and Clb2 has redundant functions, as the single mutants are viable, whereas a double mutant is lethal (Surana *et al.*, 1991). The cyclins Clb5 and Clb6 can also compensate for each other, as the single mutants are viable (Kühne and Linder, 1993). The double mutant is also viable, but the phenotype shows differences compared to the wildtype (Kühne and Linder, 1993). A mutational study indicates that the cyclin pair Clb3,4 can compensate for Clb5,6 functions (Schwob and Nasmyth, 1993). The CC-CNW accounts for Cdc28 cyclin redundancy, such that the pairs Clb1,2 and Clb5,6 have the same targets. Regulation of *CLB4* has not been reported, yet. For this reason, the CC-CNW does not account for Cdc28–Clb3,4 substrates, as this would render its targets constitutively active, which is not observed. The cyclins Cln1,2,3 also compensate for each other, with the exception of the substrate Sic1. In the CC-CNW, Sic1 is only a substrate of Cdc28–Cln1,2, due to the discrepancy between qualitative and quantitative modeling. This is an outcome of the gap-filling process, and discussed in Sections 6.1.1 and 6.3. In the CC-CNW, the functional redundancy between the cyclin pairs is used as a hypothesis for all Cdc28 phosphorylation reactions, in which empirical studies have not demonstrated a different observation. The references are listed in Table A.4, with the hypothesized cyclin pair function redundancy indicated.

The lower part of Figure 5.11 shows the Pho85 module. Similar to Cdc28, Pho85 requires cyclin binding in order to acquire kinase activity (Measday *et al.*, 1997). Though it appears likely that Pho85 has a similar upstream regulation to Cdc28, empirical evidence is missing (Nishizawa *et al.*, 1999; Huang *et al.*, 2007). The CC-CNW accounts for the Pho85 cyclins Pcl1,2 and Pcl9. In the CC-CNW, Pho85 kinase activity is established upon the interaction between Pho85 and one of its cyclins. During G_1, the CDK Pho85 has a redundant role with Cdc28 in antagonizing Whi5 and Sic1 (Huang *et al.*, 2007), which is accounted for in the CC-CNW.

5.4.2 *Cdc14*

To antagonize Cdc28 and Pho85-mediated phosphorylations, the phosphatase Cdc14 must be activated towards the end of the cell cycle (Figure 5.12). The CC-CNW accounts for Cdc14 activity regulation in the following way: Cdc14 bound to Net1 inhibits Cdc14 substrate access. This interaction implies Cdc14 retention at the nucleolus (Shou *et al.*, 1999). Hence, the interaction between Cdc14 and Net1 must be relieved for Cdc14 activation, accounted for by a mechanism involving Cdc5/Cdc28 and Dbf2. Cdc28 and Cdc5 phosphorylate Net1. In the CC-CNW, Cdc28–Clb1,2 first phosphorylates Net1, and primes it for phosphorylation by Cdc5 based on Queralt *et al.* (2006). This activational order, however, is controversial, as a study by Azzam *et al.* (2004) showed contradictory results. Dbf2 is a kinase which phosphorylates Cdc14, thereby contributing to the dissociation between Cdc14 and Net1 (Mohl *et al.*, 2009). To fine tune Cdc14 activation, the kinase Dbf2 is required to phosphorylate Cdc14 and induce its dissociation from Net1. Dbf2 is activated upon correct SPB positioning, as described in Section 5.7.6.

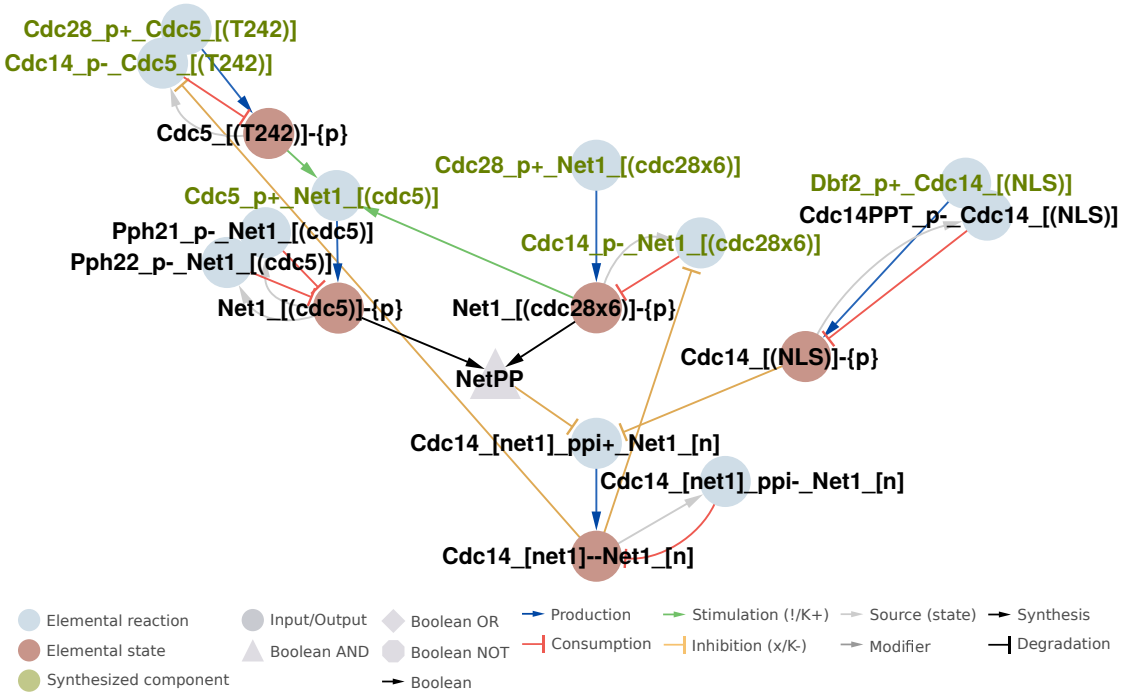

Figure 5.12. *Regulation of Cdc14.* Cdc14 is retained and kept inactive at the nucleolus, accounted for by its interaction with Net1. Relief from the nucleolus requires Net1 phosphorylation by Cdc28–Clb1,2 and Cdc5, and Cdc14 phosphorylation by Dbf2 in response to the spindle position checkpoint (SPOC, Figure 5.23).

5.5 The macroscopic cycles

The CC-CNW accounts for three individual macroscopic events: DNA replication, SPB duplication, and the formation and growth of a bud. These three macroscopic events are essential to cell cycle progression and survival of *S. cerevisiae*. The macroscopic reactions describe several states of the cell and use *Cell* as a component. The different cell states do not refer to measurable biochemical modifications, but to properties observed at a macroscopic scale. Hence, these macroscopic events cannot be described with standard elemental reactions and were implemented as new reaction types in the rxncon model base. Figure 5.13 shows the macroscopic reactions in a regulatory graph. Table 5.5 lists the reaction names and how they are expressed in rxncon language, Table A.5 lists the skeleton rules. These macroscopic reactions use inputs which collect certain elemental states and in turn, produce outputs that act upon elemental reactions. The inputs and outputs create the intersection between the macroscopic properties of the network and the regulatory, biochemical network expressed. Each macroscopic cycle starts with a neutral state (not shown) and reaches a state which is considered to be final at the end of the cell cycle. The macroscopic *Cytokinesis* reaction *Cell_CYT_Cell* collects these final states and returns their values to neutral in order to restart the cell cycle.

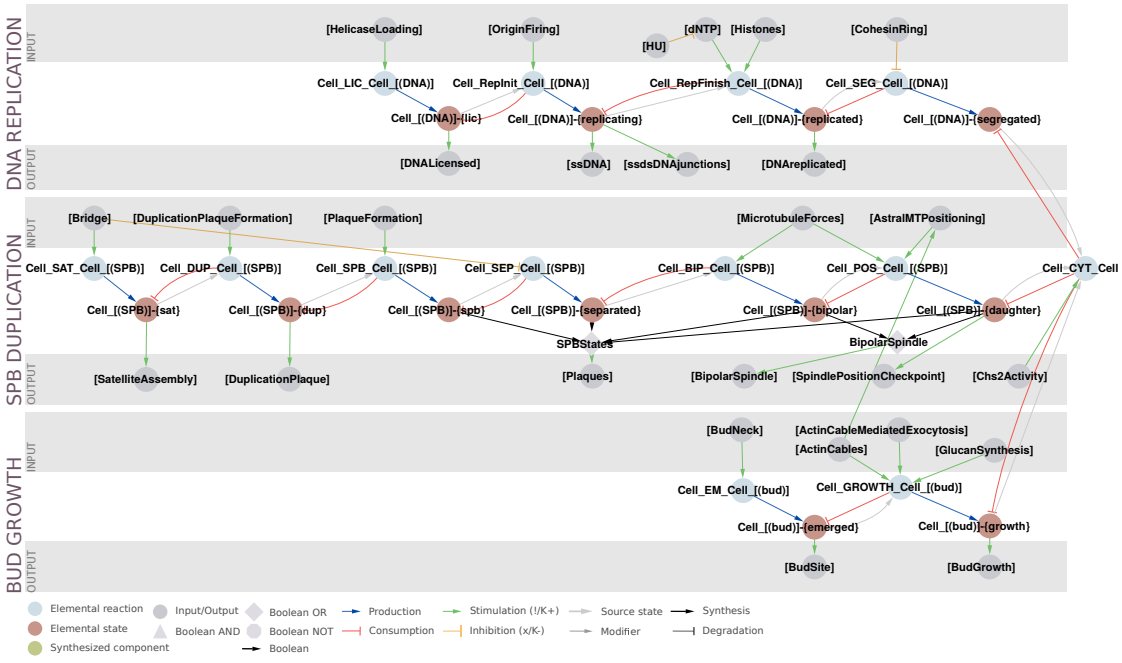

Figure 5.13. *Macroscopic reactions and states.* The three macroscopic cycles in the CC-CNW are DNA replication, SPB duplication and bud growth. Each of these cycles traverses certain macroscopic properties of the cell during the cell cycle. The macroscopic reactions do not correspond to canonical elemental reactions. To separate the two layers, the macroscopic reactions use inputs and outputs which are connected to the regulatory part of the CC-CNW.

The three macroscopic cycles describe DNA replication, SPB duplication, and bud growth. The chromosome cycle (Section 5.6) consists of four macroscopic reactions and describes DNA replication initiation, ongoing DNA replication, the finishing of DNA replication, and finally, segregation of the duplicated DNA. The SPB cycle (Section 5.7) consists of six macroscopic reactions and describes the assembly of a new SPB, starting with the formation of a bridge, which matures into a satellite, enabling the formation of duplication plaques. The SPB cycle continues with the regulation of SPB separation, its bipolar alignment, and the movement of one SPB into the daughter cell. Bud emergence and growth is described with two macroscopic reactions (Section 5.8). The first reaction describes the events of cell membrane polarization, enable bud emergence, the second reaction describes the regulation of bud growth. These three cycles are connected to the *Cytokinesis* reaction, which is required to reset cell cycle conditions to a state corresponding to G_1. These macroscopic cycles are controlled by a regulatory, biochemical network, which synchronizes the macroscopic events, accounting for the observed events during cell cycle progression.

Table 5.5. *Macroscopic reactions.* The macroscopic reactions created for the CC-CNW describe DNA replication, SPB duplication and bud growth. The *Cytokinesis* reaction returns all elemental states to their neutral values.

Reaction name	Macroscopic reaction	State(s) consumed	State(s) produced
DNA licensing	Cell_LIC_Cell_[(DNA)]	Cell_[(DNA)]-{0}	Cell_[(DNA)]-{lic}
DNA replication initiation	Cell_RepInit_Cell_[(DNA)]	Cell_[(DNA)]-{lic}	Cell_[(DNA)]-{replicating}
DNA replication termination	Cell_RepFinish_Cell_[(DNA)]	Cell_[(DNA)]-{replicating}	Cell_[(DNA)]-{replicated}
DNA segregation	Cell_SEG_Cell_[(DNA)]	Cell_[(DNA)]-{replicated}	Cell_[(DNA)]-{segregated}
SPB satellite initiation	Cell_SAT_Cell_[(SPB)]	Cell_[(SPB)]-{0}	Cell_[(SPB)]-{sat}
SPB duplication plaque initiation	Cell_DUP_Cell_[(SPB)]	Cell_[(SPB)]-{sat}	Cell_[(SPB)]-{dup}
SPB duplication	Cell_SPB_Cell_[(SPB)]	Cell_[(SPB)]-{dup}	Cell_[(SPB)]-{spb}
SPB separation initiation	Cell_SEP_Cell_[(SPB)]	Cell_[(SPB)]-{spb}	Cell_[(SPB)]-{separated}
SPB bipolar initiation	Cell_BIP_Cell_[(SPB)]	Cell_[(SPB)]-{separated}	Cell_[(SPB)]-{bipolar}
SPB daughter positioning initiation	Cell_POS_Cell_[(SPB)]	Cell_[(SPB)]-{bipolar}	Cell_[(SPB)]-{daughter}
Bud emergence initiation	Cell_EM_Cell_[(bud)]	Cell_[(bud)]-{0}	Cell_[(bud)]-{emerged}
Bud growth	Cell_GROWTH_Cell_[(bud)]	Cell_[(bud)]-{emerged}	Cell_[(bud)]-{growth}
Cytokinesis	Cell_CYT_Cell	Cell_[(DNA)]-{segregated}, Cell_[(SPB)]-{daughter}, Cell_[(bud)]-{growth}	Cell_[(DNA)]-{0}, Cell_[(SPB)]-{0}, Cell_[(bud)]-{0}

5.6 The chromosome cycle

The chromosome cycle in the CC-CNW describes the regulation of DNA replication with four macroscopic reactions. In the CC-CNW, the chromosome cycle traverses the macroscopic steps DNA licensing, DNA replication initiation, DNA replication, DNA replication termination, DNA segregation and resetting of the last state to the initial default, neutral state via the *Cytokinesis* reaction.

5.6.1 *DNA licensing*

The chromosome cycle starts with the *DNA licensing* reaction *Cell_LIC_Cell_[(DNA)]* (Figure 5.14), accounting for the licensing of DNA. The CC-CNW accounts for the recruitment of two complexes, the origin recognition complex (ORC) and the Mcm2–7 helicase complex, which are required for licensing. ORC consists of six subunits, Orc1–6, and binds to origin DNA via Orc1 (Müller *et al.*, 2010). ORC recruits the helicase Mcm2–7 to the origins via interaction between Orc1 and Cdc6, as well as Cdt1 and Cdc6 (Bell and Labib, 2016).

CDC6 and *MCM2–7* are synthesized dependent on Mcm1 cluster activation (Section 5.2). Recruitment of ORC is restricted to a time window before Cdc28–Clb5,6 becomes active, accounted for by the phosphorylation of Orc2 and Orc6 by Cdc28–Clb5,6, inhibiting ORC recruitment to the origins (Nguyen *et al.*, 2001). Relicensing is additionally inhibited by Cdc28–Clb1,2 phosphorylation of Mcm3, inhibiting nuclear localization of the Mcm2–7 complex (Liku *et al.*, 2005). Binding between Cdt1 and Orc6 is the crucial step to link the Mcm2–7 complex to the ORC complex, resulting in helicase loading at the origins. The CC-CNW accounts for regulation of helicase recruitment, but not explicitly for helicase dimerization (Evrin *et al.*, 2013). Instead, it is assumed that dimerization occurs upon recruitment of the Mcm2–7 complex. Successful loading of the helicase to the origins is implemented as output *[HelicaseLoading]*, which is a requirement for the *Cell_LIC_Cell_[(DNA)]* reaction to execute. This reaction produces the *Cell_[(DNA)]-{lic}* state, representing licensed DNA.

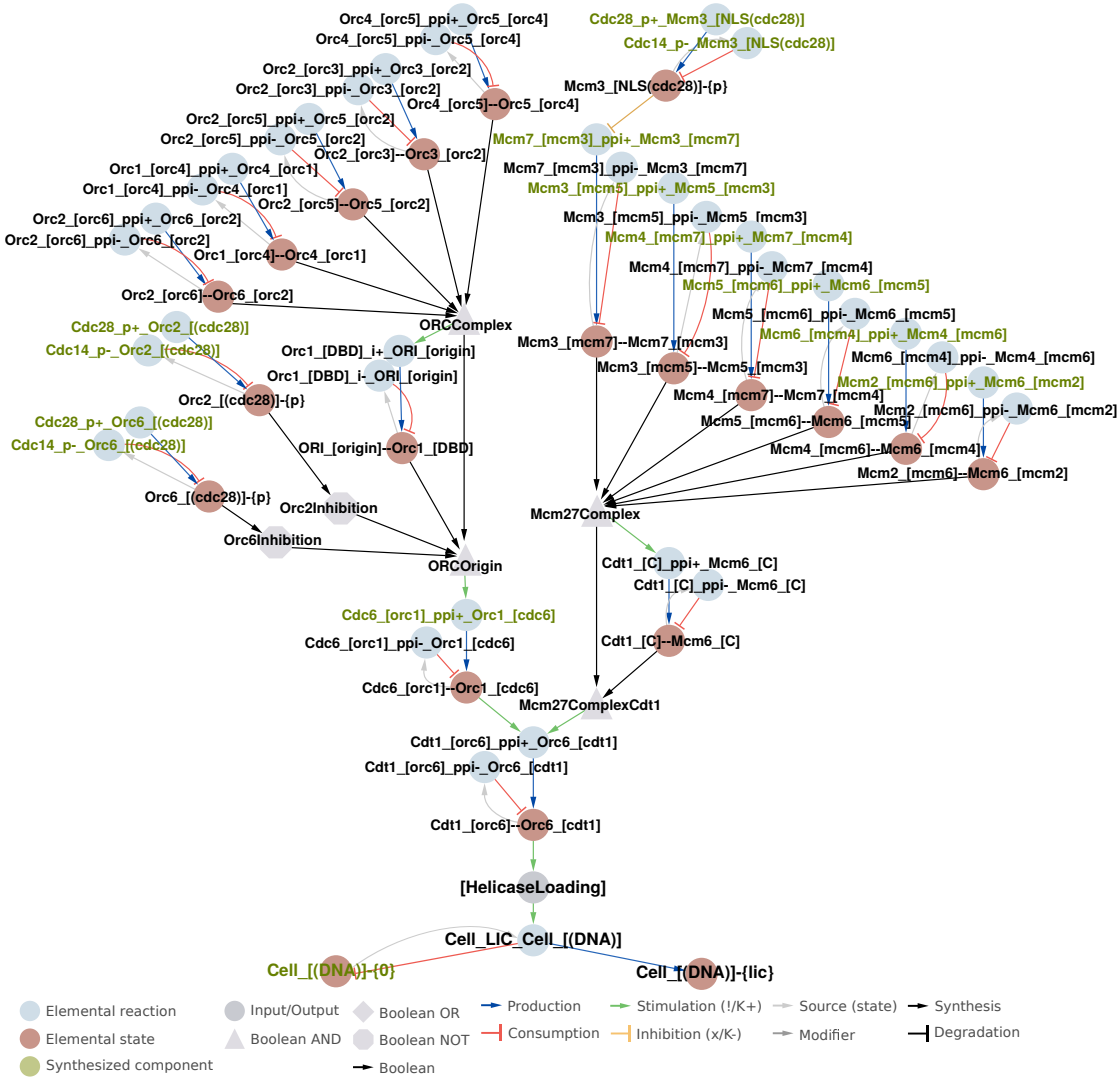

Figure 5.14. *DNA licensing.* DNA licensing requires the recruitment of the ORC complex and the Mcm2–7 complex. Licensing is restricted to a time window before Cdc28–Clb5,6 becomes active, as phosphorylation of Orc2,6 and Mcm3 prevents licensing. Cdc28–Clb1,2 prevents licensing by phosphorylating Mcm3.

5.6.2 *DNA replication initiation*

DNA licensing is followed by the macroscopic *DNA replication initiation* reaction *Cell_RepInit_Cell_[(DNA)]* (Figure 5.15), collecting the prerequisites for origin firing. In this step, several factors are recruited to the licensed origins. Cdc45 and Sld3 are recruited to the Mcm2–7 complex via Mcm4 and Mcm6, resulting in the complex named *MCMCdc45Sld3* in the CC-CNW. This recruitment strictly depends on phosphorylation of Mcm4 and Mcm6 by the Dbf4-dependent kinase (DDK) Cdc7 (Bell and Labib, 2016). DDK activity has no regulation in the CC-CNW. Both subunits are furthermore always present in the CC-CNW. To ensure timely DDK activity, the output *[DNAlicensed]*, an indicator of the state *Cell_[(DNA)]-{lic}*, is additionally required. This is a model hypothesis. Dbf4 is permanently present in the CC-CNW, as it is the output of the unregulated *DBF4* gene. A possible cell cycle regulated transcription pattern of *DBF4*, which may contribute to DDK activity regulation, is disputed (Spellman *et al.*, 1998). DDK substrates, however, may require priming by other kinases (Bell and Labib, 2016). Assembly of the complex *MCMCdc45Sld3* is required for recruitment of Dpb11, Pol2, Psf1 and Sld2 to form the Cdc45/Mcm2–7/GINS (CMG) complex, combined in the *CMG* node. Pol2 is the catalytic subunit of DNA polymerase II. CMG assembly is further regulated by Cdc28–Clb5,6-mediated phosphorylation of Sld2 and Sld3 (Loog and Morgan, 2005; Enserink and Kolodner, 2010), allowing their binding to Dpb11 (Yeeles *et al.*, 2015; Bell and Labib, 2016). Origin firing also requires Mcm10 (Rüthnick and Schiebel, 2016; Lõoke *et al.*, 2017). Mcm10 stimulates helicase activity, however, this is not explicitly accounted for in the CC-CNW, as helicase activity cannot be expressed in rxncon language. Instead, the CC-CNW accounts for Mcm10 indirectly by making its recruitment via Mcm2 a requirement for origin firing. Upon recruitment of all necessary factors and formation of the CMG complex, origin firing starts, implemented as the output node *[OriginFiring]* as a requirement for the reaction *Cell_RepInit_Cell_[(DNA)]*. The reaction produces the *Cell_[(DNA)]-{replicating}* state, which represents ongoing DNA replication.

Explicit DNA replication cannot be described in rxncon language in a feasible way, as this would require one elemental reaction for the addition of each base and corresponding contingencies. Instead, in the CC-CNW, the control of DNA replication is explicitly described, and DNA replication itself is indirectly accounted for by the recruitment of Pol2 to the CMG complex in the context of origin firing. The CC-CNW does not discriminate between the leading and lagging DNA strands.

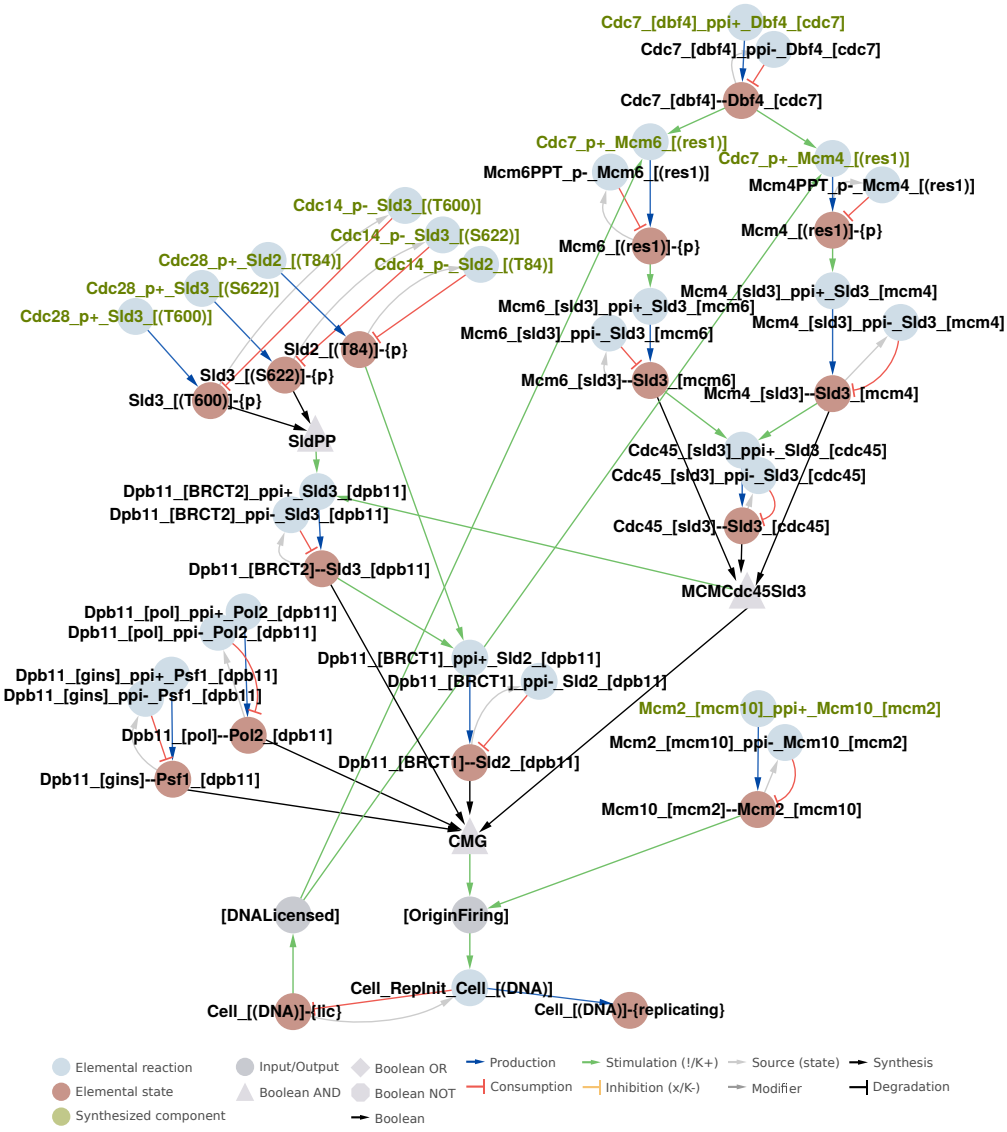

Figure 5.15. *DNA replication initiation.* Licensed DNA initiates the recruitment of Cdc45, Sld3, Dpb11, Pol2 and Psf1. This recruitment is further regulated by Cdc28- and Cdc7-mediated phosphorylation. The recruitment of these factors leads to the establishment of the CMG complex, and in addition with Mcm1 initiates origin firing.

5.6.3 *DNA replication termination*

The *Cell_[(DNA)]-{replicating}* state initiates the next steps, activation of the DNA replication checkpoint and termination of DNA replication (Figure 5.16). Ongoing DNA replication creates replication forks, which are characterized by single-stranded/double-stranded (ss/ds) DNA junctions, implemented in the CC-CNW with the node *[ssdsDNAjunctions]*. In addition, ssDNA occurs during DNA replication, accounted for with the node *[ssDNA]*. These two nodes are implemented to distinguish between processes at the replication forks and ssDNA. The junctions together with ssDNA only occur

during DNA replication and are thus an indicator of ongoing DNA replication.

The proteins Rfa1-3 form the replication protein A (RPA) complex (Iftode *et al.*, 1999), represented as *RPA*. The complex is recruited to ssDNA via Rfa1 and Rfa2, a hypothesis based on Iftode *et al.* (1999). To express the dependence on RPA recruitment to ssDNA, the interaction between Rfa1,2 and ssDNA additionally requires the *[ssDNA]* node. RPA recruited to ssDNA, combined in the *RPAssDNA* node, together with recruitment of the DNA replication checkpoint proteins Lcd1–Mec1 (Wakayama *et al.*, 2001) to Rfa1 (a hypothesis based on Rouse and Jackson (2002)), forms the complex *RPAssDNALcd1Mec*.

The replication forks recruit several replication factors, represented as the complex *DNARFCCtf18Pol2Mrc1*. The replication factor C (RFC) complex is simplified in the CC-CNW to a single component (RFC) and binds to ssDNA. RFC recruits Ctf18 and Pol2, the catalytic subunit of DNA polymerase II. The assembly of this complex together with *RPAssDNALcd1Mec1* is hypothesized to be required for the interaction between Mec1 and Mrc1 based on García-Rodríguez *et al.* (2015) and Hegnauer *et al.* (2012). This interaction activates a phosphorylation cascade which monitors ongoing DNA replication and resembles the DNA replication checkpoint. First, Mec1 phosphorylates Mrc1 (Pardo *et al.*, 2017; Chen and Zhou, 2009). Phosphorylated Mrc1 binds to Rad53 (Chen and Zhou, 2009). The complex between Mec1, Mrc1 and Rad53, combined in the node *Mec1Mrc1Rad53* is the prerequisite for Mec1 phosphorylation of Rad53 (Chen and Zhou, 2009). This phosphorylation by Mec1 activates Rad53, which in turn signals ongoing DNA replication by phosphorylating its substrates. Thus, the CC-CNW accounts for Rad53 activity in the context of ongoing DNA replication. Rad53 phosphorylates and inhibits the MBF repressor Nrm1 (Travesa *et al.*, 2012), maintaining MBF regulated transcription until DNA replication has finished. Simultaneously, Rad53 phosphorylates Ndd1, inhibiting activation of the genes regulated by Ndd1, Fkh2 and Mcm1. These phosphorylations are hypothesized to occur in the context of activated Rad53 (Chen *et al.*, 2007b). Furthermore, activated Rad53 phosphorylates Dun1 (Chen *et al.*, 2007b), which in turn phosphorylates Sml1 (Chen and Zhou, 2009; Pardo *et al.*, 2017). Phosphorylated Sml1 dissociates from the reductase Rnr1, thereby allowing Rnr1 activity, which is required for synthesis of deoxynucleoside triphosphate (dNTP), represented by the output node *[dNTP]*. DNA replication also requires histones. The CC-CNW does not explicitly account for histones and uses instead *[Histones]* as input for the *DNA replication termination* reaction *Cell_RepFinish_Cell_[(DNA)]*. This produces the state *Cell_[(DNA)]-{replicated}*, which represents completed DNA replication. Simultaneously, the *Cell_[(DNA)]-{replicating}* state disappears and along with it, the indicators of ongoing DNA replication. This deactivates the DNA replication pathway in the CC-CNW, and leads to the inactivation of MBF regulated transcription, and to the activation of transcription of the genes regulated by Fkh2Ndd1Mcm1. Furthermore, the *Cell_[(DNA)]-{replicated}* state activates the output *[DNAreplicated]*, which is used as an input for kinetochore attachment (Section 5.7). The CC-CNW accounts for the effects of HU, by inhibiting dNTP synthesis, thereby arresting cell cycle progression.

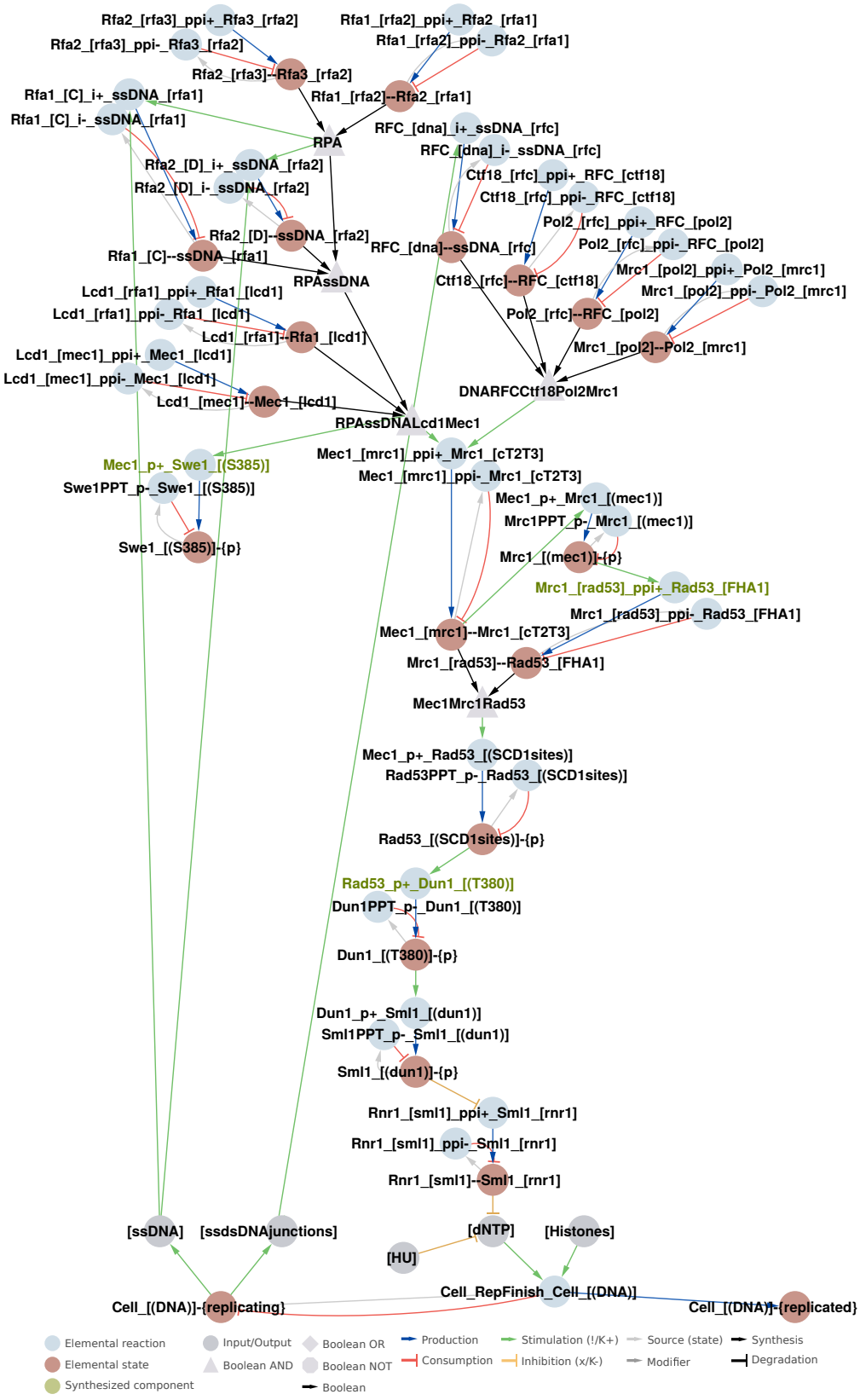

Figure 5.16. *DNA replication.* Ongoing DNA replication creates replication forks. Replication checkpoint proteins are recruited to these replication forks, leading to the activation of the kinase Rad53. The checkpoint is active until DNA replication has finished.

5.6.4 *DNA separation*

The two sister chromatids retrieved after termination of DNA replication are held together by cohesin rings. In anaphase, these cohesin rings must be destroyed to allow separation of the sister chromatids (Figure 5.17). Correct chromosome separation and segregation is a prerequisite for chromosome stability. Hence, DNA separation must be performed in the correct cell cycle phase to ensure survival of the cell. The CC-CNW does not explicitly account for chromatids. Instead, the CC-CNW describes the regulation of the cohesin rings. Their assembly and destruction implies sister chromatid attachment and separation. The CC-CNW accounts for cohesin ring assembly with two steps. First, in an initial cohesin loading step, combined in the *CohesinLoading* node, the cohesin ring subunits Scc1, Scc2, Scc4 are recruited. These associate with each other and bind to centromeric regions of the DNA via Scc4 (Marston, 2014). Second, the subunits Irr1, Smc1 and Smc3 are recruited, forming the complete ring, combined in the node *[CohesinRing]*. *SCC1* is regulated by MBF (Section 5.2). Desintegration of the cohesin ring requires truncation of the Scc1 subunit. Scc1 truncation is performed by the separase Esp1. Both Scc1 and Esp1 are regulated in order to accomplish timely cohesin ring destruction. The CC-CNW accounts for the regulation of Scc1 truncation in the following way: Pds1 binds and inhibits Esp1 (Ciosk *et al.*, 1998; Uhlmann *et al.*, 1999). This inhibition is antagonized by APC/C-mediated degradation of Pds1 (Section 5.3). *PDS1* is MBF regulated and the protein Pds1 becomes phosphorylated by Cdc28–Cln1,2,3 in G_1 phase, which protects it from degradation. Upon activation of Cdc14, Pds1 is dephosphorylated and can be degraded. Scc1 must furthermore be phosphorylated by Cdc5 (Alexandru *et al.*, 2001), which is hypothesized to require active Cdc5 (Rodriguez-Rodriguez *et al.*, 2016). These processes are restricted to a time window with Cdc14 activity, during which it is assured that DNA replication has finished and the bipolar spindle is correctly aligned (Section 5.7). Phosphorylated Scc1 and active Esp1 are the requirements as accounted for in the CC-CNW for Scc1 truncation by Esp1. Truncated Scc1 destroys the *[CohesinRing]*. This allows the *DNA segregation* reaction *Cell_SEG_Cell_[(DNA)]* to execute, producing the *Cell_[(DNA)]-{segregated}* state. The segregation reaction is the last macroscopic reaction in the chromosome cycle. The *Cell_[(DNA)]-{segregated}* state is one of three macroscopic states required for the execution of cytokinesis.

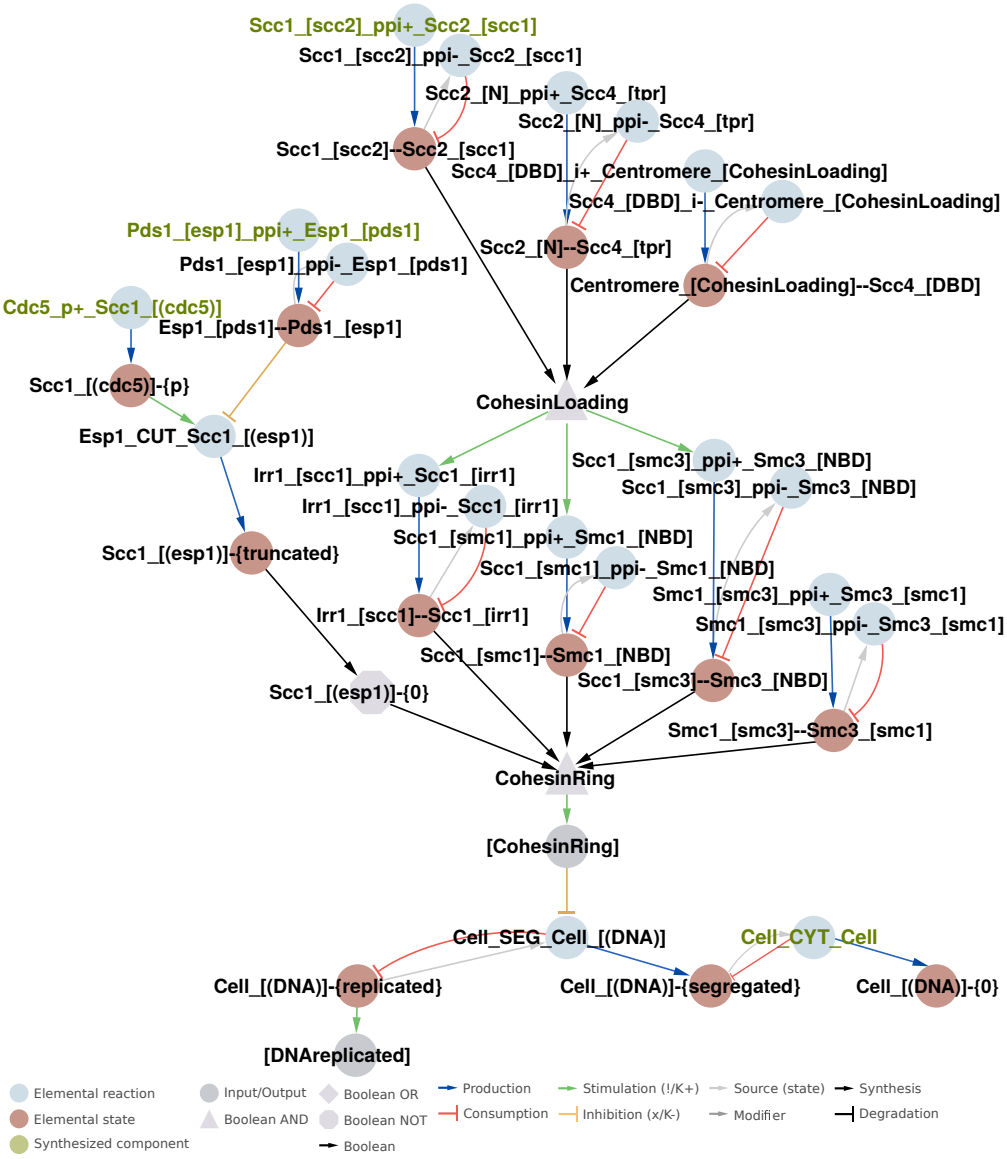

Figure 5.17. *DNA segregation.* DNA segregation requires the disassembly of the cohesin ring. This is regulated by activation of Esp1, which truncates the cohesin ring subunit Scc1, leading to the disintegration of the cohesin ring.

5.7 Spindle pole body duplication

The CC-CNW accounts for SPB duplication, separation, bipolar alignment, chromosome attachment and movement of one SPB attached to one set of chromosomes into the daughter cell with six macroscopic reactions. These reactions represent the formation of the SPB bridge, satellite, duplication plaque, assembly and maturation of a complete second SPB, separation of the two SPBs, their bipolar alignment and finally, the movement of one SPB into the daughter cell. The last state is then reset to the initial default, neutral state of the SPB duplication cycle via the *Cytokinesis* reaction.

It is assumed that these macroscopic reactions are carried out at the inherited SPB in the mother cell. Hence, the existence of the inherited SPB is implied, and here, only the reactions required to duplicate the SPB are considered. From the two SPBs, microtubules emanate and attach to the kinetochores connected to sister chromatids. Upon correct attachment, the two chromosome sets are partitioned: One chromosome set remains in the mother cell, one chromosome set is moved to the daughter cell. The movement of one chromosome set into the daughter cell activates the *spindle position checkpoint*, which ultimately leads to the activation of the chitinase Chs2 required to separate the two yeast cells at the end of the cell cycle. The CC-CNW accounts for the spindle position checkpoint machinery towards the end of the SPB duplication process.

5.7.1 *Bridge formation*

The SPB duplication cycle starts with the transformation of the half-bridge at the inherited SPB into a bridge, priming it for satellite formation (Figure 5.18). The *SPB satellite initiation* reaction *Cell_SAT_Cell_[(SPB)]* in the SPB duplication cycle refers to the formation of a bridge at the inherited SPB, priming it for satellite formation by producing the *Cell_[(SPB)]-{sat}* state. In this first step, the half-bridge at the inherited SPB, formed by an Sfi1 molecule with a free C-terminal, transforms into a full bridge by recruiting a second Sfi1 molecule. The second Sfi1 molecule binds with its C-terminal to the C-terminal of the Sfi1 attached to the mother SPB, thereby forming the bridge (Rüthnick and Schiebel, 2016). This dimerization is regulated such that SPB duplication can only occur once per cell cycle. The CC-CNW accounts for regulation of Sfi1 dimerization via phosphorylation of Sfi1 by Cdc5 and Cdc28–Cln1,2,3. Cdc5 phosphorylation on one of three sites inhibits Sfi1 dimerization (Elserafy *et al.*, 2014), combined in the *Cdc5Phosphorylation* node. Cdc5 is hypothesized to attain kinase activity by Cdc28–Clb1,2-mediated phosphorylation on residue T242, based on Rodriguez-Rodriguez *et al.* (2016). Additionally, six Cdc28 sites in Sfi1 have been identified to contribute to the inhibition of Sfi1 dimerization upon phosphorylation (Elserafy *et al.*, 2014), combined in the *Cdc28Phosphorylation* node. The kinase Mps1 is also involved in regulation of Sfi1 dimerization (Elserafy *et al.*, 2014). However, its role in bridge formation and its regulation on a mechanistic level is not yet established. Hence, Mps1 is omitted here. Along with Sfi1 recruitment, the additional components Cdc31 and Kar1 associate with the bridge (Rüthnick and Schiebel, 2016). The Sfi1

dimer, together with Cdc31 and Kar1, constitutes the bridge, combined in the node *[BridgeComponents]*, forming the prerequisite for the *Cell_SAT_Cell_[(SPB)]* reaction to execute. This reaction produces the *Cell_[(SPB)]-{sat}* state, which represents the SPB primed for satellite formation.

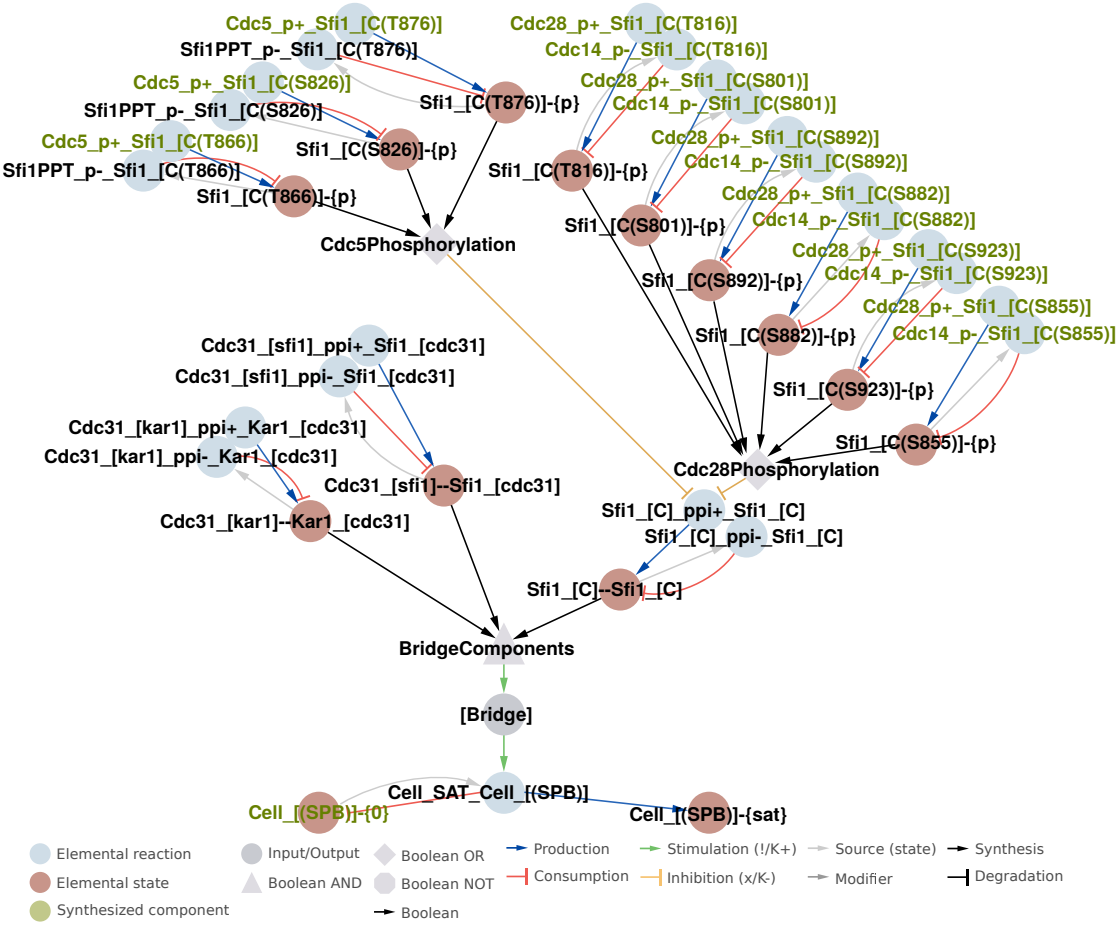

Figure 5.18. *SPB bridge formation.* The inherited SPB contains an Sfi1 molecule with a free C-terminal, serving as a template for bridge formation. Bridge formation involves binding of a second Sfi1 as well as recruitment of the additional bridge components Cdc31 and Kar1. Bridge formation can only occur during a window of low Cdc28 and Cdc5 activity, ensuring that SPB duplication can only be initiated once in each cell cycle. Bridge assembly primes the SPB to initiate satellite formation.

5.7.2 *SPB satellite and duplication plaque*

Assembly of the second SPB continues with the formation of a satellite and duplication plaque (Figure 5.19), requiring the *Cell_[(SPB)]-{sat}* state from the previous step. The *SPB duplication plaque formation* reaction *Cell_DUP_Cell_[(SPB)]* describes the formation of a satellite and duplication plaque, resulting in the production of the *Cell_[(SPB)]-{dup}* state, which is required for the formation of the inner and outer plaques in the next step. The transition from satellite to duplication plaque has no

empirically identified regulatory mechanism. Hence, these processes are captured in one macroscopic reaction.

The satellite forms at the bridge by recruiting Spc42 to the free N-terminal of Sfi1 (Rüthnick and Schiebel, 2016). The CC-CNW accounts for the regulation of this interaction with the strict requirement of Cdc28–Cln1,2,3 and Mps1 mediated phosphorylation of Spc42. The contribution of these phosphorylations is not entirely clear. In the CC-CNW it is hypothesized, that either of the Cdc28-mediated phosphorylations, combined in the node *Spc42Cdc28Phosphorylation*, or Mps1-mediated phosphorylation is sufficient to induce the interaction between Sfi1 and Spc42, combined in the *Spc42Phosphorylation* node, based on Jaspersen *et al.* (2004). Additionally, it is assumed that this interaction takes place after formation of the bridge. This is accounted for by the requirement of the *[SatelliteAssembly]* state, representing the bridge primed for satellite formation. Spc42 forms the central plaque in the daughter SPB by recruiting other Spc42 molecules to form a crystalline structure (Bullitt *et al.*, 1997). The crystallization process is difficult to express in rxncon language, as it would require one elemental reaction for each Spc42 interaction, and additionally, knowledge about the crystal topology. The CC-CNW accounts for this process implicitly with the Spc42 dimerization reaction, which also implies the formation and growth of the satellite. The CC-CNW accounts for transcriptional regulation of *SPC42* by MBF and turnover of Spc42 by degradation (Figure 5.4). The degradational reaction, however, is unregulated and hence, Spc42 stability depends on maintenance of *SPC42* transcription. From this follows that Spc42 is degraded as soon as the MBF cluster becomes inactive. In the context of SPB duplication, degradation of Spc42 would force the disassembly of the SPBs, which is not observed. Hence, in the CC-CNW it is hypothesized that crystallized Spc42 is protected from degradation, based on Bullitt *et al.* (1997). This is implemented by the node *Spc42Crystal*, which requires either of the nodes *[DuplicationPlaqueFormation]* (shown), *[DuplicationPlaque]*, *[PlaqueFormation]*, or *[Plaques]*. *[DuplicationPlaque]* is an output created by the state *Cell_[(SPB)]-{dup}*. *[PlaqueFormation]* is an output and depends on the formation of the inner and outer plaques as described in Section 5.7.3. *[Plaques]* monitors the four states of the SPB cycle in which complete plaques have formed, *Cell_[(SPB)]-{spb}*, *Cell_[(SPB)]-{separated}*, *Cell_[(SPB)]-{bipolar}*, and *Cell_[(SPB)]-{daughter}*. Together, these states indicate the states of the SPB at which Spc42 has acquired a crystalline structure. The *Spc42Crystal* node in turn, inhibits Spc42 degradation. The satellite recruits Cnm67 and Nud1 (Fu *et al.*, 2015), thereby expanding the satellite into the duplication plaque, combined in the node *DuplicationPlaque*. The implemented hierarchy of the recruitment of duplication plaque components is hypothesized and based on Fu *et al.* (2015). Along with duplication plaque formation, the growing second SPB is embedded into the nuclear envelope. This process, however, is not expressed explicitly in the CC-CNW. The *DuplicationPlaque* node is a prerequisite for the node *[DuplicationPlaque-Formation]*, required for the *Cell_DUP_Cell_[(SPB)]* reaction to execute, producing the state *Cell_[(SPB)]-{dup}*. This state represents the SPB with a duplication plaque, ready

to mature into a complete SPB. Both SPBs are still connected to each other via the bridge and rest next to each other in the nuclear envelope.

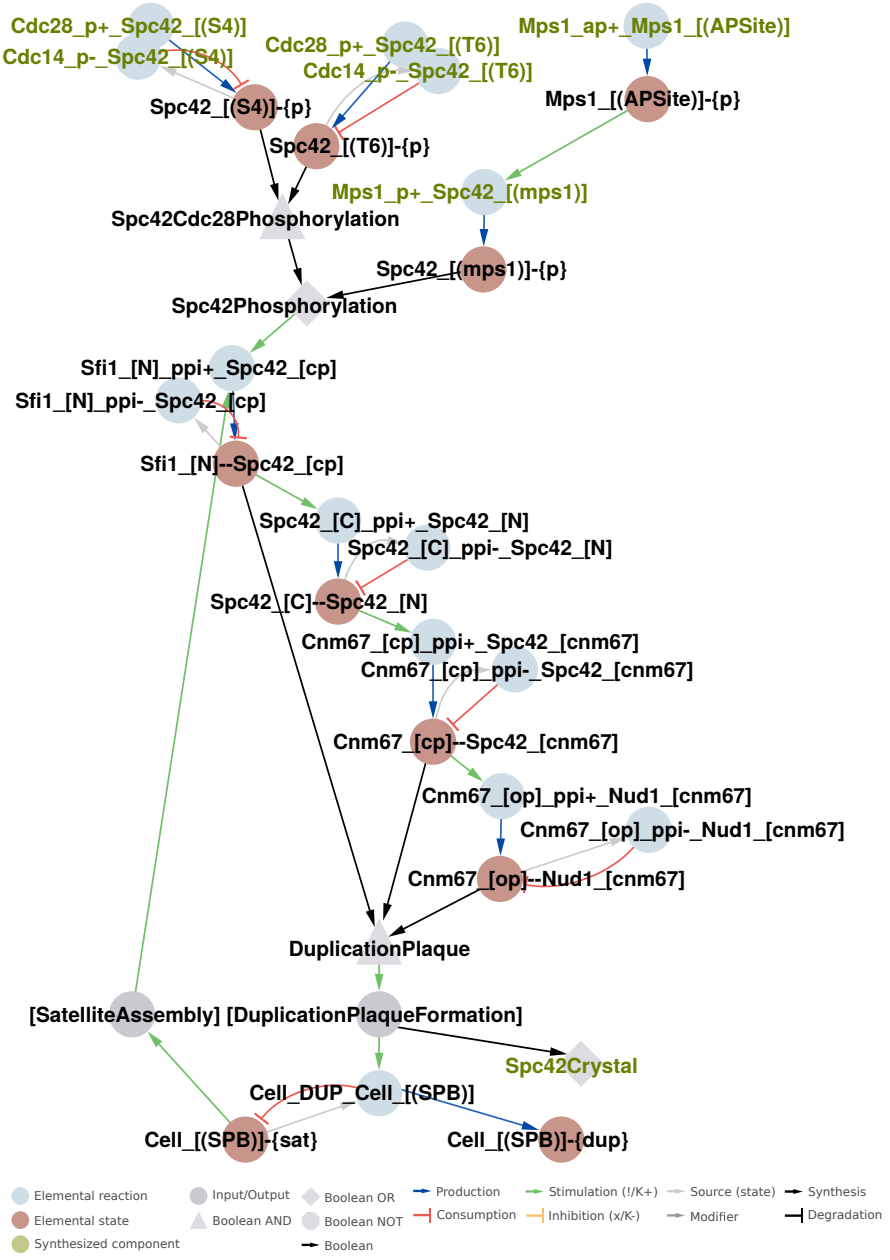

Figure 5.19. *SPB satellite formation.* The dimerized Sfi1 with a free N-terminal recruits Spc42. Spc42 forms a crystalline structure, here simplified with the Spc42 dimerization reaction between the C- and N-termini of two Spc42 molecules. The dimerization of Spc42 represents the crystallization process leading to the formation of a duplication plaque which requires the recruitment of Cnm67 and Nud1. Satellite formation is regulated via Cdc28–Cln1,2,3- and Mps1-mediated phosphorylation.

5.7.3 *SPB maturation and separation*

The next two steps (Figure 5.20) describe completion of the formation of the second SPB and the separation of the two SPBs. First, the duplication plaque matures into a complete SPB, represented by the *SPB duplication* reaction *Cell_SPB_Cell_[(SPB)]*, producing the state *Cell_[(SPB)]-{spb}*. This state represents the mother SPB and the newly formed daughter SPB together, still connected to each other via the bridge. Second, for spindle alignment, the two SPBs must be separated, represented by the *SPB separation initiation* reaction *Cell_SEP_Cell_[(SPB)]*, producing the *Cell_[(SPB)]-{separated}* state. The CC-CNW accounts for the regulation of these two reactions.

The *Cell_[(SPB)]-{dup}* state from the previous reaction produces the node *[DuplicationPlaque]*, implying the existence of a duplication plaque structure. This structure serves as a platform for the recruitment of the proteins forming the inner and outer plaques of the SPB. The CC-CNW accounts for recruitment of the outer plaque component Spc72 via Nud1 (Winey and Bloom, 2012; Fu *et al.*, 2015), combined in the node *OuterPlaque*. The CC-CNW accounts for recruitment of the inner plaque components Spc29, Cmd1 and Spc110 via Spc42 (Winey and Bloom, 2012; Fu *et al.*, 2015), combined in the node *InnerPlaque*. Additionally, both the inner and outer plaques serve as a docking platform for the recruitment of the γ–tubulin complex, consisting of Spc97, Spc98 and Tub4 (Winey and Bloom, 2012). The γ–tubulin complex binds to the receptor proteins Spc72 at the outer plaque and Spc110 at the inner plaque (Erlemann *et al.*, 2012; Winey and Bloom, 2012). This complex serves as the platform for microtubule polymerization and is combined in the node *γTubulinSmallComplex*. Recruitment of the γ–tubulin complex to Spc110 is regulated by phosphorylation. It was demonstrated that Cdc28–Cln1,2,3 phosphorylation of Spc110 is important for its ability to recruit and activate the γ–tubulin complex (Lin *et al.*, 2014), accounted for with the positive influence of the *Spc110Phos* node on Spc98 and Spc110 association.

Upon successful formation of the inner and outer plaques, combined in the node *[PlaqueFormation]*, the *Cell_SPB_Cell_[(SPB)]* reaction can execute, producing the state *Cell_[(SPB)]-{spb}*. This state represents the two SPBs, which are still connected to each other via the bridge.

The reaction *Cell_SEP_Cell_[(SPB)]* represents the detachment of the two SPBs and depends on the destruction of the bridge, regulated by Cdc28- and Cdc5-mediated phosphorylation of Sfi1 (Jaspersen *et al.*, 2004). Severing of the bridge is not deciphered. As discussed by Winey and Bloom (2012), there are indications that dissociation is mediated by Cdc28 and Cdc5, which is also the hypothesis in the CC-CNW. Additionally, pulling forces exerted by microtubules seem to contribute to SPB separation. However, according to Winey and Bloom (2012), the two SPBs can separate without the involvement of microtubules. Upon maturation of the second SPB and destruction of the bridge, the two SPBs separate, but remain in proximity to each other, represented by the *Cell_[(SPB)]-{separated}* state. Formation of the inner, central and outer plaques is regulated. Due to this regulation, the reactions creating these structures may be become

inactive, which would imply the disassembly of the plaques. It is assumed in the CC-CNW that, upon formation of the second SPB, the inner, central and outer plaques are stable structures. To account for this, at least one of the four macroscopic states of the SPB *Cell_[(SPB)]-{spb}*, *Cell_[(SPB)]-{separated}*, *Cell_[(SPB)]-{bipolar}*, *Cell_[(SPB)]-{daughter}*, which imply the existence of a mature second SPB, is required to maintain the *SPBstates* node. This node in turn is required for the output node *[Plaques]*, which is used as an indicator of completed SPB duplication.

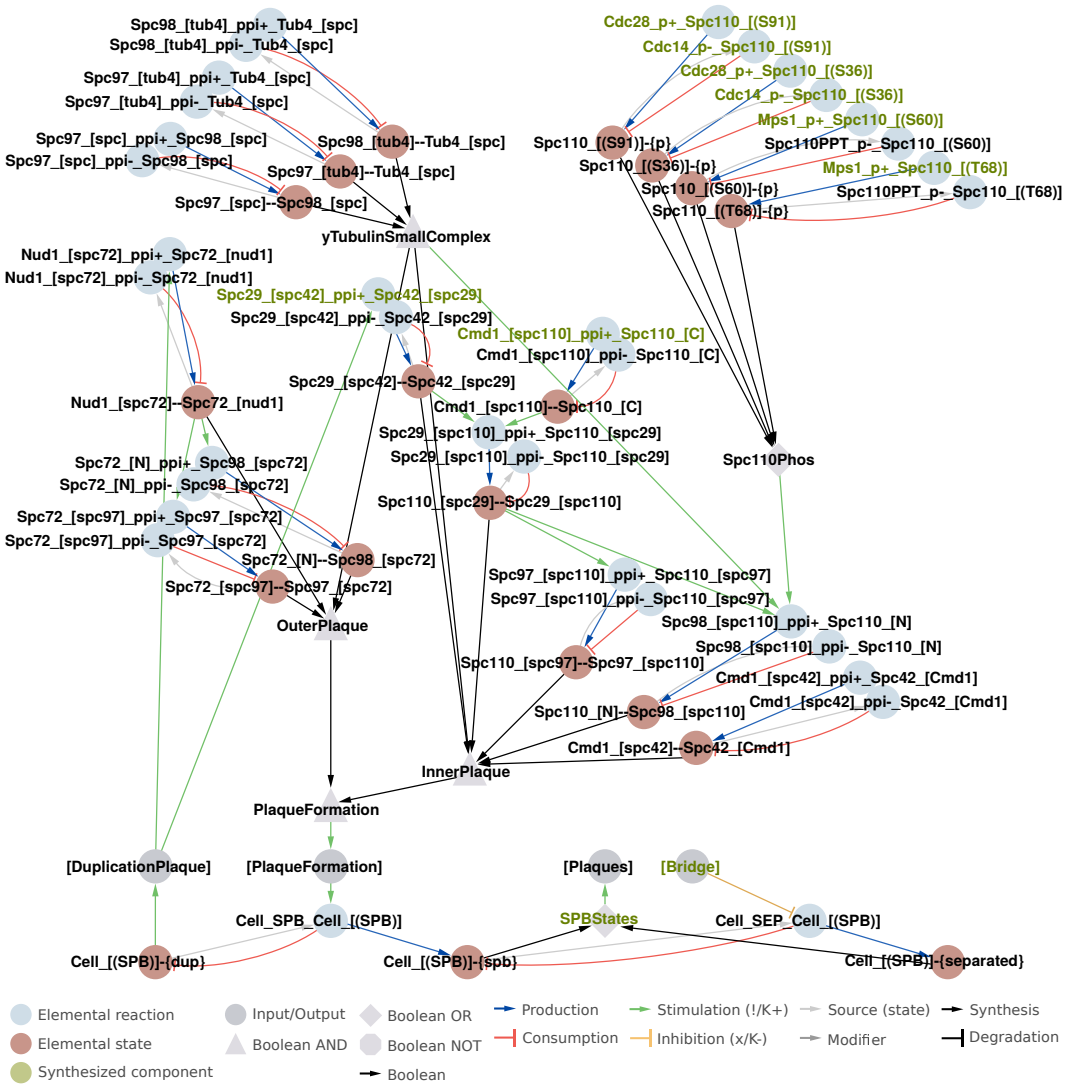

Figure 5.20. *Maturation of second SPB and separation.* During duplication plaque formation, proteins are recruited to the central plaque, forming the outer and inner plaques. Simultaneously, the growing second SPB is inserted into the nuclear pore and maturates. The two SPBs are connected to each other via the bridge until Cdc28 activity alleviates dissociation. After the destruction of the bridge, the two SPBs remain in proximity to each other.

5.7.4 *Bipolar alignment*

In the next step (Figure 5.21), the two SPBs must be separated and pushed away from each other for spindle elongation. Initially, this is accomplished by microtubules and kinesin motor proteins acting on the *SPB bipolar initiation* reaction *Cell_BIP_Cell_[(SPB)]*, producing the *Cell_[(SPB)]-{bipolar}* state. This state represents the two SPBs positioned at opposite poles of the nucleus. The SPBs are then pushed and pulled farther away from each other, described by the *SPB daughter positioning initiation* reaction *Cell_POS_Cell_[(SPB)]*. This reaction produces the state *Cell_[(SPB)]-{daughter}*. Either of the states *Cell_[(SPB)]-{bipolar}* and *Cell_[(SPB)]-{daughter}* represents the state of the cell which allows movement of one chromosome set to the daughter cell. This is combined in the node *BipolarSpindle* and explained in Figure 5.22.

Bipolar SPB alignment involves microtubules and kinesin motor proteins. The CCCNW distinguishes between microtubules emanating from the outer plaques of the SPBs, forming astral microtubules, and microtubules emanating from the inner plaques of the SPBs, the nuclear microtubules. This distinction allows to discriminate between the functions which the different microtubules are involved in. From the γ–tubulin complexes attached to the inner and outer plaques, tubulin dimers consisting of either Tub1–Tub2 or Tub2–Tub3, combined in the node *TubulinDimer*, bind to Tub4 and start to polymerize. Polymerization itself cannot be expressed in rxncon language in a meaningful way. Instead, the association between the tubulin dimers and the γ–tubulin complex represents microtubule polymerization. Furthermore, tubulin polymerization is a highly dynamic process with polymerization and depolymerization occurring frequently. The rxncon language cannot capture these dynamics in a meaningful way. Nuclear microtubules emanating from the inner plaques are combined in the node *NuclearMTpolymerization*. Nuclear microtubules emanating from the two opposite SPBs interacting with each other are called interpolar microtubules. They form an antiparallel overlap called midzone (Scholey *et al.*, 2016). The protein Ase1 crosslinks these interpolar microtubules, accounted for by the binding of Ase1 dimers to Tub1 (Schuyler *et al.*, 2003), forming the node *CrosslinkedInterpolarMT* in the model. Cdc28–Clb1,2 phosphorylates Tub4 (Keck *et al.*, 2011). This phosphorylation has a negative influence on the formation of interpolar microtubules (Nazarova *et al.*, 2013), and is also accounted for as a prerequisite for the Boolean node *CrosslinkedInterpolarMT*. The formation of interpolar microtubules and their continuing polarization is one force pushing the two SPBs away from each other. In addition to this mechanism, the kinesin motor proteins Cin8 and Kip1 bind to the midzone (Hildebrandt *et al.*, 2006; Scholey *et al.*, 2016), combined in the nodes *Cin8Tetramer* and *Kip1Motor*. These two nodes together represent the kinesin motors acting at the midzone, combined in the node *KinesinMotors*. They can actively push the two SPBs away from each other. The contribution from each of these mechanisms is not clear (Scholey *et al.*, 2016). In the CCCNW, the node *InterpolarMTSlidingApart* requires both forces in order to mediate bipolar alignment Scholey *et al.* (2016). This node creates the output *[MicrotubuleForces]*, which is

the prerequisite for the *SPB daughter positioning initiation* reaction *Cell_BIP_Cell_[(SPB)]* to execute. The CC-CNW reaches the *Cell_[(SPB)]-{bipolar}* state.

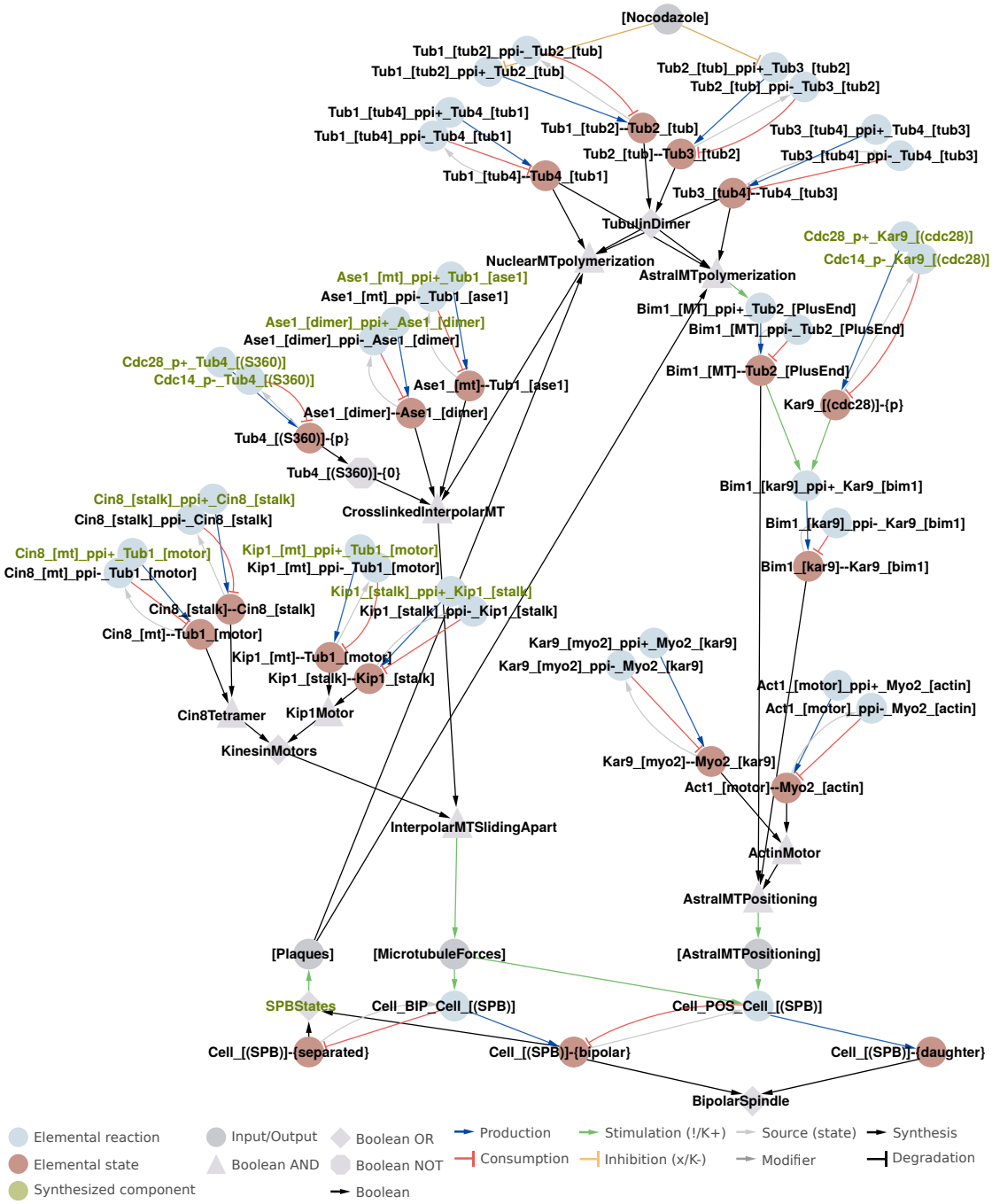

Figure 5.21. *Bipolar SPB alignment.* After their separation, the two SPBs are pushed away from each other, accomplished by interpolar microtubules and astral microtubules.

The two SPBs continue their separation and spindle elongation with one SPB being pushed or pulled towards the daughter. In addition to nuclear microtubules, the astral microtubules contribute to this process. They emanate from the outer plaques, captured in the node *AstralMTpolymerization*. The astral microtubules attach to the cell cortex via Bim1 and Kar9, where Bim1 binds to the plus ends of the microtubules (Markus *et al.*, 2012), and also recruits Kar9 (Enserink and Kolodner, 2010). This interaction requires phosphorylation of Kar9 by Cdc28–Clb5,6 (Moore and Miller, 2007). Kar9 in turn binds to Myo2, which is connected to actin cables via Act1 (Yin *et al.*, 2000; Liu *et al.*, 2010), combined in the *ActinMotor* node. The interaction between actin cables and cell cortex localized proteins is omitted. Astral microtubules connected to Bim1 and the actin cables constitute the microtubules connecting the SPBs to the cell cortex, combined in the nodes *AstralMTPositioning* and *[AstralMTPositioning]*. The astral and interpolar nuclear microtubules contribute to spindle elongation. These are the necessary prerequisites for the *Cell_POS_Cell_[(SPB)]* reaction to execute, producing the *Cell_[(SPB)]-{daughter}* state. It is important to note that this state signals that chromosome attachment to the SPBs can be initiated, which is described in the next step (Figure 5.22). Additionally, the CC-CNW accounts for nocodazole treatment. Nocodazole inhibits the polymerization of microtubules, implemented as the inhibitory action of the node *[Nocodazole]* towards tubulin dimerization. Formation of the bipolar spindle has additional regulatory layers than accounted for in the CC-CNW (Winey and Bloom, 2012). However, the exact mechanisms and contribution of these regulatory layers remain to be investigated.

The *Cell_[(SPB)]-{daughter}* state, produced in the last reaction of the SPB duplication cycle, contributes to the initiation of two processes. First, the attachment of nuclear microtubules to chromosomes, their separation and movement of one chromosome set into the daughter cell, initiated by the *[BipolarSpindle]* node (Figure 5.22). This process depends on the node *BipolarSpindle*, which is represented by either of the states *Cell_[(SPB)]-{bipolar}* or *Cell_[(SPB)]-{daughter}*. Second, the initiation of the *[SpindlePositionCheckpoint]* node, which ultimately allows activation of the Dbf2 kinase, required to activate the chitinase Chs2 for cell separation (Figure 5.23), and to activate the CDK antagonist Cdc14 (Figure 5.12).

5.7.5 *SPB movement into daughter cell*

The *[BipolarSpindle]* is the prerequisite for the process in which nuclear microtubules attach to kinetochores, leading to chromosome segregation and partitioning (Figure 5.22). The kinetochore is a protein structure consisting of several complexes attaching to the centromeric region of the DNA. The outer part of the kinetochore allows attachment to microtubules. Two kinetochore structures are attached to the opposite sides of a sister chromatid. Correct microtubule–kinetochore attachment requires that microtubules emanating from the two opposite SPBs attach to the same sister chromatid pair. These two microtubules must furthermore attach to the correct kinetochore, respectively. This

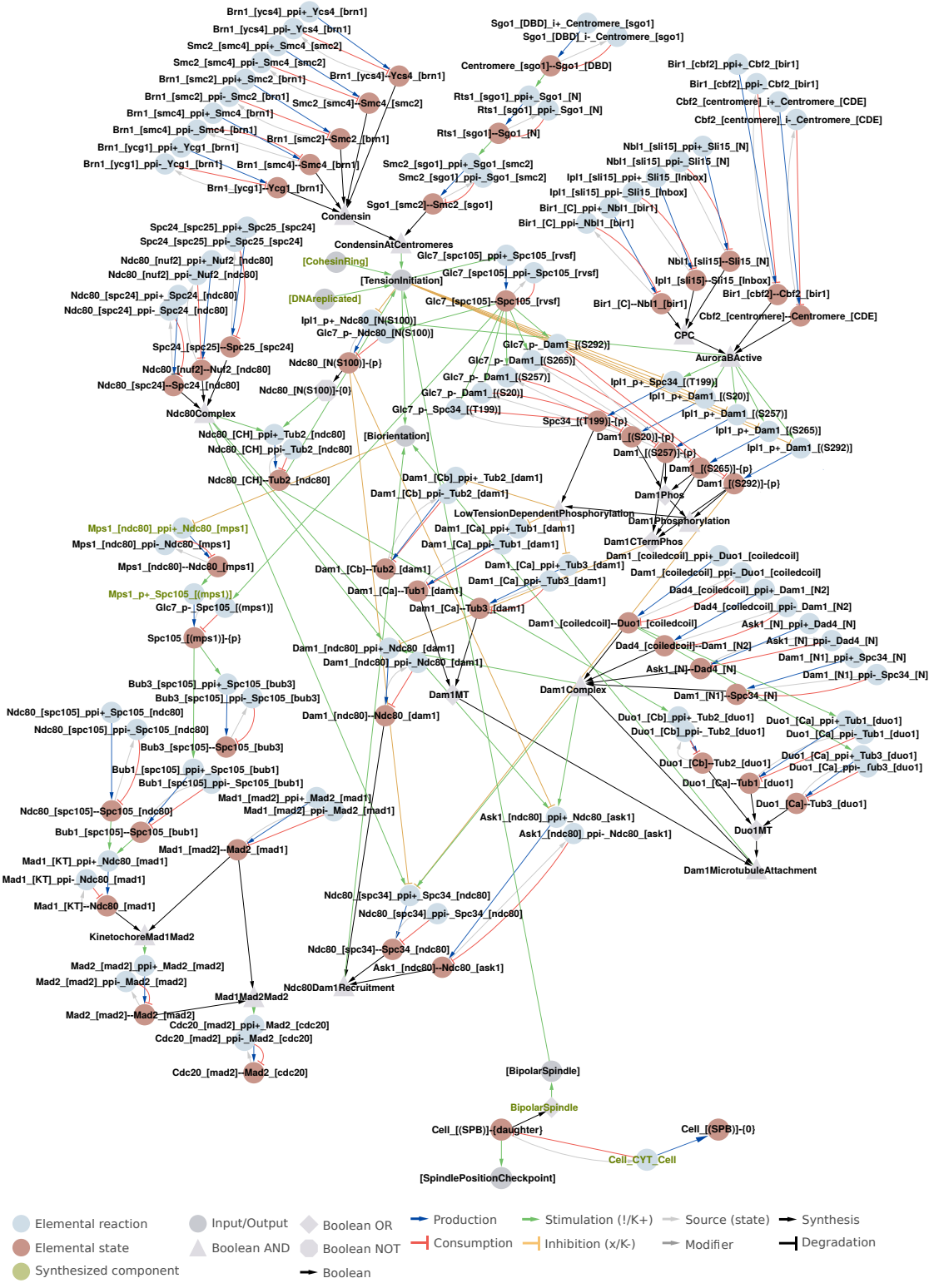

Figure 5.22. *SPB movement into daughter cell.* In this step, the microtubules emanating from the SPB attach to the kinetochores which have formed around the sister chromatids. For each kinetochore, the microtubules attaching must be from opposite poles, and only upon correct attachment, tension is exerted, leading to the deactivation of Ipl1 and stabilizing the bond between Ndc80 and Tub2.

type of interaction is referred to as biorientation or amphitelic attachment (Biggins, 2013). There are several possibilities for incorrect microtubule–kinetochore attachments. A description of all possible attachments would require a distinction between the SPBs and the two kinetochore complexes attached to one sister chromatid pair. These distinctions are not possible to express in rxncon language, as they would require spatial expressiveness. Thus, the CC-CNW only accounts for the mechanism involved in amphitelic attachment. This mechanism is tension sensitive. Tension sensing acts on the balance between phosphorylation and dephosphorylation of substrates involved in stabilization of microtubule–kinetochore attachments. Unless amphitelic attachment is accomplished, tension-sensitive aurora kinase Ipl1 phosphorylates several subunits of the kinetochore, thereby destabilizing microtubule–kinetochore attachment. Upon amphitelic attachment, the interaction between the microtubules and kinetochores exerts tension at the sister chromatids, leading to the deactivation of Ipl1, followed by dephosphorylation of its substrates. The CC-CNW accounts for the two kinetochore complexes Ndc80 and Dam1. The CC-CNW accounts for the Ndc80 complex subunits Spc24, Spc25, Nuf2 and Ndc80 (Biggins, 2013), combined in the *Ndc80Complex* node. The Dam1 complex consists of the subunits Ask1, Dad4, Dam1, Duo1 and Spc34 (Legal *et al.*, 2016), as accounted for and combined in the *Dam1Complex* node. Both complexes interact with each other via Dam1–Ndc80, Ask1–Ndc80, and Ndc80–Spc34 (Kim *et al.*, 2017). These protein complex interactions are accounted for and combined in the node *Ndc80Dam1Recruitment*.

Ipl1 is part of the chromosomal passenger complex (CPC). The CC-CNW accounts for its subunits Nbl1, Sli15, Ipl1, Bir1 (Nakajima *et al.*, 2009), combined in the node *CPC*. The CPC must furthermore be located in proximity to its substrates at the centromeres, accounted for by the requirement of Bir1 being bound to the kinetochore protein Cbf2 (Yoon and Carbon, 1999), which in turn is attached to centromeric regions of the DNA (Biggins, 2013). These conditions together with CPC form the active Ipl1 kinase complex which can reach its substrates, combined in the node *AuroraBActive*. Ipl1 phosphorylates Ndc80, subunit of the Ndc80 complex, and the Dam1 complex subunits Spc34 and Dam1 (Cheeseman *et al.*, 2002). Several Dam1 phosphorylations by Ipl1 are accounted for in the CC-CNW. Dam1 phosphorylation at at least one of three phosphorylations at S20, S257 or S64, combined in the node *Dam1Phos*, together with the phosphorylation at S292, combined in the node *Dam1Phosphorylation*, have been identified (Cheeseman *et al.*, 2002). These Dam1 phosphorylation combinations together with Spc34 phosphorylation at T199 combine into the node *LowTensionDependentPhosphorylation*, representing Ipl1-mediated phosphorylations, which inhibit and destabilize the interaction between the Dam1 complex subunit Dam1 and the microtubule subunits Tub1 and Tub2 (Cheeseman *et al.*, 2002). Additionally, phosphorylations in the Dam1 C-terminal, represented by the node *Dam1CTermPhos*, inhibit its interaction with Ndc80 (Kim *et al.*, 2017).

The CC-CNW accounts for stable kinetochore-microtubule attachment in two steps. In the first step, tension is initiated, represented by the node *[TensionInitiation]*, and

reinforced in a second step by stabilization of the interaction between the Ndc80 and Dam1 complexes, which combines into the node *[Biorientation]*. First, Ndc80 as part of the Ndc80 complex binds to Tub2. This interaction represents amphitelic attachment and requires that Ndc80 is unphosphorylated on residue S100 (Yamagishi *et al.*, 2014). Ndc80 bound to Tub2 is one prerequisite for the establishment of tension in the CC-CNW, which is presented by the *[TensionInitiation]* node. This node captures and collects additional states necessary to stabilize kinetochore-microtubules attachments. *[TensionInitiation]* requires the *[BipolarSpindle]* from the previous step, accounting for bipolar alignment of the SPBs. It is hypothesized that correct kinetochore-microtubule attachments require completed DNA replication, represented by *[DNAreplicated]* as another prerequisite for *[TensionInitiation]*. Tension establishment furthermore requires the condensin and cohesin protein complexes (Biggins, 2013; Marston, 2014), accounted for by the nodes *[CohesinRing]* and *CondensinAtCentromeres*. Condensin has a potential role in the DNA coiling process (Biggins, 2013), whereas cohesin might contribute to force transduction (Marston, 2014). The CC-CNW accounts for the condensin subunits Brn1, Smc2, Smc4 Ycg1, and Ycs4 (Marston, 2014). Smc4 is a Cdc28 substrate (Robellet *et al.*, 2015). However, the physiological role of these phosphorylations is not determined.

The node *[TensionInitiation]* represents correct kinetochore-microtubule attachment, establishing tension at the centromeres. This first tension generation initiates the second part of the stabilization of kinetochore-microtubules in which kinetochore-microtubule attachment is reinforced, represented by the node *[Biorientation]*. The initially generated tension is inhibitory towards Ipl1 activity (Liu *et al.*, 2009). Now, the activity of Glc7, the Ipl1 antagonist, dominates, resulting in the dephosphorylation of Ipl1 substrates (Francisco *et al.*, 1994). The activity of Glc7 is positively influenced by its interaction with Spc105 (Rosenberg *et al.*, 2011). The wave of dephosphorylation allows the stabilization of Dam1 complex interaction with microtubules, thereby strengthening kinetochore-microtubule attachment. Dam1 complex interaction with microtubules is combined in the node *Dam1MicrotubuleAttachment*, and requires interaction of the Dam1 complex subunits Duo1 and Dam1 with microtubules. Dephosphorylation of Dam1 allows its interaction with the tubulins Tub1 and Tub3 (Cheeseman *et al.*, 2002), combined in the node *Dam1MT*. Duo1 as Dam1 complex subunit is allowed to bind to tubulins Tub1, Tub2 and Tub3 (Miranda *et al.*, 2007), combined in the node *Duo1MT*. In the CC-CNW, it is hypothesized that Duo1–microtubule attachment furthermore requires kinetochore interaction via Ndc80, based on Legal *et al.* (2016). The interactions between the Dam1 complex subunits Dam1 and Duo1 and microtubules, represented by the nodes *Dam1MT* and *Duo1MT*, are combined in the node *Dam1MicrotubuleAttachment*, allowing the stabilization of the interaction between the Dam1 complex and microtubules by their positive influence on the *[Biorientation]* node. The *[Biorientation]* node furthermore requires the interaction between the Dam1 and Ndc80 complexes, combined in the node *Ndc80Dam1Recruitment*. The stabilization of the interaction between these two

complexes is achieved upon dephosphorylation of the subunits which are Ipl1 subunits. Lastly, *[Biorientation]* in the CC-CNW requires the initial step in the establishment of bioriented chromosomes *[TensionInitiation]*.

The node *[Biorientation]* represents stabilized microtubule–kinetochore attachments and bioriented chromosomes. At this stage, the cell can commit to segregate the chromosomes and partition them between the mother and daughter cell. In other words, the cell passes the spindle assembly checkpoint (SAC). SAC initiates the release of Cdc20, a prerequisite for APC/C–Cdc20 activation. Cdc20 release by SAC as implemented in the CC-CNW is accomplished by a signaling cascade starting with the inhibition of the interaction between Mps1 and Ndc80 requiring *[Biorientation]*. Before passing SAC, Cdc20 is part of a kinetochore complex including Bub1, Bub3, Mad1, Mad2 and Ndc80. This complex allows Mad2 dimerization (Zich and Hardwick, 2010), combining into the node *Mad1Mad2Mad2*. This is the prerequisite for the interaction between Cdc20 and Mad20, which retains Cdc20 at the kinetochores and thus, inhibits its interaction with the APC/C (Biggins, 2013). This complex assembles in the absence of stable kinetochore-microtubule attachment. Complex assembly is initiated by Mps1 interaction with Ndc80, allowing Mps1 to phosphorylate Spc105. Phosphorylated Spc105 recruits Bub1, Bub3, Mad1 and Mad2, combined in the node *KinetochoreMad1Mad2*. This allows Mad2 dimerization, combined in the node *Mad1Mad2Mad2*. The complex disassembles upon biorientation, initiated by the dissociation between Mps1 and Ndc80, which leads to the deactivation of Spc105 and its ability to interact with the remaining subunits. Cdc20 release allows it to interact with APC/C (Biggins, 2013), initiating a wave of degradation (Figure 5.8).

5.7.6 *Dbf2 activation*

The *Cell_[(SPB)]-{daughter}* state, retrieved in the last macroscopic reaction of the SPB cycle, passes the spindle position checkpoint (SPOC), represented by the node *[SpindlePositionCheckpoint]* (Figure 5.23). Upon passing SPOC, the mitotic exit network (MEN) is initiated, leading to the activation of the kinase Dbf2. Dbf2 activates Cdc14 (Figure 5.12) and the chitinase Chs2. The CC-CNW accounts for MEN activation in response to SPOC via Tem1 and Cdc15 activation. Tem1 is a GTPase which stimulates its own activity (Geymonat *et al.*, 2009). Tem1 in complex with Nud1 and Cdc15 activates Cdc15 (Weiss, 2012), combined in the node *Cdc15Active*. It was hypothesized that the GTP-bound form of Tem1 is additionally required for Cdc15 activity (Weiss, 2012), and also accounted for in the CC-CNW. Tem1 activity is antagonized by its guanosine triphosphate (GTP) GTPase activating protein (GAP) Bub2, which binds via Bfa1 to Tem1, combined in the node *Tem1ActivationInhibition*. In the CC-CNW, it is hypothesized that Bfa1 must furthermore be phosphorylated by Kin4 to inhibit Tem1 activity, based on Bertazzi *et al.* (2011). This phosphorylation requires Kin4 kinase activity, accomplished by Elm1 phosphorylation (Caydasi *et al.*, 2010), as accounted for in the CC-CNW. Kin4 is furthermore regulated via Lte1, which binds to Kin4 and de-

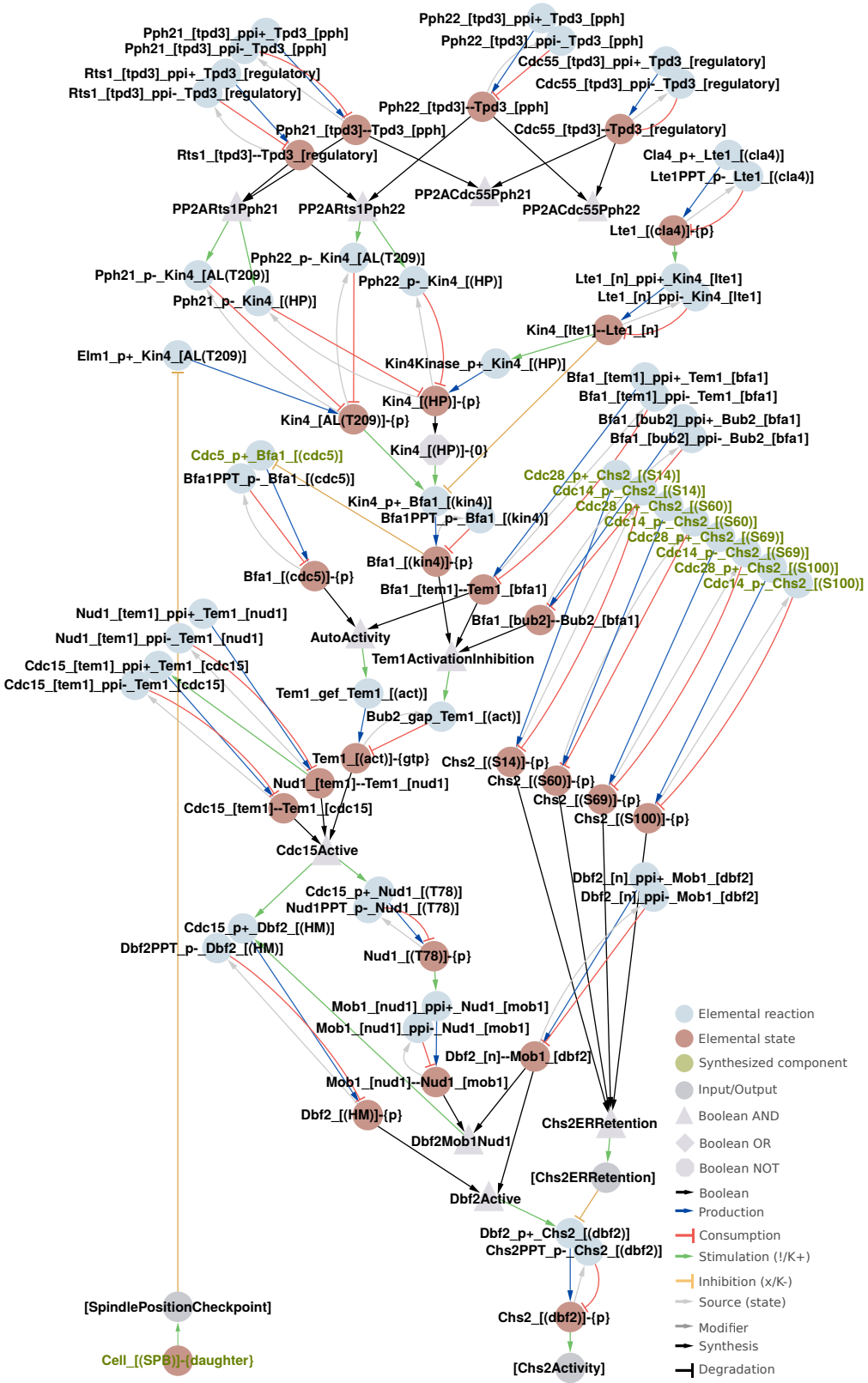

Figure 5.23. *SPB position checkpoint.* Correct spindle alignment activates the spindle position checkpoint (SPOC), which activates the mitotic exit network (MEN) by activating the kinase Dbf2. Active Dbf2 leads to the activation of Cdc14 and Chs2.

creases Kin4 activity. This is possibly mediated via a yet unidentified Kin4 kinase, which hyperphosphorylates Kin4 and contributes to its inactivation (Bertazzi *et al.*, 2011). Phosphorylation of Kin4 at T209 by Elm1 is crucial for Kin4 activity (Caydasi *et al.*, 2010). The molecular mechanism which regulates Elm1 activity remains unclear (Caydasi *et al.*, 2010). However, Elm1 phosphorylation of Kin4 depends on SPOC (Caydasi *et al.*, 2010), accounted for by the inhibitory effect of *[SpindlePositionCheckpoint]* towards Elm1 activity. Deactivated Elm1 in response to the correctly aligned spindle reverses Kin4 phosphorylation, accomplished by PP2A (Chan and Amon, 2009). Unphosphorylated Bfa1 allows Cdc5 to phosphorylate Bfa1 (Weiss, 2012). Bfa1 phosphorylated by Cdc5 forms a dimer with Tem1, enabling Tem1 GTPase activity as combined in the *AutoActivity* node. Active Tem1 can now stimulate Cdc15 kinase activity. Cdc15 is active in a complex consisting of Tem1, Nud1 and Cdc15, represented by the node *Cdc15Active*. Active Cdc15 phosphorylates Nud1 (Weiss, 2012; Rock *et al.*, 2013), enabling Nud1 to bind Mob1 (Rock *et al.*, 2013). This dimer together with Dbf2 forms a complex, combined in the node *Dbf2MobNud1*. Dbf2 as part of this complex is phosphorylated by active Cdc15 (Mah *et al.*, 2001; Weiss, 2012). This phosphorylation enables Dbf2 kinase activity, combined in the node *Dbf2Active*. Dbf2 can now phosphorylate Cdc14 and contribute to Cdc14 activation (Figure 5.12). Cdc14 activation initiates a wave of dephosphorylation of CDK targets, thus, resetting the cell to a state in which it can commence a new cell cycle. One of these Cdc14 targets is the chitinase Chs2, which, upon Cdc28–Clb1,2-mediated phosphorylation is retained and kept inactive at the endoplasmic reticulum (ER) (Teh *et al.*, 2009), combined in the node *[Ch2ERRetention]*. Chs2 dephosphorylation by Cdc14 releases Chs2, which is a prerequisite for Chs2 activation. ER release primes Chs2 for Dbf2 phosphorylation, resulting in the activation of Chs2, combined in the node *[Chs2Activity]*. This node represents the active chitinase complex, which is required to separate the mother from the daughter cell. The *[Chs2Activity]* is hence, also required as an input to the macroscopic *Cytokinesis* reaction.

5.8 Bud growth

The CC-CNW accounts for bud emergence and growth with two macroscopic reactions. First, the *Bud emergence initiation* reaction describes the regulation and establishment of a bud site. Second, the *Bud growth* reaction describes the regulation of bud growth and produces the state *Cell_[(bud)]-{growth}*. This state signals to the morphogenesis checkpoint, thereby inducing degradation of the Cdc28 inhibitor Swe1. The *Cytokinesis* reaction uses this state produced by the last reaction of the bud growth cycle and returns it to its neutral value.

5.8.1 *Bud site establishment*

Bud site establishment (Figure 5.25) starts with membrane polarization and assembly of the budneck, represented by the *Bud emergence initiation* reaction *Cell_EM_Cell_[(bud)]*. This reaction is regulated by a network responsible for membrane polarization and

recruitment of the proteins required for bud neck assembly, accounting for bud site establishment at the site of polarization. Membrane polarization requires local accumulation and activation of the GTPase Cdc42 (Bi and Park, 2012). Several hypotheses have been proposed to explain polarized Cdc42 accumulation and activation, as the exact mechanism is not entirely clear (Bi and Park, 2012; Howell and Lew, 2012). In brief, the two major hypotheses rely on positive feedback mechanisms and explain membrane polarization with either, Cdc42 accumulation via landmark proteins, or, an actin-cable based transport system, which sequesters Cdc42 to a spontaneously formed cluster. The actin-cable based mechanism, however, is contradictory (Bi and Park, 2012), and not accounted for in the CC-CNW. The CC-CNW accounts for membrane polarization via localized activation of Cdc42 by its guanine nucleotide exchange factor (GEF) Cdc24, mediated via Rsr1 or Bem1 complexes.

First, Cdc42 must become locally activated, which is accomplished by bringing Cdc42 in proximity with its GEF Cdc24 and the GAPs Bem2, Bem3, Rga1 and Rga2. In this view, it is assumed that Cdc24 first becomes locally active, whereas the deactivating GAPs Bem2, Bem3, Rga1 and Rga2 are equally distributed. This enables localized guanosine diphosphate (GDP)/GTP shuttling of Cdc42, and hence, enables membrane polarization. Cdc24 localization is accomplished by landmark proteins and Rsr1. Depending on the cell type, different landmark proteins are involved, resulting in different polarization patterns. Haploid cells have an axial polarization pattern, whereas diploid cells have a bipolar one (Bi and Park, 2012). The CC-CNW accounts for Bud3, Bud4 and Axl1 (Figure A.2). However, their physiological role and contribution to polarization establishment is not conclusively determined (Kang *et al.*, 2014). For this reason, the landmark proteins involved in polarity established are simplified in the CC-CNW. Rsr1 is recruited to landmark proteins via its GTPase Bud5 (Howell and Lew, 2012), which interacts with landmark proteins named *Lmproteins* in the CC-CNW. Bud5 interaction with the landmark proteins stimulates Rsr1 activation, which in turn enhances Rsr1 interaction with Cdc42 and Cdc24, forming the *Rsr1MediatedLocalization* complex. However, the cell is able to polarize Cdc42 in the absence of spatial markers, which requires Bem1. The CC-CNW accounts for this by Bem1-mediated recruitment of Cdc24 and Cdc42, combined in the node *Bem1MediatedLocalization*, another prerequisite for Cdc42 localized activation. The interaction between Bem1 and Cdc24 is hypothesized to depend on Cdc28–Cln1,2,3-mediated phosphorylation of Bem1, based on Bi and Park (2012). Either of the complexes *Rsr1MediatedLocalization* or *Bem1MediatedLocalization*, combined in the node *Cdc42LocalizedActivation*, is required to stimulate GEF Cdc24 activity. To enforce a positive feedback loop, only GDP-bound Cdc42 can interact with Rsr1 (Howell and Lew, 2012). It is assumed that the landmark proteins are localized to a single site in the cell membrane. Bem1 localization, however, has no distinct localization pattern, and hence, the CC-CNW cannot explain the establishment of a single polarization site in the

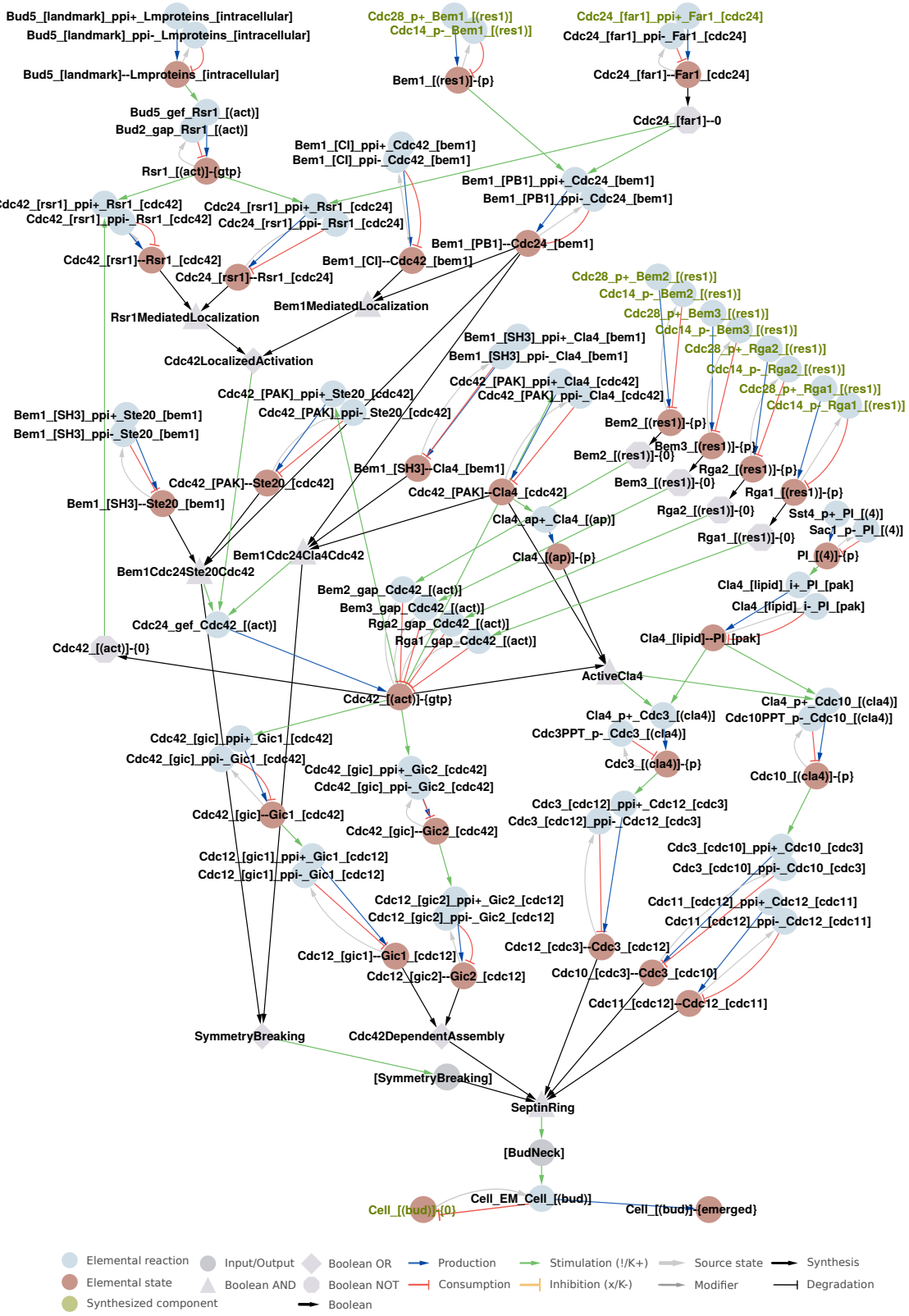

Figure 5.24. *Bud site establishment.* Bud site establishment requires the local accumulation and activation of Cdc42, leading to the polarization of the cell membrane. At the same time, proteins required for bud neck establishment are recruited to the site of polarization.

absence of Rsr1. Bem1 forms two different complexes with Cdc42 and Cdc24. One involves Bem1, Cdc24, Ste20, and Cdc42, combined in the node *Bem1Cdc24Ste20Cdc42*. The other one involves Bem1, Cdc24, Cla4, and Cdc42, combined in *Bem1Cdc24Cla4Cdc42*. Hence, these two complexes also contribute to Cdc24 stimulation, as implemented. Moreover, in the absence of Rsr1, either of these two complexes is thought to establish a site of polarization (Howell and Lew, 2012), which is accounted for by requiring either of these nodes for symmetry breaking, which is represented by the nodes *Symmetry-Breaking* and *[SymmetryBreaking]*.

Localized Cdc42 activation enables assembly of a septin ring at the polarization site. Recruitment and assembly of the septin ring subunits depends on Cla4 and Cdc42. First, Cla4 is activated by autophosphorylation (Versele and Thorner, 2004), which is supposedly supported by its interaction with active Cdc42, a hypothesis based on the same study. Active Cla4, combined in the node *ActiveCla4*, can now phosphorylate Cdc3 and Cdc10 (Perez *et al.*, 2016; Versele and Thorner, 2004). Cla4 is furthermore thought to be recruited to the cell membrane via its interaction with phosphatidylinositol (PI) 4-phosphate (Wild *et al.*, 2004). Phosphorylated Cdc3 and Cdc10 enables them to interact with each other and with Cdc12. The Cdc3–Cdc12 and Cdc10 dimers, in addition with Cdc11-Cdc12 are required to establish the septin ring (Bertin *et al.*, 2008), combined in the node *SeptinRing*. The exact topology of the septin ring, however, is not entirely resolved. The additional septin ring component Shs1 is omitted in the CC-CNW due to its redundant role.

Recruitment of septin ring proteins to the site of polarization was shown to require Gic1 and Gic2 (Iwase *et al.*, 2006). This is accounted for by the interaction between Cdc42–GTP and Gic1 or Gic2, combined in the node *Cdc42DependentAssembly*, as a prerequisite for septin ring assembly. The node *SeptinRing* collects all prerequisites accounted for in the CC-CNW and matures into a bud neck. Maturation is not explicitly accounted for, but represented by the node *[BudNeck]*, which depends on the formation of the *SeptinRing*. *[BudNeck]* is the prerequisite for the *Cell_EM_Cell_[(bud)]* reaction to execute, producing the *Cell_[(bud)]-{emerged}* state. The *Cell_[(bud)]-{emerged}* state represents the establishment of a bud site with a bud neck. The bud neck is required to enable bud growth (Figure 5.25) and for morphogenesis signaling (Figure 5.26).

Additionally, the CC-CNW accounts for pheromone treatment via Far1 in the presence of pheromone. Far1 then interacts with Cdc24, thereby inhibiting Cdc24 interaction with Bem1 (Butty *et al.*, 2002) and Rsr1 (Enserink and Kolodner, 2010). This ultimately inhibits the cell to establish a bud site.

5.8.2 *Bud emergence and growth*

In the next step (Figure 5.25), a bud starts to emerge and grow at the bud site, described by the *Bud growth* reaction *Cell_GROWTH_Cell_[(bud)]*, producing the state *Cell_[(bud)]-{growth}*. Bud growth in *S. cerevisiae* is polarized, initially. Polarized bud growth requires that the material and enzymes needed to enlarge the daughter cell are sequestered

towards the site of polarization. The material is transported in vesicles to the plasma membrane, where the vesicles dock and fuse with the plasma membrane, accomplished by polarized exocytosis. Polarized exocytosis requires the localization and activation of the exocyst complex at the site of polarization to stimulate vesicle fusion. Actin cables mediate polarized exocytosis.

The CC-CNW accounts for polarized growth in the following way: First, the exocyst complex is localized to the polarization site via Cdc42-GTP. The CC-CNW accounts for the exocyst complex subunits Sec3 and Exo70. It was shown that Exo70 interacts with Cdc42-GTP (Wu *et al.*, 2010), and the same study suggested that also Sec3 interacts with Cdc42. The remaining subunits of the exocyst are omitted in the CC-CNW. The exocyst complex furthermore recruits Rho1, which is required to direct actin cables towards the site of polarization, and to activate glucan synthase, required to remodel the cell wall of the bud. Rho1 is recruited to the exocyst complex by interaction with Sec3 (Guo *et al.*, 2001). Cdc42-GTP interaction with Exo70 and Sec3, as well as the interaction between Rho1 and Sec3 are combined in the node *Rho1Exocyst*, representing the recruitment of Rho1 to the exocyst and its localization to the site of polarization via Cdc42-GTP. Second, the exocyst targets proteins to the membrane, which requires its localization to the membrane. The CC-CNW accounts for exocyst membrane targeting via interaction of the exocyst subunits Exo70 and Sec3 with the membrane localized PI 4,5-bisphosphate ($PI(4,5)P_2$) (He *et al.*, 2007). $PI(4,5)P_2$ is represented by the node *PI45P2* and, in turn, regulated via the kinase–phosphatase pair Sst4/Mss4 and Sac1/Inp51 (Yoshida *et al.*, 1994; Stolz *et al.*, 1998; Foti *et al.*, 2001; Audhya and Emr, 2002). The interaction between Rho1 as part of the exocyst in combination with its docking to the membrane enables exocytosis (Abe *et al.*, 2003; Roumanie *et al.*, 2005; He *et al.*, 2007), represented by the node *Exocytosis*. Third, Rho1 is activated upon membrane targeting by bringing it together with its GEF Rom2 (Ozaki *et al.*, 1996; Roumanie *et al.*, 2005), which is localized to the membrane by interaction with $PI(4,5)P_2$ (Audhya and Emr, 2002). Fourth, either of two cell wall integrity pathway sensors, Slg1 or Mid2, additionally interact with Rom2, thereby enhancing the activity of Rom2 (Philip and Levin, 2001). This is accounted for by the interactions between Rom2 and Slg1, and Rom2 and Mid2, respectively, combined in the node *Rom2CWI*. Together, these four requirements build the *Rho1MembraneTargeting* prerequisite, leading to the activation of Rho1 by its GEF Rom2 at the site of polarization. Furthermore, Rho1 can be activated by Tus1 (Schmelzle *et al.*, 2002), another Rho1 GEF. Tus1 activation requires phosphorylation by Cdc5 and Cdc28–Cln1,2,3 (Yoshida *et al.*, 2006; Kono *et al.*, 2008), as accounted for in the CC-CNW. The Rho1 GAP Bem2, together with the Rho1 GEFs Rom2 and Tus1 enables Rho1 activity. In the CC-CNW, Rho1 activation at the site of polarization is hypothesized to occur without actin cables, based on Sahin *et al.* (2008).

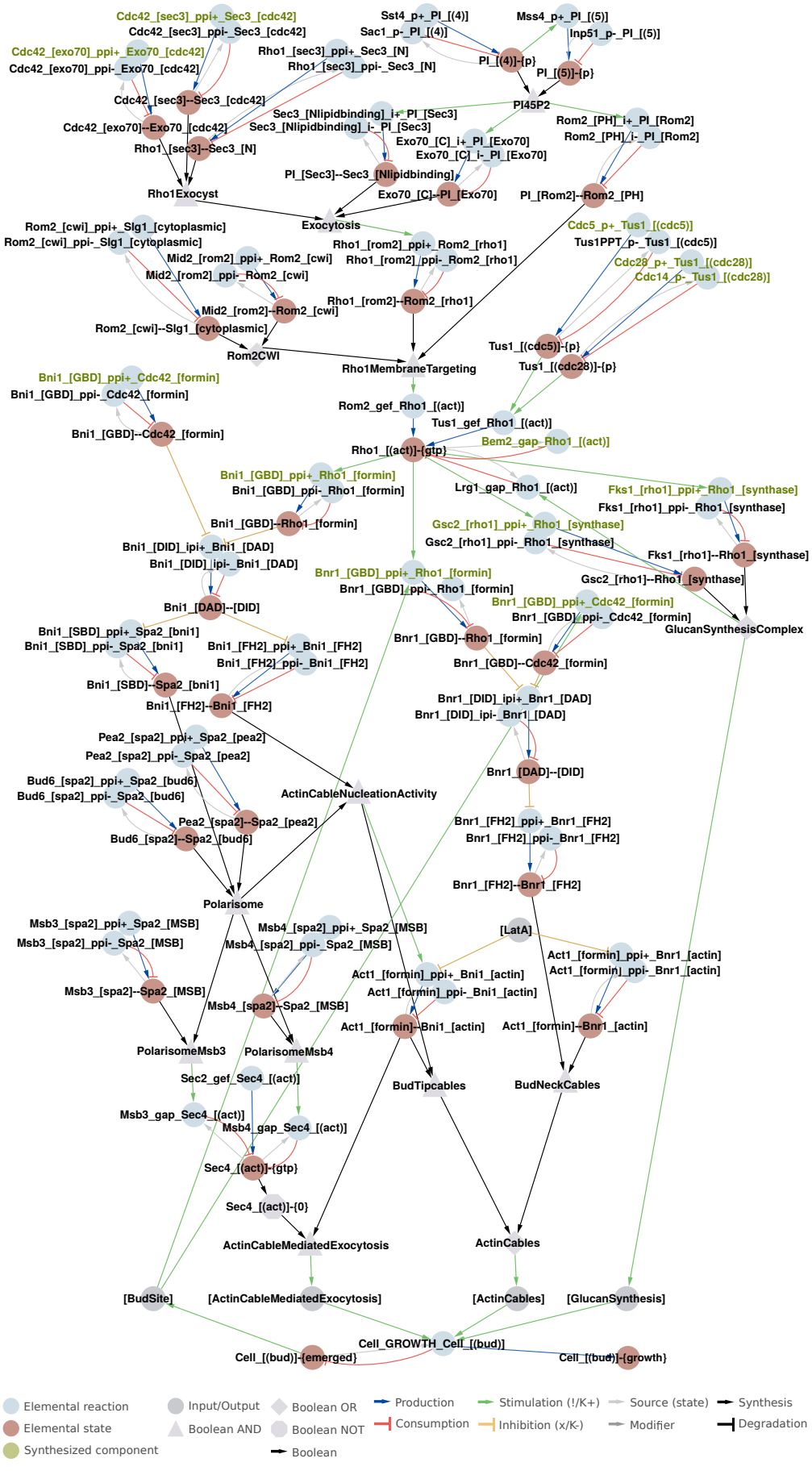

Figure 5.25. *Bud emergence.* Cell membrane polarization and recruitment of bud neck proteins leads to the formation of a bud. Polarized bud growth is enabled via actin cable mediated exocytosis.

Next, Rho1 activates the glucan synthesis complex at the site of polarization by binding to the subunits Fks2 and Gsc2. Either of these Rho1-glucan synthase complexes is required for glucan synthesis activity (Qadota *et al.*, 1996; Bi and Park, 2012), represented by the node *GlucanSynthesisComplex*, which is the prerequisite for *[GlucanSynthase]*, one of three requirements to establish bud growth as accounted for in the CC-CNW.

Polarized bud growth requires actin cable mediated exocytosis. Actin cables orient towards the site of polarization in a manner dependent on the formins Bni1 and Bnr1 (Evangelista *et al.*, 2002). The formins are required for actin cable orientation and nucleation, where Bni1 nucleates actin cables in the daughter cell at the bud tip, Bnr1 nucleates actin cables in the mother cell at the bud neck (Bi and Park, 2012). Bni1 was shown to interact intramolecularly with its C-terminal diaphanous autoregulatory domain (DAD) and GTPase binding domain (GBD) (Alberts, 2001; Dong *et al.*, 2003). This intramolecular interaction inhibits Bni1 activity. In the CC-CNW, it is hypothesized that the same autoinhibitory mechanism applies to Bnr1, based on the studies by Alberts (2001) and Dong *et al.* (2003), and structural similarities between Bni1 and Bnr1 (Dong *et al.*, 2003). The domain names used here for the intramolecular interactions of Bni1 and Bnr1 (DAD and N-terminal diaphanous inhibitory domain (DID), where DID is equivalent to GBD) are according to the convention in Bi and Park (2012). In the CC-CNW, this autoinhibition is relieved by binding of Rho1 or Cdc42 to Bni1 (Kohno *et al.*, 1996; Evangelista *et al.*, 1997), as discussed by Bi and Park (2012). Similarly, the CC-CNW accounts for Bnr1 relief of autoinhibition by Cdc42 or Rho1 binding, a model hypothesis based on Kohno *et al.* (1996) and Evangelista *et al.* (1997) due to similarity between Bni1 and Bnr1. Additionally, in the CC-CNW, it is hypothesized that Bni1 and Bnr1 interactions with Cdc42 or Rho1 require *[SymmetryBreaking]*, as discussed in Howell and Lew (2012), allowing polarized growth at the bud tip. Bni1 is then allowed to interact with the polarisome via Spa2. The CC-CNW accounts furthermore for the polarisome subunits Bud6 and Pea2, both of which bind to the scaffold protein Spa2, combined in the node *Polarisome*. The polarisome interacts via Spa2 with either Msb3 or Msb4, accounted for in the nodes *PolarisomeMsb3* and *PolarisomeMsb4*, respectively. Msb3 and Msb4 are GAPs of Sec4. Together with the Sec4 GEF Sec2, the polarisome allows for vesicle tethering via active Sec4, which is the prerequisite for active exocytosis at the site of polarization, accounted for by the node *ActinCableMediatedExocytosis*. The CC-CNW does not explicitly describe the molecular process of vesicle tethering. Exocytosis is accomplished by actin cables, which is the second prerequisite for *ActinCableMediatedExocytosis*. The CC-CNW accounts for actin cable polymerization towards the bud tip by the dimerization of Bni1 at its formin homology 2 (FH) domain (Xu *et al.*, 2004), allowing it to nucleate actin cables. The actin cables are directed towards the bud tip, which is also accounted for by the requirement of Bni1 to be part of the polarisome. Both requirements are combined in the node *ActinCableNucleationActivity*, which is the prerequisite for Bni1 interaction with actin via Act1 (Pruyne *et al.*, 2002). This node creates the output *[ActinCableMediatedExocytosis]*,

which is the second prerequisite for the *BudGrowth* reaction to occur.

The third and last prerequisite for the *BudGrowth* reaction to occur are the *[ActinCables]*. This requirement accounts for the fact that the two formins Bni1 and Bnr1 can compensate for each other (Imamura *et al.*, 1997). In the CC-CNW, this is accomplished by the interaction of Bnr1 with Cdc42 or Rho1, which, similar to Bni1, relieves the autoinhibitory interaction of the DID and DAD domains of Bnr1. This mechanism is a model hypothesis and based on similarity between Bni1 and Bnr1 as discussed in Bi and Park (2012). The Bnr1 nucleated cables emerge at the bud site at the mother cell, accounted for with *[BudSite]* as an additional requirement for Bnr1 activation by Rho1 or Cdc42. Bnr1, as accounted for in the CC-CNW, can then interact with its FH2 domains, which enables it to bind to actin via Act1. This interaction enables Bnr1 to nucleate actin cables from the bud neck, combined in the node *BudNeckCables*. In a similar fashion, the ability to form bud tip cables depends on relief of autoinhibition of Bni1, enabling to nucleate actin cables at the bud tip, combined in the node *BudTipCables*. Since either of these actin cables contribute to polarized bud growth, they are combined in the node *[ActinCables]*, and constitute the third and last prerequisite, as accounted for in the CC-CNW, to enable polarized bud growth. The CC-CNW does not explicitly account for actin cable polymerization. Upon activation of the reaction *Cell_GROWTH_Cell_[(bud)]*, the state *Cell_[(bud)]-{growth}* is produced, representing a growing cell.

The CC-CNW accounts for LatA treatment, a cell cycle arrest chemical which inhibits the polymerization of the actin skeleton. This is implemented indirectly by the inhibitory action of the input node *[LatA]* towards the interaction between Act1 and the formins Bni1 and Bnr1.

5.8.3 *Morphogenesis checkpoint*

The establishment of a growing bud is the prerequisite for the morphogenesis checkpoint to initiate the downregulation of Swe1. Swe1 acts as a Cdc28–Clb1,2 inhibitor (Keaton *et al.*, 2007), ensuring that CDK-Clb1,2 regulated processes, such as DNA segregation, occur after bud formation.

The CC-CNW accounts for Swe1 (Figure 5.26) regulation in the following way: First, Hsl1 and Hsl7 are recruited to the bud neck via Cdc3 (Howell and Lew, 2012). This recruitment depends on the input node *[BudGrowth]* in the CC-CNW, an outcome of the gap-filling process as described in Section 6.1.1. The input node *[BudGrowth]* represents a cell with a mature bud neck and ongoing bud growth. This input depends on the macroscopic state *Cell_[(bud)]-{growth}*, retrieved from the macroscopic reaction *Bud growth* in the bud growth cycle. Swe1 recruitment to the bud neck via Hsl7 then enables Cdc28–Clb1,2 to phosphorylate Swe1 (Lee *et al.*, 2005; Enserink and Kolodner, 2010; Howell and Lew, 2012). The Swe1 interaction with Hsl7 also primes Swe1 for Cdc5-mediated phosphorylation (Asano *et al.*, 2005). The CDK-mediated phosphorylation of Swe1 is thought to have a positive influence on Cdc5 phosphorylation (Howell

and Lew, 2012). In the CC-CNW, it is furthermore hypothesized that Cdc5 requires Cdc28–Clb1,2 mediated phosphorylation on T242 (Mortensen *et al.*, 2005; Rodriguez-Rodriguez *et al.*, 2016) for kinase activity. This hypothesis is based on the study by Rodriguez-Rodriguez *et al.* (2016). Phosphorylation of Swe1 by Cdc5 or Cdc28 primes it for degradation (Howell and Lew, 2012), combined in the node *Swe1DegPhosphorylation*. Phosphorylated Swe1 enables Met30–SCF-mediated ubiquitination and subsequent degradation (Section 5.3.2).

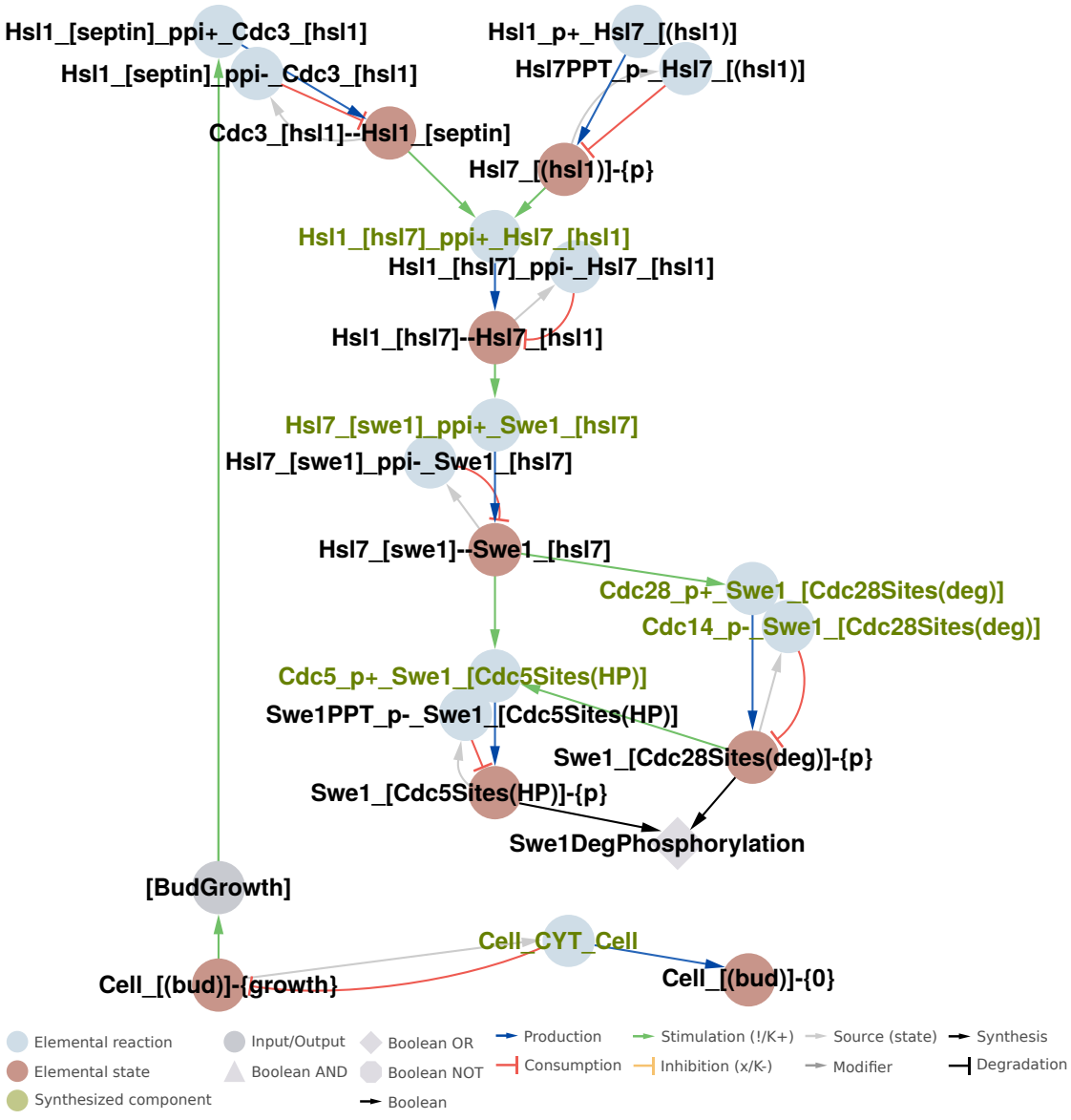

Figure 5.26. *Bud growth.* Bud growth is enabled by a mature bud neck. The bud neck recruits the septins Hsl1 and Hsl7, a prerequisite for Swe1 recruitment. Cdc28–Clb1,2 and Cdc5 phosphorylate bud neck localized Swe1 and prime it for degradation.

Swe1 substrates are antagonized by the phosphatase Mih1 (Howell and Lew, 2012), which is also accounted for. In the unperturbed cell cycle, the role of Swe1 seems to be minor. However, its role becomes more distinct and important when the cell is exposed to stresses (as discussed by Howell and Lew (2012)). As the CC-CNW describes an unperturbed cell cycle, the role of Swe1 upon cell cycle perturbations is omitted.

5.9 Network comparison

The CC-CNW was compared to the Kaizu model with regard to the proteins both models account for. The translation of the Kaizu model resulted in the identification of 969 elemental reactions listed in Table A.6, where the bidirectional reactions were counted once. From these elemental reactions, 318 proteins were extracted. 96 of these proteins were considered to be out of scope for the comparison between the CC-CNW and Kaizu model, as they belong to signal transduction pathways, metabolic processes, or processes with an unclear connection to cell cycle control. The remaining 222 proteins were compared to the 229 proteins of the CC-CNW. The protein overlap between the Kaizu model and the CC-CNW is shown in the Venn diagram in Figure 5.27. The two models have an overlap of 148 proteins, the CC-CNW uniquely accounts for 81 proteins, and the Kaizu model uniquely accounts for 74 proteins. Table A.1 lists the protein names according to the three disjunct sets in Figure 5.27, and, additionally, 96 proteins which were excluded from the comparison. The proteins excluded from the comparison are briefly discussed in Section A.1.1.

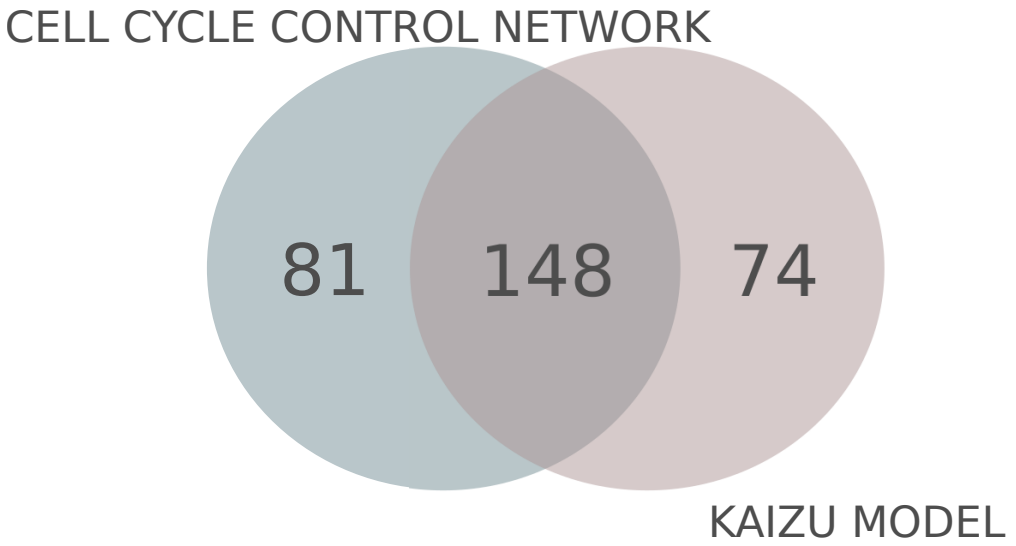

Figure 5.27. *Network comparison.* The Venn diagram shows the overlapping and unique proteins of the CC-CNW and the Kaizu model. Protein names are listed in Table A.1.

The components uniquely identified in the Kaizu model include the subunits of the APC/C (Apc1, Apc11, Apc2, Apc4, Apc5, Apc9, Cdc16, Cdc23, Cdc26, Cdc27,

Doc1, Mnd2, Swm1) (Schreiber *et al.*, 2011). The CC-CNW does not explicitly account for APC/C subunits for reasons discussed in Section 5.3.1. Furthermore, regulation of APC/C activity is accounted for as described in Subsections 5.3.1 and 5.7.5, the latter including SAC. The Kaizu model accounts explicitly for proteins comprising histones and histone regulation (Ash1, Esa1, Gcn5, Hda1, Hhf1, Hhf2, Hht1, Hht2, Htb1, Htb2, Vps75). Histones and their regulation are not explicitly described in the CC-CNW, but accounted for indirectly as input *[Histones]* in the DNA replication process (Section 5.6.3). Histone regulation plays an important role in genomic reprogramming (Jaiswal *et al.*, 2016), and is hence, not part of core cell cycle control. However, histone regulation is an important target for future extensions of the CC-CNW. The Kaizu model explicitly accounts for proteins involved in bud site selection (Axl2, Bud8, Bud9, Rax1, Rax2). The role and contribution to bud site selection is not clearly established (Bi and Park, 2012). Furthermore, the CC-CNW describes a haploid cell, and does not require proteins involved in bipolar budding (Bud8, Bud9, Rax1, Rax2). The Kaizu model accounts for the SBF/MBF associated proteins Msa1 and Msa2 (Ashe *et al.*, 2008). Both proteins contribute to fine tuning of SBF/MBF regulation (Ashe *et al.*, 2008) and play a role in quiescence. However, a mechanistic connection has not been reported, yet. Hence, Msa1 and Msa2 are omitted in the CC-CNW. The Kaizu model accounts for the nuclear pore complex (NPC) protein Nup53 , which is associated with the nuclear envelope. The CC-CNW does not account for nuclear transport explicitly, and hence, the NPC is not accounted for. Mlp1 is also associated with the NPC (Niepel *et al.*, 2013), however, its mechanistic relevance in the context of the CC-CNW could not be established. Dia2 is a SCF F-box protein, but the CC-CNW does not account for any of its substrates. However, Dia2 has a role in cell cycle progression (Koepp *et al.*, 2006), and is a target for future extension of the CC-CNW. Similarly, the protein Amn1 has a role in MEN (Wang *et al.*, 2003), and also a target for future CC-CNW extensions.

The remaining proteins accounted for in the Kaizu model but not in the CC-CNW are involved in diverse processes, such as mother bud separation, chromosome regulation, cell growth, but a clear mechanistic role relevant to cell cycle control could not be established.

5.10 Discussion

The presented CC-CNW accounts for 229 proteins, involved in 1246 elemental reactions and regulated by 801 contingencies, which together form the rxncon model base. The CC-CNW describes the cell cycle control network of a mitotic budding yeast cell. The reconstruction is based on selected, published empirical studies and review papers relevant to cell cycle control in *S. cerevisiae*, and the interpretation and translation of the empirical findings into rxncon language. In the CC-CNW, several hypotheses were introduced. Section 5.10.1 discusses the CC-CNW on the basis of the selection and interpretation of this data, discusses the main hypotheses, and limitations of the model. Section 5.10.2 discusses the CC-CNW in light of its scope in comparison to the Kaizu

model, and potential network extension.

5.10.1 *Data selection, hypotheses, and network limitations*

Data selection. The CC-CNW is based on empirical studies and review papers relevant to cell cycle control. Empirical data was selected based on demonstrated biochemical evidence *in vivo* and *in vitro*. There are, however, cell cycle regulated processes where conclusive empirical support is missing, for example, with regard to transcriptional regulation of *CLB4* and *DBF4*, bud site selection, regulation of bud growth, CDK cyclin redundancy, and the role of Bnr1 in polarized growth in the daughter cell.

The underlying data of the CC-CNW is partially based on review papers. Review papers summarize and discuss the current knowledge of different biological processes, but also constitute an interpretation of primary data. Thus, the quality of the CC-CNW could be improved by refinement and reinspection of the underlying data to use primary data without exception. The underlying data used to reconstruct the CC-CNW was carefully selected and interpreted, and is referenced in Tables A.2 to A.4. Due to the rich amount of data available, in combination with manual literature curation, the CC-CNW is based on a strong empirical foundation.

Hypotheses. The CC-CNW makes use of several hypotheses. Two global hypotheses were stated in Section 5.1. The first global hypothesis regards the antagonism of phosphorylations by hypothesized phosphatases, the second regards the turnover of mRNA transcripts. Another hypothesis was stated in Section 5.4, regarding the Cdc28-cyclin redundancy. The CC-CNW furthermore relies on hypotheses accounting for the redundant functions of Cdc28 and Pho85 during G_1. The CC-CNW introduced hypotheses regarding the control of bud growth, and actin cable polymerization.

The first global hypothesis stated in Section 5.1 regards the antagonism of physiologically relevant phosphorylations. These phosphorylations are likely to be antagonized in order to restrict the function of a phosphorylation to a certain process during the cell cycle. Phosphorylation antagonism can be achieved by dephosphorylation, or by priming a phosphorylated protein for degradation. To account for phosphorylation antagonism of a protein where this mechanism is unknown, dephosphorylation reactions carried out by hypothetical phosphatases were introduced. This was a necessary step in order to account for temporal restriction of the function of phosphorylated proteins. The hypothetical dephosphorylation reactions require minimal assumptions to antagonize protein phosphorylation. Furthermore, phosphatases tend to be less specific compared to kinases, based on the number of known kinases and phosphatases in yeast (Breitkreutz *et al.*, 2010). Hence, it is likely that several of the proposed hypothetical phosphatases are identical. It would require dedicated empirical work to identify the phosphatases, or alternative downregulation mechanisms to antagonize the physiologically relevant phosphorylations in the CC-CNW.

The second global hypothesis stated in Section 5.1 regards the decay of mRNA. The mRNA transcripts are the output of active transcription and hence, directly reflect the

activity of a gene. In the CC-CNW, the majority of the considered genes are regulated and active for a specific period. Hence, gene activity must also be reflected in the transcriptional output. The CC-CNW accounts for downregulation of the transcriptional output via decay reactions which antagonize mRNA transcripts. This is a model hypothesis as there are several possibilities to counteract mRNAs. For example, the mRNA itself may be spatially regulated, possibly via a retention mechanism. With the exception of *CLN3* mRNA, data to support this was not encountered for the remaining individual mRNA transcripts. Furthermore, mRNA transcripts may not be accessible to ribosomes due to a change in the ratio between mRNA transcripts and cellular volume, making it less likely for the mRNA to encounter ribosomes. Such spatial mechanisms, however, are not possible to account for in a qualitative model as the CC-CNW.

The stability of mRNA transcripts is determined by the length of its polyadenylated tails. Exonucleases shorten the mRNA transcripts, thereby destabilizing them (Das *et al.*, 2017). The CC-CNW does not account for this step explicitly, as the molecular mechanisms remain unknown (Das *et al.*, 2017). However, in the future, the study of mRNA decay might reveal an additional layer of regulation in cell cycle progression. Hence, the model hypothesis stating that mRNA transcripts are turned over in a decay mechanism requires minimal assumptions for mRNA downregulation.

In Section 5.4, it was hypothesized that the Cdc28 cyclins can functionally compensate for each other pairwise. This hypothesis is based on the similarity between the cyclins, together with the associated mutant phenotypes, and enables the CC-CNW to account for single and double cyclin mutant phenotypes. Furthermore, restricting Cdc28 substrates to a certain cyclin implies that the other cyclins have been ruled out empirically, which is not always the case. Hence, this hypothesis is less restrictive towards the exclusion of Cdc28-cyclins in accordance with data. However, the CC-CNW does not functionally account for Clb3 or Clb4 due to insufficient knowledge about their regulation and redundancy. Hence, the CC-CNW cannot distinguish between the functional overlap of Clb3,4 and the remaining cyclins. Furthermore, Cdc28 and Pho85 antagonize Sic1 during G_1. In the CC-CNW, it is hypothesized that both CDKs modify the same Sic1 residues, based on the studies by Nishizawa *et al.* (1998) and Nash *et al.* (2001). The residues accounted for in the CC-CNW have been explicitly shown only in the case of Cdc28.

The CC-CNW accounts for actin cable polymerization by either Bni1 or Bnr1, required for bud growth. The molecular mechanism of Bnr1 involvement in bud growth, however, is not completely deciphered. In the CC-CNW, it is hypothesized that the two formins Bni1 and Bnr1 can compensate for each other in the process of actin cable polymerization in the bud. The hypothesis is based on the observation that single formin mutants are viable, whereas a double formin mutant is not (Imamura *et al.*, 1997). The CC-CNW does not account for the redundant role of Bnr1 in actin cable mediated exocytosis, and hence, the CC-CNW cannot account for a cell lacking Bni1 (Section 6.2.2).

The CC-CNW describes macroscopic properties of a yeast cell during the cell cycle

with macroscopic reactions. These macroscopic reactions do not comply with elemental reactions which can be measured biochemically. The macroscopic reactions describe three individual events of the cell cycle, DNA replication, SPB duplication, and bud growth. These three individual cycles underly regulational control, but occur without regulation of each other. Yet, the cell cycle follows a specific order of events, and the macroscopic reactions, controlled by the regulatory layer, ensure the physiological and synchronized occurrence of these events.

Limitations. The CC-CNW is formulated in rxncon language. The rxncon language lacks spatial expressiveness and hence, spatial processes cannot be described directly on the level of elemental reactions and contingencies. The CC-CNW accounts for spatial effects indirectly as described in Section 5.1. There are, however, spatial observations which the CC-CNW cannot account for, such as the observation that the dividing yeast cell activates different transcriptional programs in the mother and daughter cell (Colman-Lerner *et al.*, 2001). Furthermore, asymmetric protein distributions and regulatory mechanisms have been reported involving the spindle (reviewed in Smeets and Segal (2002)). The CC-CNW cannot account for these asymmetries, as it would require a distinction between the different compartments, and the strict association of these processes with their respective compartments. Hence, the CC-CNW can not distinguish age related differences between a mother and daughter cell (Denoth Lippuner *et al.*, 2014).

The rxncon language has limited expressiveness for quantitative statements. Regulated reactions either require certain molecular context, indicated by a strict contingency (!/x), or they can be positively or negatively influenced by K+/K- contingencies. However, this distinction does not permit the description of dynamic processes leading to macroscopic properties such as the establishment of a single site, as opposed to multiple sites, of polarization. Such processes should rather be formulated in quantitative model languages, such as reaction-diffusion systems (Giese *et al.*, 2015). Other quantitative properties such as cell cycle duration, cell size during the different cell cycle stages and the influence of volume on kinetic processes cannot be described in rxncon language. To do so, other modeling formalisms are required which can handle quantitative data, such as rule-based or ODE-based modeling.

5.10.2 *Network comparison*

The scope of the Kaizu model (Kaizu *et al.*, 2010) covers cell cycle control, and signal transduction pathways and metabolic processes interfering with the cell cycle. Hence, the Kaizu model covers a larger range of processes than the CC-CNW. For the comparison between the models, the proteins which overlap in scope have been identified. The Kaizu model and the CC-CNW were compared on the level of the proteins both models account for. Both models have an overlap of 148 proteins, which is a relative overlap of approximately 67% for the Kaizu model, and 65% for the CC-CNW. The proteins accounted for exclusively in the Kaizu model are discussed in Section 5.9. Some of

these proteins were identified as peripheral to the scope to the CC-CNW. With regard to the requirement of regulatory, molecular knowledge to reconstruct the CC-CNW, it is currently difficult to account for the remaining proteins. However, the Kaizu model offers an excellent overview of targets to select for future model extensions, such as the connection to signal transduction processes which interfere with the cell cycle.

The network comparison is a qualitative measure based on the proteins both networks account for. However, such a comparison neglects other important information, such as if these proteins have physiologically relevant functions in the respective networks. Such a comparison would require the determination of the number of microstates which are connected in each network. An approximation of such a comparison is the estimation of the number of microstates in each network. The Kaizu model is published in an explicit format and reports 880 microstates in the complete network. Hence, the states which are not shown in the Kaizu model have been omitted. These omissions should be supported by literature. However, it is more likely that the omitted states are simplifications in the network, which also explains why the number of microstates in the CC-CNW is much higher compared to the Kaizu model, despite their large overlap in scope. The estimation of the number of microstates in the CC-CNW was attempted by exporting the CC-CNW to BNGL, enabling its translation into a microstate-based format. However, this translation could not proceed completely due to insufficient computational power, and was interrupted after three iterations, yielding 66773 microstates[1]. The true number of microstates in the CC-CNW is higher. Already at this point, the difference between the number of microstates in both networks is two orders of magnitude. The true number of physiologically relevant states accounted for in the CC-CNW is higher compared to the Kaizu model. Hence, the CC-CNW accounts for a much higher number of physiologically relevant states in cell cycle control.

5.10.3 *Summary*

To briefly summarize, the CC-CNW accounts for the molecular processes which control cell cycle progression in budding yeast. These molecular processes are based on empirical studies and hypotheses as described above. The collected empirical findings could be brought into context with each other, and constitute the description of a complete cell cycle on the level of molecular reactions and their regulation. The CC-CNW furthermore relies on few hypotheses, which are based on published studies, and which can be tested empirically in the future.

[1] Translation was performed on a Dell PowerEdge R815 4x AMD Opteron 6276 processor with 512 GB RAM.

6

The bipartite Boolean model

THIS CHAPTER PRESENTS the results from the gap-filling process of the CC-CNW candidate QlM, and the analysis of the gap-filled bipartite Boolean model. The candidate QlM was translated into an initial bipartite Boolean model. Section 6.1 describes the gap-filling process of the initial bipartite Boolean model. The gap-filling process resulted in a validated QlM, the final CC-CNW. The final CC-CNW was then translated into the bipartite Boolean formalism, and the behavior of the final bipartite Boolean model was analyzed. Section 6.2 shows the mutant analysis performed on the final bipartite Boolean model of the CC-CNW. Section 6.3 summarizes and discusses the results from this chapter.

6.1 Model validation by gap-filling

The reconstruction step of the cell cycle control network resulted in a candidate QlM, which was translated into an initial bipartite Boolean model using the formalism described in Section 3.4. This initial version of the bipartite Boolean model was computationally interrogated in order to study its functionality and adapt its behavior by gap-filling. The gap-filling step aims to analyze whether the bipartite Boolean model can reproduce the expected wildtype behavior, and which model changes need to be applied to the candidate QlM in order to achieve this.

The expected behavior of a wildtype budding yeast cell depends on the availability of nutrients. In starvational conditions, a wildtype cell in G_1 phase cannot commit to

cell cycle progression. Thus, the bipartite Boolean model should reflect this behavior and is expected to have a point attractor corresponding to G_1 phase. In the presence of nutrients, a wildtype cell shows oscillatory behavior, as it traverses the different stages of the cell cycle multiple times. Nutrient dependency is implemented in the candidate QlM, and upon nutrient availability, the bipartite Boolean model is expected to have a cyclic attractor which traverses the macroscopic states according to the physiological stages of a wildtype cell.

This section first, describes the gap-filling process resulting in the final CC-CNW and bipartite Boolean model (Section 6.1.1), and second, presents the behavior of the final bipartite Boolean model after gap-filling (Section 6.1.2).

6.1.1 *Gap-filling*

The gap-filling process of the bipartite Boolean model was performed in two steps. The aim of the first step (step 1) was to gap-fill the Boolean model to achieve the expected behavior of a wildtype cell in the absence of nutrients. The aim of the second step (step 2) was to use the model version retrieved from step 1 and gap-fill it to achieve the expected behavior of a wildtype cell in the presence of nutrients.

The gap-filling process furthermore required the definition of an initial state used in the simulations of the Boolean model. As a Boolean model with n nodes has 2^n possible initial states, rendering a complete search for all initial states infeasible, it was instrumental to use *a priori* knowledge in order to define an initial state which corresponds to G_1 phase. The translation of the QlM from rxncon language into the bipartite Boolean formalism provides a default initial state vector where all reaction nodes, input-output nodes, and non-neutral elemental states are set to false, and all neutral elemental states are set to true. The default initial state vector was changed according to *a priori* knowledge regarding the activity of the gene clusters considered in the model. From the six gene clusters (Table 5.1), only the Mcm1 cluster is active during early G_1 phase in the absence of nutrients. This was accounted for in the initial state by setting the Mcm1 gene products to true, and the gene products of the remaining five clusters to false. In addition, the SBF cluster is inhibited by Whi5 and the HDACs Hos3 and Rpd3 in G_1 phase, which was accounted for in the initial vector by setting the elemental states mediating the inhibition to true. The default initial state vector was changed accordingly, and used for simulation.

In step 1, the Boolean model was simulated and the trajectory analyzed iteratively, using this initial state definition based on *a priori* knowledge. The expected outcome of the simulation is a trajectory resulting in a point attractor without premature activation of gene clusters and macroscopic states downstream of Mcm1 activation. However, several unexpected observations were detected which required model adaptation. Table 6.1 summarizes the observations and the changes applied to the candidate QlM.

Table 6.1. *Gap-filling step 1.* These observations of the initial bipartite Boolean model did not correlate with wildtype behavior and required changes to the candidate QlM. *refers to Fkh2, Ndd1, and Mcm1.

Observation	Change	Reference
MBF regulated cluster constitutively active	Swi6 phosphorylation requirement for MBF cluster activation	Palumbo *et al.* (2016)
Fkh2* regulated cluster constitutively active	Fkh2 phosphorylation requirement for Fkh2* cluster activation	Pic-Taylor *et al.* (2004)
Clb2,5 not degraded in G_1	Degradation linked to both APC machineries	Wäsch and Cross (2002), Lu *et al.* (2014)
SBF inhibition not functional	Change of Boolean signs	
Pcl9 degradation not regulated	Degradation equivalent to Pcl1,2	Hernández-Ortega *et al.* (2013)
Pho85-Pcl9 phosphorylation of Whi5 overrules Cdc28 regulation	Change from strict requirement to positive influence	

Simulation of the initial bipartite Boolean model revealed constitutive activation of the MBF and Fkh2, Ndd1, Mcm1 controlled clusters, causing premature activation of their targets. Furthermore, the initial implementation of SBF inhibition did not work as anticipated, resulting in premature SBF cluster activation. The wave of activation of the three gene clusters resulted in the production of Clb2 and Clb5, two proteins which are unstable during G_1 phase. However, the two proteins remained in the system even after deactivation of the gene clusters. Furthermore, it was observed that the presence of the Pho85-cyclin Pcl9 caused permanent deactivation of the SBF inhibitor Whi5. Whi5 deactivation occurs in a Cdc28–Cln3 dependent manner in a wildtype cell and should depend on nutrient availability. In the following, the model adaptations applied to correct the model behavior are described.

Constitutive activation of the MBF regulated cluster in the bipartite Boolean model was caused by a lack of MBF regulation. This is in agreement with the lack of conclusive data describing the regulatory mechanism of MBF activation (Enserink and Kolodner, 2010). The Boolean model, however, requires strict regulation to allow periodic activation and deactivation. In the study by Palumbo *et al.* (2016), MBF activation depends on Swi6 phosphorylation by Cdc28–Cln1,2,3 at four CDK sites. This mechanism was then implemented as a strict requirement for MBF regulation in the CC-CNW. However, the regulation of MBF is experimentally not conclusively verified, and a Swi6 mutant with alanine substitutions at the CDK sites is viable (Wagner *et al.*, 2009).

Activation of the cluster controlled by Fkh2, Ndd1, and Mcm1, depends on the interaction between Fkh2 and Ndd1, and this interaction was initially regulated by a positive influence of the Cdc28–Clb1,2,5,6 mediated phosphorylation of Fkh2. Since the bipartite Boolean model ignores such quantitative statements, the cluster controlled by Fkh2, Ndd1, and Mcm1 remained constitutively active. To prevent premature activation, the positive influence of phosphorylated Fkh2 on its interaction with Ndd1 was changed

to a strict requirement. This strict requirement underlies cell cycle dependent control and hence, the gene activity in this cluster follows periodic activation.

The pulse of the Fkh2, Ndd1, Mcm1 controlled cluster activation resulted in the production of Clb2 and Clb5, which are normally unstable in G_1. To account for this, the degradation of Clb2 and Clb5 was extended from APC/C-Cdc20-mediated degradation to degradation by both APC/C machineries, supported by the studies Wäsch and Cross (2002), and Lu *et al.* (2014).

The SBF activated cluster is inhibited by Whi5 in early G_1. The initial mechanism accounted for Whi5-mediated inhibition via a requirement of Swi6 being unbound to Whi5 in order to permit SBF activation. The Whi5-free Swi6 molecule, however, is always present in the network, and hence, inhibition of SBF could not be achieved. The inhibitory effect of Whi5 towards SBF cluster activation was changed to explicit SBF inhibition by the Swi6–Whi5 dimer. The Swi6–Whi5 dimer in turn, is regulated by a phosphorylation mechanism as explained in Section 5.2.2 and shown in Figure 5.3. The reimplementation of Whi5-mediated SBF inhibition was then functional.

Constitutive SBF cluster activation was also caused by unregulated Pho85-Pcl9-mediated phosphorylation of Whi5, inducing dissociation between Whi5 and the HDACs, which resulted in SBF cluster activation. This effect was caused by the permanent presence of Pcl9 in the simulation, causing constitutive Pho85 activation, and due to the strictly inhibitory effect of Pho85-mediated phosphorylation of Whi5 on HDAC dissociation. This was counteracted by two hypotheses. First, Pcl9 degradation was included with a hypothetical mechanism similar to Pcl1,2 degradation based on Hernández-Ortega *et al.* (2013). As the transcription of *PCL9* is periodic, accounted for in the CC-CNW by Ace2/Swi5-mediated control (Section 5.2.6), the protein Pcl9 should also be present periodically to ensure its temporal activation. The implementation of regulated degradation of Pcl9 accounts for periodic presence of Pcl9. Second, the initial rule which forced the dissociation of Whi5 from the HDACs by Pcl9-mediated phosphorylation of Whi5 dominated the regulatory machinery of Cdc28–Cln1-3-mediated phosphorylation. However, a pho85Δ mutant is viable (Huang *et al.*, 2009), which was not reflected in the initial implementation. Furthermore, the Pho85 phosphorylation sites in Whi5 are unknown. In order to account for the current knowledge, the effect of Pho85–Pcl9-mediated phosphorylation of Whi5 was then changed to a negative influence on the association between Whi5 and the HDACs.

After implementation of the changes to the candidate QlM, listed in Table 6.1, the bipartite Boolean model was exported again, and simulated using the adapted initial state. The simulation trajectory did not reveal premature transcriptional activation anymore, and resulted in a point attractor. Hence, the updated candidate QlM was considered to be functional at this stage, and the point attractor from the simulation using the updated initial state was considered to be the G_1 point attractor.

In step 2 (Table 6.2), the point attractor retrieved from step 1 was used as the initial state but now with nutrient availability set to true. The expected outcome of the second

gap-filling step was a model simulation which, given the updated initial state, shows progression through the macroscopic cycles, starting with their neutral states, and returning to their neutral states in a cyclic manner. In other words, the outcome of the second gap-filling should reveal a model which has a cyclic attractor, where the transcriptional activation and progression through the macroscopic events appear in physiological order corresponding to wildtype behavior.

Table 6.2. *Gap-filling step 2.* These observations of the bipartite Boolean model after step 1 did not correlate with wildtype behavior in the presence of nutrients and required changes to the QIM.

Observation	Change
Mcm1 inhibition not functional	Change of Boolean signs
Discrepancy between Boolean and physiological time	Introduction of transcriptional delays
Sic1 deactivation too early	Change to phosphorylation by Cdc28-Cln1,2
Bud growth module insufficiently regulated	Introduction of regulation via macroscopic states and outputs
Stable complexes not maintained	Boolean statements added in SPB cycle
Rad53 transcriptional deactivation causing premature Rad53 depletion (Rad53 deg not regulated)	Strict requirement to K+ of MBF regulation
Resetting of G_1 not achieved	Introduction of equilibrium delays

The model retrieved from step 1 was simulated with the point attractor as initial state, and nutrient availability set to true. This simulation should show subsequent activation of SBF, MBF, and Fkh2,Ndd1,Mcm1 regulated clusters, and deactivation of the Mcm1 cluster. However, the simulation trajectory revealed several discrepancies between expected and observed behavior. The simulation revealed that the MBF cluster, which should maintain activity until DNA replication is finished, was inactivated prematurely. The simulation also revealed premature Sic1 deactivation, non-functional Mcm1 inhibition, premature interruption of the DNA replication checkpoint due to Rad53 depletion, and an incomplete resetting of all dynamic states to G_1. These observations were made iteratively, and the changes were applied iteratively.

In the presence of nutrients, the Mcm1 cluster activates Cln3, and Cln3 is the activator of SBF and MBF. Activation of these clusters also mediates Hcm1 activation and in turn, two inhibitors of Mcm1 become active, Yhp1 and Yox1. Their binding to Mcm1 inhibits the ability of Mcm1 to bind to promoters. In the initial implementation, this was accounted for by a requirement of Mcm1 being unbound to either of these inhibitors. However, similar to the case of SBF inhibition, this was not functional as the unbound state of Mcm1 is always present in the model. Instead, Mcm1 bound to either of its inhibitors was implemented as inhibitory for Mcm1 transcription.

Step 2 furthermore revealed premature inactivation of the repressor Sic1. Initially, Sic1 was phosphorylated by Cdc28–Cln1,2,3 and primed for degradation. Since Cln3 is the earliest cyclin, Sic1 was antagonized as soon as Cln3 was present and before the Cln1,2 cyclins became fully active. This was counteracted by making Sic1 phosphorylation

dependent on Cdc28–Cln1,2, only. This is a model hypothesis which accounts for the quantitative effects observed in experiments, but which cannot be considered in the Boolean model.

Next, it was observed that MBF inactivation occurred prior to DNA replication termination, which is not in accordance with empirical data. The reason for this is the discrepancy between Boolean time and physiological time: In the Boolean model, the rules are updated synchronously. This means that the linear flow of information depends on the distance between nodes and hence, the number of Boolean reactions which separate them. In a physiological environment, chemical reactions have different reactions times. This is exemplified by the amount of time it takes to express genes in comparison to signaling reactions. The transcriptional clusters in the CC-CNW in general only require transcription factor binding, transcription and translation. These processes in Boolean time do not provide a sufficient amount of time to activate the DNA replication checkpoint and act on MBF activity maintenance. This happens because there are more steps between DNA replication initiation and activation of the checkpoint measured by Rad53 kinase activation compared to the number of steps between activation and autoinhibition of the MBF cluster. The discrepancy between Boolean and physiological time can potentially occur in every gene cluster. To circumvent this problem, an artificial time delay was applied to each regulated gene cluster. The time delay consists of 20 input-output nodes based on the distance between DNA replication checkpoint activation and MBF inhibition. The same delay was implemented for all clusters. In addition to the transcriptional delays, an equilibrium delay was implemented and connected to the Mcm1 cluster. This implementation was necessary to equilibrate the state of the system to full inactivation. The implementation of the time delays showed transcriptional activation of the gene clusters in a manner similar to a wildtype yeast cell.

The second gap-filling step revealed that the bud growth cycle was not sufficiently regulated, which is not in accordance with the observations. To account for the observation that actin cables in the bud are polymerized from the site of polymerization, the recruitment of Bni1 to Cdc42 and Rho1 was made dependent on the output *[SymmetryBreaking]*. Similarly, the actin cables in the daughter cell are polymerized from the bud neck, which was accounted for by the requirement *[BudNeck]* for Bnr1 interaction with Cdc42 and Rho1. Swe1 monitors bud morphology and is degraded when a bud has formed. Swe1 degradation is initiated by a signaling cascade involving Hsl1 and Hsl7 (Howell and Lew, 2012). To account for the activation of this cascade in response to bud formation, the interaction between Hsl1 and Cdc3, in the CC-CNW the most upstream interaction of the cascade, was made dependent on the input *[BudGrowth]*. *[BudGrowth]* in turn depends on the macroscopic state *Cell_[(bud)]-{growth}*, which represents a cell with a growing bud.

The second gap-filling step revealed that the SPB subunit Spc42 was degraded before a complete SPB could be assembled. Spc42 forms a crystalline structure in the SPB,

which presumably protects it from degradation (Bullitt *et al.*, 1997). To account for degradational protection, all SPB states which imply the formation of a Spc42 crystalline structure were collected in a Boolean node *Spc42Crystal*, which protects Spc42 from degradation as described in Section 5.7.2.

Towards the end of the cell cycle, the states must be returned to their initial values, ensuring the resetting of the cell cycle. However, the simulation of the model revealed that the initial states were not reset. Similar to the transcriptional delay, an equilibrium delay with 20 steps, which was found to be sufficient, was implemented to allow the system to equilibrate and reset.

6.1.2 *Qualitative network model*

The CC-CNW is reconstructed in rxncon language and based on empirical data. However, macroscopic properties of the cell during different cell cycle stages are difficult to describe with elemental reactions corresponding to biochemical reactions, and hence, macroscopic reactions were implemented (Section 5.5) to describe these properties. This section shows how these macroscopic reactions and their corresponding states behave in a bipartite Boolean model without smoothing strategy and regulation. Next, the behavior of the regulated macroscopic states is shown as part of the complete network in the hybrid bipartite Boolean model, and finally, the behavior of the complete bipartite Boolean model of the CC-CNW is presented.

Figure 6.1 shows the behavior of unregulated macroscopic states in a bipartite Boolean system without smoothing. The initial state of the system, corresponding to G_1, starts with the neutral elemental states of the DNA, SPB and bud growth cycles set to true. The simulation has a cyclic attractor, as the initial values are reached again at the end of the simulation. The cytokinetic reaction takes the last state of each of these cycles and resets the states to their neutral, initial values. The cyclic attractor of the unregulated macroscopic states has a period of seven Boolean time steps. The period of the cyclic attractor in this system only depends on the number of macroscopic reactions within each of the cycles. The simulation demonstrates that the macroscopic states within one cycle are mutually exclusive. This is desired as their physiological counterparts are mutually exclusive, too. Figure 6.1 also demonstrates that the implementation of the macroscopic reactions is functional on a technical level, and that these macroscopic reactions reproduce the anticipated biological behavior.

In the complete CC-CNW, these macroscopic reactions are regulated by a biochemical network as described in Chapter 5. The CC-CNW translated into the bipartite Boolean formalism has 2506 nodes. Due to the size of the CC-CNW, the complete simulation trajectory for all nodes cannot be shown in detail. Instead, Figure 6.2 shows the attractors of the macroscopic states in the context of this biochemical regulatory network using the initial state vector identified after the gap-filling process. The CC-CNW has a point attractor in the absence of nutrients, shown to the left in Figure 6.2. The cell cycle is arrested in early G_1, which is observed by the macroscopic states of the DNA and

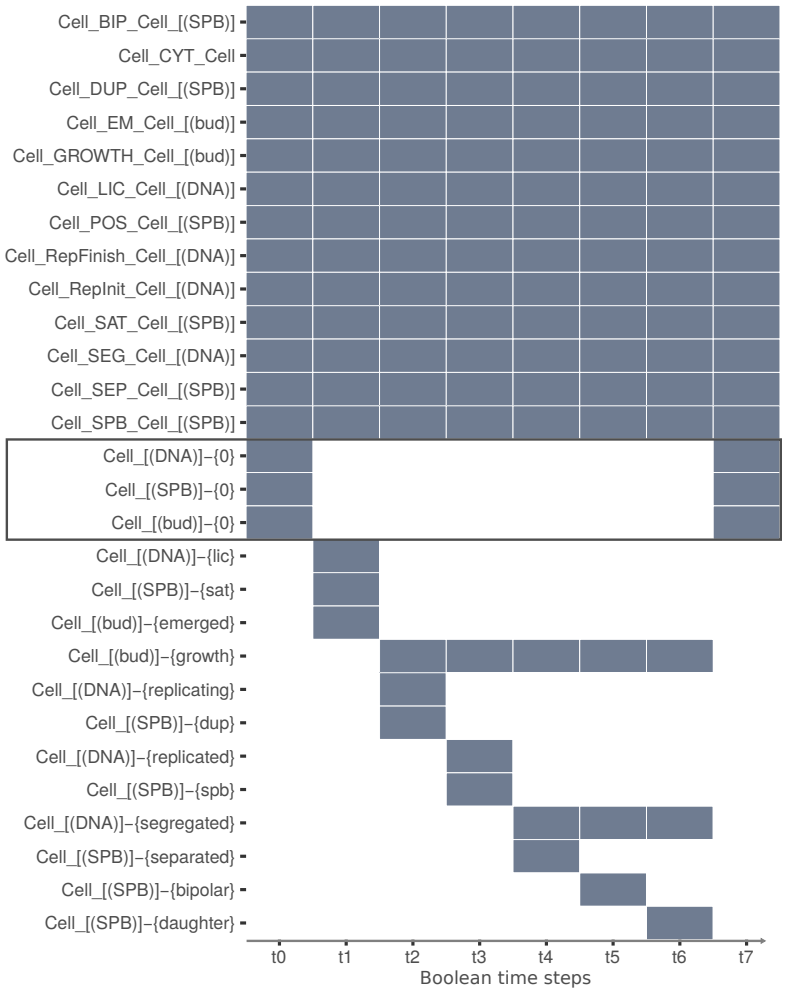

Figure 6.1. *Macroscopic cycles simulation.* The simulation trajectory of the macroscopic states without smoothing. The Boolean system of the macroscopic cycles has a cyclic attractor with a period of 7 Boolean time steps. The neutral elemental states are marked with a box to emphasize that the system is able to reset the states to their initial values. Blue: Active states; white: inactive states.

SPB cycles, where DNA is licensed and the satellite formation is primed. These processes are accomplished before Cdc28 becomes active. The bud has furthermore not emerged, as this requires Cdc28-mediated polarization in the CC-CNW. Hence, the cell does not pass G_1. In the presence of nutrients, the Boolean model has a cyclic attractor with a period of 165 Boolean time steps. Figure 6.2 shows a compressed trajectory of the complete cyclic attractor on the right side. The gray boxes show where the attractor was truncated, and the numbers inside the gray box indicate how many time steps were omitted in the figure. The figure demonstrates that the bipartite Boolean model can reproduce the expected physiological behavior of a yeast wildtype cell.

The different cell cycle phases were interpreted on the basis of the macroscopic states. G_1 phase was defined as the period where DNA replication has not started, indicated

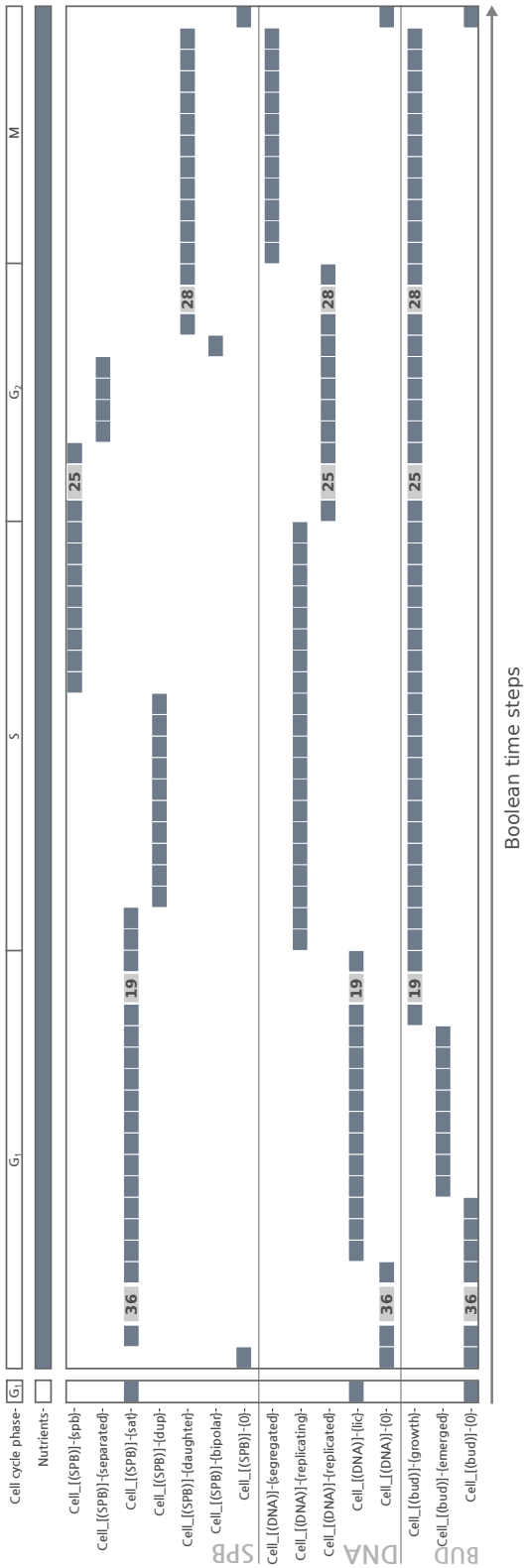

Figure 6.2. *Trajectory of macroscopic states in the CC-CNW.* The regulation of the macroscopic states of the cyclic attractor. The cyclic attractor shows that the neutral states are active in the beginning and reactivated at the end of the cycle. During the simulation, the other macroscopic states are traversed in the expected order and only once. Due to space limitations, non-dynamic periods were cut and the number of steps are shown in the figure. Blue: Active states; white: inactive states.

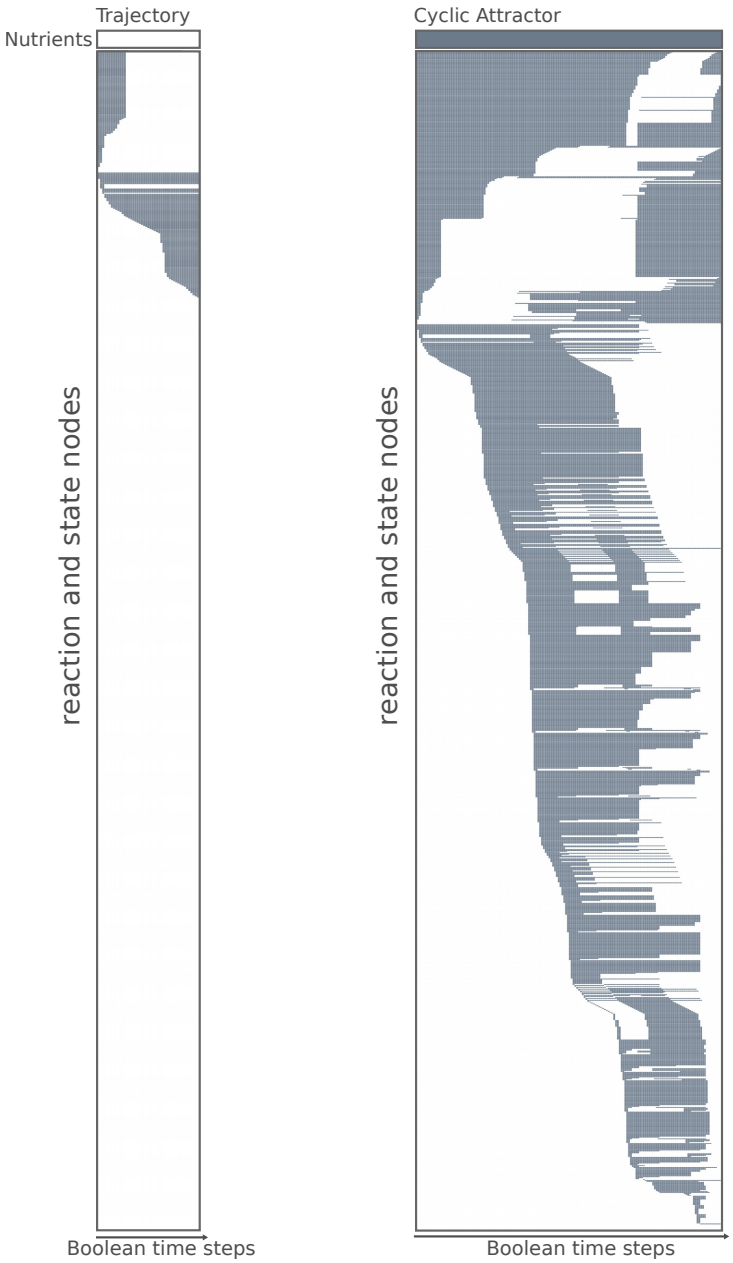

Figure 6.3. *Attractors of the cell cycle control network.* Left: Trajectory without nutrients. The simulation reaches a point attractor in step 47. Right: The cyclic attractor has a period of 165 steps. In both figures, the dynamic states and the states which are never activated are shown. The constitutively active states are omitted. The lines between the two figures do not match, as they are ordered according to their dynamics. Blue: Active states; white: inactive states.

by the macroscopic states *Cell_[(DNA)]-{o}* and *Cell_[(DNA)]-{lic}*. Similarly, S phase was observed by the macroscopic state *Cell_[(DNA)]-{replicating}*, as this is an indicator of ongoing DNA synthesis. During S phase, the yeast cell has started budding, which is here indicated by the macroscopic states *Cell_[(bud)]-{emerged}* or *Cell_[(bud)]-{growth}*, where

the *Cell_[(bud)]-{growth}* state occurs simultaneously with ongoing DNA replication. Onset of G_2 phase is characterized by budded cells, indicated by the macroscopic states *Cell_[(bud)]-{emerged}* or *Cell_[(bud)]-{growth}*. At this stage, the cells are not binuclear. Hence, the two macroscopic states *Cell_[(DNA)]-{segregated}* and *Cell_[(SPB)]-{daughter}* are not active simultaneously. M phase is interpreted as the period where the cell is binuclear, indicated by the states *Cell_[(DNA)]-{segregated}* and *Cell_[(SPB)]-{daughter}* occurring simultaneously. This interpretation of the cell cycle phases on the basis of the macroscopic states is based on the morphogenic changes a yeast cell undergoes as described in Howell and Lew (2012). Figure 6.3 shows the two attractors of the complete bipartite Boolean model of the CC-CNW using the previously identified initial state in the absence (left side), and in the presence (right side) of nutrients. To reduce the size of the figures, only the dynamic states, and the states which are not activated during one simulation are shown. The nodes which are constitutively active are omitted. The left side of Figure 6.3 shows the simulation trajectory of the bipartite Boolean model using the initial state retrieved after the gap-filling process, and with nutrients set to false. The simulation culminates in a point attractor, corresponding to time step 47 in the simulation. This behavior is in congruence with the expected wildtype behavior of a yeast cell in nutrient depleted conditions. The macroscopic states show that the cell has licensed DNA, formed a bridge primed for satellite formation, and a non-growing bud (Figure 6.2). These states can be reached without activated Cdc28. The state shown on the left side of Figure 6.3 hence, corresponds to G_1.

The right side of Figure 6.3 shows a complete simulation trajectory of the bipartite Boolean model using the same initial values as in the left side, but with nutrients available. The shown trajectory corresponds to a cyclic attractor with 165 Boolean time steps. In this scenario, nutrients are available, and the cell can grow and divide. This behavior is reflected in the overall simulation, which shows oscillatory behavior. The cell starts with the conditions previously identified corresponding to G_1. The cell traverses all macroscopic states, and resets all microscopic states to G_1 conditions. Indeed, the simulation reproduces the wildtype behavior of a yeast cell at birth until it gives birth to a new offspring. The model retrieved after gap-filling and the initial state identified in the process were considered to be a functional cell cycle control network. This control network was used for analysis as described in Section 6.2.

6.2 Model analysis

The gap-filled CC-CNW from the previous step was analyzed for three different scenarios to further validate the model behavior: (i) Induction of cell cycle arrest via chemicals (Section 6.2.1), (ii) mutational study (Section 6.2.2), and a (iii) residue substitution study (Section 6.2.3). The simulations of this analysis were interpreted in the following way: A phenotype was declared as viable if it could traverse the macroscopic states, and if the simulation reproduced a cyclic attractor. A phenotype was considered inviable if it either produced a cyclic attractor without passing all

macroscopic states, or if it produced a point attractor.

6.2.1 *Cell cycle arrest*

The effects of four cell cycle arrest inducing chemicals were implemented in the CC-CNW, and the model behavior tested in presence of each of these chemicals. These chemicals are pheromone, causing G_1 arrest; nocodazole, inhibiting actin polymerization and causing arrest at G_2/M; LatA, depleting the dNTP pool and causing arrest at G_2/M; and HU, which inhibits DNA replication, causing arrest in S phase. Table 6.3 shows the arrest points in the bipartite Boolean model and compares it to the observed cell cycle arrest. The *in silico* cell cycle phases were interpreted on the basis of the macroscopic states as described in Section 6.1.2.

Figure 6.4 shows the attractors of the macroscopic states for each treatment. Pheromone, hydroxyurea and nocodazole treatment result in a global point attractor, whereas LatA treatment results in a global cyclic attractor. However, the macroscopic states do not cycle. Hence, all four chemicals induce cell cycle arrest in the bipartite Boolean model. The cell cycle arrest induced by these chemicals could be reproduced in the bipartite Boolean model.

Table 6.3. *Implemented cell cycle arrest points.* The table shows the different mutants investigated with simulations, and how they compare to phenotypes.

Chemical	Model	Experiment
Pheromone	G_1	G_1
Hydroxyurea	S	S
Nocodazole	G_2/M	G_2/M
Latrunculin A	G_2/M	G_2/M

Pheromone treatment resulted in a point attractor with licensed DNA. Since DNA replication could not be induced, the cell is arrested before S phase, hence, the cell is arrested in G_1 phase. HU treatment resulted in a growing cell, indicated by *Cell_[(bud)]-{growth}*, with ongoing DNA replication, indicated by the *Cell_[(DNA)]-{replicating}* state. Hence, cell cycle arrest occurred during S phase. Nocodazole treatment permitted the cell to finish S phase, as the macroscopic state of the DNA cycle reached the *Cell_[(DNA)]-{replicated}* state. A bud had also formed, indicated by the state *Cell_[(bud)]-{growth}*. However, the cell is mononuclear, as the DNA could not be segregated and distributed to the daughter cell. Hence, the cell was arrested in G_2 phase. Similarly, LatA treatment also arrested a budded cell after S phase. However, as the DNA could be segregated, indicated by the *Cell_[(DNA)]-{segregated}* state, it was not yet positioned in the daughter cell. Hence, LatA also induced arrest in G_2 phase.

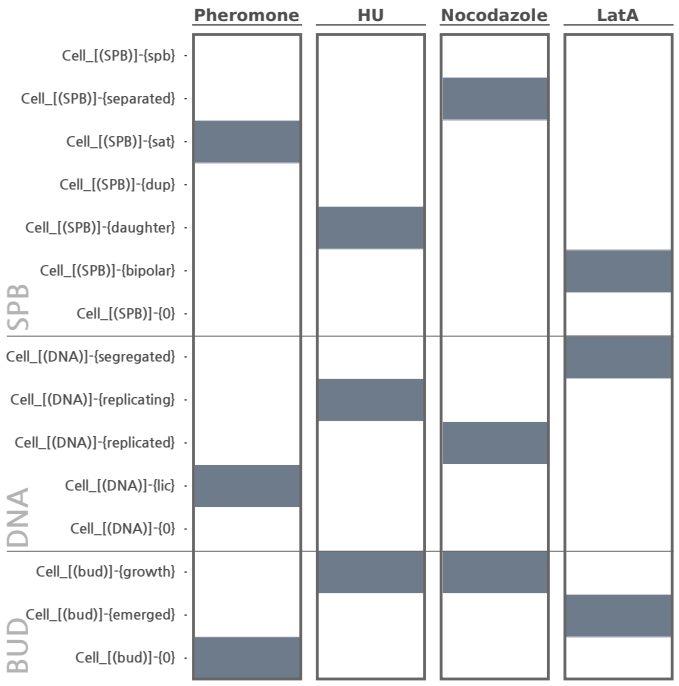

Figure 6.4. *Cell cycle arrest points.* The attractors of the macroscopic states for each treatment are shown. Pheromone, HU, and nocodazole treatment result in a global point attractor. LatA treatment results in a global cyclic attractor, however, the macroscopic states do not show cyclic behavior. Blue: Active states; white: inactive states.

6.2.2 *Gene knockouts*

The model behavior was further investigated with a knockout analysis for known mutant phenotypes (Table 6.4). For this analysis, the indicated genes were inactivated in the model, corresponding to gene knockouts. In total, 32 gene knockout mutants were tested, with 27 single mutants, four double mutants, and one triple mutant.

Figure 6.5 shows the arrest points of the macroscopic states of the mutants which were inviable. The analysis revealed that the bipartite Boolean model could reproduce the phenotypes of 29 mutants of the 32 tested gene knockout mutants. The phenotype of the *bni1*Δ mutant could not be reproduced in the bipartite Boolean model. Bni1 is one of two formins involved in actin cable polymerization, and has redundant functions with Bnr1 (Imamura *et al.*, 1997). The CC-CNW accounts for the redundant function between Bni1 and Bnr1 with regard to actin cable polymerization. However, the mechanism of Bnr1 involved in exocytosis is not known and hence, is not accounted for in the CC-CNW.

The phenotype of the *cln3*Δ mutant could not be reproduced in the bipartite Boolean model. In the CC-CNW, Cln3 is responsible for the activation of the SBF cluster. Hence, in the *cln3*Δ mutant, the SBF cluster cannot be activated and the cell cycle not proceed. In a wildtype cell, the cyclins Cln1 and Cln2 contribute to SBF activation, which is not

accounted for in the CC-CNW. Cln1 and Cln2 are activated by SBF, and hence, they cannot be present before their own activation in a Boolean model. The phenotype of the *clb5*Δ*clb6*Δ mutant could not be reproduced in the bipartite Boolean model. The cyclins Clb5 and Clb6 have redundant roles with the cyclins Clb3 and Clb4. The CC-CNW does not account for Clb3 and Clb4 functionality as their functional regulation remains to be deciphered.

Table 6.4. *Investigated mutants.* The table shows the different mutants investigated in the simulation and their comparison to phenotypes. The SGD entries for some pheontypes were used as indicated (`www.yeastgenome.org`, Cherry *et al.* (2011)).

Mutant	Model	Experiment	Reference
*bnr1*Δ	viable	viable	Imamura *et al.* (1997)
*cdc55*Δ	viable	viable	SGD
*clb1*Δ	viable	viable	Surana *et al.* (1991)
*clb2*Δ	viable	viable	Surana *et al.* (1991)
*clb5*Δ	viable	viable	Schwob and Nasmyth (1993)
*clb6*Δ	viable	viable	Schwob and Nasmyth (1993)
*cln1*Δ	viable	viable	SGD
*cln2*Δ	viable	viable	SGD
*cln1*Δ*cln2*Δ	viable	viable	Dirick *et al.* (1995)
*cln3*Δ*whi5*Δ	viable	viable	Huang *et al.* (2009)
*cdc3*Δ	inviable	inviable	SGD
*cdc4*Δ	inviable	inviable	SGD
*cdc5*Δ	inviable	inviable	SGD
*cdc6*Δ	inviable	inviable	SGD
*cdc7*Δ	inviable	inviable	SGD
*cdc10*Δ	inviable	inviable	SGD
*cdc11*Δ	inviable	inviable	SGD
*cdc12*Δ	inviable	inviable	SGD
*cdc14*Δ	inviable	inviable	SGD
*cdc15*Δ	inviable	inviable	SGD
*cdc20*Δ	inviable	inviable	SGD
*cdc24*Δ	inviable	inviable	SGD
*cdc28*Δ	inviable	inviable	SGD
*cdc31*Δ	inviable	inviable	SGD
*cdc34*Δ	inviable	inviable	SGD
*cdc42*Δ	inviable	inviable	SGD
*cdc53*Δ	inviable	inviable	SGD
*clb1*Δ*clb2*Δ	inviable	inviable	Surana *et al.* (1991)
*cln1*Δ*cln2*Δ*cln3*Δ	inviable	inviable	Richardson *et al.* (1989)
*bni1*Δ	inviable	viable	Imamura *et al.* (1997)
*clb5*Δ*clb6*Δ	inviable	viable	Kühne and Linder (1993)
*cln3*Δ	inviable	viable	SGD

The remaining 29 tested mutants did reproduce the expected *in vivo* phenotypes on the level of viability. The *in silico* mutants can be investigated further with regard to the cell cycle phase in which they are arrested. Such an analysis, however, requires the consultation of other types of data, and is not within the scope of this study.

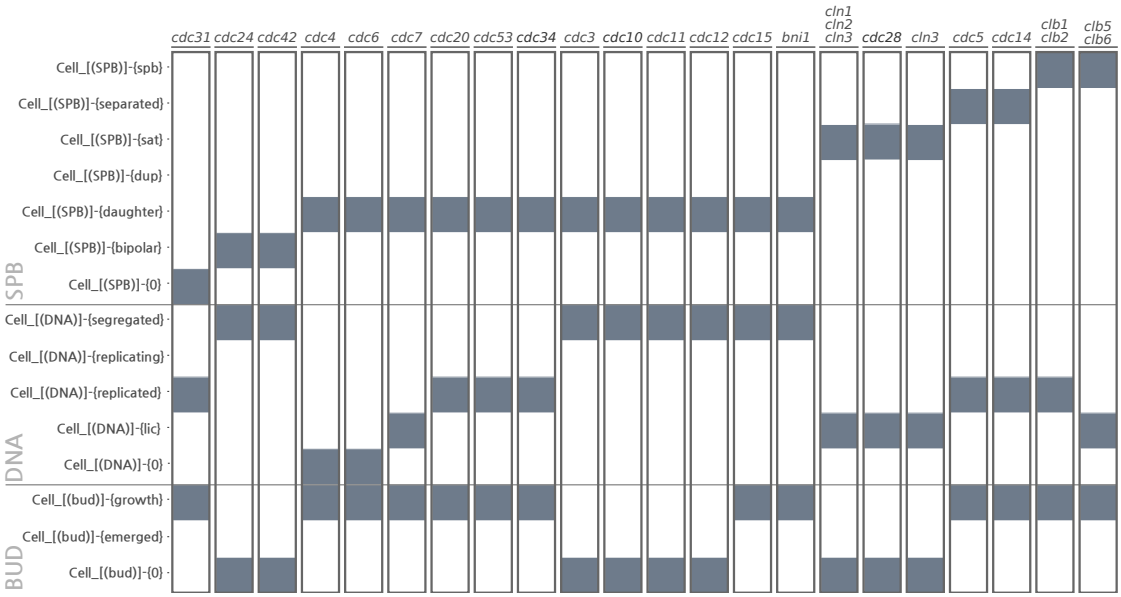

Figure 6.5. *Mutant analysis.* The inviable mutants and their attractor states of the macroscopic states are shown. Blue: Active states; white: inactive states.

6.2.3 *Residue substitution*

The resolution of data in rxncon language permits the analysis of mutations on the level of residue substitutions in the bipartite Boolean model. Thus, the third analysis was performed to analyze the behavior of versions of the bipartite Boolean model corresponding to alanine substitution mutants (Table 6.5). Five residue mutants were considered, three of which could reproduce the associated phenotpyes. Figure 6.6 shows the attractors of the macroscopic states of the two mutants which could not reproduce the phenotype.

Table 6.5. *Residue substitution analysis.* The table shows the substitutions analyzed and the comparison to phenotypes.

Mutant	Model	Experiment	Reference
whi5-12A	viable	viable	Wagner *et al.* (2009)
swi6-4A	inviable	viable	Wagner *et al.* (2009)
spc110-2A CDK	viable	viable	Lin *et al.* (2014)
spc110-2A Mps1	viable	viable	Lin *et al.* (2014)
spc110-4A	inviable	viable	Lin *et al.* (2014)

The bipartite Boolean model could not reproduce the viable phenotype of a swi6-4A mutant. In the CC-CNW, the phosphorylation of four CDK sites is strictly required for activation of MBF regulated genes. This requirement was introduced in the gap-filling process (Section 6.1.1) in order to account for MBF regulation and is based on the study by Palumbo *et al.* (2016). The study by Wagner *et al.* (2009), however, demonstrated

that the swi6-4A mutant is viable. The discrepancy between the *in silico* and *in vivo* phenotypes is hence, not a surprise. This strict requirement, however, is not crucial in a quantitative model and can be changed accordingly.

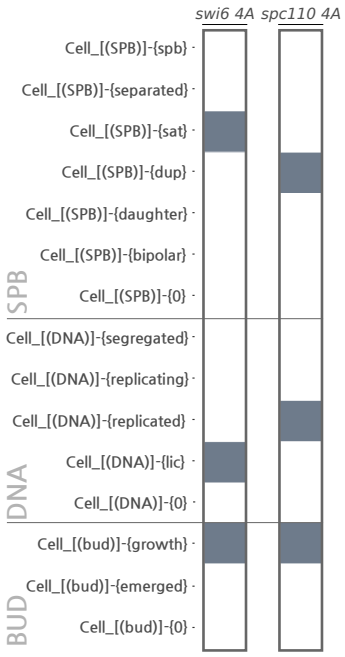

Figure 6.6. *Residue substitution.* The inviable mutants and their attractor states of the macroscopic states are shown. Blue: Active states; white: inactive states.

The bipartite Boolean model reproduces the behavior of two spc110 mutants with substituted CDK and Mps1 sites, respectively. The CC-CNW accounts for two of the three reported Mps1 sites, hence, the CC-CNW is functionally equivalent to the triple Mps1-site mutant.However, a CC-CNW mutant with four alanine substituted sites is not viable, as opposed to observation (Lin *et al.*, 2014). The phosphorylation at at least one of these sites is a strict requirement for Spc110 interaction with Spc98 in the CC-CNW. To account for viability of this mutant, this strict requirement can be changed to a positive influence.

6.3 Discussion

Empirical data was collected to reconstruct the CC-CNW in rxncon language, resulting in a candidate QlM. The candidate QlM was then translated from rxncon language into a bipartite Boolean formalism, introduced in Section 3.4.1. Next, the bipartite Boolean model was used in a gap-filling process according to the description in Section 4.2. The gap-filling required the estimation of an initial state for the Boolean model and was

based on *a priori* knowledge. Hence, the functional analysis of the CC-CNW could proceed without the requirement of additional estimation of parameters or kinetic laws. The gap-filling process enabled the analysis of the functionality of the CC-CNW, that is, to analyze whether the information flow in the network can proceed, and that the regulation of the information flow results in a model behavior expected from biological observation.

The gap-filling process revealed mechanistic gaps of both technical and biological nature. The technical gaps regarded the initial implementation of inhibitory mechanisms for SBF and Mcm1. These gaps could be anticipated without changing the underlying biological knowledge. Furthermore, the analysis of the Boolean model demonstrated that the discrepancy between physiological and Boolean time lead to transcriptional activation of a cluster which should become active after DNA replication has finished, as the transcriptional process required less Boolean time steps compared to the activation of the pathway which regulates it. This was solved by adding artificial delays to the network, without changing the underlying biological knowledge. In a similar way, the gap-filling process showed that Spc42 was degraded before a second SPB was assembled. Spc42 in the SPB forms a crystalline structure which likely protects it from degradation (Bullitt *et al.*, 1997). Hence, the introduced states *Spc42Crystal* which imply Spc42 as part of the forming SPB, are in accordance with biological data.

Other gaps required the reinterpretation of empirically supported contingencies to enable network regulation. To this end, quantitative contingencies were changed to strict requirements, as in the case for Fkh2, Ndd1, Mcm1 cluster activation. The positive influence of Fkh2 phosphorylation in Fkh2, Ndd1, Mcm1 cluster activation was changed to a strict requirement. Similarly, MBF regulation had to be added to the model, as its otherwise constitutive activation is not in congruence with empirical findings. As MBF regulation is not completely known, a hypothetical requirement of Swi6 phosphorylation was added. As the Boolean model cannot distinguish quantitative effects, Cdc28–Cln1,2,3-mediated phosphorylation of Sic1 had to be changed to be carried out by Cdc28–Cln1,2, only. Without this change, SBF and MBF activation occurs simultaneously to Mcm1 cluster activation, which is not observed. The bud growth cycle required implementation of regulation via macroscopic states and outputs to ensure the observed order of processes associated with bud emergence and growth. These additional requirements underly the observation that a yeast cell polarizes its membrane, polymerizes actin cables from these sites of polarization, and has a means of internally assessing bud morphology to allow cell cycle progression.

Analysis of the model identified unexpected stability of Clb2 and Clb5 during G_1, and premature Rad53 depletion. Both observations could be adapted in accordance with biological measurements.

The initial implementation of Pcl9 contribution to SBF cluster activation had to be changed, as the implemented mechanism dominated the effect of the empirically observed machinery mediated by Cdc28–Cln1,2,3. The final implementation is in

accordance with the supporting role of Pho85–Pcl9 in SBF regulation, future empirical studies might reveal more mechanistic details.

Overall, the gaps the CC-CNW were of technical nature in some cases, and occurred due to insufficient empirical data in other cases. The model changes are reported, and, where applicable, substantiated with empirical observation. These changes lead to a model version which was functional in terms of cell cycle progression. Functionality was observed by model simulation using the initial state previously defined: The trajectories of the macroscopic states, in absence of nutrients arrest the cell cycle in G_1. In the presence of nutrients, the macroscopic states traverse a complete cell cycle, while being regulated by a biochemical network.

Furthermore, the functionality of the network could be demonstrated by the analysis of its response to cell cycle inhibitors, and of mutant phenotypes. The model was found to correctly arrest in the presence of the four tested cell cycle inhibitors, and reproduced the behavior of 32 out of 37 tested mutant phenotypes. The mutants could be tested on the level of gene knockout, and on the level of residue substitutions. The five phenotypes which could not be reproduced are explained in Sections 6.2.2 and 6.2.3.

The results from this chapter show that the empirical knowledge in combination with the macroscopic states and reactions, suffices to explain the cell cycle behavior by simulation of the network as a bipartite Boolean model. The gaps revealed in this study can be followed up by refining the underlying rxncon network when more information about the mechanistic details becomes available.

7

Conclusion and outlook

> Chaos was the oft-quoted blind play of atoms, which, in mechanistic and positivistic philosophy, appeared to represent ultimate reality, with life as an accidental product of physical processes, and mind as an epi-phenomenon.
>
> *(Ludwig von Bertalanffy)*

THIS THESIS PRESENTS A large-scale reconstruction of the cell cycle control network in *S. cerevisiae*, the CC-CNW. The reconstruction in rxncon language puts the current knowledge of the network controlling cell cycle progression into context, and, gap-filled and translated into a bipartite Boolean model, shows that it can explain the cyclic behavior of the cell cycle. This chapter concludes this study and proposes suggestions for further investigations (Section 7.1), gives an outlook into the future (Section 7.2), and Section 7.3 closes the thesis.

7.1 Conclusion and future work

This study presents a reconstruction in rxncon language of the biochemical knowledge of the processes which control the cell cycle in *S. cerevisiae*. In Chapter 5, the biomolecular details of the CC-CNW are shown and discussed. For the reconstruction process, biochemical evidence on the level of elemental reactions and contingencies

was used. On this level of resolution, a large part of the cell cycle control network could be reconstructed, as demonstrated by the references to the data which was used (Tables A.2 to A.4).

In Section 1.4, four questions were identified at the core of this study. First, is the current knowledge sufficient to link the relevant components of the cell cycle control network mechanistically? This study showed that the empirical knowledge is sufficient to link and regulate the events of three independent cycles, DNA replication, SPB duplication, and bud growth. However, from these studies only, the global properties of the cell cycle regulatory network cannot be observed, which connects to the second question: Can we reproduce the oscillatory behavior of the cell cycle? These three cycles had to be linked to each other via macroscopic reactions, which refer to macroscopic properties of a cell. The CC-CNW required the introduction of new reaction types, the macroscopic reactions, which represent macroscopic properties of the DNA replication, SPB duplication, and bud growth cycles. The regulatory layer of the CC-CNW controls these macroscopic reactions via inputs, and the macroscopic states evolving from the macroscopic reactions control the biochemical regulatory network. In connection with the macroscopic states, the three independent cycles could be synchronized with each other. Together, they can reproduce the oscillatory behavior of a dividing yeast cell and represent a yeast cell at birth, giving birth to a new yeast cell towards the end of the cell cycle. In other words, the biological information which encodes and controls cell cycle progression cannot be followed by biochemical regulation alone. Hence, the biochemical regulatory layer of the CC-CNW itself does not account for the cyclic behavior of the cell cycle. Can we identify gaps in the network? Chapter 6 shows how the collected knowledge behaves in a bipartite Boolean model. The analysis of the initial bipartite Boolean model revealed that the collected knowledge had regulatory gaps, which were addressed in the gap-filling process. The reconstruction and gap-filling processes together revealed that the available regulatory knowledge of cell cycle control lacks a mechanism for MBF cluster activation, the control of *CLB4* and *DBF4* regulation, insufficient data to describe Cdc28 cyclin dependence and functional redundance, and insufficient data to account in mechanistic detail for the Pho85-mediated activation of SBF. Finally, does the reconstructed network reproduce known phenotypes? The CC-CNW reproduces 32 out of 37 tested phenotypes. This analysis can be extended in future work to include more mutants and to refine the CC-CNW to account for additional mechanistic detail.

The CC-CNW was reconstructed and analyzed with the rxncon approach. The CC-CNW is based on a few simplifications, such as the omission of explicit DNA polymerization reactions, or Spc42 crystal topology. However, the CC-CNW accounts for 229 proteins which have been identified to be involved in cell cycle progression. The CC-CNW is in scope and comprehensiveness similar to the Kaizu model (Kaizu *et al.*, 2010). However, the microstate-based comparison between the CC-CNW and Kaizu model revealed that the CC-CNW accounts for a much higher number of microstates.

The CC-CNW describes more than $6.6 \cdot 10^4$ microstates compared to the 880 microstates accounted for in the Kaizu model. Yet, the reconstruction in rxncon language only requires 1246 elemental reactions and 801 contingencies to describe these macrostates. Moreover, the Kaizu model is not simulatable in SBML, as it does not have specified rate laws or parameters. Hence, the Kaizu model cannot be analyzed with regard to its functionality and collective properties. In this study, it was shown that the rxncon model base of the CC-CNW could be simulated after translation into the bipartite Boolean formalism, but also that the information does convey the biochemical information, and, moreover, oscillates in accordance with wildtype behavior, given an initial state. Such an analysis was previously shown in Boolean networks with a small number of nodes, such as in the studies by Li *et al.* (2004) and Irons (2009). The bipartite Boolean formalism not only allowed the study of the wildtype and gene knockout mutants, but also the analysis on the level of protein residue mutants. Overall, this study demonstrated that the rxncon approach enables large-scale reconstruction of a cell cycle control network in mechanistic detail, yet maintaining congruence with empirical findings, which together form a functional and simulatable network that can reproduce yeast cell cycle behavior.

There are two different kinds of investigations that should be addressed in future work. The first regards the extension of the CC-CNW itself, the second regards the development of analysis tools for bipartite Boolean models of large-scale reconstructions.

Model extension. The CC-CNW describes the processes which control progression of the cell cycle in *S. cerevisiae*. The CC-CNW does not explicitly account for APC/C topology and its potential assembly regulation. The CC-CNW also omits explicit histone regulation. These processes are involved in cell cycle regulation, but were omitted here, due to insufficient biochemical data. Hence, the APC/C and histone regulation should be addressed in a future extension of the model, when more empirical data becomes available. Furthermore, there are several signal transduction pathways and stress responses which interfere with the cell cycle. These processes perturb the cell cycle and often require a cellular adaptation. The cell cycle only resumes after the adaptation. These pathways include the response to hyperosmotic stress (Saito and Posas, 2012), the response to pheromone signaling (Haber, 2012), and radiation induced DNA replication stress (Boiteux and Jinks-Robertson, 2013), some of which the Kaizu model accounts for. The inclusion of such pathways requires not only knowledge about how they operate on a molecular level, but also which cell cycle related processes they interrupt, and how this interruption is lifted to allow resumption of cell cycle progression. A reconstruction of these pathways and their molecular connection to cell cycle progression gives a more complete view of how the cell cycle is controlled.

Methods development. The rxncon toolbox provides the export from a rxncon model base into a bipartite Boolean formalism. Such a Boolean model can be analyzed with regard to the number and type of attractors (cyclic or acyclic), as well as the number of initial states which result in a certain attractor. This analysis enables the

identification of the attractors which are relevant in a study without using *a priori* knowledge. Furthermore, such an analysis allows to study the robustness of a network, as shown in Li *et al.* (2004). For a Boolean network with n nodes there are 2^n possible initial states. The bipartite Boolean model corresponding to the information in the QlM of the CC-CNW has 2506 nodes, and hence, 2^{2506} possible initial states, rendering an exhaustive search infeasible. Moreover, finding the point attractors of a Boolean network is known to be an NP-hard problem (Akutsu *et al.*, 1998), and finding cyclic attractors is considered to be at least equally complex. It was proposed that the estimation of the feedback vertex sets in a Boolean model can be used to identify point attractors, as well as to identify nodes which contribute to global dynamics in a Boolean network (Akutsu *et al.*, 1998; Mochizuki *et al.*, 2013). The integration of such an analysis tool into the rxncon toolbox facilitates network analysis with regard to its global properties, such as robustness.

7.2 Outlook

The ultimate goal in systems biology is to understand organisms holistically. Such an endeavor requires the integration of different kinds of biological information to describe the different intracellular and, where applicable, intercellular processes. Section 1.3.3 describes the properties of signal transduction pathways, and how these properties challenge reconstruction of large-scale signal transduction pathways. This study demonstrates that the rxncon approach successfully addresses these challenges, enabling the reconstruction of large-scale signal transduction processes in a scalable way, and allowing their computational interrogation. The rxncon approach harbors the potential to enable modeling of large-scale systems such as whole cell systems. This is an important step in order to understand not only yeast cells, but also other eukaryotic cells, such as human cells. Ultimately, this requires to allow to account for differences of the same type of cells between individuals. This is important to explain and act upon the individual propensity to develop certain diseases, and to find a personalized cure, which is the mission of the P4 medicine research project (Hood, 2013).

7.3 A map of life

In his autobiography, Richard Feynman describes an encounter with a librarian, from whom he requested a *map of a cat* (Feynman, 2010). Feynman was referring to a zoological chart of the anatomy of a cat. Such a map enables an immediate association between a cat and its inner structure. This kind of map is special with regard to the deduction we can do. These maps are an abstraction, yet tangible for general comprehension. The regulatory graphs presented in this thesis represent the cell cycle control network in yeast. Ultimately, the cell cycle is the molecular machinery underlying the process of life. However, usually, from these maps, the phenomenon of life cannot be deduced by looking at these maps, as life is an emergent property

of an intricate biomolecular mechanism. Capturing life in its entirety on a map is an endeavor for the future.

Bibliography

Abe, M., H. Qadota, A. Hirata, and Y. Ohya (2003). Lack of GTP-bound Rho1p in secretory vesicles of *Saccharomyces cerevisiae*. *The Journal of Cell Biology*, 162(1):85–97.

Agarwal, R. and O. Cohen-Fix (2002). Phosphorylation of the mitotic regulator Pds1/securin by Cdc28 is required for efficient nuclear localization of Esp1/separase. *Genes & Development*, 16(11):1371–1382.

Akutsu, T., S. Kuhara, O. Maruyama, and S. Miyano (1998). A system for identifying genetic networks from gene expression patterns produced by gene disruptions and overexpressions. *Genome Informatics*, 9:151–160.

Alberts, A. S. (2001). Identification of a carboxyl-terminal diaphanous-related formin homology protein autoregulatory domain. *Journal of Biological Chemistry*, 276(4):2824–2830.

Alcasabas, A. A., A. J. Osborn, J. Bachant, F. Hu, P. J. Werler, K. Bousset, K. Furuya, J. F. Diffley, A. M. Carr, and S. J. Elledge (2001). Mrc1 transduces signals of DNA replication stress to activate Rad53. *Nature Cell Biology*, 3(11):958–965.

Alexandru, G., F. Uhlmann, K. Mechtler, M.-A. Poupart, and K. Nasmyth (2001). Phosphorylation of the cohesin subunit Scc1 by Polo/Cdc5 kinase regulates sister chromatid separation in yeast. *Cell*, 105(4):459–472.

Archambault, V., E. J. Chang, B. J. Drapkin, F. R. Cross, B. T. Chait, and M. P. Rout (2004). Targeted proteomic study of the cyclin-Cdk module. *Molecular Cell*, 14(6):699–711.

Asano, S., J.-E. Park, K. Sakchaisri, L.-R. Yu, S. Song, P. Supavilai, T. D. Veenstra, and K. S. Lee (2005). Concerted mechanism of Swe1/Wee1 regulation by multiple kinases in budding yeast. *The EMBO Journal*, 24(12):2194–2204.

Ashe, M., R. A. de Bruin, T. Kalashnikova, W. H. McDonald, J. R. Yates, and C. Wittenberg (2008). The SBF-and MBF-associated protein Msa1 is required for proper timing of G1-specific transcription in Saccharomyces cerevisiae. *Journal of Biological Chemistry*, 283(10):6040–6049.

Audhya, A. and S. D. Emr (2002). Stt4 PI 4-kinase localizes to the plasma membrane and functions in the Pkc1-mediated MAP kinase cascade. *Developmental Cell*, 2(5):593–605.

Aung, H. W., S. A. Henry, and L. P. Walker (2013). Revising the representation of fatty acid, glycerolipid, and glycerophospholipid metabolism in the consensus model of yeast metabolism. *Industrial biotechnology*, 9(4):215–228.

Azzam, R., S. L. Chen, W. Shou, A. S. Mah, G. Alexandru, K. Nasmyth, R. S. Annan, S. A. Carr, and R. J. Deshaies (2004). Phosphorylation by cyclin B-Cdk underlies release of mitotic exit activator Cdc14 from the nucleolus. *Science*, 305(5683):516–519.

Barberis, M., E. Klipp, M. Vanoni, and L. Alberghina (2007). Cell size at S phase initiation: an emergent property of the G1/S network. *PLoS Computational Biology*, 3(4):e64.

Barberis, M., R. G. Todd, and L. van der Zee (2017). Advances and challenges in logical modeling of cell cycle regulation: perspective for multi-scale, integrative yeast cell models. *FEMS Yeast Research*, 17(1):fow103.

Barbet, N. C., U. Schneider, S. B. Helliwell, I. Stansfield, M. F. Tuite, and M. N. Hall (1996). TOR controls translation initiation and early G1 progression in yeast. *Molecular Biology of the Cell*, 7(1):25–42.

Bashkirov, V. I., E. V. Bashkirova, E. Haghnazari, and W.-D. Heyer (2003). Direct kinase-to-kinase signaling mediated by the FHA phosphoprotein recognition domain of the Dun1 DNA damage checkpoint kinase. *Molecular and Cellular Biology*, 23(4):1441–1452.

Bastajian, N., H. Friesen, and B. J. Andrews (2013). Bck2 acts through the MADS box protein Mcm1 to activate cell-cycle-regulated genes in budding yeast. *PLoS Genetics*, 9(5):e1003507.

Bean, J. M., E. D. Siggia, and F. R. Cross (2005). High functional overlap between MluI cell-cycle box binding factor and Swi4/6 cell-cycle box binding factor in the G1/S transcriptional program in *Saccharomyces cerevisiae*. *Genetics*, 171(1):49–61.

Bell, S. P. and K. Labib (2016). Chromosome duplication in *Saccharomyces cerevisiae*. *Genetics*, 203(3):1027–1067.

Benner, S. A. (2010). Defining life. *Astrobiology*, 10(10):1021–1030.

Bertazzi, D. T., B. Kurtulmus, and G. Pereira (2011). The cortical protein Lte1 promotes mitotic exit by inhibiting the spindle position checkpoint kinase Kin4. *The Journal of Cell Biology*, 193(6):1033–1048.

Bertin, A., M. A. McMurray, P. Grob, S.-S. Park, G. Garcia, I. Patanwala, H.-l. Ng, T. Alber, J. Thorner, and E. Nogales (2008). *Saccharomyces cerevisiae* septins: supramolecular organization of heterooligomers and the mechanism of filament assembly. *Proceedings of the National Academy of Sciences*, 105(24):8274–8279.

Bi, E. and H.-O. Park (2012). Cell polarization and cytokinesis in budding yeast. *Genetics*, 191(2):347–387.

Biggins, S. (2013). The Composition, Functions, and Regulation of the Budding Yeast Kinetochore. *Genetics*, 194(4):817–846.

Blinov, M. L., J. R. Faeder, B. Goldstein, and W. S. Hlavacek (2004). BioNetGen: software for rule-based modeling of signal transduction based on the interactions of molecular domains. *Bioinformatics*, 20(17):3289–3291.

Blondel, M., J.-M. Galan, Y. Chi, C. Lafourcade, C. Longaretti, R. J. Deshaies, and M. Peter (2000). Nuclear-specific degradation of Far1 is controlled by the localization of the F-box protein Cdc4. *The EMBO Journal*, 19(22):6085–6097.

Boiteux, S. and S. Jinks-Robertson (2013). DNA repair mechanisms and the bypass of DNA damage in *Saccharomyces cerevisiae*. *Genetics*, 193(4):1025–1064.

Bose, I., J. E. Irazoqui, J. J. Moskow, E. S. Bardes, T. R. Zyla, and D. J. Lew (2001). Assembly of scaffold-mediated complexes containing Cdc42p, the exchange factor Cdc24p, and the effector Cla4p required for cell cycle-regulated phosphorylation of Cdc24p. *Journal of Biological Chemistry*, 276(10):7176–7186.

Braunewell, S. and S. Bornholdt (2007). Superstability of the yeast cell-cycle dynamics: Ensuring causality in the presence of biochemical stochasticity. *Journal of Theoretical Biology*, 245(4):638–643.

Breitkreutz, A., H. Choi, J. R. Sharom, L. Boucher, V. Neduva, B. Larsen, Z.-Y. Lin, B.-J. Breitkreutz, C. Stark, G. Liu, *et al.* (2010). A Global Protein Kinase and Phosphatase Interaction Network in Yeast. *Science*, 328(5981):1043–1046.

Brill, S. J. and S. Bastin-Shanower (1998). Identification and characterization of the fourth single-stranded-DNA binding domain of replication protein A. *Molecular and Cellular Biology*, 18(12):7225–7234.

Broach, J. R. (2012). Nutritional Control of Growth and Development in Yeast. *Genetics*, 192(1):73–105.

Bullitt, E., M. P. Rout, J. V. Kilmartin, and C. W. Akey (1997). The yeast spindle pole body is assembled around a central crystal of Spc42p. *Cell*, 89(7):1077–1086.

Butty, A.-C., N. Perrinjaquet, A. Petit, M. Jaquenoud, J. E. Segall, K. Hofmann, C. Zwahlen, and M. Peter (2002). A positive feedback loop stabilizes the guanine-nucleotide exchange factor Cdc24 at sites of polarization. *The EMBO Journal*, 21(7):1565–1576.

Caplan, A. J., D. M. Cyr, and M. G. Douglas (1992). YDJ1p facilitates polypeptide translocation across different intracellular membranes by a conserved mechanism. *Cell*, 71(7):1143–1155.

Cappellaro, C., V. Mrsa, and W. Tanner (1998). New Potential Cell Wall Glucanases ofSaccharomyces cerevisiae and Their Involvement in Mating. *Journal of bacteriology*, 180(19):5030–5037.

Caron, E., S. Ghosh, Y. Matsuoka, D. Ashton-Beaucage, M. Therrien, S. Lemieux, C. Perreault, P. P. Roux, and H. Kitano (2010). A comprehensive map of the mTOR signaling network. *Molecular Systems Biology*, 6(1):453.

Caydasi, A. K., B. Kurtulmus, M. I. Orrico, A. Hofmann, B. Ibrahim, and G. Pereira (2010). Elm1 kinase activates the spindle position checkpoint kinase Kin4. *The Journal of Cell Biology*, 190(6):975–989.

Chan, L. Y. and A. Amon (2009). The protein phosphatase 2A functions in the spindle position checkpoint by regulating the checkpoint kinase Kin4. *Genes & Development*, 23(14):1639–1649.

Chang, S. (1988). Planetary environments and the conditions of life. *Philosophical Transactions of the Royal Society of London. Series A, Mathematical and Physical Sciences*, Pp. 601–610.

Chee, M. K. and S. B. Haase (2010). B-cyclin/CDKs Regulate Mitotic Spindle Assembly by Phosphorylating Kinesins-5 in Budding Yeast. *PLoS Genetics*, 6(5):e1000935.

Cheeseman, I. M., S. Anderson, M. Jwa, E. M. Green, J.-s. Kang, J. R. Yates, C. S. Chan, D. G. Drubin, and G. Barnes (2002). Phospho-regulation of kinetochore-microtubule attachments by the Aurora kinase Ipl1p. *Cell*, 111(2):163–172.

Chen, K. C., L. Calzone, A. Csikasz-Nagy, F. R. Cross, B. Novak, and J. J. Tyson (2004). Integrative analysis of cell cycle control in budding yeast. *Molecular Biology of the Cell*, 15(8):3841–3862.

Chen, S., M. A. de Vries, and S. P. Bell (2007a). Orc6 is required for dynamic recruitment of Cdt1 during repeated Mcm2–7 loading. *Genes & Development*, 21(22):2897–2907.

Chen, S.-h., M. B. Smolka, and H. Zhou (2007b). Mechanism of Dun1 activation by Rad53 phosphorylation in *Saccharomyces cerevisiae*. *Journal of Biological Chemistry*, 282(2):986–995.

Chen, S.-h. and H. Zhou (2009). Reconstitution of Rad53 activation by Mec1 through adaptor protein Mrc1. *Journal of Biological Chemistry*, 284(28):18593–18604.

Chen, Y.-C., J. Kenworthy, C. Gabrielse, C. Hänni, P. Zegerman, and M. Weinreich (2013). DNA Replication Checkpoint Signaling Depends on a Rad53–Dbf4 N-Terminal Interaction in *Saccharomyces cerevisiae*. *Genetics*, 194(2):389–401.

Cheng, A., K. E. Ross, P. Kaldis, and M. J. Solomon (1999). Dephosphorylation of cyclin-dependent kinases by type 2C protein phosphatases. *Genes & Development*, 13(22):2946–2957.

Cherry, J. M., E. L. Hong, C. Amundsen, R. Balakrishnan, G. Binkley, E. T. Chan, K. R. Christie, M. C. Costanzo, S. S. Dwight, S. R. Engel, *et al.* (2011). *Saccharomyces* Genome Database: the genomics resource of budding yeast. *Nucleic Acids Research*, P. gkr1029.

Chilkova, O., P. Stenlund, I. Isoz, C. M. Stith, P. Grabowski, E.-B. Lundström, P. M. Burgers, and E. Johansson (2007). The eukaryotic leading and lagging strand DNA polymerases are loaded onto primer-ends via separate mechanisms but have comparable processivity in the presence of PCNA. *Nucleic Acids Research*, 35(19):6588–6597.

Cho, R. J., M. J. Campbell, E. A. Winzeler, L. Steinmetz, A. Conway, L. Wodicka, T. G. Wolfsberg, A. E. Gabrielian, D. Landsman, D. J. Lockhart, *et al.* (1998). A genome-wide transcriptional analysis of the mitotic cell cycle. *Molecular Cell*, 2(1):65–73.

Chylek, L. A., V. Akimov, J. Dengjel, K. T. Rigbolt, B. Hu, W. S. Hlavacek, and B. Blagoev (2014). Phosphorylation site dynamics of early T-cell receptor signaling. *PLoS One*, 9(8):e104240.

Cid, V. J., J. Jiménez, M. Molina, M. Sánchez, C. Nombela, and J. W. Thorner (2002). Orchestrating the cell cycle in yeast: sequential localization of key mitotic regulators at the spindle pole and the bud neck. *Microbiology*, 148(9):2647–2659.

Ciliberto, A., B. Novak, and J. J. Tyson (2003). Mathematical model of the morphogenesis checkpoint in budding yeast. *The Journal of Cell Biology*, 163(6):1243–1254.

Ciosk, R., W. Zachariae, C. Michaelis, A. Shevchenko, M. Mann, and K. Nasmyth (1998). An ESP1/PDS1 complex regulates loss of sister chromatid cohesion at the metaphase to anaphase transition in yeast. *Cell*, 93(6):1067–1076.

Colman-Lerner, A., T. E. Chin, and R. Brent (2001). Yeast Cbk1 and Mob2 activate daughter-specific genetic programs to induce asymmetric cell fates. *Cell*, 107(6):739–750.

Colvin, J., M. I. Monine, R. N. Gutenkunst, W. S. Hlavacek, D. D. Von Hoff, and R. G. Posner (2010). RuleMonkey: software for stochastic simulation of rule-based models. *BMC Bioinformatics*, 11(1):404.

Costanzo, M., O. Schub, and B. Andrews (2003). G1 transcription factors are differentially regulated in *Saccharomyces cerevisiae* by the Swi6-binding protein Stb1. *Molecular and Cellular Biology*, 23(14):5064–5077.

Coué, M., S. L. Brenner, I. Spector, and E. D. Korn (1987). Inhibition of actin polymerization by latrunculin A. *FEBS letters*, 213(2):316–318.

Crabbé, L., A. Thomas, V. Pantesco, J. De Vos, P. Pasero, and A. Lengronne (2010). Analysis of replication profiles reveals key role of RFC-Ctf18 in yeast replication stress response. *Nature Structural & Molecular Biology*, 17(11):1391–1397.

Crasta, K., P. Huang, G. Morgan, M. Winey, and U. Surana (2006). Cdk1 regulates centrosome separation by restraining proteolysis of microtubule-associated proteins. *The EMBO Journal*, 25(11):2551–2563.

Creamer, M. S., E. C. Stites, M. Aziz, J. A. Cahill, C. W. Tan, M. E. Berens, H. Han, K. J. Bussey, D. D. Von Hoff, W. S. Hlavacek, *et al.* (2012). Specification, annotation, visualization and simulation of a large rule-based model for ERBB receptor signaling. *BMC Systems Biology*, 6(1):107.

Csikász-Nagy, A. (2009). Computational systems biology of the cell cycle. *Briefings in Bioinformatics*, 10(4):424–434.

Cullen, P. J. and G. F. Sprague (2012). The Regulation of Filamentous Growth in Yeast. *Genetics*, 190(1):23–49.

Culotti, J. and L. Hartwell (1971). Genetic control of the cell division cycle in yeast: III. Seven genes controlling nuclear division. *Experimental Cell Research*, 67(2):389–401.

Cyert, M. S. and C. C. Philpott (2013). Regulation of Cation Balance in *Saccharomyces cerevisiae*. *Genetics*, 193(3):677–713.

Cyr, D. M. and M. G. Douglas (1994). Differential regulation of Hsp70 subfamilies by the eukaryotic DnaJ homologue YDJ1. *Journal of Biological Chemistry*, 269(13):9798–9804.

Darieva, Z., R. Bulmer, A. Pic-Taylor, K. S. Doris, M. Geymonat, S. G. Sedgwick, B. A. Morgan, and A. D. Sharrocks (2006). Polo Kinase Controls Cell Cycle-Dependent Transcription by Direct Targeting of a Coactivator Protein. *Nature*, 444(7118):494.

Das, S., D. Sarkar, and B. Das (2017). The interplay between transcription and mRNA degradation in *Saccharomyces cerevisiae*. *Microbial Cell*, 4(7):212.

de Bruin, R. A., T. I. Kalashnikova, C. Chahwan, W. H. McDonald, J. Wohlschlegel, J. Yates, P. Russell, and C. Wittenberg (2006). Constraining G1-specific transcription to late G1 phase: the MBF-associated corepressor Nrm1 acts via negative feedback. *Molecular cell*, 23(4):483–496.

de Bruin, R. A., T. I. Kalashnikova, and C. Wittenberg (2008). Stb1 collaborates with other regulators to modulate the G1-specific transcriptional circuit. *Molecular and Cellular Biology*, 28(22):6919–6928.

Demir, E., M. P. Cary, S. Paley, K. Fukuda, C. Lemer, I. Vastrik, G. Wu, P. D'eustachio, C. Schaefer, J. Luciano, *et al.* (2010). The BioPAX community standard for pathway data sharing. *Nature Biotechnology*, 28(9):935–942.

Denoth Lippuner, A., T. Julou, and Y. Barral (2014). Budding yeast as a model organism to study the effects of age. *FEMS Microbiology Reviews*, 38(2):300–325.

Di Camillo, B., A. Carlon, F. Eduati, and G. M. Toffolo (2016). A rule-based model of insulin signalling pathway. *BMC Systems Biology*, 10(1):38.

Dial, J. M., E. V. Petrotchenko, and C. H. Borchers (2007). Inhibition of APCCdh1 activity by Cdh1/Acm1/Bmh1 ternary complex formation. *Journal of Biological Chemistry*, 282(8):5237–5248.

Dirick, L., T. Böhm, and K. Nasmyth (1995). Roles and regulation of Cln-Cdc28 kinases at the start of the cell cycle of *Saccharomyces cerevisiae*. *The EMBO Journal*, 14(19):4803.

Donaldson, A. D. and J. V. Kilmartin (1996). Spc42p: a phosphorylated component of the *S. cerevisiae* spindle pole body (SPB) with an essential function during SPB duplication. *The Journal of Cell Biology*, 132(5):887–901.

Dong, Y., D. Pruyne, and A. Bretscher (2003). Formin-dependent actin assembly is regulated by distinct modes of Rho signaling in yeast. *The Journal of cell biology*, 161(6):1081–1092.

Dougherty, E. R. and I. Shmulevich (2012). On the limitations of biological knowledge. *Current Genomics*, 13(7):574–587.

Douglas, M. E. and J. F. Diffley (2016). Recruitment of Mcm10 to sites of replication initiation requires direct binding to the minichromosome maintenance (Mcm) complex. *Journal of Biological Chemistry*, 291(11):5879–5888.

Edenberg, E. R., K. G. Mark, and D. P. Toczyski (2015). Ndd1 Turnover by SCFGrr1 Is Inhibited by the DNA Damage Checkpoint in *Saccharomyces cerevisiae*. *PLoS Genetics*, 11(4):e1005162.

Elliott, S., M. Knop, G. Schlenstedt, and E. Schiebel (1999). Spc29p is a component of the Spc110p subcomplex and is essential for spindle pole body duplication. *Proceedings of the National Academy of Sciences*, 96(11):6205–6210.

Elsasser, S., Y. Chi, P. Yang, and J. L. Campbell (1999). Phosphorylation controls timing of Cdc6p destruction: a biochemical analysis. *Molecular Biology of the Cell*, 10(10):3263–3277.

Elserafy, M., M. Šarić, A. Neuner, T.-c. Lin, W. Zhang, C. Seybold, L. Sivashanmugam, and E. Schiebel (2014). Molecular mechanisms that restrict yeast centrosome duplication to one event per cell cycle. *Current Biology*, 24(13):1456–1466.

Enquist-Newman, M., M. Sullivan, and D. O. Morgan (2008). Modulation of the mitotic regulatory network by APC-dependent destruction of the Cdh1 inhibitor Acm1. *Molecular Cell*, 30(4):437–446.

Enserink, J. M. and R. D. Kolodner (2010). An overview of Cdk1-controlled targets and processes. *Cell Division*, 5:11.

Epstein, C. B. and F. R. Cross (1992). CLB5: a novel B cyclin from budding yeast with a role in S phase. *Genes & Development*, 6(9):1695–1706.

Erlemann, S., A. Neuner, L. Gombos, R. Gibeaux, C. Antony, and E. Schiebel (2012). An extended γ-tubulin ring functions as a stable platform in microtubule nucleation. *The Journal of Cell Biology*, 197(1):59–74.

Evangelista, M., K. Blundell, M. S. Longtine, C. J. Chow, N. Adames, J. R. Pringle, M. Peter, and C. Boone (1997). Bni1p, a yeast formin linking Cdc42p and the actin cytoskeleton during polarized morphogenesis. *Science*, 276(5309):118–122.

Evangelista, M., D. Pruyne, D. C. Amberg, C. Boone, and A. Bretscher (2002). Formins direct Arp2/3-independent actin filament assembly to polarize cell growth in yeast. *Nature Cell Biology*, 4(1):32.

Evrin, C., A. Fernández-Cid, A. Riera, J. Zech, P. Clarke, M. C. Herrera, S. Tognetti, R. Lurz, and C. Speck (2013). The ORC/Cdc6/MCM2-7 complex facilitates MCM2-7 dimerization during prereplicative complex formation. *Nucleic Acids Research*, 42(4):2257–2269.

Faeder, J. R., M. L. Blinov, and W. S. Hlavacek (2009). Rule-based modeling of biochemical systems with BioNetGen. *Systems biology*, Pp. 113–167.

Fauré, A., A. Naldi, C. Chaouiya, and D. Thieffry (2006). Dynamical analysis of a generic Boolean model for the control of the mammalian cell cycle. *Bioinformatics*, 22(14):e124–e131.

Fauré, A., A. Naldi, F. Lopez, C. Chaouiya, A. Ciliberto, and D. Thieffry (2009). Modular logical modelling of the budding yeast cell cycle. *Molecular BioSystems*, 5(12):1787–1796.

Feng, L., B. Wang, L. Wu, and A. Jong (2000). Loss control of Mcm5 interaction with chromatin in cdc6-1 mutated in CDC-NTP motif. *DNA and Cell Biology*, 19(7):447–457.

Feret, J., V. Danos, J. Krivine, R. Harmer, and W. Fontana (2009). Internal coarse-graining of molecular systems. *Proceedings of the National Academy of Sciences*, 106(16):6453–6458.

Fernius, J., O. O. Nerusheva, S. Galander, F. de Lima Alves, J. Rappsilber, and A. L. Marston (2013). Cohesin-dependent association of Scc2/4 with the centromere initiates pericentromeric cohesion establishment. *Current Biology*, 23(7):599–606.

Ferrell, J. E., T. Y.-C. Tsai, and Q. Yang (2011). Modeling the cell cycle: why do certain circuits oscillate? *Cell*, 144(6):874–885.

Feynman, R. P. (2010). *" Surely You're Joking, Mr. Feynman!": Adventures of a Curious Character: Adventures of a Curious Character*. WW Norton & Company.

Finley, D., H. D. Ulrich, T. Sommer, and P. Kaiser (2012). The ubiquitin–proteasome system of *Saccharomyces cerevisiae*. *Genetics*, 192(2):319–360.

Fisher, J. and T. A. Henzinger (2007). Executable cell biology. *Nature Biotechnology*, 25(11):1239–1249.

Flöttmann, M., F. Krause, E. Klipp, and M. Krantz (2013). Reaction-contingency based bipartite Boolean modelling. *BMC Syst Biol*, 7:58.

Flöttmann, M., T. Scharp, and E. Klipp (2012). A stochastic model of epigenetic dynamics in somatic cell reprogramming. *Frontiers in Physiology*, 3.

Foti, M., A. Audhya, and S. D. Emr (2001). Sac1 lipid phosphatase and Stt4 phosphatidylinositol 4-kinase regulate a pool of phosphatidylinositol 4-phosphate that functions in the control of the actin cytoskeleton and vacuole morphology. *Molecular Biology of the Cell*, 12(8):2396–2411.

Francisco, L., W. Wang, and C. Chan (1994). Type 1 protein phosphatase acts in opposition to IpL1 protein kinase in regulating yeast chromosome segregation. *Molecular and Cellular Biology*, 14(7):4731–4740.

Fridman, V., A. Gerson-Gurwitz, O. Shapira, N. Movshovich, S. Lakämper, C. F. Schmidt, and L. Gheber (2013). Kinesin-5 Kip1 is a bi-directional motor that stabilizes microtubules and tracks their plus-ends in vivo. *J Cell Sci*, 126(18):4147–4159.

Fu, J., I. M. Hagan, and D. M. Glover (2015). The centrosome and its duplication cycle. *Cold Spring Harbor Perspectives in Biology*, 7(2):a015800.

Fujiwara, T., K. Tanaka, A. Mino, M. Kikyo, K. Takahashi, K. Shimizu, and Y. Takai (1998). Rho1p-Bni1p-Spa2p Interactions: Implication in Localization of Bni1p at the Bud Site and Regulation of the Actin Cytoskeleton in *Saccharomyces cerevisiae*. *Molecular Biology of the Cell*, 9(5):1221–1233.

Funahashi, A., Y. Matsuoka, A. Jouraku, M. Morohashi, N. Kikuchi, and H. Kitano (2008). CellDesigner 3.5: a versatile modeling tool for biochemical networks. *Proceedings of the IEEE*, 96(8):1254–1265.

Gallone, B., J. Steensels, T. Prahl, L. Soriaga, V. Saels, B. Herrera-Malaver, A. Merlevede, M. Roncoroni, K. Voordeckers, L. Miraglia, *et al.* (2016). Domestication and divergence of *Saccharomyces cerevisiae* beer yeasts. *Cell*, 166(6):1397–1410.

Gao, X.-D., S. Albert, S. E. Tcheperegine, C. G. Burd, D. Gallwitz, and E. Bi (2003). The GAP activity of Msb3p and Msb4p for the Rab GTPase Sec4p is required for efficient exocytosis and actin organization. *The Journal of Cell Biology*, 162(4):635–646.

García-Rodríguez, L. J., G. De Piccoli, V. Marchesi, R. C. Jones, R. D. Edmondson, and K. Labib (2015). A conserved Polϵ binding module in Ctf18-RFC is required for S-phase checkpoint activation downstream of Mec1. *Nucleic Acids Research*, 43(18):8830–8838.

Garí, E., T. Volpe, H. Wang, C. Gallego, B. Futcher, and M. Aldea (2001). Whi3 binds the mRNA of the G1 cyclin CLN3 to modulate cell fate in budding yeast. *Genes & Development*, 15(21):2803–2808.

Gartner, A., A. Jovanović, D.-I. Jeoung, S. Bourlat, F. R. Cross, and G. Ammerer (1998). Pheromone-dependent G1 cell cycle arrest requires Far1 phosphorylation, but may not involve inhibition of Cdc28-Cln2 kinase, in vivo. *Molecular and Cellular Biology*, 18(7):3681–3691.

Gasch, A. P., P. T. Spellman, C. M. Kao, O. Carmel-Harel, M. B. Eisen, G. Storz, D. Botstein, and P. O. Brown (2000). Genomic Expression Programs in the Response of Yeast Cells to Environmental Changes. *Molecular Biology of the Cell*, 11(12):4241–4257.

Geymonat, M., A. Spanos, G. de Bettignies, and S. G. Sedgwick (2009). Lte1 contributes to Bfa1 localization rather than stimulating nucleotide exchange by Tem1. *The Journal of Cell Biology*, 187(4):497–511.

Geymonat, M., A. Spanos, S. J. Smith, E. Wheatley, K. Rittinger, L. H. Johnston, and S. G. Sedgwick (2002). Control of Mitotic Exit in Budding Yeast *In vitro* Regulation of Tem1 GTPase by Bub2 and Bfa1. *Journal of Biological Chemistry*, 277(32):28439–28445.

Giese, W., M. Eigel, S. Westerheide, C. Engwer, and E. Klipp (2015). Influence of cell shape, inhomogeneities and diffusion barriers in cell polarization models. *Physical Biology*, 12(6):066014.

Glotzer, M. (2009). The 3Ms of central spindle assembly: microtubules, motors and MAPs. *Nature Reviews. Molecular Cell Biology*, 10(1):9.

Goffeau, A., B. G. Barrell, H. Bussey, R. Davis, *et al.* (1996). Life with 6000 genes. *Science*, 274(5287):546.

Goldbeter, A. (1991). A minimal cascade model for the mitotic oscillator involving cyclin and cdc2 kinase. *Proceedings of the National Academy of Sciences*, 88(20):9107–9111.

Gross, M. (2012). The search for life on Earth and other planets.

Gruneberg, U., K. Campbell, C. Simpson, J. Grindlay, and E. Schiebel (2000). Nud1p links astral microtubule organization and the control of exit from mitosis. *The EMBO Journal*, 19(23):6475–6488.

Guo, W., F. Tamanoi, and P. Novick (2001). Spatial regulation of the exocyst complex by Rho1 GTPase. *Nature Cell Biology*, 3(4):353–360.

Haase, S. B. and C. Wittenberg (2014). Topology and control of the cell-cycle-regulated transcriptional circuitry. *Genetics*, 196(1):65–90.

Haber, J. E. (2012). Mating-type genes and MAT switching in *Saccharomyces cerevisiae*. *Genetics*, 191(1):33–64.

Hadwiger, J., C. Wittenberg, M. Mendenhall, and S. Reed (1989). The *Saccharomyces cerevisiae* CKS1 gene, a homolog of the *Schizosaccharomyces pombe* suc1+ gene, encodes a subunit of the Cdc28 protein kinase complex. *Molecular and Cellular Biology*, 9(5):2034–2041.

Han, B.-K., L. M. Bogomolnaya, J. M. Totten, H. M. Blank, L. J. Dangott, and M. Polymenis (2005). Bem1p, a scaffold signaling protein, mediates cyclin-dependent control of vacuolar homeostasis in Saccharomyces cerevisiae. *Genes & Development*, 19(21):2606–2618.

Harashima, H., N. Dissmeyer, and A. Schnittger (2013). Cell Cycle control across the eukaryotic kingdom. *Trends in Cell Biology*, 23(7):345–356.

Harris, L. A., J. S. Hogg, J.-J. Tapia, J. A. Sekar, S. Gupta, I. Korsunsky, A. Arora, D. Barua, R. P. Sheehan, and J. R. Faeder (2016). BioNetGen 2.2: advances in rule-based modeling. *Bioinformatics*, P. btw469.

Hartwell, L. (1971a). Genetic control of the cell division cycle in yeast: IV. Genes controlling bud emergence and cytokinesis. *Experimental Cell Research*, 69(2):265–276.

Hartwell, L. H. (1971b). Genetic control of the cell division cycle in yeast: II. Genes controlling DNA replication and its initiation. *Journal of Molecular Biology*, 59(1):183IN17185–184IN18194.

Hartwell, L. H., J. Culotti, J. R. Pringle, and B. J. Reid (1974). Genetic controlof the cell division cycle in yeast. *Science (Wash. DC)*, 183:46–51.

Hartwell, L. H., J. Culotti, and B. Reid (1970). Genetic control of the cell-division cycle in yeast, I. Detection of mutants. *Proceedings of the National Academy of Sciences*, 66(2):352–359.

Hartwell, L. H., R. K. Mortimer, J. Culotti, and M. Culotti (1973). Genetic control of the cell division cycle in yeast: V. Genetic analysis of cdc mutants. *Genetics*, 74(2):267–286.

He, B., F. Xi, X. Zhang, J. Zhang, and W. Guo (2007). Exo70 interacts with phospholipids and mediates the targeting of the exocyst to the plasma membrane. *The EMBO Journal*, 26(18):4053–4065.

Hegnauer, A. M., N. Hustedt, K. Shimada, B. L. Pike, M. Vogel, P. Amsler, S. M. Rubin, F. Van Leeuwen, A. Guénolé, H. Van Attikum, *et al.* (2012). An N-terminal acidic region of Sgs1 interacts with Rpa70 and recruits Rad53 kinase to stalled forks. *The EMBO Journal*, 31(18):3768–3783.

Hernández-Ortega, S., S. Bru, N. Ricco, S. Ramírez, N. Casals, J. Jiménez, M. Isasa, B. Crosas, and J. Clotet (2013). Defective in mitotic arrest 1 (Dma1) ubiquitin ligase controls G1 cyclin degradation. *Journal of Biological Chemistry*, 288(7):4704–4714.

Heusden, G. P. H., D. J. Griffiths, J. C. Ford, P. A. Schrader, A. M. Carr, H. Y. Steensma, *et al.* (1995). The 14-3-3 Proteins Encoded by the BMH1 and BMH2 Genes are Essential in the Yeast *Saccharomyces cerevisiae* and Can be Replaced by a Plant Homologue. *The FEBS Journal*, 229(1):45–53.

Hildebrandt, E. R., L. Gheber, T. Kingsbury, and M. A. Hoyt (2006). Homotetrameric form of Cin8p, a *Saccharomyces cerevisiae* kinesin-5 motor, is essential for its in vivo function. *Journal of Biological Chemistry*, 281(36):26004–26013.

Hilioti, Z., Y.-S. Chung, Y. Mochizuki, C. F. Hardy, and O. Cohen-Fix (2001). The anaphase inhibitor Pds1 binds to the APC/C-associated protein Cdc20 in a destruction box-dependent manner. *Current Biology*, 11(17):1347–1352.

Hinshaw, S. M., V. Makrantoni, A. Kerr, A. L. Marston, and S. C. Harrison (2015). Structural evidence for Scc4-dependent localization of cohesin loading. *Elife*, 4:e06057.

Hlavacek, W. S., J. R. Faeder, M. L. Blinov, A. S. Perelson, and B. Goldstein (2003). The complexity of complexes in signal transduction. *Biotechnology and Bioengineering*, 84(7):783–794.

Hlavacek, W. S., M. I. Monnie, J. Colvin, and J. Faseder (2008). Simulation of large-scale rule-based models. *Bioinformatics*, 25(LA-UR-08-04860; LA-UR-08-4860).

Hoffman, G. R., N. Nassar, and R. A. Cerione (2000). Structure of the Rho family GTP-binding protein Cdc42 in complex with the multifunctional regulator RhoGDI. *Cell*, 100(3):345–356.

Holmes, K. J., D. M. Klass, E. L. Guiney, and M. S. Cyert (2013). Whi3, an *S. cerevisiae* RNA-binding protein, is a component of stress granules that regulates levels of its target mRNAs. *PLoS One*, 8(12):e84060.

Holt, L. J., A. N. Krutchinsky, and D. O. Morgan (2008). Positive feedback sharpens the anaphase switch. *Nature*, 454(7202):353.

Hood, L. (2013). Systems Biology and P4 Medicine: Past, Present, and Future. *Rambam Maimonides Medical Journal*, 4(2).

Hoops, S., S. Sahle, R. Gauges, C. Lee, J. Pahle, N. Simus, M. Singhal, L. Xu, P. Mendes, and U. Kummer (2006). COPASI–a complex pathway simulator. *Bioinformatics*, 22(24):3067–3074.

Horak, C. E., N. M. Luscombe, J. Qian, P. Bertone, S. Piccirrillo, M. Gerstein, and M. Snyder (2002). Complex transcriptional circuitry at the G1/S transition in *Saccharomyces cerevisiae*. *Genes & Development*, 16(23):3017–3033.

Howell, A. S. and D. J. Lew (2012). Morphogenesis and the cell cycle. *Genetics*, 190(1):51–77.

Huang, D., H. Friesen, and B. Andrews (2007). Pho85, a multifunctional cyclin-dependent protein kinase in budding yeast. *Molecular Microbiology*, 66(2):303–314.

Huang, D., S. Kaluarachchi, D. van Dyk, H. Friesen, R. Sopko, W. Ye, N. Bastajian, J. Moffat, H. Sassi, M. Costanzo, *et al.* (2009). Dual regulation by pairs of cyclin-dependent protein kinases and histone deacetylases controls G1 transcription in budding yeast. *PLoS Biology*, 7(9):e1000188.

Hucka, M., A. Finney, H. M. Sauro, H. Bolouri, J. C. Doyle, H. Kitano, A. P. Arkin, B. J. Bornstein, D. Bray, A. Cornish-Bowden, *et al.* (2003). The systems biology markup language (SBML): a medium for representation and exchange of biochemical network models. *Bioinformatics*, 19(4):524–531.

Hunt, C. A., G. E. Ropella, S. Park, and J. Engelberg (2008). Dichotomies between computational and mathematical models. *Nature Biotechnology*, 26(7):737–738.

Iftode, C., Y. Daniely, and J. A. Borowiec (1999). Replication protein A (RPA): the eukaryotic SSB. *Critical Reviews in Biochemistry and Molecular Biology*, 34(3):141–180.

Imamura, H., K. Tanaka, T. Hihara, M. Umikawa, T. Kamei, K. Takahashi, T. Sasaki, and Y. Takai (1997). Bni1p and Bnr1p: downstream targets of the Rho family small G-proteins which interact with profilin and regulate actin cytoskeleton in *Saccharomyces cerevisiae*. *The EMBO Journal*, 16(10):2745–2755.

Irons, D. (2009). Logical analysis of the budding yeast cell cycle. *Journal of Theoretical Biology*, 257(4):543–559.

Iwase, M., J. Luo, S. Nagaraj, M. Longtine, H. B. Kim, B. K. Haarer, C. Caruso, Z. Tong, J. R. Pringle, and E. Bi (2006). Role of a Cdc42p effector pathway in recruitment of the yeast septins to the presumptive bud site. *Molecular Biology of the Cell*, 17(3):1110–1125.

Jackson, L. P., S. I. Reed, and S. B. Haase (2006). Distinct mechanisms control the stability of the related S-phase cyclins Clb5 and Clb6. *Molecular and Cellular Biology*, 26(6):2456–2466.

Jaiswal, D., R. Turniansky, and E. M. Green (2016). Choose your own adventure: the role of histone modifications in yeast cell fate. *Journal of Molecular Biology*.

Jaspersen, S. L., B. J. Huneycutt, T. H. Giddings, K. A. Resing, N. G. Ahn, and M. Winey (2004). Cdc28/Cdk1 regulates spindle pole body duplication through phosphorylation of Spc42 and Mps1. *Developmental Cell*, 7(2):263–274.

Jiang, Y. and J. R. Broach (1999). Tor proteins and protein phosphatase 2A reciprocally regulate Tap42 in controlling cell growth in yeast. *The EMBO Journal*, 18(10):2782–2792.

Juang, Y.-L., J. Huang, J.-M. Peters, M. E. McLaughlin, C.-Y. Tai, and D. Pellman (1997). APC-mediated Proteolysis of Ase1 and the Morphogenesis of the Mitotic Spindle. *Science*, 275(5304):1311–1314.

Kaiser, P., R. A. Sia, E. G. Bardes, D. J. Lew, and S. I. Reed (1998). Cdc34 and the F-box protein Met30 are required for degradation of the Cdk-inhibitory kinase Swe1. *Genes & Development*, 12(16):2587–2597.

Kaizu, K., S. Ghosh, Y. Matsuoka, H. Moriya, Y. Shimizu-Yoshida, and H. Kitano (2010). A comprehensive molecular interaction map of the budding yeast cell cycle. *Mol. Syst. Biol.*, 6:415.

Kang, J.-s., I. M. Cheeseman, G. Kallstrom, S. Velmurugan, G. Barnes, and C. S. Chan (2001). Functional cooperation of Dam1, Ipl1, and the inner centromere protein (INCENP)–related protein Sli15 during chromosome segregation. *The Journal of Cell Biology*, 155(5):763–774.

Kang, P. J., M. E. Lee, and H.-O. Park (2014). Bud3 activates Cdc42 to establish a proper growth site in budding yeast. *The Journal of Cell Biology*, 206(1):19–28.

Kantake, N., T. Sugiyama, R. D. Kolodner, and S. C. Kowalczykowski (2003). The recombination-deficient mutant RPA (rfa1-t11) is displaced slowly from single-stranded DNA by Rad51 protein. *Journal of Biological Chemistry*, 278(26):23410–23417.

Kauffman, S. A. (1969). Metabolic stability and epigenesis in randomly constructed genetic nets. *Journal of Theoretical Biology*, 22(3):437–467.

Kawakami, E., V. K. Singh, K. Matsubara, T. Ishii, Y. Matsuoka, T. Hase, P. Kulkarni, K. Siddiqui, J. Kodilkar, N. Danve, *et al.* (2016). Network analyses based on comprehensive molecular interaction maps reveal robust control structures in yeast stress response pathways. *npj Systems Biology and Applications*, 2:15018.

Keaton, M. A., E. S. Bardes, A. R. Marquitz, C. D. Freel, T. R. Zyla, J. Rudolph, and D. J. Lew (2007). Differential susceptibility of yeast S and M phase CDK complexes to inhibitory tyrosine phosphorylation. *Current Biology*, 17(14):1181–1189.

Keck, J. M., M. H. Jones, C. C. Wong, J. Binkley, D. Chen, S. L. Jaspersen, E. P. Holinger, T. Xu, M. Niepel, M. P. Rout, *et al.* (2011). A cell cycle phosphoproteome of the yeast centrosome. *Science*, 332(6037):1557–1561.

Kemmler, S., M. Stach, M. Knapp, J. Ortiz, J. Pfannstiel, T. Ruppert, and J. Lechner (2009). Mimicking Ndc80 phosphorylation triggers spindle assembly checkpoint signalling. *The EMBO Journal*, 28(8):1099–1110.

Kim, J., G. Luo, Y. Y. Bahk, and K. Song (2012). Cdc5-dependent asymmetric localization of Bfa1 fine-tunes timely mitotic exit. *PLoS Genetics*, 8(1):e1002450.

Kim, J. o., A. Zelter, N. T. Umbreit, A. Bollozos, M. Riffle, R. Johnson, M. J. MacCoss, C. L. Asbury, and T. N. Davis (2017). The Ndc80 complex bridges two Dam1 complex rings. *eLife*, 6:e21069.

Kitano, H. (2002). Systems biology: a brief overview. *Science*, 295(5560):1662–1664.

Klipp, E., W. Liebermeister, A. Helbig, A. Kowald, and J. Schaber (2007). Systems biology standardsâĂŤthe community speaks. *Nature Biotechnology*, 25(4):390–391.

Klipp, E., W. Liebermeister, C. Wierling, A. Kowald, and R. Herwig (2016). *Systems Biology: A Textbook*. John Wiley & Sons.

Knapp, D., L. Bhoite, D. J. Stillman, and K. Nasmyth (1996). The transcription factor Swi5 regulates expression of the cyclin kinase inhibitor p40SIC1. *Molecular and Cellular Biology*, 16(10):5701–5707.

Kobayashi, O., N. Hayashi, R. Kuroki, and H. Sone (1998). Region of Flo1 proteins responsible for sugar recognition. *Journal of Bacteriology*, 180(24):6503–6510.

Koch, C., T. Moll, M. Neuberg, H. Ahorn, and K. Nasmyth (1993). A role for the transcription factors Mbp1 and Swi4 in progression from G1 to S phase. *Science*, 261(5128):1551–1558.

Koch, C., A. Schleiffer, G. Ammerer, and K. Nasmyth (1996). Switching transcription on and off during the yeast cell cycle: Cln/Cdc28 kinases activate bound transcription factor SBF (Swi4/Swi6) at start, whereas Clb/Cdc28 kinases displace it from the promoter in G2. *Genes & Development*, 10(2):129–141.

Koepp, D. M., A. C. Kile, S. Swaminathan, and V. Rodriguez-Rivera (2006). The F-box protein Dia2 regulates DNA replication. *Molecular Biology of the Cell*, 17(4):1540–1548.

Kohno, H., K. Tanaka, A. Mino, M. Umikawa, H. Imamura, T. Fujiwara, Y. Fujita, K. Hotta, H. Qadota, T. Watanabe, *et al.* (1996). Bni1p implicated in cytoskeletal control is a putative target of Rho1p small GTP binding protein in *Saccharomyces cerevisiae*. *The EMBO Journal*, 15(22):6060.

Kõivomägi, M., E. Valk, R. Venta, A. Iofik, M. Lepiku, D. O. Morgan, and M. Loog (2011). Dynamics of Cdk1 substrate specificity during the cell cycle. *Molecular Cell*, 42(5):610–623.

Kolch, W., M. Halasz, M. Granovskaya, and B. N. Kholodenko (2015). The dynamic control of signal transduction networks in cancer cells. *Nature Reviews Cancer*, 15(9):515–527.

Komarnitsky, S. I., Y.-C. Chiang, F. C. Luca, J. Chen, J. H. Toyn, M. Winey, L. H. Johnston, and C. L. Denis (1998). DBF2 protein kinase binds to and acts through the cell cycle-regulated MOB1 protein. *Molecular and Cellular Biology*, 18(4):2100–2107.

Kono, K., S. Nogami, M. Abe, M. Nishizawa, S. Morishita, D. Pellman, and Y. Ohya (2008). G1/S cyclin-dependent kinase regulates small GTPase Rho1p through phosphorylation of RhoGEF Tus1p in *Saccharomyces cerevisiae*. *Molecular Biology of the Cell*, 19(4):1763–1771.

Koren, R., L. Rainis, and T. Kleinberger (2004). The scaffolding A/Tpd3 subunit and high phosphatase activity are dispensable for Cdc55 function in the *Saccharomyces cerevisiae* spindle checkpoint and in cytokinesis. *Journal of Biological Chemistry*, 279(47):48598–48606.

Koshland, D. E. (2002). The seven pillars of life. *Science*, 295(5563):2215–2216.

Kraikivski, P., K. C. Chen, T. Laomettachit, T. Murali, and J. J. Tyson (2015). From START to FINISH: computational analysis of cell cycle control in budding yeast. *Npj Systems Biology And Applications*, 1:15016.

Kühne, C. and P. Linder (1993). A new pair of B-type cyclins from *Saccharomyces cerevisiae* that function early in the cell cycle. *The EMBO Journal*, 12(9):3437.

Lampert, F., P. Hornung, and S. Westermann (2010). The Dam1 complex confers microtubule plus end–tracking activity to the Ndc80 kinetochore complex. *The Journal of Cell Biology*, 189(4):641–649.

Landry, B. D., J. P. Doyle, D. P. Toczyski, and J. A. Benanti (2012). F-box protein specificity for g1 cyclins is dictated by subcellular localization. *PLoS Genetics*, 8(7):e1002851.

Landry, B. D., C. E. Mapa, H. E. Arsenault, K. E. Poti, and J. A. Benanti (2014). Regulation of a transcription factor network by Cdk1 coordinates late cell cycle gene expression. *The EMBO Journal*, 33(9):1044–1060.

Le Novere, N., B. Bornstein, A. Broicher, M. Courtot, M. Donizelli, H. Dharuri, L. Li, H. Sauro, M. Schilstra, B. Shapiro, *et al.* (2006). BioModels Database: a free, centralized database of curated, published, quantitative kinetic models of biochemical and cellular systems. *Nucleic Acids Research*, 34(suppl_1):D689–D691.

Le Novere, N., M. Hucka, H. Mi, S. Moodie, F. Schreiber, A. Sorokin, E. Demir, K. Wegner, M. I. Aladjem, S. M. Wimalaratne, *et al.* (2009). The systems biology graphical notation. *Nature Biotechnology*, 27(8):735–741.

Lee, K. S., S. Asano, J.-E. Park, K. Sakchaisri, and R. L. Erikson (2005). Monitoring the cell cycle by multi-kinase-dependent regulation of Swe1/Wee1 in budding yeast. *Cell Cycle*, 4(10):1346–1349.

Lee, S. E., S. Jensen, L. M. Frenz, A. L. Johnson, D. Fesquet, and L. H. Johnston (2001). The Bub2-dependent mitotic pathway in yeast acts every cell cycle and regulates cytokinesis. *Journal of Cell Science*, 114(12):2345–2354.

Legal, T., J. Zou, A. Sochaj, J. Rappsilber, and J. P. Welburn (2016). Molecular architecture of the Dam1 complex–microtubule interaction. *Open Biology*, 6(3):150237.

Levin, D. E. (2011). Regulation of cell wall biogenesis in *Saccharomyces cerevisiae*: the cell wall integrity signaling pathway. *Genetics*, 189(4):1145–1175.

Li, F., T. Long, Y. Lu, Q. Ouyang, and C. Tang (2004). The yeast cell-cycle network is robustly designed. *Proceedings of the National Academy of Sciences of the United States of America*, 101(14):4781–4786.

Liku, M. E., V. Q. Nguyen, A. W. Rosales, K. Irie, and J. J. Li (2005). CDK phosphorylation of a novel NLS-NES module distributed between two subunits of the Mcm2-7 complex prevents chromosomal rereplication. *Molecular Biology of the Cell*, 16(10):5026–5039.

Limson, M. V. and K. S. Sweder (2009). Rapamycin inhibits yeast nucleotide excision repair independently of Tor kinases. *Toxicological Sciences*, 113(1):77–84.

Lin, T.-c., A. Neuner, Y. T. Schlosser, E. Schiebel, A. N. Scharf, and L. Weber (2014). Cell-cycle dependent phosphorylation of yeast pericentrin regulates γ-TuSC-mediated microtubule nucleation. *Elife*, 3:e02208.

Linke, C., A. Chasapi, A. González-Novo, I. Al Sawad, S. Tognetti, E. Klipp, M. Loog, S. Krobitsch, F. Posas, I. Xenarios, *et al.* (2017). A Clb/Cdk1-mediated regulation of Fkh2 synchronizes CLB expression in the budding yeast cell cycle. *npj Systems Biology and Applications*, 3:1.

Liu, B., L. Larsson, A. Caballero, X. Hao, D. Öling, J. Grantham, and T. Nyström (2010). The polarisome is required for segregation and retrograde transport of protein aggregates. *Cell*, 140(2):257–267.

Liu, D., G. Vader, M. J. Vromans, M. A. Lampson, and S. M. Lens (2009). Sensing chromosome bi-orientation by spatial separation of aurora B kinase from kinetochore substrates. *Science*, 323(5919):1350–1353.

Ljungdahl, P. O. and B. Daignan-Fornier (2012). Regulation of Amino Acid, Nucleotide, and Phosphate Metabolism in *Saccharomyces cerevisiae*. *Genetics*, 190(3):885–929.

Lloyd, C. M., M. D. Halstead, and P. F. Nielsen (2004). CellML: its future, present and past. *Progress in Biophysics and Molecular Biology*, 85(2):433–450.

Loewith, R. and M. N. Hall (2011). Target of rapamycin (TOR) in nutrient signaling and growth control. *Genetics*, 189(4):1177–1201.

Loog, M. and D. O. Morgan (2005). Cyclin specificity in the phosphorylation of cyclin-dependent kinase substrates. *Nature*, 434(7029):104–108.

Lõoke, M., M. F. Maloney, and S. P. Bell (2017). Mcm10 regulates DNA replication elongation by stimulating the CMG replicative helicase. *Genes & Development*, 31(3):291–305.

Lopez, C. F., J. L. Muhlich, J. A. Bachman, and P. K. Sorger (2013). Programming biological models in Python using PySB. *Molecular Systems Biology*, 9(1):646.

Lopez-Mosqueda, J., N. L. Maas, Z. O. Jonsson, L. G. D. Eli, J. Wohlschlegel, and D. P. Toczyski (2010). Damage-induced phosphorylation of Sld3 is important to block late origin firing. *Nature*, 467(7314):479.

Lou, H., M. Komata, Y. Katou, Z. Guan, C. C. Reis, M. Budd, K. Shirahige, and J. L. Campbell (2008). Mrc1 and DNA polymerase ϵ function together in linking DNA replication and the S phase checkpoint. *Molecular Cell*, 32(1):106–117.

Lu, D., J. Y. Hsiao, N. E. Davey, V. A. Van Voorhis, S. A. Foster, C. Tang, and D. O. Morgan (2014). Multiple mechanisms determine the order of APC/C substrate degradation in mitosis. *The Journal of Cell Biology*, 207(1):23–39.

Lubitz, T., J. Hahn, F. T. Bergmann, E. Noor, E. Klipp, and W. Liebermeister (2016). SBtab: a flexible table format for data exchange in systems biology. *Bioinformatics*, 32(16):2559.

Lubitz, T., N. Welkenhuysen, S. Shashkova, L. Bendrioua, S. Hohmann, E. Klipp, and M. Krantz (2015). Network reconstruction and validation of the Snf1/AMPK pathway in baker's yeast based on a comprehensive literature review. *npj Systems Biology and Applications*, 1:15007.

Lyon, A. S., G. Morin, M. Moritz, K. C. B. Yabut, T. Vojnar, A. Zelter, E. Muller, T. N. Davis, and D. A. Agard (2016). Higher-order oligomerization of Spc110p drives γ-tubulin ring complex assembly. *Molecular Biology of the Cell*, 27(14):2245–2258.

MacIsaac, K. D., T. Wang, D. B. Gordon, D. K. Gifford, G. D. Stormo, and E. Fraenkel (2006). An improved map of conserved regulatory sites for *Saccharomyces cerevisiae*. *BMC Bioinformatics*, 7(1):113.

Maekawa, H., C. Priest, J. Lechner, G. Pereira, and E. Schiebel (2007). The yeast centrosome translates the positional information of the anaphase spindle into a cell cycle signal. *The Journal of Cell Biology*, 179(3):423–436.

Mah, A. S., J. Jang, and R. J. Deshaies (2001). Protein kinase Cdc15 activates the Dbf2-Mob1 kinase complex. *Proceedings of the National Academy of Sciences*, 98(13):7325–7330.

Malo, M. E., S. D. Postnikoff, T. G. Arnason, and T. A. Harkness (2016). Mitotic degradation of yeast Fkh1 by the Anaphase Promoting Complex is required for normal longevity, genomic stability and stress resistance. *Aging (Albany NY)*, 8(4):810.

Margolin, W. and R. Bernander (2004). How do prokaryotic cells cycle? *Current Biology*, 14(18):R768–R770.

Markus, S. M., K. A. Kalutkiewicz, and W.-L. Lee (2012). Astral microtubule asymmetry provides directional cues for spindle positioning in budding yeast. *Experimental Cell Research*, 318(12):1400–1406.

Marston, A. L. (2014). Chromosome segregation in budding yeast: sister chromatid cohesion and related mechanisms. *Genetics*, 196(1):31–63.

Masumoto, H., A. Sugino, and H. Araki (2000). Dpb11 controls the association between DNA polymerases α and ϵ and the autonomously replicating sequence region of budding yeast. *Molecular and Cellular Biology*, 20(8):2809–2817.

Matsuoka, Y., H. Matsumae, M. Katoh, A. J. Eisfeld, G. Neumann, T. Hase, S. Ghosh, J. E. Shoemaker, T. J. Lopes, T. Watanabe, *et al.* (2013). A comprehensive map of the influenza A virus replication cycle. *BMC Systems Biology*, 7(1):97.

McCusker, D., C. Denison, S. Anderson, T. A. Egelhofer, J. R. Yates, S. P. Gygi, and D. R. Kellogg (2007). Cdk1 coordinates cell-surface growth with the cell cycle. *Nature Cell Biology*, 9(5):506–515.

Measday, V., L. Moore, R. Retnakaran, J. Lee, M. Donoviel, A. Neiman, and B. Andrews (1997). A family of cyclin-like proteins that interact with the Pho85 cyclin-dependent kinase. *Molecular and Cellular Biology*, 17(3):1212–1223.

Meitinger, F., S. Palani, B. Hub, and G. Pereira (2013). Dual function of the NDR-kinase Dbf2 in the regulation of the F-BAR protein Hof1 during cytokinesis. *Molecular Biology of the Cell*, 24(9):1290–1304.

Mendenhall, M. D. and A. E. Hodge (1998). Regulation of Cdc28 cyclin-dependent protein kinase activity during the cell cycle of the yeast *Saccharomyces cerevisiae*. *Microbiology and Molecular Biology Reviews*, 62(4):1191–1243.

Miranda, J. L., D. S. King, and S. C. Harrison (2007). Protein arms in the kinetochore-microtubule interface of the yeast DASH complex. *Molecular Biology of the Cell*, 18(7):2503–2510.

Mirkin, E. V. and S. M. Mirkin (2007). Replication fork stalling at natural impediments. *Microbiology and Molecular Biology Reviews*, 71(1):13–35.

Mochizuki, A., B. Fiedler, G. Kurosawa, and D. Saito (2013). Dynamics and control at feedback vertex sets. II: A faithful monitor to determine the diversity of molecular activities in regulatory networks. *Journal of Theoretical Biology*, 335:130–146.

Mohl, D. A., M. J. Huddleston, T. S. Collingwood, R. S. Annan, and R. J. Deshaies (2009). Dbf2–Mob1 drives relocalization of protein phosphatase Cdc14 to the cytoplasm during exit from mitosis. *The Journal of Cell Biology*, 184(4):527–539.

Moll, T., G. Tebb, U. Surana, H. Robitsch, and K. Nasmyth (1991). The role of phosphorylation and the CDC28 protein kinase in cell cycle-regulated nuclear import of the *S. cerevisiae* transcription factor SW15. *Cell*, 66(4):743–758.

Moore, J. K. and R. K. Miller (2007). The cyclin-dependent kinase Cdc28p regulates multiple aspects of Kar9p function in yeast. *Molecular Biology of the Cell*, 18(4):1187–1202.

Morano, K. A., C. M. Grant, and W. S. Moye-Rowley (2012). The Response to Heat shock and Oxidative Stress in *Saccharomyces cerevisiae*. *Genetics*, 190(4):1157–1195.

Mortensen, E. M., W. Haas, M. Gygi, S. P. Gygi, and D. R. Kellogg (2005). Cdc28-dependent regulation of the Cdc5/Polo kinase. *Current Biology*, 15(22):2033–2037.

Müller, P., S. Park, E. Shor, D. J. Huebert, C. L. Warren, A. Z. Ansari, M. Weinreich, M. L. Eaton, D. M. MacAlpine, and C. A. Fox (2010). The conserved bromo-adjacent homology domain of yeast Orc1 functions in the selection of DNA replication origins within chromatin. *Genes & Development*, 24(13):1418–1433.

Münzner, U., T. Lubitz, E. Klipp, and M. Krantz (2017). Toward Genome–scale Models of Signal Transduction Networks. In *Systems Biology*, J. Nielsen and S. Hohmann, eds., chapter 8, Pp. 215–242. Wiley–VCH.

Müssel, C., M. Hopfensitz, and H. A. Kestler (2010). BoolNet–an R package for generation, reconstruction and analysis of Boolean networks. *Bioinformatics*, 26(10):1378–1380.

Nakajima, Y., R. G. Tyers, C. C. Wong, J. R. Yates, D. G. Drubin, and G. Barnes (2009). Nbl1p: a Borealin/Dasra/CSC-1-like protein essential for Aurora/Ipl1 complex function and integrity in *Saccharomyces cerevisiae*. *Molecular Biology of the Cell*, 20(6):1772–1784.

Nash, P., X. Tang, S. Orlicky, Q. Chen, F. B. Gertler, M. D. Mendenhall, F. Sicheri, T. Pawson, and M. Tyers (2001). Multisite phosphorylation of a CDK inhibitor sets a threshold for the onset of DNA replication. *Nature*, 414(6863):514–521.

Nasmyth, K. and L. Dirick (1991). The role of SWI4 and SWI6 in the activity of G1 cyclins in yeast. *Cell*, 66(5):995–1013.

Nazarova, E., E. O'Toole, S. Kaitna, P. Francois, M. Winey, and J. Vogel (2013). Distinct roles for antiparallel microtubule pairing and overlap during early spindle assembly. *Molecular Biology of the Cell*, 24(20):3238–3250.

Neiman, A. M. (2011). Sporulation in the budding yeast *Saccharomyces cerevisiae*. *Genetics*, 189(3):737–765.

Nelson, B., C. Kurischko, J. Horecka, M. Mody, P. Nair, L. Pratt, A. Zougman, L. D. McBroom, T. R. Hughes, C. Boone, *et al.* (2003). RAM: a conserved signaling network that regulates Ace2p transcriptional activity and polarized morphogenesis. *Molecular Biology of the Cell*, 14(9):3782–3803.

Nern, A. and R. A. Arkowitz (1999). A Cdc24p-Far1p-G$\beta\gamma$ protein complex required for yeast orientation during mating. *The Journal of Cell Biology*, 144(6):1187–1202.

Nguyen, V. Q., J. J. Li, *et al.* (2001). Cyclin-dependent kinases prevent DNA re-replication through multiple mechanisms. *Nature*, 411(6841):1068–1073.

Niepel, M., K. R. Molloy, R. Williams, J. C. Farr, A. C. Meinema, N. Vecchietti, I. M. Cristea, B. T. Chait, M. P. Rout, and C. Strambio-De-Castillia (2013). The nuclear basket proteins Mlp1p and Mlp2p are part of a dynamic interactome including Esc1p and the proteasome. *Molecular Biology of the Cell*, 24(24):3920–3938.

Nishizawa, M., M. Kawasumi, M. Fujino, and A. Toh-e (1998). Phosphorylation of sic1, a cyclin-dependent kinase (Cdk) inhibitor, by Cdk including Pho85 kinase is required for its prompt degradation. *Molecular Biology of the Cell*, 9(9):2393–2405.

Nishizawa, M., K. Suzuki, M. Fujino, T. Oguchi, and A. Toh-e (1999). The Pho85 kinase, a member of the yeast cyclin-dependent kinase (Cdk) family, has a regulation mechanism different from Cdks functioning throughout the cell cycle. *Genes to Cells*, 4(11):627–642.

Nogales, E., M. Whittaker, R. A. Milligan, and K. H. Downing (1999). High-resolution model of the microtubule. *Cell*, 96(1):79–88.

Norris, D., B. Dunn, and M. A. Osley (1988). The effect of histone gene deletions on chromatin structure in *Saccharomyces cerevisiae*. *Science*, 242(4879):759–761.

Nurse, P. (2000). A long twentieth century of the cell cycle and beyond. *Cell*, 100(1):71–78.

Oda, K. and H. Kitano (2006). A comprehensive map of the toll-like receptor signaling network. *Molecular Systems Biology*, 2(1).

Oda, K., Y. Matsuoka, A. Funahashi, and H. Kitano (2005). A comprehensive pathway map of epidermal growth factor receptor signaling. *Molecular Systems Biology*, 1(1).

Oh, Y., K.-J. Chang, P. Orlean, C. Wloka, R. Deshaies, and E. Bi (2012). Mitotic exit kinase Dbf2 directly phosphorylates chitin synthase Chs2 to regulate cytokinesis in budding yeast. *Molecular Biology of the Cell*, 23(13):2445–2456.

Orth, J. D., T. M. Conrad, J. Na, J. A. Lerman, H. Nam, A. M. Feist, and B. Ø. Palsson (2011). A comprehensive genome-scale reconstruction of Escherichia coli metabolism–2011. *Molecular Systems Biology*, 7(1):535.

Ostapenko, D., J. L. Burton, and M. J. Solomon (2012). Identification of anaphase promoting complex substrates in *S. cerevisiae*. *PLoS One*, 7(9):e45895.

Ostapenko, D., J. L. Burton, R. Wang, and M. J. Solomon (2008). Pseudosubstrate inhibition of the anaphase-promoting complex by Acm1: regulation by proteolysis and Cdc28 phosphorylation. *Molecular and Cellular Biology*, 28(15):4653–4664.

Ostapenko, D. and M. J. Solomon (2011). Anaphase promoting complex–dependent degradation of transcriptional repressors Nrm1 and Yhp1 in *Saccharomyces cerevisiae*. *Molecular Biology of the Cell*, 22(13):2175–2184.

Ozaki, K., K. Tanaka, H. Imamura, T. Hihara, T. Kameyama, H. Nonaka, H. Hirano, Y. Matsuura, and Y. Takai (1996). Rom1p and Rom2p are GDP/GTP exchange proteins (GEPs) for the Rho1p small GTP binding protein in *Saccharomyces cerevisiae*. *The EMBO Journal*, 15(9):2196.

Palou, G., R. Palou, F. Zeng, A. A. Vashisht, J. A. Wohlschlegel, and D. G. Quintana (2015). Three different pathways prevent chromosome segregation in the presence of DNA damage or replication stress in budding yeast. *PLoS Genetics*, 11(9):e1005468.

Palumbo, P., M. Vanoni, V. Cusimano, S. Busti, F. Marano, C. Manes, and L. Alberghina (2016). Whi5 phosphorylation embedded in the G1/S network dynamically controls critical cell size and cell fate. *Nature Communications*, 7.

Pardo, B., L. Crabbé, and P. Pasero (2017). Signaling pathways of replication stress in yeast. *FEMS Yeast Research*, 17(2).

Park, C. J., J.-E. Park, T. S. Karpova, N.-K. Soung, L.-R. Yu, S. Song, K. H. Lee, X. Xia, E. Kang, I. Dabanoglu, *et al.* (2008). Requirement for the budding yeast polo kinase Cdc5 in proper microtubule growth and dynamics. *Eukaryotic Cell*, 7(3):444–453.

Patton, E. E., A. R. Willems, D. Sa, L. Kuras, D. Thomas, K. L. Craig, and M. Tyers (1998). Cdc53 is a scaffold protein for multiple Cdc34/Skp1/F-box protein complexes that regulate cell division and methionine biosynthesis in yeast. *Genes & Development*, 12(5):692–705.

Peplowska, K., A. U. Wallek, and Z. Storchova (2014). Sgo1 regulates both condensin and Ipl1/Aurora B to promote chromosome biorientation. *PLoS Genetics*, 10(6):e1004411.

Perez, A. M., G. C. Finnigan, F. M. Roelants, and J. Thorner (2016). Septin-associated protein kinases in the yeast *Saccharomyces cerevisiae*. *Frontiers in Cell and Developmental Biology*, 4.

Perkins, G., L. S. Drury, and J. F. Diffley (2001). Separate SCF CDC4 recognition elements target Cdc6 for proteolysis in S phase and mitosis. *The EMBO Journal*, 20(17):4836–4845.

Peter, M. and I. Herskowitz (1994). Direct inhibition of the yeast cyclin-dependent kinase Cdc28-Cln by Far1. *Science*, 265(5176):1228–1232.

Philip, B. and D. E. Levin (2001). Wsc1 and Mid2 are cell surface sensors for cell wall integrity signaling that act through Rom2, a guanine nucleotide exchange factor for Rho1. *Molecular and Cellular Biology*, 21(1):271–280.

Philipova, D., J. R. Mullen, H. S. Maniar, J. Lu, C. Gu, and S. J. Brill (1996). A hierarchy of SSB protomers in replication protein A. *Genes & Development*, 10(17):2222–2233.

Pic-Taylor, A., Z. Darieva, B. A. Morgan, and A. D. Sharrocks (2004). Regulation of cell cycle-specific gene expression through cyclin-dependent kinase-mediated phosphorylation of the forkhead transcription factor Fkh2p. *Molecular and Cellular Biology*, 24(22):10036–10046.

Poch, O., E. Schwob, F. de Fraipont, A. Camasses, R. Bordonné, and R. P. Martin (1994). RPK1, an essential yeast protein kinase involved in the regulation of the onset of mitosis, shows homology to mammalian dual-specificity kinases. *Molecular and General Genetics MGG*, 243(6):641–653.

Poli, J., O. Tsaponina, L. Crabbé, A. Keszthelyi, V. Pantesco, A. Chabes, A. Lengronne, and P. Pasero (2012). dNTP pools determine fork progression and origin usage under replication stress. *The EMBO Journal*, 31(4):883–894.

Pramila, T., S. Miles, D. GuhaThakurta, D. Jemiolo, and L. L. Breeden (2002). Conserved homeodomain proteins interact with MADS box protein Mcm1 to restrict ECB-dependent transcription to the M/G1 phase of the cell cycle. *Genes & Development*, 16(23):3034–3045.

Pramila, T., W. Wu, S. Miles, W. S. Noble, and L. L. Breeden (2006). The Forkhead transcription factor Hcm1 regulates chromosome segregation genes and fills the S-phase gap in the transcriptional circuitry of the cell cycle. *Genes & Development*, 20(16):2266–2278.

Pruyne, D., M. Evangelista, C. Yang, E. Bi, S. Zigmond, A. Bretscher, and C. Boone (2002). Role of formins in actin assembly: nucleation and barbed-end association. *Science*, 297(5581):612–615.

Pruyne, D., L. Gao, E. Bi, and A. Bretscher (2004). Stable and dynamic axes of polarity use distinct formin isoforms in budding yeast. *Molecular Biology of the Cell*, 15(11):4971–4989.

Qadota, H., C. P. Python, S. B. Inoue, M. Arisawa, Y. Anraku, Y. Zheng, T. Watanabe, D. E. Levin, and Y. Ohya (1996). Identification of yeast Rho1p GTPase as a regulatory subunit of 1, 3-β-glucan synthase. *Science*, Pp. 279–281.

Queralt, E., C. Lehane, B. Novak, and F. Uhlmann (2006). Downregulation of PP2A Cdc55 phosphatase by separase initiates mitotic exit in budding yeast. *Cell*, 125(4):719–732.

Quilis, I. and J. C. Igual (2017). A comparative study of the degradation of yeast cyclins Cln1 and Cln2. *FEBS open bio*, 7(1):74–87.

R Core Team (2013). *R: A Language and Environment for Statistical Computing*. R Foundation for Statistical Computing, Vienna, Austria.

Rane, C. K. and A. Minden (2014). P21 activated kinases: structure, regulation, and functions. *Small GTPases*, 5(1):e28003.

Reynard, G. J., W. Reynolds, R. Verma, and R. J. Deshaies (2000). Cks1 Is Required for G1Cyclin–Cyclin-Dependent Kinase Activity in Budding Yeast. *Molecular and Cellular Biology*, 20(16):5858–5864.

Reynolds, D., B. J. Shi, C. McLean, F. Katsis, B. Kemp, and S. Dalton (2003). Recruitment of Thr 319-phosphorylated Ndd1p to the FHA domain of Fkh2p requires Clbkinase activity: a mechanism for CLB cluster gene activation. *Genes & Development*, 17(14):1789–1802.

Richardson, H. E., C. Wittenberg, F. Cross, and S. I. Reed (1989). An essential G1 function for cyclin-like proteins in yeast. *Cell*, 59(6):1127–1133.

Riedel, C. G., V. L. Katis, Y. Katou, S. Mori, T. Itoh, W. Helmhart, M. Gálová, M. Petronczki, J. Gregan, B. Cetin, *et al.* (2006). Protein phosphatase 2A protects centromeric sister chromatid cohesion during meiosis I. *Nature*, 441(7089):53–61.

Rienksma, R. A., M. Suarez-Diez, L. Spina, P. J. Schaap, and V. A. M. dos Santos (2014). Systems-level modeling of mycobacterial metabolism for the identification of new (multi-) drug targets. In *Seminars in Immunology*, volume 26, Pp. 610–622. Elsevier.

Robellet, X., Y. Thattikota, F. Wang, T.-L. Wee, M. Pascariu, S. Shankar, É. Bonneil, C. M. Brown, and D. D'Amours (2015). A high-sensitivity phospho-switch triggered by Cdk1 governs chromosome morphogenesis during cell division. *Genes & Development*, 29(4):426–439.

Rock, J. M., D. Lim, L. Stach, R. W. Ogrodowicz, J. M. Keck, M. H. Jones, C. C. Wong, J. R. Yates, M. Winey, S. J. Smerdon, *et al.* (2013). Activation of the yeast Hippo pathway by phosphorylation-dependent assembly of signaling complexes. *Science*, 340(6134):871–875.

Rodriguez-Rodriguez, J.-A., Y. Moyano, S. Játiva, and E. Queralt (2016). Mitotic Exit Function of Polo-like Kinase Cdc5 Is Dependent on Sequential Activation by Cdk1. *Cell Reports*, 15(9):2050–2062.

Romers, J., S. Thieme, U. Münzner, and M. Krantz . Using rxncon to develop rule–based models. *under review*.

Romers, J. C. and M. Krantz (2017). rxncon 2.0: a language for executable molecular systems biology. *bioRxiv*.

Rosenberg, J. S., F. R. Cross, and H. Funabiki (2011). KNL1/Spc105 recruits PP1 to silence the spindle assembly checkpoint. *Current Biology*, 21(11):942–947.

Ross, K. E., P. Kaldis, and M. J. Solomon (2000). Activating phosphorylation of the *Saccharomyces cerevisiae* cyclin-dependent kinase, Cdc28p, precedes cyclin binding. *Molecular Biology of the Cell*, 11(5):1597–1609.

Rother, M., U. Münzner, S. Thieme, and M. Krantz (2013). Information content and scalability in signal transduction network reconstruction formats. *Molecular BioSystems*, 9(8):1993–2004.

Roumanie, O., H. Wu, J. N. Molk, G. Rossi, K. Bloom, and P. Brennwald (2005). Rho GTPase regulation of exocytosis in yeast is independent of GTP hydrolysis and polarization of the exocyst complex. *The Journal of Cell Biology*, 170(4):583–594.

Rouse, J. and S. P. Jackson (2002). Lcd1p recruits Mec1p to DNA lesions in vitro and in vivo. *Molecular Cell*, 9(4):857–869.

Rüthnick, D. and E. Schiebel (2016). Duplication of the yeast spindle pole body once per cell cycle. *Molecular and Cellular Biology*, 36(9):1324–1331.

Ryan, K. J., J. M. McCaffery, and S. R. Wente (2003). The Ran GTPase cycle is required for yeast nuclear pore complex assembly. *The Journal of Cell Biology*, 160(7):1041–1053.

Sahin, A., B. Daignan-Fornier, and I. Sagot (2008). Polarized growth in the absence of F-actin in *Saccharomyces cerevisiae* exiting quiescence. *PLoS One*, 3(7):e2556.

Sahin, Ö., H. Fröhlich, C. Löbke, U. Korf, S. Burmester, M. Majety, J. Mattern, I. Schupp, C. Chaouiya, D. Thieffry, A. Poustka, S. Wiemann, T. Beissbarth, and D. Arlt (2009). Modeling ERBB receptor-regulated G1/S transition to find novel targets for de novo trastuzumab resistance. *BMC Systems Biology*, 3(1):1.

Saito, H. and F. Posas (2012). Response to Hyperosmotic Stress. *Genetics*, 192(2):289–318.

Sbia, M., E. J. Parnell, Y. Yu, A. E. Olsen, K. L. Kretschmann, W. P. Voth, and D. J. Stillman (2008). Regulation of the yeast Ace2 transcription factor during the cell cycle. *Journal of Biological Chemistry*, 283(17):11135–11145.

Schmelzle, T., S. B. Helliwell, and M. N. Hall (2002). Yeast protein kinases and the RHO1 exchange factor TUS1 are novel components of the cell integrity pathway in yeast. *Molecular and Cellular Biology*, 22(5):1329–1339.

Scholey, J. M., G. Civelekoglu-Scholey, and I. Brust-Mascher (2016). Anaphase B. *Biology*, 5(4):51.

Schreiber, A., F. Stengel, Z. Zhang, R. I. Enchev, E. H. Kong, E. P. Morris, C. V. Robinson, P. C. da Fonseca, and D. Barford (2011). Structural basis for the subunit assembly of the anaphase-promoting complex. *Nature*, 470(7333):227.

Schrum, J. P., T. F. Zhu, and J. W. Szostak (2010). The Origins of Cellular Life. *Cold Spring Harbor Perspectives in Biology*, 2(9):a002212.

Schuyler, S. C., J. Y. Liu, and D. Pellman (2003). The molecular function of Ase1p. *The Journal of Cell Biology*, 160(4):517–528.

Schwob, E. and K. Nasmyth (1993). CLB5 and CLB6, a new pair of B cyclins involved in S phase and mitotic spindle formation in *S. cerevisiae*. *Genes & Development*, 7:1160–1175.

Seol, J. H., R. R. Feldman, W. Zachariae, A. Shevchenko, C. C. Correll, S. Lyapina, Y. Chi, M. Galova, J. Claypool, S. Sandmeyer, *et al.* (1999). Cdc53/cullin and the essential Hrt1 RING–H2 subunit of SCF define a ubiquitin ligase module that activates the E2 enzyme Cdc34. *Genes & Development*, 13(12):1614–1626.

Shannon, P., A. Markiel, O. Ozier, N. S. Baliga, J. T. Wang, D. Ramage, N. Amin, B. Schwikowski, and T. Ideker (2003). Cytoscape: a software environment for integrated models of biomolecular interaction networks. *Genome Research*, 13(11):2498–2504.

Shou, W., R. Azzam, S. L. Chen, M. J. Huddleston, C. Baskerville, H. Charbonneau, R. S. Annan, S. A. Carr, and R. J. Deshaies (2002). Cdc5 influences phosphorylation of Net1 and disassembly of the RENT complex. *BMC Molecular Biology*, 3(1):3.

Shou, W., J. H. Seol, A. Shevchenko, C. Baskerville, D. Moazed, Z. S. Chen, J. Jang, A. Shevchenko, H. Charbonneau, and R. J. Deshaies (1999). Exit from mitosis is triggered by Tem1-dependent release of the protein phosphatase Cdc14 from nucleolar RENT complex. *Cell*, 97(2):233–244.

Shu, Y., H. Yang, E. Hallberg, and R. Hallberg (1997). Molecular genetic analysis of Rts1p, a B'regulatory subunit of *Saccharomyces cerevisiae* protein phosphatase 2A. *Molecular and Cellular Biology*, 17(6):3242–3253.

Sia, R., H. A. Herald, and D. J. Lew (1996). Cdc28 tyrosine phosphorylation and the morphogenesis checkpoint in budding yeast. *Molecular Biology of the Cell*, 7(11):1657–1666.

Siegmund, R. F. and K. A. Nasmyth (1996). The *Saccharomyces cerevisiae* Start-specific transcription factor Swi4 interacts through the ankyrin repeats with the mitotic Clb2/Cdc28 kinase and through its conserved carboxy terminus with Swi6. *Molecular and Cellular Biology*, 16(6):2647–2655.

Simon, I., J. Barnett, N. Hannett, C. T. Harbison, N. J. Rinaldi, T. L. Volkert, J. J. Wyrick, J. Zeitlinger, D. K. Gifford, T. S. Jaakkola, *et al.* (2001). Serial regulation of transcriptional regulators in the yeast cell cycle. *Cell*, 106(6):697–708.

Skowyra, D., K. L. Craig, M. Tyers, S. J. Elledge, and J. W. Harper (1997). F-box proteins are receptors that recruit phosphorylated substrates to the SCF ubiquitin-ligase complex. *Cell*, 91(2):209–219.

Smeets, M. F. and M. Segal (2002). Spindle polarity in *S. cerevisiae*: MEN can tell. *Cell Cycle*, 1(5):308–311.

Sneddon, M. W., J. R. Faeder, and T. Emonet (2011). Efficient modeling, simulation and coarse-graining of biological complexity with NFsim. *Nature Methods*, 8(2):177–183.

Song, S. and K. S. Lee (2001). A novel function of *Saccharomyces cerevisiae* CDC5 in cytokinesis. *The Journal of Cell Biology*, 152(3):451–470.

Sopko, R., D. Huang, J. C. Smith, D. Figeys, and B. J. Andrews (2007). Activation of the Cdc42p GTPase by cyclin-dependent protein kinases in budding yeast. *The EMBO Journal*, 26(21):4487–4500.

Speck, C., Z. Chen, H. Li, and B. Stillman (2005). ATPase-dependent, cooperative binding of ORC and Cdc6p to origin DNA. *Nature Structural & Molecular Biology*, 12(11):965.

Spellman, P. T., G. Sherlock, M. Q. Zhang, V. R. Iyer, K. Anders, M. B. Eisen, P. O. Brown, D. Botstein, and B. Futcher (1998). Comprehensive identification of cell cycle–regulated genes of the yeast *Saccharomyces cerevisiae* by microarray hybridization. *Molecular Biology of the Cell*, 9(12):3273–3297.

Spiesser, T. W., C. Müller, G. Schreiber, M. Krantz, and E. Klipp (2012). Size homeostasis can be intrinsic to growing cell populations and explained without size sensing or signalling. *FEBS J.*, 279(22):4213–30.

Stolz, L. E., W. J. Kuo, J. Longchamps, M. K. Sekhon, and J. D. York (1998). INP51, a yeast inositol polyphosphate 5-phosphatase required for phosphatidylinositol 4, 5-bisphosphate homeostasis and whose absence confers a cold-resistant phenotype. *Journal of Biological Chemistry*, 273(19):11852–11861.

Sullivan, M., C. Lehane, and F. Uhlmann (2001). Orchestrating anaphase and mitotic exit: separase cleavage and localization of Slk19. *Nature Cell Biology*, 3(9):771–777.

Sun, J., H. Kawakami, J. Zech, C. Speck, B. Stillman, and H. Li (2012). Cdc6-induced conformational changes in ORC bound to origin DNA revealed by cryo-electron microscopy. *Structure*, 20(3):534–544.

Surana, U., H. Robitsch, C. Price, T. Schuster, I. Fitch, A. B. Futcher, and K. Nasmyth (1991). The role of CDC28 and cyclins during mitosis in the budding yeast *S. cerevisiae*. *Cell*, 65(1):145–161.

Takahata, S., Y. Yu, and D. J. Stillman (2009). The E2F functional analogue SBF recruits the Rpd3 (L) HDAC, via Whi5 and Stb1, and the FACT chromatin reorganizer, to yeast G1 cyclin promoters. *The EMBO Journal*, 28(21):3378–3389.

Tanaka, S., Y. Komeda, T. Umemori, Y. Kubota, H. Takisawa, and H. Araki (2013). Efficient initiation of DNA replication in eukaryotes requires Dpb11/TopBP1-GINS interaction. *Molecular and Cellular Biology*, 33(13):2614–2622.

Tanaka, S., T. Umemori, K. Hirai, S. Muramatsu, Y. Kamimura, and H. Araki (2007). CDK-dependent phosphorylation of Sld2 and Sld3 initiates DNA replication in budding yeast. *Nature*, 445(7125):328.

Teh, E. M., C. C. Chai, and F. M. Yeong (2009). Retention of Chs2p in the ER requires N-terminal CDK1-phosphorylation sites. *Cell Cycle*, 8(18):2965–2976.

Tennyson, C. N., J. Lee, and B. J. Andrews (1998). A role for the Pcl9-Pho85 cyclin–cdk complex at the M/G1 boundary in *Saccharomyces cerevisiae*. *Molecular Microbiology*, 28(1):69–79.

Tessera, M. (2011). Origin of evolution versus origin of life: a shift of paradigm. *International Journal of Molecular Sciences*, 12(6):3445–3458.

Thiele, I. and B. Ø. Palsson (2010). A protocol for generating a high-quality genome-scale metabolic reconstruction. *Nature Protocols*, 5(1):93–121.

Thieme, S., J. C. Romers, U. Münzner, and M. Krantz (2017). Bipartite Boolean modelling - a method for mechanistic simulation and validation of large-scale signal transduction networks. *bioRxiv*.

Thomas, D. and Y. Surdin-Kerjan (1997). Metabolism of sulfur amino acids in *Saccharomyces cerevisiae*. *Microbiology and Molecular Biology Reviews*, 61(4):503–532.

Thompson, D., A. Regev, and S. Roy (2015). Comparative analysis of gene regulatory networks: from network reconstruction to evolution. *Annual review of cell and developmental biology*, 31:399–428.

Tiger, C.-F., F. Krause, G. Cedersund, R. Palmér, E. Klipp, S. Hohmann, H. Kitano, and M. Krantz (2012). A framework for mapping, visualisation and automatic model creation of signal-transduction networks. *Molecular Systems Biology*, 8(1).

Travesa, A., T. I. Kalashnikova, R. A. de Bruin, S. R. Cass, C. Chahwan, D. E. Lee, N. F. Lowndes, and C. Wittenberg (2013). Repression of G1/S transcription is mediated via interaction of the GTB motifs of Nrm1 and Whi5 with Swi6. *Molecular and Cellular Biology*, 33(8):1476–1486.

Travesa, A., D. Kuo, R. A. De Bruin, T. I. Kalashnikova, M. Guaderrama, K. Thai, A. Aslanian, M. B. Smolka, J. R. Yates, T. Ideker, *et al.* (2012). DNA replication stress differentially regulates G1/S genes via Rad53-dependent inactivation of Nrm1. *The EMBO Journal*, 31(7):1811–1822.

Truman, A. W., K. Kristjansdottir, D. Wolfgeher, N. Hasin, S. Polier, H. Zhang, S. Perrett, C. Prodromou, G. W. Jones, and S. J. Kron (2012). CDK-dependent Hsp70 Phosphorylation controls G1 cyclin abundance and cell-cycle progression. *Cell*, 151(6):1308–1318.

Tsokolov, S. A. (2009). Why is the definition of life so elusive? Epistemological considerations. *Astrobiology*, 9(4):401–412.

Tummler, K., T. Lubitz, M. Schelker, and E. Klipp (2014). New types of experimental data shape the use of enzyme kinetics for dynamic network modeling. *The FEBS journal*, 281(2):549–571.

Uhlmann, F., F. Lottspeich, and K. Nasmyth (1999). Sister-chromatid separation at anaphase onset is promoted by cleavage of the cohesin subunit Scc1. *Nature*, 400(6739):37.

Valerio-Santiago, M. and F. Monje-Casas (2011). Tem1 localization to the spindle pole bodies is essential for mitotic exit and impairs spindle checkpoint function. *The Journal of Cell Biology*, Pp. jcb–201007044.

Vergés, E., N. Colomina, E. Garí, C. Gallego, and M. Aldea (2007). Cyclin Cln3 is retained at the ER and released by the J chaperone Ydj1 in late G1 to trigger cell cycle entry. *Molecular Cell*, 26(5):649–662.

Versele, M. and J. Thorner (2004). Septin collar formation in budding yeast requires GTP binding and direct phosphorylation by the PAK, Cla4. *The Journal of Cell Biology*, 164(5):701–715.

Visintin, R., K. Craig, E. S. Hwang, S. Prinz, M. Tyers, and A. Amon (1998). The phosphatase Cdc14 triggers mitotic exit by reversal of Cdk-dependent phosphorylation. *Molecular Cell*, 2(6):709–718.

Wagner, M. V., M. B. Smolka, R. A. De Bruin, H. Zhou, C. Wittenberg, and S. F. Dowdy (2009). Whi5 regulation by site specific CDK-phosphorylation in *Saccharomyces cerevisiae*. *PLoS One*, 4(1):e4300.

Wakayama, T., T. Kondo, S. Ando, K. Matsumoto, and K. Sugimoto (2001). Pie1, a protein interacting with Mec1, controls cell growth and checkpoint responses in *Saccharomyces cerevisiae*. *Molecular and Cellular Biology*, 21(3):755–764.

Wang, H., E. Garí, E. Verges, C. Gallego, and M. Aldea (2004). Recruitment of Cdc28 by Whi3 restricts nuclear accumulation of the G1 cyclin–Cdk complex to late G1. *The EMBO Journal*, 23(1):180–190.

Wang, H., D. Liu, Y. Wang, J. Qin, and S. J. Elledge (2001). Pds1 phosphorylation in response to DNA damage is essential for its DNA damage checkpoint function. *Genes & Development*, 15(11):1361–1372.

Wang, Y., T. Shirogane, D. Liu, J. W. Harper, and S. J. Elledge (2003). Exit from exit: resetting the cell cycle through Amn1 inhibition of G protein signaling. *Cell*, 112(5):697–709.

Wäsch, R. and F. R. Cross (2002). APC-dependent proteolysis of the mitotic cyclin Clb2 is essential for mitotic exit. *Nature*, 418(6897):556.

Watanabe, D., M. Abe, and Y. Ohya (2001). Yeast Lrg1p acts as a specialized RhoGAP regulating 1, 3-β-glucan synthesis. *Yeast*, 18(10):943–951.

Webster, C. R., P. R. Mahaffy, S. K. Atreya, G. J. Flesch, M. A. Mischna, P.-Y. Meslin, K. A. Farley, P. G. Conrad, L. E. Christensen, A. A. Pavlov, *et al.* (2015). Mars methane detection and variability at Gale crater. *Science*, 347(6220):415–417.

Weiss, E. L. (2012). Mitotic exit and separation of mother and daughter cells. *Genetics*, 192(4):1165–1202.

Wild, A. C., W. Y. Jong, M. A. Lemmon, and K. J. Blumer (2004). The p21-activated protein kinase-related kinase Cla4 is a coincidence detector of signaling by Cdc42 and phosphatidylinositol 4-phosphate. *Journal of Biological Chemistry*, 279(17):17101–17110.

Winey, M. and K. Bloom (2012). Mitotic spindle form and function. *Genetics*, 190(4):1197–1224.

Woods, B., C.-C. Kuo, C.-F. Wu, T. R. Zyla, and D. J. Lew (2015). Polarity establishment requires localized activation of Cdc42. *The Journal of Cell Biology*, 211(1):19–26.

Wu, H., C. Turner, J. Gardner, B. Temple, and P. Brennwald (2010). The Exo70 subunit of the exocyst is an effector for both Cdc42 and Rho3 function in polarized exocytosis. *Molecular biology of the cell*, 21(3):430–442.

Wu, R., J. Wang, and C. Liang (2012). Cdt1p, through its interaction with Mcm6p, is required for the formation, nuclear accumulation and chromatin loading of the MCM complex. *J Cell Sci*, 125(1):209–219.

Xu, Y., J. B. Moseley, I. Sagot, F. Poy, D. Pellman, B. L. Goode, and M. J. Eck (2004). Crystal structures of a Formin Homology-2 domain reveal a tethered dimer architecture. *Cell*, 116(5):711–723.

Yaglom, J., M. Linskens, S. Sadis, D. M. Rubin, B. Futcher, and D. Finley (1995). p34Cdc28-mediated control of Cln3 cyclin degradation. *Molecular and Cellular Biology*, 15(2):731–741.

Yaglom, J. A., A. L. Goldberg, D. Finley, and M. Y. Sherman (1996). The molecular chaperone Ydj1 is required for the p34CDC28-dependent phosphorylation of the cyclin Cln3 that signals its degradation. *Molecular and Cellular Biology*, 16(7):3679–3684.

Yamagishi, Y., T. Sakuno, Y. Goto, and Y. Watanabe (2014). Kinetochore composition and its function: lessons from yeasts. *FEMS Microbiology Reviews*, 38(2):185–200.

Yeeles, J. T., T. D. Deegan, A. Janska, A. Early, and J. F. Diffley (2015). Regulated eukaryotic DNA replication origin firing with purified proteins. *Nature*, 519(7544):431–435.

Yelamanchi, S. K., J. Veis, D. Anrather, H. Klug, and G. Ammerer (2014). Genotoxic stress prevents Ndd1-dependent transcriptional activation of G2/M-specific genes in *Saccharomyces cerevisiae*. *Molecular and Cellular Biology*, 34(4):711–724.

Yin, H., D. Pruyne, T. C. Huffaker, and A. Bretscher (2000). Myosin V orientates the mitotic spindle in yeast. *Nature*, 406(6799):1013.

Yoon, H.-J. and J. Carbon (1999). Participation of Bir1p, a member of the inhibitor of apoptosis family, in yeast chromosome segregation events. *Proceedings of the National Academy of Sciences*, 96(23):13208–13213.

Yoshida, S., K. Kono, D. M. Lowery, S. Bartolini, M. B. Yaffe, Y. Ohya, and D. Pellman (2006). Polo-like kinase Cdc5 controls the local activation of Rho1 to promote cytokinesis. *Science*, 313(5783):108–111.

Yoshida, S., Y. Ohya, M. Goebl, A. Nakano, and Y. Anraku (1994). A novel gene, STT4, encodes a phosphatidylinositol 4-kinase in the PKC1 protein kinase pathway of *Saccharomyces cerevisiae*. *Journal of Biological Chemistry*, 269(2):1166–1172.

Yoshida, S. and A. Toh-e (2002). Budding yeast Cdc5 phosphorylates Net1 and assists Cdc14 release from the nucleolus. *Biochemical and biophysical research communications*, 294(3):687–691.

Zhang, X., R. L. Lester, and R. C. Dickson (2004). Pil1p and Lsp1p Negatively Regulate the 3-Phosphoinositide-dependent Protein Kinase-like Kinase Pkh1p and Downstream Signaling Pathways Pkc1p and Ypk1p. *Journal of Biological Chemistry*, 279(21):22030–22038.

Zhao, X., E. G. Muller, and R. Rothstein (1998). A suppressor of two essential checkpoint genes identifies a novel protein that negatively affects dNTP pools. *Molecular Cell*, 2(3):329–340.

Zheng, J., D. Zhang, P. F. Przytycki, R. Zielinski, J. Capala, and T. M. Przytycka (2010). SimBoolNet – a Cytoscape plugin for dynamic simulation of signaling networks. *Bioinformatics*, 26(1):141–142.

Zheng, P., D. Fay, J. Burton, H. Xiao, J. Pinkham, and D. Stern (1993). SPK1 is an essential S-phase-specific gene of *Saccharomyces cerevisiae* that encodes a nuclear serine/threonine/tyrosine kinase. *Molecular and Cellular Biology*, 13(9):5829–5842.

Zheng, Y., R. Cerione, and A. Bender (1994). Control of the yeast bud-site assembly GTPase Cdc42. Catalysis of guanine nucleotide exchange by Cdc24 and stimulation of GTPase activity by Bem3. *Journal of Biological Chemistry*, 269(4):2369–2372.

Zich, J. and K. G. Hardwick (2010). Getting down to the phosphorylated 'nuts and bolts' of spindle checkpoint signalling. *Trends in Biochemical Sciences*, 35(1):18–27.

List of Figures

List of Tables

Abbreviations

APC/C	anaphase promoting complex/cyclosome
BNG	BioNetGen
BNGL	BNG language
CC-CNW	cell cycle control network
CDK	cyclin dependent kinase
CDKI	CDK inhibitor
CMG	Cdc45/Mcm2–7/GINS
COPASI	COmplex PAthway SImulator
DAD	C-terminal diaphanous autoregulatory domain
DDK	Dbf4-dependent kinase
DID	N-terminal diaphanous inhibitory domain
dNTP	deoxynucleoside triphosphate
ER	endoplasmic reticulum
FH	formin homology 2
G_1	gap phase 1
G_2	gap phase 2
GAP	GTPase activating protein
GBD	GTPase binding domain
GDP	guanosine diphosphate
GEF	guanine nucleotide exchange factor
GTP	guanosine triphosphate
HDAC	histone deacetylase
HU	hydroxyurea
LatA	latrunculin A
M	mitotic exit phase
MBF	Mlu1-box binding factor
MCB	Mlu1 cell cycle box
MEN	mitotic exit network
NPC	nuclear pore complex

ODE	ordinary differential equation
ORC	origin recognition complex
PDE	partial differential equation
QlM	qualitative network model
RFC	replication factor C
RPA	replication protein A
rxncon	reaction–contingency
S	synthesis phase
SAC	spindle assembly checkpoint
SBF	Swi4-Swi6 cell cycle box binding factor
SBGN	Systems Biology Graphical Notation
SBGN-PD	SBGN process diagram
SBML	Systems Biology Markup Language
SCB	Swi4/Swi6 cell cycle box
SCF	Skp, Cullin, F-box containing complex
SGD	*Saccharomyces* Genome Database
SPOC	spindle position checkpoint
ss/ds	single-stranded/double-stranded
T	threonine

A

Appendix

THE APPENDIX PRESENTS the CC-CNW in rxncon language, and the comparison of the proteins accounted for in the CC-CNW and Kaizu model (Section A.1). Section A.2 presents the elemental reactions and states which have no physiological relevance as accounted for in the CC-CNW, and presents the unregulated gene regulatory motifs. Section A.3 presents the translation of the Kaizu model into elemental reactions.

A.1 Complete cell cycle control network in rxncon language

This section presents the complete CC-CNW in rxncon language. First, the proteins of the CC-CNW and the Kaizu model are presented and compared to each other (Subsection A.1.1). Second, the completee CC-CNW in rxncon language is presented in Subsection A.1.2.

A.1.1 *Network components and comparison*

Table A.1 lists the proteins accounted for in the CC-CNW and Kaizu model. The table is divided into four columns. The first three columns show the proteins uniquely accounted for in the CC-CNW, the proteins accounted for in both, the CC-CNW and Kaizu model, and the proteins uniquely accounted for in the Kaizu model. The separation is according to the Venn diagram in Figure 5.27. The fourth column contains the proteins accounted for in the Kaizu model which have not been considered in the comparison to the CC-CNW.

The proteins excluded from the comparison were considered to be out of scope, as they belong to signal transduction pathways or metabolic processes, and hence, are not part to the core cell cycle control network. The proteins are here sorted according to the processes they are involved in. The division, however, is not strict, as some proteins can be involved in several pathways due to cross talk. The proteins Hog1, Hot1, Msb2, Och1, Opy2, Pbs2, Ptc1, Ptp2, Ptp3, Sho1, Sko1, Sln1, Smp1, Ssk1, Ssk2, Ssk22, Stl1, and Ypd1 are involved in osmoregulation (Saito and Posas, 2012). The proteins Dig1, Dig2, Fus3, Gpa1, Msg5, Msn1, Ras2, Sst2, Ste2, Ste3, Ste4, Ste5, Ste7, Ste11, Ste12, Ste18, Ste50, Tec1, and Tpk1 are involved in mating and filamentous growth (Cullen and Sprague, 2012; Haber, 2012), Exg1 is a cell wall glucanase (Cappellaro *et al.*, 1998). The proteins Ddc1, Rtt109, Esc4, Pph3, Rad6, and Rad9 are involved in DNA damage repair (Boiteux and Jinks-Robertson, 2013). The proteins Mig1, Reg1, Snf1, Stl1, Yak1 are involved in glucose repression (Broach, 2012). The proteins Bck1, Mkk1, Mkk2, Pkc1, Pkh1, Phk2, Rlm1, Sdp1, and Slt2 are involved in the PKC pathway (Levin, 2011). The proteins Lsp1 and Pil1 interfere with the PKC pathway (Zhang *et al.*, 2004). The proteins Pho2, Pho4, Pho5, Pho80, and Pho81 are involved in phosphate metabolism (Ljungdahl and Daignan-Fornier, 2012). The proteins Avo1, Avo2, Kog1, Lst8, Sch9, Tap42, Tco89, Tip41, Tor1, Tor2, Tsc11, Ypk1, and Ypk2 are involved in nutrient sensing (Loewith and Hall, 2011). Met4 is involved in sulfur amino acid metabolism (Thomas and Surdin-Kerjan, 1997). The Kaizu model also accounts for proteins involved in general stress responses, such as the proteins Cna1, Cna2, Cnb1, and Crz1 (Cyert and Philpott, 2013), and the transcription factor Msn2 (Gasch *et al.*, 2000). Hsf1 is involved in heat shock response (Morano *et al.*, 2012); Cch1 amd Pmc1 are involved in ion homeostasis (Cyert and Philpott, 2013); Bre1, Skn7, Sko1, Trr1, Trx2, and Yap1 are involved in oxidative stress, Flo1 is involved in flocculation (Kobayashi *et al.*, 1998), Bcy1 belongs to the PKA pathway (Broach, 2012), Fap1 and Fpr1 are involved in the rapamycin stress response (Limson and Sweder, 2009). Rna1 is connected to the nuclear pore complex (Ryan *et al.*, 2003).

Table A.1. *Network comparison based on proteins.* The table lists the proteins uniquely accounted for in the CC-CNW, the overlapping proteins from both networks, the proteins uniquely accounted for in the Kaizu model; and the proteins accounted for in the Kaizu model excluded from the comparison.

	Only in CC-CNW	Shared	Only in Kaizu	Excluded from Kaizu
1	Act1	Ace2	Amn1	Avo1
2	Ask1	Acm1	Apc1	Avo2
3	Bck2	Ase1	Apc11	Bck1
4	Bem2	Axl1	Apc2	Bcy1
5	Bem3	Bem1	Apc4	Bre1
6	Bim1	Bfa1	Apc5	Cch1
7	Bnr1	Bir1	Apc9	Cna1
8	Brn1	Bmh1	Asf1	Cna2
9	Bud6	Bmh2	Ash1	Cnb1
10	Cdc11	Bni1	Axl2	Crz1
11	Cdc12	Boi1	Bit61	Ddc1
12	Cdc31	Boi2	Bud8	Dig1
13	Cdc45	Bub1	Bud9	Dig2
14	Cdt1	Bub2	Cdc16	Exg1
15	Chs2	Bub3	Cdc23	Fap1
16	Cmd1	Bud2	Cdc26	Flo1
17	Cnm67	Bud3	Cdc27	Fpr1
18	Ctf18	Bud4	Cka1	Fus3
19	Dad4	Bud5	Cka2	Gpa1
20	Dma1	Cak1	Ckb1	Hog1
21	Duo1	Cbf2	Cts1	Hot1
22	Exo70	Cbk1	Cyc8	Hsf1
23	Fks1	Cdc10	Dia2	Kog1
24	Hos3	Cdc14	Doc1	Lsp1
25	Hym1	Cdc15	Eco1	Lst8
26	Inp51	Cdc20	Egt2	Met4
27	Kar1	Cdc24	Esa1	Mig1
28	Kic1	Cdc28	Fob1	Mkk1
29	Lrg1	Cdc3	Gcn5	Mkk2
30	Mcm10	Cdc34	Gin4	Msb2
31	Mcm4	Cdc4	Gsp1	Msg5
32	Mcm6	Cdc42	Hda1	Msn1
33	Mid2	Cdc5	Hhf1	Msn2
34	Mrc1	Cdc53	Hhf2	Och1
35	Msb3	Cdc55	Hht1	Opy2
36	Msb4	Cdc6	Hht2	Pbs2
37	Mss4	Cdc7	Hrr25	Pho2
38	Myo2	Cdh1	Htb1	Pho4
39	Nbl1	Chk1	Htb2	Pho5
40	Ndc80	Cin8	Ime2	Pho80
41	Nuf2	Cks1	Mck1	Pho81
42	Orc1	Cla4	Mlp1	Pil1
43	Orc3	Clb1	Mnd2	Pkc1
44	Orc4	Clb2	Msa1	Pkh1
45	Orc5	Clb3	Msa2	Pkh2
46	Pcl9	Clb4	Myo3	Pmc1
47	Pea2	Clb5	Nop7	Pph3
48	Pol2	Clb6	Nup53	Ptc1
49	Psf1	Cln1	Pmr2	Ptp2
50	Ptc2	Cln2	Ppm1	Ptp3
51	Ptc3	Cln3	Rax1	Rad6
52	Rfa3	Dam1	Rax2	Rad9
53	Rga1	Dbf2	Rec8	Ras2
54	Sac1	Dbf4	Rfx1	Reg1
55	Scc2	Dpb11	Sap155	Rlm1
56	Scc4	Dun1	Sap185	Rna1
57	Sec2	Elm1	Sap190	Rtt107
58	Sec3	Esp1	Shs1	Rtt109
59	Sec4	Far1	Sir2	Sch9
60	Sfi1	Fin1	Sir3	Sdp1
61	Sgs1	Fkh1	Sir4	Sho1
62	Sld3	Fkh2	Sit4	Skn7
63	Slg1	Gic1	Spo12	Sko1
64	Smc2	Gic2	Ssn3	Sln1
65	Smc4	Glc7	Ssn8	Slt2
66	Sog2	Grr1	Stu2	Smp1
67	Spa2	Gsc2	Swm1	Snf1
68	Spc105	Hcm1	Tup1	Ssk1
69	Spc24	Hof1	Ubp10	Ssk2
70	Spc25	Hrt1	Vps75	Ssk22
71	Spc29	Hsl1	Yck1	Sst2
72	Spc97	Hsl7	Yck2	Ste11
73	Sst4	Ipl1	Ypa1	Ste12

Table A.1 – *Continued from previous page*

	Only in CC-CNW	Shared	Only in Kaizu	Excluded from Kaizu
74	Tao3	Irr1	Ypa2	Ste18
75	Tgl4	Kar9		Ste2
76	Tub1	Kin4		Ste3
77	Tub2	Kip1		Ste4
78	Tub3	Lcd1		Ste5
79	Tub4	Lte1		Ste50
80	Ycg1	Mad1		Ste7
81	Ycs4	Mad2		Stl1
82		Mad3		Tap42
83		Mbp1		Tco89
84		Mcm1		Tec1
85		Mcm2		Tip41
86		Mcm3		Tor1
87		Mcm5		Tor2
88		Mcm7		Tpk1
89		Mec1		Trr1
90		Met30		Trx2
91		Mih1		Tsc11
92		Mob1		Yak1
93		Mob2		Yap1
94		Mps1		Ypd1
95		Ndd1		Ypk1
96		Net1		Ypk2
97		Nrm1		
98		Nud1		
99		Orc2		
100		Orc6		
101		Pcl1		
102		Pcl2		
103		Pds1		
104		Pho85		
105		Pph21		
106		Pph22		
107		Rad53		
108		Rdi1		
109		Rfa1		
110		Rfa2		
111		Rga2		
112		Rho1		
113		Rnr1		
114		Rom2		
115		Rpd3		
116		Rsr1		
117		Rts1		
118		Scc1		
119		Sgo1		
120		Sic1		
121		Skp1		
122		Sld2		
123		Sli15		
124		Slk19		
125		Smc1		
126		Smc3		
127		Sml1		
128		Spc110		
129		Spc34		
130		Spc42		
131		Spc72		
132		Spc98		
133		Ssa1		
134		Ssa2		
135		Stb1		
136		Ste20		
137		Swe1		
138		Swi4		
139		Swi5		
140		Swi6		
141		Tem1		
142		Tpd3		
143		Tus1		
144		Whi3		
145		Whi5		
146		Ydj1		
147		Yhp1		
148		Yox1		

A.1.2 *Cell cycle control network in rxncon language*

The complete CC-CNW in rxncon language (Tables A.2 to A.5) is presented. The tables containing the rxncon information of the CC-CNW are divided into three tables: Table A.2 lists all Boolean statements used in the CC-CNW. Table A.3 lists the definitions of the outputs used in the CC-CNW. Table A.4 contains the complete list of reactions and contingencies which are part of the CC-CNW. Table A.5 lists the skeleton rules of the macroscopic reactions.

Table A.2. *Booleans in the CC-CNW.* C: Contingency.

	Boolean	C	State	Reference
1	⟨Acm1Bmh12⟩	OR	Acm1_[bmh]–Bmh1_[acm1]	Dial *et al.* (2007); Heusden *et al.* (1995)
2	⟨Acm1Bmh12⟩	OR	Acm1_[bmh]–Bmh2_[acm1]	Dial *et al.* (2007); Heusden *et al.* (1995)
3	⟨Acm1Phosphorylation⟩	OR	Acm1_[(S31)]-{P}	Ostapenko *et al.* (2008); Hypothesis
4	⟨Acm1Phosphorylation⟩	OR	Acm1_[(S3)]-{P}	Ostapenko *et al.* (2008); Hypothesis
5	⟨Acm1Phosphorylation⟩	OR	Acm1_[(S48)]-{P}	Ostapenko *et al.* (2008); Hypothesis
6	⟨Acm1Phosphorylation⟩	OR	Acm1_[(T161)]-{P}	Ostapenko *et al.* (2008); Hypothesis
7	⟨Acm1PseudosubstrateBinding⟩	NOT	⟨CAB⟩	Dial *et al.* (2007)
8	⟨ActinCableMediatedExocytosis⟩	AND	Act1_[formin]–Bni1_[actin]	Pruyne *et al.* (2002); Hypothesis
9	⟨ActinCableMediatedExocytosis⟩	AND	Sec4_[(act)]-{0}	Bi and Park (2012); Hypothesis
10	⟨ActinCableNucleationActivity⟩	AND	Bni1@8_[FH2]–Bni1@9_[FH2]	Pruyne *et al.* (2002); Hypothesis
11	⟨ActinCableNucleationActivity⟩	AND	⟨Polarisome⟩	Bi and Park (2012); Hypothesis
12	⟨ActinCables⟩	OR	⟨BudNeckCables⟩	Pruyne *et al.* (2004)
13	⟨ActinCables⟩	OR	⟨BudTipcables⟩	Pruyne *et al.* (2004)
14	⟨ActinMotor⟩	AND	Act1_[motor]–Myo2_[actin]	Liu *et al.* (2010), Yin *et al.* (2000)
15	⟨ActinMotor⟩	AND	Kar9_[myo2]–Myo2_[kar9]	Liu *et al.* (2010), Yin *et al.* (2000)
16	⟨ActiveCla4⟩	AND	Cdc42_[(act)]-{GTP}	Versele and Thorner (2004); Hypothesis
17	⟨ActiveCla4⟩	AND	Cdc42_[PAK]–Cla4_[cdc42]	Versele and Thorner (2004); Hypothesis
18	⟨ActiveCla4⟩	AND	Cla4_[(ap)]-{P}	Versele and Thorner (2004)
19	⟨ActiveCondensin⟩	AND	⟨Condensin⟩	Robellet *et al.* (2015)
20	⟨ActiveCondensin⟩	AND	⟨Smc4Phosphorylation⟩	Robellet *et al.* (2015)
21	⟨ActiveYdj1⟩	OR	Ssa1_[ydj1]–Ydj1_[ssa]	Cyr and Douglas (1994)
22	⟨ActiveYdj1⟩	OR	Ssa2_[ydj1]–Ydj1_[ssa]	Cyr and Douglas (1994)
23	⟨APCCdh1Active⟩	AND	⟨Acm1PseudosubstrateBinding⟩	Dial *et al.* (2007)
24	⟨APCCdh1Active⟩	AND	APC_[cdh1]–Cdh1_[APC]	Dial *et al.* (2007)
25	⟨APCCdh1Cdc20⟩	OR	APC_[cdc20]–Cdc20_[APC]	Boolean combination
26	⟨APCCdh1Cdc20⟩	OR	⟨APCCdh1Active⟩	Boolean combination
27	⟨AstralMTpolymerization⟩	AND	[Plaques]	Gap-filling step 2
28	⟨AstralMTpolymerization⟩	AND	Tub1_[tub4]–Tub4_[tub1]	Nogales *et al.* (1999); Hypothesis
29	⟨AstralMTpolymerization⟩	AND	Tub3_[tub4]–Tub4_[tub3]	Nogales *et al.* (1999); Hypothesis
30	⟨AstralMTpolymerization⟩	AND	⟨TubulinDimer⟩	Winey and Bloom (2012)
31	⟨AstralMTPositioning⟩	AND	⟨ActinMotor⟩	Markus *et al.* (2012)
32	⟨AstralMTPositioning⟩	AND	Bim1_[kar9]–Kar9_[bim1]	Markus *et al.* (2012)
33	⟨AstralMTPositioning⟩	AND	Bim1_[MT]–Tub2_[PlusEnd]	Markus *et al.* (2012)
34	⟨AuroraBActive⟩	AND	Bir1_[cbf2]–Cbf2_[bir1]	Nakajima *et al.* (2009); Hypothesis
35	⟨AuroraBActive⟩	AND	Cbf2_[centromere]–Centromere_[CDE]	Nakajima *et al.* (2009); Hypothesis
36	⟨AuroraBActive⟩	AND	⟨CPC⟩	Nakajima *et al.* (2009)
37	⟨Bem1Cdc24Cla4Cdc42⟩	AND	Bem1_[PB1]–Cdc24_[bem1]	Howell and Lew (2012)
38	⟨Bem1Cdc24Cla4Cdc42⟩	AND	Bem1_[SH3]–Cla4_[bem1]	Howell and Lew (2012)
39	⟨Bem1Cdc24Cla4Cdc42⟩	AND	Cdc42_[PAK]–Cla4_[cdc42]	Versele and Thorner (2004); Hypothesis
40	⟨Bem1Cdc24Ste20Cdc42⟩	AND	Bem1_[PB1]–Cdc24_[bem1]	Howell and Lew (2012)
41	⟨Bem1Cdc24Ste20Cdc42⟩	AND	Bem1_[SH3]–Ste20_[bem1]	Howell and Lew (2012)
42	⟨Bem1Cdc24Ste20Cdc42⟩	AND	Cdc42_[PAK]–Ste20_[cdc42]	Howell and Lew (2012)
43	⟨Bem1MediatedLocalization⟩	AND	Bem1_[CI]–Cdc42_[bem1]	Woods *et al.* (2015); Hypothesis
44	⟨Bem1MediatedLocalization⟩	AND	Bem1_[PB1]–Cdc24_[bem1]	Woods *et al.* (2015)
45	⟨BipolarSpindle⟩	OR	Cell_[(SPB)]-{bipolar}	Gap-filling step 2
46	⟨BipolarSpindle⟩	OR	Cell_[(SPB)]-{daughter}	Gap-filling step 2
47	⟨BridgeComponents⟩	AND	Cdc31_[kar1]–Kar1_[cdc31]	Rüthnick and Schiebel (2016)
48	⟨BridgeComponents⟩	AND	Cdc31_[sfi1]–Sfi1_[cdc31]	Rüthnick and Schiebel (2016)
49	⟨BridgeComponents⟩	AND	Sfi1@3_[C]–Sfi1@4_[C]	Rüthnick and Schiebel (2016)
50	⟨BudNeckCables⟩	AND	Act1_[formin]–Bnr1_[actin]	Pruyne *et al.* (2004); Hypothesis
51	⟨BudNeckCables⟩	AND	Bnr1@2_[FH2]–Bnr1@3_[FH2]	Pruyne *et al.* (2004); Hypothesis
52	⟨BudTipcables⟩	AND	Act1_[formin]–Bni1_[actin]	Pruyne *et al.* (2004)
53	⟨BudTipcables⟩	AND	⟨ActinCableNucleationActivity⟩	Pruyne *et al.* (2004)
54	⟨CAB⟩	AND	⟨Acm1Bmh12⟩	Dial *et al.* (2007)
55	⟨CAB⟩	AND	Acm1_[cdh1]–Cdh1_[acm1]	Dial *et al.* (2007)
56	⟨Cdc15Active⟩	AND	Cdc15_[tem1]–Tem1_[cdc15]	Weiss (2012)
57	⟨Cdc15Active⟩	AND	Nud1_[tem1]–Tem1_[nud1]	Weiss (2012)
58	⟨Cdc15Active⟩	AND	Tem1_[(act)]-{GTP}	Weiss (2012); Hypothesis
59	⟨Cdc28Clb1⟩	AND	Cdc28_[cyclin]–Clb1_[cdc28]	Surana *et al.* (1991)
60	⟨Cdc28Clb1⟩	AND	Cdc28_[sic1]–0	Mendenhall and Hodge (1998)
61	⟨Cdc28Clb1⟩	AND	Cdc28_[Tloop(T169)]-{P}	Ross *et al.* (2000); Hypothesis
62	⟨Cdc28Clb1⟩	AND	Cdc28_[whi3]–0	Wang *et al.* (2004); Hypothesis

Table A.2 – *Continued from previous page*

	Boolean Name	C	State	Reference
63	⟨Cdc28Clb1⟩	AND	Cdc28_[(Y19)]-{0}	Keaton *et al.* (2007)
64	⟨Cdc28Clb12⟩	OR	⟨Cdc28Clb1⟩	Boolean combination
65	⟨Cdc28Clb12⟩	OR	⟨Cdc28Clb2⟩	Boolean combination
66	⟨Cdc28Clb1256⟩	OR	⟨Cdc28Clb12⟩	Boolean combination
67	⟨Cdc28Clb1256⟩	OR	⟨Cdc28Clb56⟩	Boolean combination
68	⟨Cdc28Clb2⟩	AND	Cdc28_[cyclin]–Clb2_[cdc28]	Surana *et al.* (1991)
69	⟨Cdc28Clb2⟩	AND	Cdc28_[sic1]–0	Mendenhall and Hodge (1998)
70	⟨Cdc28Clb2⟩	AND	Cdc28_[Tloop(T169)]-{P}	Ross *et al.* (2000); Hypothesis
71	⟨Cdc28Clb2⟩	AND	Cdc28_[whi3]–0	Wang *et al.* (2004); Hypothesis
72	⟨Cdc28Clb2⟩	AND	Cdc28_[(Y19)]-{0}	Keaton *et al.* (2007)
73	⟨Cdc28Clb3⟩	AND	Cdc28_[cyclin]–Clb3_[cdc28]	Surana *et al.* (1991)
74	⟨Cdc28Clb3⟩	AND	Cdc28_[sic1]–0	Mendenhall and Hodge (1998)
75	⟨Cdc28Clb3⟩	AND	Cdc28_[Tloop(T169)]-{P}	Ross *et al.* (2000); Hypothesis
76	⟨Cdc28Clb3⟩	AND	Cdc28_[whi3]–0	Wang *et al.* (2004); Hypothesis
77	⟨Cdc28Clb34⟩	OR	⟨Cdc28Clb3⟩	Boolean combination
78	⟨Cdc28Clb34⟩	OR	⟨Cdc28Clb4⟩	Boolean combination
79	⟨Cdc28Clb4⟩	AND	Cdc28_[cyclin]–Clb4_[cdc28]	Surana *et al.* (1991)
80	⟨Cdc28Clb4⟩	AND	Cdc28_[sic1]–0	Mendenhall and Hodge (1998)
81	⟨Cdc28Clb4⟩	AND	Cdc28_[Tloop(T169)]-{P}	Ross *et al.* (2000); Hypothesis
82	⟨Cdc28Clb4⟩	AND	Cdc28_[whi3]–0	Wang *et al.* (2004); Hypothesis
83	⟨Cdc28Clb5⟩	AND	Cdc28_[cyclin]–Clb5_[cdc28]	Epstein and Cross (1992)
84	⟨Cdc28Clb5⟩	AND	Cdc28_[sic1]–0	Mendenhall and Hodge (1998)
85	⟨Cdc28Clb5⟩	AND	Cdc28_[Tloop(T169)]-{P}	Ross *et al.* (2000); Hypothesis
86	⟨Cdc28Clb5⟩	AND	Cdc28_[whi3]–0	Wang *et al.* (2004); Hypothesis
87	⟨Cdc28Clb56⟩	OR	⟨Cdc28Clb5⟩	Boolean combination
88	⟨Cdc28Clb56⟩	OR	⟨Cdc28Clb6⟩	Boolean combination
89	⟨Cdc28Clb6⟩	AND	Cdc28_[cyclin]–Clb6_[cdc28]	Schwob and Nasmyth (1993)
90	⟨Cdc28Clb6⟩	AND	Cdc28_[sic1]–0	Mendenhall and Hodge (1998)
91	⟨Cdc28Clb6⟩	AND	Cdc28_[Tloop(T169)]-{P}	Ross *et al.* (2000); Hypothesis
92	⟨Cdc28Clb6⟩	AND	Cdc28_[whi3]–0	Wang *et al.* (2004); Hypothesis
93	⟨Cdc28Cln1⟩	AND	Cdc28_[cks1]–Cks1_[cdc28]	Reynard *et al.* (2000)
94	⟨Cdc28Cln1⟩	AND	Cdc28_[cyclin]–Cln1_[cdc28]	Richardson *et al.* (1989)
95	⟨Cdc28Cln1⟩	AND	Cdc28_[far1]–0	Peter and Herskowitz (1994)
96	⟨Cdc28Cln1⟩	AND	Cdc28_[Tloop(T169)]-{P}	Ross *et al.* (2000); Hypothesis
97	⟨Cdc28Cln12⟩	OR	⟨Cdc28Cln1⟩	Boolean combination
98	⟨Cdc28Cln12⟩	OR	⟨Cdc28Cln2⟩	Boolean combination
99	⟨Cdc28Cln123⟩	OR	⟨Cdc28Cln1⟩	Boolean combination
100	⟨Cdc28Cln123⟩	OR	⟨Cdc28Cln2⟩	Boolean combination
101	⟨Cdc28Cln123⟩	OR	⟨Cdc28Cln3⟩	Boolean combination
102	⟨Cdc28Cln2⟩	AND	Cdc28_[cks1]–Cks1_[cdc28]	Reynard *et al.* (2000)
103	⟨Cdc28Cln2⟩	AND	Cdc28_[cyclin]–Cln2_[cdc28]	Richardson *et al.* (1989)
104	⟨Cdc28Cln2⟩	AND	Cdc28_[far1]–0	Peter and Herskowitz (1994)
105	⟨Cdc28Cln2⟩	AND	Cdc28_[Tloop(T169)]-{P}	Ross *et al.* (2000); Hypothesis
106	⟨Cdc28Cln3⟩	AND	Cdc28_[cks1]–Cks1_[cdc28]	Reynard *et al.* (2000)
107	⟨Cdc28Cln3⟩	AND	Cdc28_[cyclin]–Cln3_[cdc28]	Richardson *et al.* (1989)
108	⟨Cdc28Cln3⟩	AND	Cdc28_[far1]–0	Peter and Herskowitz (1994)
109	⟨Cdc28Cln3⟩	AND	Cdc28_[Tloop(T169)]-{P}	Ross *et al.* (2000); Hypothesis
110	⟨Cdc28Cln3⟩	AND	Cdc28_[whi3]–0	Wang *et al.* (2004)
111	⟨Cdc28Cln3⟩	AND	Cln3_[Jdomain]–Ydj1_[cln3]	Vergés *et al.* (2007)
112	⟨Cdc28Phosphorylation⟩	OR	Sfi1_[C(S801)]-{P}	Elserafy *et al.* (2014)
113	⟨Cdc28Phosphorylation⟩	OR	Sfi1_[C(S855)]-{P}	Elserafy *et al.* (2014)
114	⟨Cdc28Phosphorylation⟩	OR	Sfi1_[C(S882)]-{P}	Elserafy *et al.* (2014)
115	⟨Cdc28Phosphorylation⟩	OR	Sfi1_[C(S892)]-{P}	Elserafy *et al.* (2014)
116	⟨Cdc28Phosphorylation⟩	OR	Sfi1_[C(S923)]-{P}	Elserafy *et al.* (2014)
117	⟨Cdc28Phosphorylation⟩	OR	Sfi1_[C(T816)]-{P}	Elserafy *et al.* (2014)
118	⟨Cdc42DependentAssembly⟩	OR	Cdc12_[gic1]–Gic1_[cdc12]	Iwase *et al.* (2006); Hypothesis
119	⟨Cdc42DependentAssembly⟩	OR	Cdc12_[gic2]–Gic2_[cdc12]	Iwase *et al.* (2006); Hypothesis
120	⟨Cdc42LocalizedActivation⟩	OR	⟨Bem1MediatedLocalization⟩	Woods *et al.* (2015)
121	⟨Cdc42LocalizedActivation⟩	OR	⟨Rsr1MediatedLocalization⟩	Woods *et al.* (2015); Hypothesis
122	⟨Cdc5Phosphorylation⟩	OR	Sfi1_[C(S826)]-{P}	Elserafy *et al.* (2014)
123	⟨Cdc5Phosphorylation⟩	OR	Sfi1_[C(T866)]-{P}	Elserafy *et al.* (2014)
124	⟨Cdc5Phosphorylation⟩	OR	Sfi1_[C(T876)]-{P}	Elserafy *et al.* (2014)
125	⟨Chs2ERRetention⟩	AND	Chs2_[(S100)]-{P}	Teh *et al.* (2009)
126	⟨Chs2ERRetention⟩	AND	Chs2_[(S14)]-{P}	Teh *et al.* (2009)
127	⟨Chs2ERRetention⟩	AND	Chs2_[(S60)]-{P}	Teh *et al.* (2009)
128	⟨Chs2ERRetention⟩	AND	Chs2_[(S69)]-{P}	Teh *et al.* (2009)
129	⟨Cin8Tetramer⟩	AND	Cin8@1_[stalk]–Cin8@2_[stalk]	Hildebrandt *et al.* (2006)
130	⟨Cin8Tetramer⟩	AND	Cin8@2_[stalk]–Cin8@3_[stalk]	Hildebrandt *et al.* (2006)
131	⟨Cin8Tetramer⟩	AND	Cin8@3_[stalk]–Cin8@4_[stalk]	Hildebrandt *et al.* (2006)
132	⟨Cin8Tetramer⟩	AND	Cin8_[mt]–Tub1_[motor]	Scholey *et al.* (2016)
133	⟨CMG⟩	AND	Dpb11_[BRCT1]–Sld2_[dpb11]	Bell and Labib (2016)
134	⟨CMG⟩	AND	Dpb11_[BRCT2]–Sld3_[dpb11]	Bell and Labib (2016)
135	⟨CMG⟩	AND	Dpb11_[gins]–Psf1_[dpb11]	Bell and Labib (2016)
136	⟨CMG⟩	AND	Dpb11_[pol]–Pol2_[dpb11]	Bell and Labib (2016)
137	⟨CMG⟩	AND	⟨MCMCdc45Sld3⟩⟩	Bell and Labib (2016), Yeeles *et al.* (2015)
138	⟨CohesinLoading⟩	AND	Scc1_[scc2]–Scc2_[scc1]	Marston (2014)
139	⟨CohesinLoading⟩	AND	Scc2_[N]–Scc4_[tpr]	Marston (2014)

Table A.2 – *Continued from previous page*

	Boolean Name	C	State	Reference
140	⟨CohesinLoading⟩	AND	Scc4_[DBD]–Centromere_[CohesinLoading]	Marston (2014)
141	⟨CohesinRing⟩	AND	Scc1_[(esp1)]-{0}	Marston (2014)
142	⟨CohesinRing⟩	AND	Irr1_[scc1]–Scc1_[irr1]	Marston (2014)
143	⟨CohesinRing⟩	AND	Scc1_[smc1]–Smc1_[NBD]	Marston (2014)
144	⟨CohesinRing⟩	AND	Scc1_[smc3]–Smc3_[NBD]	Marston (2014)
145	⟨CohesinRing⟩	AND	Smc1_[smc3]–Smc3_[smc1]	Marston (2014)
146	⟨Condensin⟩	AND	Brn1_[smc2]–Smc2_[brn1]	Marston (2014)
147	⟨Condensin⟩	AND	Brn1_[smc4]–Smc4_[brn1]	Marston (2014)
148	⟨Condensin⟩	AND	Brn1_[ycg1]–Ycg1_[brn1]	Marston (2014)
149	⟨Condensin⟩	AND	Brn1_[ycs4]–Ycs4_[brn1]	Marston (2014)
150	⟨Condensin⟩	AND	Smc2_[smc4]–Smc4_[smc2]	Marston (2014)
151	⟨CondensinAtCentromeres⟩	AND	⟨Condensin⟩	Marston (2014)
152	⟨CondensinAtCentromeres⟩	AND	Smc2_[sgo1]–Sgo1_[smc2]	Peplowska *et al.* (2014)
153	⟨CPC⟩	AND	Bir1_[C]–Nbl1_[bir1]	Nakajima *et al.* (2009)
154	⟨CPC⟩	AND	Ipl1_[sli15]–Sli15_[Inbox]	Nakajima *et al.* (2009)
155	⟨CPC⟩	AND	Nbl1_[sli15]–Sli15_[N]	Nakajima *et al.* (2009)
156	⟨CrosslinkedInterpolarMT⟩	AND	Ase1@1_[dimer]–Ase1@2_[dimer]	Scholey *et al.* (2016)
157	⟨CrosslinkedInterpolarMT⟩	AND	Ase1_[mt]–Tub1_[ase1]	Scholey *et al.* (2016)
158	⟨CrosslinkedInterpolarMT⟩	AND	⟨NuclearMTpolymerization⟩	Scholey *et al.* (2016)
159	⟨CrosslinkedInterpolarMT⟩	AND	Tub4_[(S360)]-{0}	Nazarova *et al.* (2013)
160	⟨Dam1Complex⟩	AND	Ask1_[N]–Dad4_[N]	Legal *et al.* (2016)
161	⟨Dam1Complex⟩	AND	Dad4_[coiledcoil]–Dam1_[N2]	Legal *et al.* (2016)
162	⟨Dam1Complex⟩	AND	Dam1_[coiledcoil]–Duo1_[coiledcoil]	Legal *et al.* (2016)
163	⟨Dam1Complex⟩	AND	Dam1_[N1]–Spc34_[N]	Legal *et al.* (2016)
164	⟨Dam1CTermPhos⟩	OR	Dam1_[(S257)]-{P}	Kim *et al.* (2017)
165	⟨Dam1CTermPhos⟩	OR	Dam1_[(S265)]-{P}	Kim *et al.* (2017)
166	⟨Dam1CTermPhos⟩	OR	Dam1_[(S292)]-{P}	Kim *et al.* (2017)
167	⟨Dam1MicrotubuleAttachment⟩	AND	⟨Dam1Complex⟩	Legal *et al.* (2016); Hypothesis
168	⟨Dam1MicrotubuleAttachment⟩	AND	⟨Dam1MT⟩	Legal *et al.* (2016); Hypothesis
169	⟨Dam1MicrotubuleAttachment⟩	AND	⟨Duo1MT⟩	Legal *et al.* (2016); Hypothesis
170	⟨Dam1MT⟩	OR	Dam1_[Ca]–Tub1_[dam1]	Legal *et al.* (2016); Hypothesis
171	⟨Dam1MT⟩	OR	Dam1_[Ca]–Tub3_[dam1]	Legal *et al.* (2016); Hypothesis
172	⟨Dam1Phos⟩	OR	Dam1_[(S20)]-{P}	Cheeseman *et al.* (2002)
173	⟨Dam1Phos⟩	OR	Dam1_[(S257)]-{P}	Cheeseman *et al.* (2002)
174	⟨Dam1Phos⟩	OR	Dam1_[(S265)]-{P}	Cheeseman *et al.* (2002)
175	⟨Dam1Phosphorylation⟩	AND	⟨Dam1Phos⟩	Cheeseman *et al.* (2002)
176	⟨Dam1Phosphorylation⟩	AND	Dam1_[(S292)]-{P}	Cheeseman *et al.* (2002)
177	⟨Dbf2Active⟩	AND	Dbf2_[(HM)]-{P}	Mah *et al.* (2001)
178	⟨Dbf2Active⟩	AND	Dbf2_[n]–Mob1_[dbf2]	Mah *et al.* (2001)
179	⟨Dbf2Mob1Nud1⟩	AND	Dbf2_[n]–Mob1_[dbf2]	Weiss (2012)
180	⟨Dbf2Mob1Nud1⟩	AND	Mob1_[nud1]–Nud1_[mob1]	Weiss (2012)
181	⟨DNARFCCtf18Pol2Mrc1⟩	AND	Ctf18_[rfc]–RFC_[ctf18]	García-Rodríguez *et al.* (2015)
182	⟨DNARFCCtf18Pol2Mrc1⟩	AND	Mrc1_[pol2]–Pol2_[mrc1]	García-Rodríguez *et al.* (2015); Hypothesis
183	⟨DNARFCCtf18Pol2Mrc1⟩	AND	Pol2_[rfc]–RFC_[pol2]	García-Rodríguez *et al.* (2015)
184	⟨DNARFCCtf18Pol2Mrc1⟩	AND	RFC_[dna]–ssDNA_[rfc]	García-Rodríguez *et al.* (2015); Hypothesis
185	⟨Duo1MT⟩	OR	Duo1_[Ca]–Tub1_[duo1]	Legal *et al.* (2016); Hypothesis
186	⟨Duo1MT⟩	OR	Duo1_[Ca]–Tub1_[duo1]	Legal *et al.* (2016); Hypothesis
187	⟨Duo1MT⟩	OR	Duo1_[Ca]–Tub3_[duo1]	Legal *et al.* (2016); Hypothesis
188	⟨Duo1MT⟩	OR	Duo1_[Cb]–Tub2_[duo1]	Legal *et al.* (2016); Hypothesis
189	⟨DuplicationPlaque⟩	AND	Cnm67_[cp]–Spc42_[cnm67]	Fu *et al.* (2015)
190	⟨DuplicationPlaque⟩	AND	Cnm67_[op]–Nud1_[cnm67]	Fu *et al.* (2015)
191	⟨DuplicationPlaque⟩	AND	Sfi1_[N]–Spc42_[cp]	Fu *et al.* (2015)
192	⟨ERReleaseSignal⟩	AND	Cdc28_[cyclin]–Cln3_[cdc28]	Yaglom *et al.* (1996); Hypothesis
193	⟨ERReleaseSignal⟩	AND	Cln3_[Jdomain]–Ydj1_[cln3]	Yaglom *et al.* (1996); Hypothesis
194	⟨Exocytosis⟩	AND	Exo70_[C]–PI	Abe *et al.* (2003), Roumanie *et al.* (2005), He *et al.* (2007)
195	⟨Exocytosis⟩	AND	⟨Rho1Exocyst⟩	Roumanie *et al.* (2005),Sahin *et al.* (2008); Hypothesis
196	⟨Exocytosis⟩	AND	Sec3_[Nlipidbinding]–PI	Abe *et al.* (2003), Roumanie *et al.* (2005), He *et al.* (2007)
197	⟨Fkh2Ndd1Mcm1⟩	AND	Fkh2_[mcm1]–Mcm1_[fkh2]	Haase and Wittenberg (2014)
198	⟨Fkh2Ndd1Mcm1⟩	AND	Fkh2_[ndd1]–Ndd1_[fkh2]	Haase and Wittenberg (2014)
199	⟨GlucanSynthesisComplex⟩	OR	Fks1_[rho1]–Rho1_[synthase]	Bi and Park (2012)
200	⟨GlucanSynthesisComplex⟩	OR	Gsc2_[rho1]–Rho1_[synthase]	Bi and Park (2012)
201	⟨HDAC⟩	OR	Hos3_[whi5]–Whi5_[hdac]	Wagner *et al.* (2009)
202	⟨HDAC⟩	OR	Rpd3_[whi5]–Whi5_[hdac]	Wagner *et al.* (2009)
203	⟨InnerPlaque⟩	AND	Cmd1_[spc42]–Spc42	Fu *et al.* (2015)
204	⟨InnerPlaque⟩	AND	Spc29_[spc110]–Spc110_[spc29]	Fu *et al.* (2015)
205	⟨InnerPlaque⟩	AND	Spc29_[spc42]–Spc42_[spc29]	Fu *et al.* (2015)
206	⟨InnerPlaque⟩	AND	Spc97_[spc110]–Spc110_[spc97]	Winey and Bloom (2012)
207	⟨InnerPlaque⟩	AND	Spc98_[spc110]–Spc110_[N]	Winey and Bloom (2012)
208	⟨InnerPlaque⟩	AND	⟨yTubulinSmallComplex⟩	Fu *et al.* (2015)
209	⟨InterpolarMTSlidingApart⟩	AND	⟨CrosslinkedInterpolarMT⟩	Scholey *et al.* (2016)
210	⟨InterpolarMTSlidingApart⟩	AND	⟨KinesinMotors⟩	Scholey *et al.* (2016)
211	⟨KinesinMotors⟩	OR	⟨Cin8Tetramer⟩	Scholey *et al.* (2016)
212	⟨KinesinMotors⟩	OR	⟨Kip1Motor⟩	Scholey *et al.* (2016)
213	⟨KinetochoreMad1Mad2⟩	AND	Mad1_[KT]–Ndc80_[mad1]	Zich and Hardwick (2010)
214	⟨KinetochoreMad1Mad2⟩	AND	Mad1_[mad2]–Mad2_[mad1]	Zich and Hardwick (2010)

Table A.2 – *Continued from previous page*

	Boolean Name	C	State	Reference
215	⟨Kip1Motor⟩	AND	Kip1@1_[stalk]–Kip1@2_[stalk]	Fridman *et al.* (2013), Scholey *et al.* (2016); Hypothesis
216	⟨Kip1Motor⟩	AND	Kip1_[mt]–Tub1_[motor]	Glotzer (2009), Fridman *et al.* (2013), Scholey *et al.* (2016); Hypothesis
217	⟨LowTensionDependentPhosphorylation⟩	AND	⟨Dam1Phosphorylation⟩	Cheeseman *et al.* (2002)
218	⟨LowTensionDependentPhosphorylation⟩	AND	Spc34_[(T199)]-{P}	Cheeseman *et al.* (2002)
219	⟨Mad1Mad2Mad2⟩	AND	Mad1@2_[mad2]–Mad2@3_[mad1]	Biggins (2013)
220	⟨Mad1Mad2Mad2⟩	AND	Mad2@3_[mad2]–Mad2@4_[mad2]	Biggins (2013)
221	⟨MBF⟩	AND	Mbp1_[swi6]–Swi6_[mbp1]	Enserink and Kolodner (2010)
222	⟨MBF⟩	AND	⟨Swi6Phosphorylation⟩	Palumbo *et al.* (2016); Hypothesis; Gap-filling step 1
223	⟨MBF⟩	AND	⟨Swi6repressed⟩	de Bruin *et al.* (2006)
224	⟨MBFHCM1⟩	AND	[MBFDelay20]	Bean *et al.* (2005)
225	⟨MBFHCM1⟩	AND	Mbp1_[mcb]–Hcm1Gene_[mcb]	Bean *et al.* (2005)
226	⟨Mcm1Bck2Transcription⟩	AND	Bck2_[mcm1]–Mcm1_[bck2]	Bastajian *et al.* (2013)
227	⟨Mcm1Bck2Transcription⟩	AND	[EquilibriumDelay20]	Gap-filling step 2
228	⟨Mcm1Transcription⟩	AND	⟨Mcm1Yhp1⟩	Pramila *et al.* (2002)
229	⟨Mcm1Transcription⟩	AND	⟨Mcm1Yox1⟩	Pramila *et al.* (2002)
230	⟨Mcm1Yhp1⟩	NOT	Mcm1_[yhp1]–Yhp1_[mcm1]	Pramila *et al.* (2002); Gap-filling step 1
231	⟨Mcm1Yox1⟩	NOT	Mcm1_[yox1]–Yox1_[mcm1]	Pramila *et al.* (2002); Gap-filling step 1
232	⟨Mcm27Complex⟩	AND	Mcm2_[mcm6]–Mcm6_[mcm2]	Bell and Labib (2016)
233	⟨Mcm27Complex⟩	AND	Mcm3_[mcm5]–Mcm5_[mcm3]	Bell and Labib (2016)
234	⟨Mcm27Complex⟩	AND	Mcm4_[mcm7]–Mcm7_[mcm4]	Bell and Labib (2016)
235	⟨Mcm27Complex⟩	AND	Mcm5_[mcm6]–Mcm6_[mcm5]	Bell and Labib (2016)
236	⟨Mcm27Complex⟩	AND	Mcm6_[mcm4]–Mcm4_[mcm6]	Bell and Labib (2016)
237	⟨Mcm27Complex⟩	AND	Mcm7_[mcm3]–Mcm3_[mcm7]	Bell and Labib (2016)
238	⟨Mcm27ComplexCdt1⟩	AND	Cdt1_[C]–Mcm6_[C]	Wu *et al.* (2012), Bell and Labib (2016)
239	⟨Mcm27ComplexCdt1⟩	AND	⟨Mcm27Complex⟩	Bell and Labib (2016)
240	⟨MCMCdc45Sld3⟩	AND	Cdc45_[sld3]–Sld3_[cdc45]	Yeeles *et al.* (2015)
241	⟨MCMCdc45Sld3⟩	AND	Mcm4_[sld3]–Sld3_[mcm4]	Yeeles *et al.* (2015)
242	⟨MCMCdc45Sld3⟩	AND	Mcm6_[sld3]–Sld3_[mcm6]	Yeeles *et al.* (2015)
243	⟨Mec1Mrc1Rad53⟩	AND	Mec1_[mrc1]–Mrc1_[cT2T3]	Chen and Zhou (2009)
244	⟨Mec1Mrc1Rad53⟩	AND	Mrc1_[rad53]–Rad53_[FHA1]	Chen and Zhou (2009)
245	⟨Ndc80Complex⟩	AND	Ndc80_[nuf2]–Nuf2_[ndc80]	Biggins (2013)
246	⟨Ndc80Complex⟩	AND	Ndc80_[spc24]–Spc24_[ndc80]	Biggins (2013)
247	⟨Ndc80Complex⟩	AND	Spc24_[spc25]–Spc25_[spc24]	Biggins (2013)
248	⟨Ndc80Dam1Recruitment⟩	AND	Ask1_[ndc80]–Ndc80_[ask1]	Kim *et al.* (2017)
249	⟨Ndc80Dam1Recruitment⟩	AND	Dam1_[ndc80]–Ndc80_[dam1]	Kim *et al.* (2017)
250	⟨Ndc80Dam1Recruitment⟩	AND	Ndc80_[spc34]–Spc34_[ndc80]	Kim *et al.* (2017)
251	⟨Ndd1Phosphorylation⟩	OR	Ndd1_[(S85)]-{P}	Darieva *et al.* (2006)
252	⟨Ndd1Phosphorylation⟩	OR	Ndd1_[(T319)]-{P}	Darieva *et al.* (2006)
253	⟨NetPP⟩	AND	Net1_[(cdc28x6)]-{P}	Yoshida and Toh-e (2002), Azzam *et al.* (2004)
254	⟨NetPP⟩	AND	Net1_[(cdc5)]-{P}	Yoshida and Toh-e (2002), Azzam *et al.* (2004)
255	⟨NuclearMTpolymerization⟩	AND	[Plaques]	Gap-filling step 2
256	⟨NuclearMTpolymerization⟩	AND	Tub1_[tub4]–Tub4_[tub1]	Nogales *et al.* (1999); Hypothesis
257	⟨NuclearMTpolymerization⟩	AND	Tub3_[tub4]–Tub4_[tub3]	Nogales *et al.* (1999); Hypothesis
258	⟨NuclearMTpolymerization⟩	AND	⟨TubulinDimer⟩	Winey and Bloom (2012)
259	⟨Orc2Inhibition⟩	NOT	Orc2_[(cdc28)]-{P}	Nguyen *et al.* (2001)
260	⟨Orc6Inhibition⟩	NOT	Orc6_[(cdc28)]-{P}	Nguyen *et al.* (2001)
261	⟨ORCComplex⟩	AND	Orc1_[orc4]–Orc4_[orc1]	Sun *et al.* (2012)
262	⟨ORCComplex⟩	AND	Orc2_[orc3]–Orc3_[orc2]	Sun *et al.* (2012)
263	⟨ORCComplex⟩	AND	Orc2_[orc5]–Orc5_[orc2]	Sun *et al.* (2012)
264	⟨ORCComplex⟩	AND	Orc2_[orc6]–Orc6_[orc2]	Sun *et al.* (2012)
265	⟨ORCComplex⟩	AND	Orc4_[orc5]–Orc5_[orc4]	Sun *et al.* (2012)
266	⟨ORCOrigin⟩	AND	Orc1_[DBD]–ORI_[origin]	Müller *et al.* (2010)
267	⟨ORCOrigin⟩	AND	⟨Orc2Inhibition⟩	Nguyen *et al.* (2001)
268	⟨ORCOrigin⟩	AND	⟨Orc6Inhibition⟩	Nguyen *et al.* (2001)
269	⟨ORCOrigin⟩	AND	⟨ORCComplex⟩	Müller *et al.* (2010), Sun *et al.* (2012)
270	⟨OuterPlaque⟩	AND	Nud1_[spc72]–Spc72_[nud1]	Fu *et al.* (2015)
271	⟨OuterPlaque⟩	AND	Spc72_[N]–Spc98_[spc72]	Winey and Bloom (2012)
272	⟨OuterPlaque⟩	AND	Spc72_[spc97]–Spc97_[spc72]	Winey and Bloom (2012)
273	⟨OuterPlaque⟩	AND	⟨yTubulinSmallComplex⟩	Fu *et al.* (2015)
274	⟨Pcl9Transcription⟩	OR	Ace2_[PBD]–Pcl9Gene_[pcl9]	Tennyson *et al.* (1998)
275	⟨Pcl9Transcription⟩	OR	Swi5_[PBD]–Pcl9Gene_[pcl9]	Tennyson *et al.* (1998)
276	⟨Pho85Cyclin⟩	OR	Pcl1_[pho85]–Pho85_[cyclin]	Measday *et al.* (1997)
277	⟨Pho85Cyclin⟩	OR	Pcl2_[pho85]–Pho85_[cyclin]	Measday *et al.* (1997)
278	⟨Pho85Cyclin⟩	OR	Pcl9_[pho85]–Pho85_[cyclin]	Measday *et al.* (1997)
279	⟨Pho85Pcl1Pcl9⟩	OR	Pcl1_[pho85]–Pho85_[cyclin]	Huang *et al.* (2009); Hypothesis
280	⟨Pho85Pcl1Pcl9⟩	OR	Pcl9_[pho85]–Pho85_[cyclin]	Huang *et al.* (2009)
281	⟨PI45P2⟩	AND	PI_[(4)]-{P}	Audhya and Emr (2002)
282	⟨PI45P2⟩	AND	PI_[(5)]-{P}	Audhya and Emr (2002)
283	⟨PlaqueFormation⟩	AND	⟨InnerPlaque⟩	Fu *et al.* (2015)
284	⟨PlaqueFormation⟩	AND	⟨OuterPlaque⟩	Fu *et al.* (2015)
285	⟨Polarisome⟩	AND	Bni1_[SBD]–Spa2_[bni1]	Bi and Park (2012)
286	⟨Polarisome⟩	AND	Bud6_[spa2]–Spa2_[bud6]	Bi and Park (2012)
287	⟨Polarisome⟩	AND	Pea2_[spa2]–Spa2_[pea2]	Bi and Park (2012)
288	⟨PolarisomeMsb3⟩	AND	Msb3_[spa2]–Spa2_[MSB]	Bi and Park (2012)
289	⟨PolarisomeMsb3⟩	AND	⟨Polarisome⟩	Bi and Park (2012)
290	⟨PolarisomeMsb4⟩	AND	Msb4_[spa2]–Spa2_[MSB]	Bi and Park (2012)

Table A.2 – *Continued from previous page*

	Boolean Name	C	State	Reference
291	⟨PolarisomeMsb4⟩	AND	⟨Polarisome⟩	Bi and Park (2012)
292	⟨PP2ACdc55Pph21⟩	AND	Cdc55_[tpd3]–Tpd3_[regulatory]	Jiang and Broach (1999); Hypothesis
293	⟨PP2ACdc55Pph21⟩	AND	Pph21_[tpd3]–Tpd3_[pph]	Jiang and Broach (1999); Hypothesis
294	⟨PP2ACdc55Pph22⟩	AND	Cdc55_[tpd3]–Tpd3_[regulatory]	Jiang and Broach (1999); Hypothesis
295	⟨PP2ACdc55Pph22⟩	AND	Pph22_[tpd3]–Tpd3_[pph]	Jiang and Broach (1999); Hypothesis
296	⟨PP2ARts1Pph21⟩	AND	Pph21_[tpd3]–Tpd3_[pph]	Shu *et al.* (1997)
297	⟨PP2ARts1Pph21⟩	AND	Rts1_[tpd3]–Tpd3_[regulatory]	Shu *et al.* (1997)
298	⟨PP2ARts1Pph22⟩	AND	Pph22_[tpd3]–Tpd3_[pph]	Shu *et al.* (1997)
299	⟨PP2ARts1Pph22⟩	AND	Rts1_[tpd3]–Tpd3_[regulatory]	Shu *et al.* (1997)
300	⟨Rho1Exocyst⟩	AND	Cdc42_[exo70]–Exo70_[cdc42]	Roumanie *et al.* (2005); Hypothesis
301	⟨Rho1Exocyst⟩	AND	Cdc42_[sec3]–Sec3_[cdc42]	Roumanie *et al.* (2005); Hypothesis
302	⟨Rho1Exocyst⟩	AND	Rho1_[sec3]–Sec3_[N]	Roumanie *et al.* (2005); Hypothesis
303	⟨Rho1MembraneTargeting⟩	AND	Rho1_[rom2]–Rom2_[rho1]	Abe *et al.* (2003)
304	⟨Rho1MembraneTargeting⟩	AND	⟨Rom2CWI⟩	Philip and Levin (2001)
305	⟨Rho1MembraneTargeting⟩	AND	Rom2_[PH]–PI	Abe *et al.* (2003)
306	⟨Rom2CWI⟩	OR	Mid2_[rom2]–Rom2_[cwi]	Philip and Levin (2001)
307	⟨Rom2CWI⟩	OR	Rom2_[cwi]–Slg1_[cytoplasmic]	Philip and Levin (2001)
308	⟨RPA⟩	AND	Rfa1_[rfa2]–Rfa2_[rfa1]	Iftode *et al.* (1999)
309	⟨RPA⟩	AND	Rfa2_[rfa3]–Rfa3_[rfa2]	Iftode *et al.* (1999)
310	⟨RPAssDNA⟩	AND	Rfa1_[C]–ssDNA_[rfa1]	Kantake *et al.* (2003)
311	⟨RPAssDNA⟩	AND	Rfa2_[D]–ssDNA_[rfa2]	Kantake *et al.* (2003)
312	⟨RPAssDNA⟩	AND	⟨RPA⟩	Kantake *et al.* (2003)
313	⟨RPAssDNALcd1Mec1⟩	AND	Lcd1_[mec1]–Mec1_[lcd1]	Rouse and Jackson (2002)
314	⟨RPAssDNALcd1Mec1⟩	AND	Lcd1_[rfa1]–Rfa1_[lcd1]	Rouse and Jackson (2002)
315	⟨RPAssDNALcd1Mec1⟩	AND	⟨RPAssDNA⟩	Rouse and Jackson (2002)
316	⟨Rsr1MediatedLocalization⟩	AND	Cdc24_[rsr1]–Rsr1_[cdc24]	Howell and Lew (2012)
317	⟨Rsr1MediatedLocalization⟩	AND	Cdc42_[rsr1]–Rsr1_[cdc42]	Howell and Lew (2012)
318	⟨SBF⟩	AND	Swi4_[swi6]–Swi6_[swi4]	Enserink and Kolodner (2010)
319	⟨SBF⟩	AND	⟨Whi5Configuration⟩	Wagner *et al.* (2009)
320	⟨SBFHCM1⟩	AND	[SBFDelay20]	Horak *et al.* (2002); Bean *et al.* (2005); Hypothesis; Gap-filling step 2
321	⟨SBFHCM1⟩	AND	Swi4_[scb]–Hcm1Gene_[scb]	Horak *et al.* (2002); Bean *et al.* (2005); Hypothesis
322	⟨SBForMBFHCM1⟩	OR	⟨MBFHCM1⟩	Horak *et al.* (2002); Bean *et al.* (2005); Hypothesis
323	⟨SBForMBFHCM1⟩	OR	⟨SBFHCM1⟩	Horak *et al.* (2002); Bean *et al.* (2005); Hypothesis
324	⟨SCF⟩	AND	Cdc34@4_[scf]–Hrt1@3_[cdc34]	Seol *et al.* (1999)
325	⟨SCF⟩	AND	Cdc53@2_[scf]–Skp1@1_[cdc53]	Seol *et al.* (1999)
326	⟨SCF⟩	AND	Hrt1@3_[scf]–Cdc53@2_[hrt1]	Seol *et al.* (1999)
327	⟨SCFCdc4⟩	AND	Cdc4_[scf]–Skp1_[Fprotein]	Skowyra *et al.* (1997)
328	⟨SCFCdc4⟩	AND	⟨SCF⟩	Seol *et al.* (1999)
329	⟨SCFCdcMet30⟩	AND	Met30_[scf]–Skp1_[Fprotein]	Kaiser *et al.* (1998)
330	⟨SCFCdcMet30⟩	AND	⟨SCF⟩	Seol *et al.* (1999)
331	⟨SCFGrr1⟩	AND	Grr1@5_[scf]–Skp1@1_[Fprotein]	Mendenhall and Hodge (1998)
332	⟨SCFGrr1⟩	AND	⟨SCF⟩	Seol *et al.* (1999)
333	⟨SeptinRing⟩	AND	Cdc11_[cdc12]–Cdc12_[cdc11]	Bertin *et al.* (2008)
334	⟨SeptinRing⟩	AND	Cdc3_[cdc10]–Cdc10_[cdc3]	Bertin *et al.* (2008)
335	⟨SeptinRing⟩	AND	Cdc3_[cdc12]–Cdc12_[cdc3]	Bertin *et al.* (2008)
336	⟨SeptinRing⟩	AND	⟨Cdc42DependentAssembly⟩	Iwase *et al.* (2006)
337	⟨SeptinRing⟩	AND	[SymmetryBreaking]	Gap-filling step 2
338	⟨Sic1Transcription⟩	OR	Ace2_[PBD]–Sic1Gene_[sic1]	Knapp *et al.* (1996)
339	⟨Sic1Transcription⟩	OR	Swi5_[PBD]–Sic1Gene_[sic1]	Knapp *et al.* (1996)
340	⟨Sic1x6P⟩	AND	Sic1_[(S76)]-{P}	Nash *et al.* (2001)
341	⟨Sic1x6P⟩	AND	Sic1_[(T2)]-{P}	Nash *et al.* (2001)
342	⟨Sic1x6P⟩	AND	Sic1_[(T33)]-{P}	Nash *et al.* (2001)
343	⟨Sic1x6P⟩	AND	Sic1_[(T45)]-{P}	Nash *et al.* (2001)
344	⟨Sic1x6P⟩	AND	Sic1_[(T5)]-{P}	Nash *et al.* (2001)
345	⟨Sic1x6P⟩	AND	⟨VariableSic1P⟩	Nash *et al.* (2001)
346	⟨SldPP⟩	AND	Sld3_[(S622)]-{P}	Tanaka *et al.* (2007)
347	⟨SldPP⟩	AND	Sld3_[(T600)]-{P}	Tanaka *et al.* (2007)
348	⟨Smc4Phosphorylation⟩	AND	Smc4_[(S109)]-{P}	Robellet *et al.* (2015)
349	⟨Smc4Phosphorylation⟩	AND	Smc4_[(S113)]-{P}	Robellet *et al.* (2015)
350	⟨Smc4Phosphorylation⟩	AND	Smc4_[(S117)]-{P}	Robellet *et al.* (2015)
351	⟨Smc4Phosphorylation⟩	AND	Smc4_[(S128)]-{P}	Robellet *et al.* (2015)
352	⟨Smc4Phosphorylation⟩	AND	Smc4_[(S4)]-{P}	Robellet *et al.* (2015)
353	⟨Smc4Phosphorylation⟩	AND	Smc4_[(T43)]-{P}	Robellet *et al.* (2015)
354	⟨Smc4Phosphorylation⟩	AND	Smc4_[(T60)]-{P}	Robellet *et al.* (2015)
355	⟨SPBStates⟩	OR	Cell_[(SPB)]-{bipolar}	Gap-filling 2
356	⟨SPBStates⟩	OR	Cell_[(SPB)]-{daughter}	Gap-filling 2
357	⟨SPBStates⟩	OR	Cell_[(SPB)]-{separated}	Gap-filling 2
358	⟨SPBStates⟩	OR	Cell_[(SPB)]-{spb}	Gap-filling 2
359	⟨Spc110Phos⟩	OR	Spc110_[(S36)]-{P}	Lin *et al.* (2014)
360	⟨Spc110Phos⟩	OR	Spc110_[(S60)]-{P}	Lin *et al.* (2014)
361	⟨Spc110Phos⟩	OR	Spc110_[(S91)]-{P}	Lin *et al.* (2014)
362	⟨Spc110Phos⟩	OR	Spc110_[(T68)]-{P}	Lin *et al.* (2014)
363	⟨Spc42Cdc28Phosphorylation⟩	AND	Spc42_[(S4)]-{P}	Jaspersen *et al.* (2004); Hypothesis
364	⟨Spc42Cdc28Phosphorylation⟩	AND	Spc42_[(T6)]-{P}	Jaspersen *et al.* (2004); Hypothesis
365	⟨Spc42Crystal⟩	OR	[DuplicationPlaque]	Gap-filling 2
366	⟨Spc42Crystal⟩	OR	[DuplicationPlaqueFormation]	Gap-filling 2

Table A.2 – *Continued from previous page*

	Boolean Name	C	State	Reference
367	⟨Spc42Crystal⟩	OR	[PlaqueFormation]	Gap-filling 2
368	⟨Spc42Crystal⟩	OR	[Plaques]	Gap-filling 2
369	⟨Spc42Phosphorylation⟩	OR	⟨Spc42Cdc28Phosphorylation⟩	Jaspersen *et al.* (2004); Hypothesis
370	⟨Spc42Phosphorylation⟩	OR	Spc42_[(mps1)]-{P}	Jaspersen *et al.* (2004); Hypothesis
371	⟨Swe1DegPhosphorylation⟩	OR	Swe1_[Cdc28Sites(deg)]-{P}	Howell and Lew (2012)
372	⟨Swe1DegPhosphorylation⟩	OR	Swe1_[Cdc5Sites(HP)]-{P}	Howell and Lew (2012)
373	⟨Swi6Phosphorylation⟩	AND	Swi6_[(S160)]-{P}	Wagner *et al.* (2009)
374	⟨Swi6Phosphorylation⟩	AND	Swi6_[(S228)]-{P}	Wagner *et al.* (2009)
375	⟨Swi6Phosphorylation⟩	AND	Swi6_[(S238)]-{P}	Wagner *et al.* (2009)
376	⟨Swi6Phosphorylation⟩	AND	Swi6_[(T179)]-{P}	Wagner *et al.* (2009)
377	⟨Swi6repressed⟩	NOT	Nrm1_[GTB]–Swi6_[nrm1]	de Bruin *et al.* (2006)
378	⟨SymmetryBreaking⟩	OR	⟨Bem1Cdc24Cla4Cdc42⟩	Howell and Lew (2012); Hypothesis
379	⟨SymmetryBreaking⟩	OR	⟨Bem1Cdc24Ste20Cdc42⟩	Howell and Lew (2012); Hypothesis
380	⟨Tem1ActivationInhibition⟩	AND	Bfa1_[bub2]–Bub2_[bfa1]	Cid *et al.* (2002)
381	⟨Tem1ActivationInhibition⟩	AND	Bfa1_[(kin4)]-{P}	Bertazzi *et al.* (2011); Hypothesis
382	⟨Tem1ActivationInhibition⟩	AND	Bfa1_[tem1]–Tem1_[bfa1]	Geymonat *et al.* (2009)
383	⟨TubulinDimer⟩	OR	Tub1_[tub2]–Tub2_[tub]	Winey and Bloom (2012)
384	⟨TubulinDimer⟩	OR	Tub2_[tub]–Tub3_[tub2]	Winey and Bloom (2012)
385	⟨VariableSic1P⟩	OR	Sic1_[(S69)]-{P}	Nash *et al.* (2001)
386	⟨VariableSic1P⟩	OR	Sic1_[(S80)]-{P}	Nash *et al.* (2001)
387	⟨Whi5Configuration⟩	NOT	⟨Whi5HDAC⟩	Wagner *et al.* (2009)
388	⟨Whi5HDAC⟩	AND	⟨HDAC⟩	Wagner *et al.* (2009)
389	⟨Whi5HDAC⟩	AND	Swi6_[whi5]–Whi5_[swi6]	Wagner *et al.* (2009)
390	⟨Whi5HyperPhos⟩	AND	Whi5_[(S154)]-{P}	Wagner *et al.* (2009)
391	⟨Whi5HyperPhos⟩	AND	Whi5_[(S156)]-{P}	Wagner *et al.* (2009)
392	⟨Whi5HyperPhos⟩	AND	Whi5_[(S161)]-{P}	Wagner *et al.* (2009)
393	⟨Whi5HyperPhos⟩	AND	Whi5_[(S215)]-{P}	Wagner *et al.* (2009)
394	⟨Whi5HyperPhos⟩	AND	Whi5_[(S262)]-{P}	Wagner *et al.* (2009)
395	⟨Whi5HyperPhos⟩	AND	Whi5_[(S59)]-{P}	Wagner *et al.* (2009)
396	⟨Whi5HyperPhos⟩	AND	Whi5_[(S62)]-{P}	Wagner *et al.* (2009)
397	⟨Whi5HyperPhos⟩	AND	Whi5_[(S88)]-{P}	Wagner *et al.* (2009)
398	⟨Whi5HyperPhos⟩	AND	Whi5_[(T143)]-{P}	Wagner *et al.* (2009)
399	⟨Whi5HyperPhos⟩	AND	Whi5_[(T57)]-{P}	Wagner *et al.* (2009)
400	⟨Whi5HyperPhosOrSwi6Phosphorylation⟩	OR	⟨Swi6Phosphorylation⟩	Wagner *et al.* (2009)
401	⟨Whi5HyperPhosOrSwi6Phosphorylation⟩	OR	⟨Whi5HyperPhos⟩	Wagner *et al.* (2009)
402	⟨Whi5PhosComb1⟩	AND	Whi5_[(S154)]-{P}	Wagner *et al.* (2009)
403	⟨Whi5PhosComb1⟩	AND	Whi5_[(S156)]-{P}	Wagner *et al.* (2009)
404	⟨Whi5PhosComb1⟩	AND	Whi5_[(S161)]-{P}	Wagner *et al.* (2009)
405	⟨Whi5PhosComb2⟩	AND	Whi5_[(S154)]-{P}	Wagner *et al.* (2009)
406	⟨Whi5PhosComb2⟩	AND	Whi5_[(S156)]-{P}	Wagner *et al.* (2009)
407	⟨Whi5PhosComb2⟩	AND	Whi5_[(S262)]-{P}	Wagner *et al.* (2009)
408	⟨Whi5PhosCombinations⟩	OR	⟨Whi5PhosComb1⟩	Wagner *et al.* (2009)
409	⟨Whi5PhosCombinations⟩	OR	⟨Whi5PhosComb2⟩	Wagner *et al.* (2009)
410	⟨yTubulinSmallComplex⟩	AND	Spc97@1_[tub4]–Tub4@2_[spc]	Winey and Bloom (2012)
411	⟨yTubulinSmallComplex⟩	AND	Spc97_[spc]–Spc98_[spc]	Winey and Bloom (2012)
412	⟨yTubulinSmallComplex⟩	AND	Spc98@1_[tub4]–Tub4@3_[spc]	Winey and Bloom (2012)

Table A.3. *Outputs in the CC-CNW.* C: Contingency.

	Output	C	Statement	Reference
1	[ActinCableMediatedExocytosis]	!	⟨ActinCableMediatedExocytosis⟩	Pruyne *et al.* (2002), Bi and Park (2012); Hypothesis
2	[ActinCables]	!	⟨ActinCables⟩	Pruyne *et al.* (2004)
3	[AstralMTPositioning]	!	[ActinCables]	Markus *et al.* (2012)
4	[AstralMTPositioning]	!	⟨AstralMTPositioning⟩	Markus *et al.* (2012)
5	[Biorientation]	!	⟨Dam1MicrotubuleAttachment⟩	Biggins (2013); Hypothesis
6	[Biorientation]	!	⟨Ndc80Dam1Recruitment⟩	Kim *et al.* (2017); Hypothesis
7	[Biorientation]	!	[TensionInitiation]	Biggins (2013); Hypothesis
8	[BipolarSpindle]	!	⟨BipolarSpindle⟩	Gap-filling step 2
9	[Bridge]	!	⟨BridgeComponents⟩	Rüthnick and Schiebel (2016)
10	[BudGrowth]	!	Cell_[(bud)]-{growth}	Howell and Lew (2012); Hypothesis
11	[BudNeck]	!	⟨SeptinRing⟩	Howell and Lew (2012)
12	[BudSite]	!	Cell_[(bud)]-{emerged}	Howell and Lew (2012); Hypothesis
13	[Chs2Activity]	!	Chs2_[(dbf2)]-{P}	Oh *et al.* (2012); Hypothesis
14	[Chs2ERRetention]	!	⟨Chs2ERRetention⟩	Teh *et al.* (2009)
15	[CohesinRing]	!	⟨CohesinRing⟩	Marston (2014)
16	[DNALicensed]	!	Cell_[(DNA)]-{lic}	Bell and Labib (2016); Hypothesis
17	[DNAreplicated]	!	Cell_[(DNA)]-{replicated}	Bell and Labib (2016); Hypothesis
18	[dNTP]	x	[HU]	Poli *et al.* (2012)
19	[dNTP]	x	Rnr1_[sml1]–Sml1_[rnr1]	Zhao *et al.* (1998)
20	[DuplicationPlaque]	!	Cell_[(SPB)]-{dup}	Fu *et al.* (2015)
21	[DuplicationPlaqueFormation]	!	⟨DuplicationPlaque⟩	Fu *et al.* (2015)
22	[EquilibriumDelay1]	!	[Mcm1Delay20]	Gap-filling step 2
23	[EquilibriumDelay10]	!	[EquilibriumDelay9]	Gap-filling step 2
24	[EquilibriumDelay11]	!	[EquilibriumDelay10]	Gap-filling step 2
25	[EquilibriumDelay12]	!	[EquilibriumDelay11]	Gap-filling step 2
26	[EquilibriumDelay13]	!	[EquilibriumDelay12]	Gap-filling step 2
27	[EquilibriumDelay14]	!	[EquilibriumDelay13]	Gap-filling step 2
28	[EquilibriumDelay15]	!	[EquilibriumDelay14]	Gap-filling step 2
29	[EquilibriumDelay16]	!	[EquilibriumDelay15]	Gap-filling step 2
30	[EquilibriumDelay17]	!	[EquilibriumDelay16]	Gap-filling step 2
31	[EquilibriumDelay18]	!	[EquilibriumDelay17]	Gap-filling step 2
32	[EquilibriumDelay19]	!	[EquilibriumDelay18]	Gap-filling step 2
33	[EquilibriumDelay2]	!	[EquilibriumDelay1]	Gap-filling step 2
34	[EquilibriumDelay20]	!	[EquilibriumDelay19]	Gap-filling step 2
35	[EquilibriumDelay3]	!	[EquilibriumDelay2]	Gap-filling step 2
36	[EquilibriumDelay4]	!	[EquilibriumDelay3]	Gap-filling step 2
37	[EquilibriumDelay5]	!	[EquilibriumDelay4]	Gap-filling step 2
38	[EquilibriumDelay6]	!	[EquilibriumDelay5]	Gap-filling step 2
39	[EquilibriumDelay7]	!	[EquilibriumDelay6]	Gap-filling step 2
40	[EquilibriumDelay8]	!	[EquilibriumDelay7]	Gap-filling step 2
41	[EquilibriumDelay9]	!	[EquilibriumDelay8]	Gap-filling step 2
42	[Fkh2Ndd1Mcm1Delay1]	!	⟨Fkh2Ndd1Mcm1⟩	Gap-filling step 2
43	[Fkh2Ndd1Mcm1Delay10]	!	[Fkh2Ndd1Mcm1Delay9]	Gap-filling step 2
44	[Fkh2Ndd1Mcm1Delay11]	!	[Fkh2Ndd1Mcm1Delay10]	Gap-filling step 2
45	[Fkh2Ndd1Mcm1Delay12]	!	[Fkh2Ndd1Mcm1Delay11]	Gap-filling step 2
46	[Fkh2Ndd1Mcm1Delay13]	!	[Fkh2Ndd1Mcm1Delay12]	Gap-filling step 2
47	[Fkh2Ndd1Mcm1Delay14]	!	[Fkh2Ndd1Mcm1Delay13]	Gap-filling step 2
48	[Fkh2Ndd1Mcm1Delay15]	!	[Fkh2Ndd1Mcm1Delay14]	Gap-filling step 2
49	[Fkh2Ndd1Mcm1Delay16]	!	[Fkh2Ndd1Mcm1Delay15]	Gap-filling step 2
50	[Fkh2Ndd1Mcm1Delay17]	!	[Fkh2Ndd1Mcm1Delay16]	Gap-filling step 2
51	[Fkh2Ndd1Mcm1Delay18]	!	[Fkh2Ndd1Mcm1Delay17]	Gap-filling step 2
52	[Fkh2Ndd1Mcm1Delay19]	!	[Fkh2Ndd1Mcm1Delay18]	Gap-filling step 2
53	[Fkh2Ndd1Mcm1Delay2]	!	[Fkh2Ndd1Mcm1Delay1]	Gap-filling step 2
54	[Fkh2Ndd1Mcm1Delay20]	!	[Fkh2Ndd1Mcm1Delay19]	Gap-filling step 2
55	[Fkh2Ndd1Mcm1Delay3]	!	[Fkh2Ndd1Mcm1Delay2]	Gap-filling step 2
56	[Fkh2Ndd1Mcm1Delay4]	!	[Fkh2Ndd1Mcm1Delay3]	Gap-filling step 2
57	[Fkh2Ndd1Mcm1Delay5]	!	[Fkh2Ndd1Mcm1Delay4]	Gap-filling step 2
58	[Fkh2Ndd1Mcm1Delay6]	!	[Fkh2Ndd1Mcm1Delay5]	Gap-filling step 2
59	[Fkh2Ndd1Mcm1Delay7]	!	[Fkh2Ndd1Mcm1Delay6]	Gap-filling step 2
60	[Fkh2Ndd1Mcm1Delay8]	!	[Fkh2Ndd1Mcm1Delay7]	Gap-filling step 2
61	[Fkh2Ndd1Mcm1Delay9]	!	[Fkh2Ndd1Mcm1Delay8]	Gap-filling step 2
62	[GlucanSynthesis]	!	⟨GlucanSynthesisComplex⟩	Bi and Park (2012)
63	[Hcm1Delay1]	!	[SBForMBF]	Gap-filling step 2
64	[Hcm1Delay10]	!	[Hcm1Delay9]	Gap-filling step 2
65	[Hcm1Delay11]	!	[Hcm1Delay10]	Gap-filling step 2
66	[Hcm1Delay12]	!	[Hcm1Delay11]	Gap-filling step 2
67	[Hcm1Delay13]	!	[Hcm1Delay12]	Gap-filling step 2
68	[Hcm1Delay14]	!	[Hcm1Delay13]	Gap-filling step 2
69	[Hcm1Delay15]	!	[Hcm1Delay14]	Gap-filling step 2
70	[Hcm1Delay16]	!	[Hcm1Delay15]	Gap-filling step 2
71	[Hcm1Delay17]	!	[Hcm1Delay16]	Gap-filling step 2
72	[Hcm1Delay18]	!	[Hcm1Delay17]	Gap-filling step 2
73	[Hcm1Delay19]	!	[Hcm1Delay18]	Gap-filling step 2
74	[Hcm1Delay2]	!	[Hcm1Delay1]	Gap-filling step 2
75	[Hcm1Delay20]	!	[Hcm1Delay19]	Gap-filling step 2

Table A.3 – *Continued from previous page*

	Output	C	Statement	Reference
76	[Hcm1Delay3]	!	[Hcm1Delay2]	Gap-filling step 2
77	[Hcm1Delay4]	!	[Hcm1Delay3]	Gap-filling step 2
78	[Hcm1Delay5]	!	[Hcm1Delay4]	Gap-filling step 2
79	[Hcm1Delay6]	!	[Hcm1Delay5]	Gap-filling step 2
80	[Hcm1Delay7]	!	[Hcm1Delay6]	Gap-filling step 2
81	[Hcm1Delay8]	!	[Hcm1Delay7]	Gap-filling step 2
82	[Hcm1Delay9]	!	[Hcm1Delay8]	Gap-filling step 2
83	[HelicaseLoading]	!	Cdt1_[orc6]–Orc6_[cdt1]	Bell and Labib (2016)
84	[MBF]	!	[MBFDelay20]	Gap-filling step 2
85	[MBFDelay1]	!	⟨MBF⟩	Gap-filling step 2
86	[MBFDelay10]	!	[MBFDelay9]	Gap-filling step 2
87	[MBFDelay11]	!	[MBFDelay10]	Gap-filling step 2
88	[MBFDelay12]	!	[MBFDelay11]	Gap-filling step 2
89	[MBFDelay13]	!	[MBFDelay12]	Gap-filling step 2
90	[MBFDelay14]	!	[MBFDelay13]	Gap-filling step 2
91	[MBFDelay15]	!	[MBFDelay14]	Gap-filling step 2
92	[MBFDelay16]	!	[MBFDelay15]	Gap-filling step 2
93	[MBFDelay17]	!	[MBFDelay16]	Gap-filling step 2
94	[MBFDelay18]	!	[MBFDelay17]	Gap-filling step 2
95	[MBFDelay19]	!	[MBFDelay18]	Gap-filling step 2
96	[MBFDelay2]	!	[MBFDelay1]	Gap-filling step 2
97	[MBFDelay20]	!	[MBFDelay19]	Gap-filling step 2
98	[MBFDelay3]	!	[MBFDelay2]	Gap-filling step 2
99	[MBFDelay4]	!	[MBFDelay3]	Gap-filling step 2
100	[MBFDelay5]	!	[MBFDelay4]	Gap-filling step 2
101	[MBFDelay6]	!	[MBFDelay5]	Gap-filling step 2
102	[MBFDelay7]	!	[MBFDelay6]	Gap-filling step 2
103	[MBFDelay8]	!	[MBFDelay7]	Gap-filling step 2
104	[MBFDelay9]	!	[MBFDelay8]	Gap-filling step 2
105	[Mcm1Delay1]	!	⟨Mcm1Transcription⟩	Gap-filling step 2
106	[Mcm1Delay10]	!	[Mcm1Delay9]	Gap-filling step 2
107	[Mcm1Delay11]	!	[Mcm1Delay10]	Gap-filling step 2
108	[Mcm1Delay12]	!	[Mcm1Delay11]	Gap-filling step 2
109	[Mcm1Delay13]	!	[Mcm1Delay12]	Gap-filling step 2
110	[Mcm1Delay14]	!	[Mcm1Delay13]	Gap-filling step 2
111	[Mcm1Delay15]	!	[Mcm1Delay14]	Gap-filling step 2
112	[Mcm1Delay16]	!	[Mcm1Delay15]	Gap-filling step 2
113	[Mcm1Delay17]	!	[Mcm1Delay16]	Gap-filling step 2
114	[Mcm1Delay18]	!	[Mcm1Delay17]	Gap-filling step 2
115	[Mcm1Delay19]	!	[Mcm1Delay18]	Gap-filling step 2
116	[Mcm1Delay2]	!	[Mcm1Delay1]	Gap-filling step 2
117	[Mcm1Delay20]	!	[Mcm1Delay19]	Gap-filling step 2
118	[Mcm1Delay3]	!	[Mcm1Delay2]	Gap-filling step 2
119	[Mcm1Delay4]	!	[Mcm1Delay3]	Gap-filling step 2
120	[Mcm1Delay5]	!	[Mcm1Delay4]	Gap-filling step 2
121	[Mcm1Delay6]	!	[Mcm1Delay5]	Gap-filling step 2
122	[Mcm1Delay7]	!	[Mcm1Delay6]	Gap-filling step 2
123	[Mcm1Delay8]	!	[Mcm1Delay7]	Gap-filling step 2
124	[Mcm1Delay9]	!	[Mcm1Delay8]	Gap-filling step 2
125	[MicrotubuleForces]	!	⟨InterpolarMTSlidingApart⟩	Scholey *et al.* (2016); Hypothesis
126	[OriginFiring]	!	⟨CMG⟩	Bell and Labib (2016); Yeeles *et al.* (2015)
127	[OriginFiring]	!	Mcm2_[mcm10]–Mcm10_[mcm2]	Douglas and Diffley (2016), Lõoke *et al.* (2017)
128	[PlaqueFormation]	!	⟨PlaqueFormation⟩	Gap-filling step 2
129	[Plaques]	!	⟨SPBStates⟩	Gap-filling step 2
130	[SatelliteAssembly]	!	Cell_[(SPB)]-{sat}	Fu *et al.* (2015); Hypothesis
131	[SBF]	!	[SBFDelay20]	Gap-filling step 2
132	[SBFDelay1]	!	⟨SBF⟩	Gap-filling step 2
133	[SBFDelay10]	!	[SBFDelay9]	Gap-filling step 2
134	[SBFDelay11]	!	[SBFDelay10]	Gap-filling step 2
135	[SBFDelay12]	!	[SBFDelay11]	Gap-filling step 2
136	[SBFDelay13]	!	[SBFDelay12]	Gap-filling step 2
137	[SBFDelay14]	!	[SBFDelay13]	Gap-filling step 2
138	[SBFDelay15]	!	[SBFDelay14]	Gap-filling step 2
139	[SBFDelay16]	!	[SBFDelay15]	Gap-filling step 2
140	[SBFDelay17]	!	[SBFDelay16]	Gap-filling step 2
141	[SBFDelay18]	!	[SBFDelay17]	Gap-filling step 2
142	[SBFDelay19]	!	[SBFDelay18]	Gap-filling step 2
143	[SBFDelay2]	!	[SBFDelay1]	Gap-filling step 2
144	[SBFDelay20]	!	[SBFDelay19]	Gap-filling step 2
145	[SBFDelay3]	!	[SBFDelay2]	Gap-filling step 2
146	[SBFDelay4]	!	[SBFDelay3]	Gap-filling step 2
147	[SBFDelay5]	!	[SBFDelay4]	Gap-filling step 2
148	[SBFDelay6]	!	[SBFDelay5]	Gap-filling step 2
149	[SBFDelay7]	!	[SBFDelay6]	Gap-filling step 2
150	[SBFDelay8]	!	[SBFDelay7]	Gap-filling step 2
151	[SBFDelay9]	!	[SBFDelay8]	Gap-filling step 2
152	[SBForMBF]	!	⟨SBForMBFHCM1⟩	Gap-filling step 2

Table A.3 – *Continued from previous page*

	Output	C	Statement	Reference
153	[SpindlePositionCheckpoint]	!	Cell_[(SPB)]-{daughter}	Winey and Bloom (2012), Bertazzi *et al.* (2011); Hypothesis
154	[ssDNA]	!	Cell_[(DNA)]-{replicating}	Mirkin and Mirkin (2007)
155	[ssdsDNAjunctions]	!	Cell_[(DNA)]-{replicating}	Mirkin and Mirkin (2007)
156	[SymmetryBreaking]	!	⟨SymmetryBreaking⟩	Howell and Lew (2012); Gap-filling step 2
157	[TensionInitiation]	!	[BipolarSpindle]	Biggins (2013); Hypothesis
158	[TensionInitiation]	!	[CohesinRing]	Biggins (2013); Hypothesis
159	[TensionInitiation]	!	⟨CondensinAtCentromeres⟩	Marston (2014); Hypothesis
160	[TensionInitiation]	!	[DNAreplicated]	Biggins (2013); Hypothesis
161	[TensionInitiation]	!	Ndc80_[CH]–Tub2_[ndc80]	Biggins (2013); Hypothesis

Table A.4. *Reactions and contingencies CC-CNW.* C: Contingency.

	Reference	Reaction	C	Statement	Reference
1	Tennyson *et al.* (1998)	Ace2_[PBD]_BIND_Pcl9Gene_[pcl9]	x	Ace2_[NLS(cdc28)]-{P}	Sbia *et al.* (2008)
2	Haase and Wittenberg (2014)	Ace2_[PBD]_BIND_Sic1Gene_[sic1]	x	Ace2_[NLS(cdc28)]-{P}	Sbia *et al.* (2008)
3	Dial *et al.* (2007)	Acm1_[bmh]_ppi_Bmh1_[acm1]			
4	Dial *et al.* (2007)	Acm1_[bmh]_ppi_Bmh2_[acm1]			
5	Enquist-Newman *et al.* (2008)	Acm1_[cdh1]_ppi_Cdh1_[acm1]			
6	Pruyne *et al.* (2002)	Act1_[formin]_ppi_Bni1_[actin]	!	<ActinCableNucleationActivity>	Pruyne *et al.* (2002); Hypothesis
7	Pruyne *et al.* (2002)	Act1_[formin]_ppi_Bni1_[actin]	x	[LatA]	Coué *et al.* (1987); Hypothesis
8	Pruyne *et al.* (2002); Hypothesis	Act1_[formin]_ppi_Bnr1_[actin]	x	[LatA]	Coué *et al.* (1987); Hypothesis
9	Liu *et al.* (2010)	Act1_[motor]_ppi_Myo2_[actin]			
10	Crasta *et al.* (2006); Weiss (2012)	APC_[cdc20]_ppi_Cdc20_[APC]	x	Cdc20_[mad2]–Mad2_[cdc20]	Biggins (2013)
11	Enserink and Kolodner (2010); Weiss (2012)	APC_[cdh1]_ppi_Cdh1_[APC]	!	Cdh1_[(cdc28)]-{0}	Enserink and Kolodner (2010), Weiss (2012)
12	Enquist-Newman *et al.* (2008)	APC_Ub+_Acm1_[(Dbox)]	!	APC_[cdc20]–Cdc20_[APC]	Enquist-Newman *et al.* (2008)
13	Enquist-Newman *et al.* (2008)	APC_Ub+_Acm1_[(Dbox)]	K-	<Acm1Phosphorylation>	Ostapenko *et al.* (2008); Hypothesis
14	Crasta *et al.* (2006)	APC_Ub+_Ase1	!	<APCCdh1Active>	Crasta *et al.* (2006)
15	Weiss (2012)	APC_Ub+_Cdc20	!	<APCCdh1Active>	Weiss (2012)
16	Weiss (2012)	APC_Ub+_Cdc5	!	<APCCdh1Active>	Crasta *et al.* (2006)
17	Crasta *et al.* (2006)	APC_Ub+_Cin8_[(apc)]	!	<APCCdh1Active>	Crasta *et al.* (2006)
18	Weiss (2012)	APC_Ub+_Clb1_[(apc)]	!	<APCCdh1Active>	Weiss (2012)
19	Wäsch and Cross (2002)	APC_Ub+_Clb2_[(apc)]	!	<APCCdh1Cdc20>	Wäsch and Cross (2002); Gap-filling step 1
20	Weiss (2012)	APC_Ub+_Clb3_[(apc)]	!	<APCCdh1Active>	Weiss (2012)
21	Weiss (2012)	APC_Ub+_Clb4_[(apc)]	!	<APCCdh1Active>	Weiss (2012)
22	Lu *et al.* (2014)	APC_Ub+_Clb5_[(apc)]	!	<APCCdh1Cdc20>	Lu *et al.* (2014); Gap-filling step 1
23	Lu *et al.* (2014)	APC_Ub+_Dbf4	!	APC_[cdc20]–Cdc20_[APC]	Lu *et al.* (2014)
24	Malo *et al.* (2016)	APC_Ub+_Fkh1_[(apc)]	!	<APCCdh1Active>	Malo *et al.* (2016)
25	Malo *et al.* (2016); Hypothesis	APC_Ub+_Fkh2_[(apc)]	!	<APCCdh1Active>	Malo *et al.* (2016), Hypothesis
26	Crasta *et al.* (2006)	APC_Ub+_Kip1	!	APC_[cdc20]–Cdc20_[APC]	Crasta *et al.* (2006)
27	Ostapenko *et al.* (2012)	APC_Ub+_Mps1_[(apc)]	!	<APCCdh1Active>	Ostapenko *et al.* (2012)
28	Ostapenko *et al.* (2012)	APC_Ub+_Mps1_[(apc)]	K-	Mps1_[(T29)]-{P}	Enserink and Kolodner (2010)
29	Ostapenko and Solomon (2011)	APC_Ub+_Nrm1_[(apc)]	!	<APCCdh1Active>	Ostapenko and Solomon (2011)
30	Hilioti *et al.* (2001)	APC_Ub+_Pds1	!	APC_[cdc20]–Cdc20_[APC]	Hilioti *et al.* (2001), Cid *et al.* (2002)
31	Hilioti *et al.* (2001)	APC_Ub+_Pds1	x	Pds1_[(cdc28)]-{P}	Holt *et al.* (2008)
32	Ostapenko and Solomon (2011)	APC_Ub+_Yhp1	!	<APCCdh1Active>	Ostapenko and Solomon (2011)
33	Haase and Wittenberg (2014)	APC_Ub+_Yox1	!	<APCCdh1Active>	Ostapenko and Solomon (2011); Hypothesis
34	Schuyler *et al.* (2003)	Ase1_[dimer]_ppi_Ase1_[dimer]			
35	Schuyler *et al.* (2003)	Ase1_[mt]_ppi_Tub1_[ase1]			
36	Kim *et al.* (2017)	Ask1_[ndc80]_ppi_Ndc80_[ask1]	!	<Dam1Complex>	Kim *et al.* (2017)
37	Kim *et al.* (2017)	Ask1_[ndc80]_ppi_Ndc80_[ask1]	!	<Ndc80Complex>	Kim *et al.* (2017)
38	Kim *et al.* (2017)	Ask1_[ndc80]_ppi_Ndc80_[ask1]	K-	Ndc80_[N(S100)]-{P}	Kim *et al.* (2017)
39	Legal *et al.* (2016)	Ask1_[N]_ppi_Dad4_[N]			
40	Kang *et al.* (2014)	Axl1_[bud3]_ppi_Bud3_[axl1]			
41	Bastajian *et al.* (2013)	Bck2_[mcm1]_ppi_Mcm1_[bck2]			
42	Bose *et al.* (2001)	Bem1_[Cl]_ppi_Cdc42_[bem1]			
43	Bi and Park (2012)	Bem1_[PB1]_ppi_Cdc24_[bem1]	!	Bem1_[(res1)]-{P}	Bi and Park (2012); Hypothesis
44	Bi and Park (2012)	Bem1_[PB1]_ppi_Cdc24_[bem1]	!	Cdc24_[far1]–0	Butty *et al.* (2002); Hypothesis
45	Bi and Park (2012)	Bem1_[SH3]_ppi_Cla4_[bem1]			
46	Bi and Park (2012)	Bem1_[SH3]_ppi_Ste20_[bem1]			
47	Bi and Park (2012)	Bem2_GAP_Cdc42_[(act)]	!	Bem2_[(res1)]-{0}	Howell and Lew (2012); Hypothesis
48	Bi and Park (2012)	Bem2_GAP_Rho1_[(act)]	!	Bem2_[(res1)]-{0}	Howell and Lew (2012); Hypothesis
49	Bi and Park (2012)	Bem3_GAP_Cdc42_[(act)]	!	Bem3_[(res1)]-{0}	Howell and Lew (2012); Hypothesis
50	Lee *et al.* (2001)	Bfa1_[bub2]_ppi_Bub2_[bfa1]			
51	Hypothesis	Bfa1PPT_P-_Bfa1_[(cdc5)]			
52	Hypothesis	Bfa1PPT_P-_Bfa1_[(kin4)]			

Table A.4 – *Continued from previous page*

	Reference	Reaction	C	Statement	Reference
53	Geymonat *et al.* (2009)	Bfa1_[tem1]_ppi_Tem1_[bfa1]			
54	Enserink and Kolodner (2010)	Bim1_[kar9]_ppi_Kar9_[bim1]	!	Bim1_[MT]–Tub2_[PlusEnd]	Markus *et al.* (2012)
55	Enserink and Kolodner (2010)	Bim1_[kar9]_ppi_Kar9_[bim1]	!	Kar9_[(cdc28)]-{P}	Moore and Miller (2007); Hypothesis
56	Markus *et al.* (2012)	Bim1_[MT]_ppi_Tub2_[PlusEnd]	!	<AstralMTpolymerization>	Markus *et al.* (2012)
57	Yoon and Carbon (1999)	Bir1_[cbf2]_ppi_Cbf2_[bir1]			
58	Nakajima *et al.* (2009)	Bir1_[C]_ppi_Nbl1_[bir1]			
59	Alberts (2001), Dong *et al.* (2003)	Bni1_[DID]_ipi_Bni1_[DAD]	x	Bni1_[GBD]–Cdc42_[formin]	Bi and Park (2012); Hypothesis
60	Alberts (2001), Dong *et al.* (2003)	Bni1_[DID]_ipi_Bni1_[DAD]	x	Bni1_[GBD]–Rho1_[formin]	Bi and Park (2012); Hypothesis
61	Xu *et al.* (2004)	Bni1_[FH2]_ppi_Bni1_[FH2]	x	Bni1_[DID]–[DAD]	Evangelista *et al.* (2002)
62	Evangelista *et al.* (1997)	Bni1_[GBD]_ppi_Cdc42_[formin]	!	Cdc42_[(act)]-{GTP}	Evangelista *et al.* (1997)
63	Evangelista *et al.* (1997)	Bni1_[GBD]_ppi_Cdc42_[formin]	!	[SymmetryBreaking]	Howell and Lew (2012); Gap-filling step 2
64	Kohno *et al.* (1996)	Bni1_[GBD]_ppi_Rho1_[formin]	!	Rho1_[(act)]-{GTP}	Kohno *et al.* (1996)
65	Kohno *et al.* (1996)	Bni1_[GBD]_ppi_Rho1_[formin]	!	[SymmetryBreaking]	Howell and Lew (2012); Gap-filling step 2
66	Fujiwara *et al.* (1998)	Bni1_[SBD]_ppi_Spa2_[bni1]	x	Bni1_[DID]–[DAD]	Evangelista *et al.* (2002); Hypothesis
67	Alberts (2001), Dong *et al.* (2003); Hypothesis	Bnr1_[DID]_ipi_Bnr1_[DAD]	x	Bnr1_[GBD]–Cdc42_[formin]	Bi and Park (2012); Hypothesis
68	Alberts (2001), Dong *et al.* (2003); Hypothesis	Bnr1_[DID]_ipi_Bnr1_[DAD]	x	Bnr1_[GBD]–Rho1_[formin]	Bi and Park (2012); Hypothesis
69	Xu *et al.* (2004); Hypothesis	Bnr1_[FH2]_ppi_Bnr1_[FH2]	x	Bnr1_[DID]–[DAD]	Evangelista *et al.* (2002); Hypothesis
70	Evangelista *et al.* (1997); Hypothesis	Bnr1_[GBD]_ppi_Cdc42_[formin]	!	[BudSite]	Howell and Lew (2012); Gap-filling step 2
71	Evangelista *et al.* (1997); Hypothesis	Bnr1_[GBD]_ppi_Cdc42_[formin]	!	Cdc42_[(act)]-{GTP}	Evangelista *et al.* (1997); Hypothesis
72	Kohno *et al.* (1996); Hypothesis	Bnr1_[GBD]_ppi_Rho1_[formin]	!	[BudSite]	Howell and Lew (2012); Gap-filling step 2
73	Kohno *et al.* (1996); Hypothesis	Bnr1_[GBD]_ppi_Rho1_[formin]	!	Rho1_[(act)]-{GTP}	Kohno *et al.* (1996); Hypothesis
74	Enserink and Kolodner (2010)	Boi1_[cdc42]_ppi_Cdc42_[boi1]	!	Boi1_[(cdc28)]-{P}	Enserink and Kolodner (2010)
75	Enserink and Kolodner (2010)	Boi1_[cdc42]_ppi_Cdc42_[boi1]	!	Cdc42_[(act)]-{GTP}	Hypothesis
76	Enserink and Kolodner (2010)	Boi2_[cdc42]_ppi_Cdc42_[boi2]	!	Boi2_[(cdc28)]-{P}	Enserink and Kolodner (2010)
77	Enserink and Kolodner (2010)	Boi2_[cdc42]_ppi_Cdc42_[boi2]	!	Cdc42_[(act)]-{GTP}	Howell and Lew (2012)
78	Marston (2014)	Brn1_[smc2]_ppi_Smc2_[brn1]			
79	Marston (2014)	Brn1_[smc4]_ppi_Smc4_[brn1]			
80	Marston (2014)	Brn1_[ycg1]_ppi_Ycg1_[brn1]			
81	Marston (2014)	Brn1_[ycs4]_ppi_Ycs4_[brn1]			
82	Biggins (2013)	Bub1_[spc105]_ppi_Spc105_[bub1]	!	Spc105_[(mps1)]-{P}	Biggins (2013)
83	Geymonat *et al.* (2002)	Bub2_GAP_Tem1_[(act)]	!	<Tem1ActivationInhibition>	Cid *et al.* (2002)
84	Biggins (2013)	Bub3_[spc105]_ppi_Spc105_[bub3]	!	Spc105_[(mps1)]-{P}	Biggins (2013)
85	Howell and Lew (2012)	Bud2_GAP_Rsr1_[(act)]			
86	Kang *et al.* (2014)	Bud3_[bud4]_ppi_Bud4_[bud3]			
87	Kang *et al.* (2014)	Bud3_[bud5]_ppi_Bud5_[bud3]			
88	Howell and Lew (2012)	Bud5_GEF_Rsr1_[(act)]	!	Bud5_[landmark]–Lmproteins_[intracellular]	Howell and Lew (2012)
89	Howell and Lew (2012)	Bud5_[landmark]_ppi_Lmproteins_[intracellular]			
90	Bi and Park (2012)	Bud6_[spa2]_ppi_Spa2_[bud6]			
91	Ross *et al.* (2000)	Cak1_P+_Cdc28_[Tloop(T169)]			
92	Biggins (2013)	Cbf2_[centromere]_i_Centromere_[CDE]			
93	Weiss (2012)	Cbk1_[mob2]_ppi_Mob2_[cbk1]			
94	Weiss (2012)	Cbk1_P+_Ace2_[(cbk1)]	!	Cbk1_[mob2]–Mob2_[cbk1]	Weiss (2012)
95	Weiss (2012)	Cbk1_[tao3]_ppi_Tao3_[cbk1]			
96	Hypothesis	Cdc10PPT_P-_Cdc10_[(cla4)]			
97	Bertin *et al.* (2008)	Cdc11_[cdc12]_ppi_Cdc12_[cdc11]			
98	Iwase *et al.* (2006)	Cdc12_[gic1]_ppi_Gic1_[cdc12]	!	Cdc42_[gic]–Gic1_[cdc42]	Iwase *et al.* (2006); Hypothesis
99	Iwase *et al.* (2006)	Cdc12_[gic2]_ppi_Gic2_[cdc12]	!	Cdc42_[gic]–Gic2_[cdc42]	Iwase *et al.* (2006); Hypothesis
100	Mohl *et al.* (2009)	Cdc14_[net1]_ppi_Net1_[n]	x	Cdc14_[(NLS)]-{P}	Mohl *et al.* (2009)
101	Weiss (2012)	Cdc14_[net1]_ppi_Net1_[n]	x	<NetPP>	Yoshida and Toh-e (2002), Azzam *et al.* (2004)
102	Enserink and Kolodner (2010)	Cdc14_P-_Ace2_[NLS(cdc28)]	x	Cdc14_[net1]–Net1_[n]	Shou *et al.* (1999)
103	Visintin *et al.* (1998); Hypothesis	Cdc14_P-_Acm1_[(S3)]	x	Cdc14_[net1]–Net1_[n]	Shou *et al.* (1999)
104	Visintin *et al.* (1998); Hypothesis	Cdc14_P-_Acm1_[(S31)]	x	Cdc14_[net1]–Net1_[n]	Shou *et al.* (1999)
105	Visintin *et al.* (1998); Hypothesis	Cdc14_P-_Acm1_[(S48)]	x	Cdc14_[net1]–Net1_[n]	Shou *et al.* (1999)

Table A.4 – *Continued from previous page*

	Reference	Reaction	C	Statement	Reference
106	Visintin *et al.* (1998); Hypothesis	Cdc14_P-_Acm1_[(T161)]	x	Cdc14_[net1]–Net1_[n]	Shou *et al.* (1999)
107	Visintin *et al.* (1998); Hypothesis	Cdc14_P-_Bem1_[(res1)]	x	Cdc14_[net1]–Net1_[n]	Shou *et al.* (1999)
108	Visintin *et al.* (1998); Hypothesis	Cdc14_P-_Bem2_[(res1)]	x	Cdc14_[net1]–Net1_[n]	Shou *et al.* (1999)
109	Visintin *et al.* (1998); Hypothesis	Cdc14_P-_Bem3_[(res1)]	x	Cdc14_[net1]–Net1_[n]	Shou *et al.* (1999)
110	Visintin *et al.* (1998); Hypothesis	Cdc14_P-_Boi1_[(cdc28)]	x	Cdc14_[net1]–Net1_[n]	Shou *et al.* (1999)
111	Visintin *et al.* (1998); Hypothesis	Cdc14_P-_Boi2_[(cdc28)]	x	Cdc14_[net1]–Net1_[n]	Shou *et al.* (1999)
112	Visintin *et al.* (1998); Hypothesis	Cdc14_P-_Cdc24_[(cdc28)]	x	Cdc14_[net1]–Net1_[n]	Shou *et al.* (1999)
113	Visintin *et al.* (1998); Hypothesis	Cdc14_P-_Cdc5_[(T238)]	x	Cdc14_[net1]–Net1_[n]	Shou *et al.* (1999)
114	Weiss (2012)	Cdc14_P-_Cdc5_[(T242)]	x	Cdc14_[net1]–Net1_[n]	Shou *et al.* (1999)
115	Weiss (2012)	Cdc14_P-_Cdh1_[(cdc28)]	x	Cdc14_[net1]–Net1_[n]	Shou *et al.* (1999)
116	Visintin *et al.* (1998); Hypothesis	Cdc14_P-_Chs2_[(S100)]	x	Cdc14_[net1]–Net1_[n]	Shou *et al.* (1999)
117	Visintin *et al.* (1998); Hypothesis	Cdc14_P-_Chs2_[(S14)]	x	Cdc14_[net1]–Net1_[n]	Shou *et al.* (1999)
118	Visintin *et al.* (1998); Hypothesis	Cdc14_P-_Chs2_[(S60)]	x	Cdc14_[net1]–Net1_[n]	Shou *et al.* (1999)
119	Visintin *et al.* (1998); Hypothesis	Cdc14_P-_Chs2_[(S69)]	x	Cdc14_[net1]–Net1_[n]	Shou *et al.* (1999)
120	Visintin *et al.* (1998); Hypothesis	Cdc14_P-_Dbf4_[(res1)]	x	Cdc14_[net1]–Net1_[n]	Shou *et al.* (1999)
121	Visintin *et al.* (1998); Hypothesis	Cdc14_P-_Fin1_[(cdc28)]	x	Cdc14_[net1]–Net1_[n]	Shou *et al.* (1999)
122	Visintin *et al.* (1998); Hypothesis	Cdc14_P-_Fkh2_[(S683)]	x	Cdc14_[net1]–Net1_[n]	Shou *et al.* (1999)
123	Visintin *et al.* (1998); Hypothesis	Cdc14_P-_Fkh2_[(T697)]	x	Cdc14_[net1]–Net1_[n]	Shou *et al.* (1999)
124	Visintin *et al.* (1998); Hypothesis	Cdc14_P-_Kar9_[(cdc28)]	x	Cdc14_[net1]–Net1_[n]	Shou *et al.* (1999)
125	Visintin *et al.* (1998); Hypothesis	Cdc14_P-_Lte1_[(cdc28)]	x	Cdc14_[net1]–Net1_[n]	Shou *et al.* (1999)
126	Visintin *et al.* (1998); Hypothesis	Cdc14_P-_Mcm3_[NLS(cdc28)]	x	Cdc14_[net1]–Net1_[n]	Shou *et al.* (1999)
127	Visintin *et al.* (1998); Hypothesis	Cdc14_P-_Mps1_[(T29)]	x	Cdc14_[net1]–Net1_[n]	Shou *et al.* (1999)
128	Visintin *et al.* (1998); Hypothesis	Cdc14_P-_Ndd1_[(T319)]	x	Cdc14_[net1]–Net1_[n]	Shou *et al.* (1999)
129	Weiss (2012)	Cdc14_P-_Net1_[(cdc28x6)]	x	Cdc14_[net1]–Net1_[n]	Shou *et al.* (1999)
130	Visintin *et al.* (1998); Hypothesis	Cdc14_P-_Orc2_[(cdc28)]	x	Cdc14_[net1]–Net1_[n]	Shou *et al.* (1999)
131	Visintin *et al.* (1998); Hypothesis	Cdc14_P-_Orc6_[(cdc28)]	x	Cdc14_[net1]–Net1_[n]	Shou *et al.* (1999)
132	Enserink and Kolodner (2010)	Cdc14_P-_Pds1_[(cdc28)]	x	Cdc14_[net1]–Net1_[n]	Shou *et al.* (1999)
133	Visintin *et al.* (1998); Hypothesis	Cdc14PPT_P-_Cdc14_[(NLS)]			
134	Visintin *et al.* (1998); Hypothesis	Cdc14_P-_Rga1_[(res1)]	x	Cdc14_[net1]–Net1_[n]	Shou *et al.* (1999)
135	Visintin *et al.* (1998); Hypothesis	Cdc14_P-_Rga2_[(res1)]	x	Cdc14_[net1]–Net1_[n]	Shou *et al.* (1999)
136	Elserafy *et al.* (2014)	Cdc14_P-_Sfi1_[C(S801)]	x	Cdc14_[net1]–Net1_[n]	Shou *et al.* (1999)
137	Elserafy *et al.* (2014)	Cdc14_P-_Sfi1_[C(S855)]	x	Cdc14_[net1]–Net1_[n]	Shou *et al.* (1999)
138	Elserafy *et al.* (2014)	Cdc14_P-_Sfi1_[C(S882)]	x	Cdc14_[net1]–Net1_[n]	Shou *et al.* (1999)
139	Elserafy *et al.* (2014)	Cdc14_P-_Sfi1_[C(S892)]	x	Cdc14_[net1]–Net1_[n]	Shou *et al.* (1999)
140	Elserafy *et al.* (2014)	Cdc14_P-_Sfi1_[C(S923)]	x	Cdc14_[net1]–Net1_[n]	Shou *et al.* (1999)
141	Elserafy *et al.* (2014)	Cdc14_P-_Sfi1_[C(T816)]	x	Cdc14_[net1]–Net1_[n]	Shou *et al.* (1999)
142	Visintin *et al.* (1998); Hypothesis	Cdc14_P-_Sld2_[(T84)]	x	Cdc14_[net1]–Net1_[n]	Shou *et al.* (1999)
143	Visintin *et al.* (1998); Hypothesis	Cdc14_P-_Sld3_[(S622)]	x	Cdc14_[net1]–Net1_[n]	Shou *et al.* (1999)
144	Visintin *et al.* (1998); Hypothesis	Cdc14_P-_Sld3_[(T600)]	x	Cdc14_[net1]–Net1_[n]	Shou *et al.* (1999)
145	Visintin *et al.* (1998); Hypothesis	Cdc14_P-_Smc4_[(S109)]	x	Cdc14_[net1]–Net1_[n]	Shou *et al.* (1999)
146	Visintin *et al.* (1998); Hypothesis	Cdc14_P-_Smc4_[(S113)]	x	Cdc14_[net1]–Net1_[n]	Shou *et al.* (1999)
147	Visintin *et al.* (1998); Hypothesis	Cdc14_P-_Smc4_[(S117)]	x	Cdc14_[net1]–Net1_[n]	Shou *et al.* (1999)
148	Visintin *et al.* (1998); Hypothesis	Cdc14_P-_Smc4_[(S128)]	x	Cdc14_[net1]–Net1_[n]	Shou *et al.* (1999)
149	Visintin *et al.* (1998); Hypothesis	Cdc14_P-_Smc4_[(S4)]	x	Cdc14_[net1]–Net1_[n]	Shou *et al.* (1999)
150	Visintin *et al.* (1998); Hypothesis	Cdc14_P-_Smc4_[(T43)]	x	Cdc14_[net1]–Net1_[n]	Shou *et al.* (1999)
151	Visintin *et al.* (1998); Hypothesis	Cdc14_P-_Smc4_[(T60)]	x	Cdc14_[net1]–Net1_[n]	Shou *et al.* (1999)
152	Visintin *et al.* (1998); Hypothesis	Cdc14_P-_Spc110_[(S36)]	x	Cdc14_[net1]–Net1_[n]	Shou *et al.* (1999)
153	Visintin *et al.* (1998); Hypothesis	Cdc14_P-_Spc110_[(S91)]	x	Cdc14_[net1]–Net1_[n]	Shou *et al.* (1999)
154	Visintin *et al.* (1998); Hypothesis	Cdc14_P-_Spc42_[(S4)]	x	Cdc14_[net1]–Net1_[n]	Shou *et al.* (1999)
155	Visintin *et al.* (1998); Hypothesis	Cdc14_P-_Spc42_[(T6)]	x	Cdc14_[net1]–Net1_[n]	Shou *et al.* (1999)
156	Visintin *et al.* (1998); Hypothesis	Cdc14_P-_Stb1_[(cdc28)]	x	Cdc14_[net1]–Net1_[n]	Shou *et al.* (1999)
157	Visintin *et al.* (1998); Hypothesis	Cdc14_P-_Swe1_[Cdc28Sites(deg)]	x	Cdc14_[net1]–Net1_[n]	Shou *et al.* (1999)
158	Visintin *et al.* (1998); Hypothesis	Cdc14_P-_Swi4_[(cdc28)]	x	Cdc14_[net1]–Net1_[n]	Shou *et al.* (1999)

Table A.4 – *Continued from previous page*

	Reference	Reaction	C	Statement	Reference
159	Visintin *et al.* (1998)	Cdc14_P-_Swi5_[NLS(cdc28)]	x	Cdc14_[net1]–Net1_[n]	Shou *et al.* (1999)
160	Visintin *et al.* (1998); Hypothesis	Cdc14_P-_Swi6_[(S160)]	x	Cdc14_[net1]–Net1_[n]	Shou *et al.* (1999)
161	Visintin *et al.* (1998); Hypothesis	Cdc14_P-_Swi6_[(S228)]	x	Cdc14_[net1]–Net1_[n]	Shou *et al.* (1999)
162	Visintin *et al.* (1998); Hypothesis	Cdc14_P-_Swi6_[(S238)]	x	Cdc14_[net1]–Net1_[n]	Shou *et al.* (1999)
163	Visintin *et al.* (1998); Hypothesis	Cdc14_P-_Swi6_[(T179)]	x	Cdc14_[net1]–Net1_[n]	Shou *et al.* (1999)
164	Visintin *et al.* (1998); Hypothesis	Cdc14_P-_Tgl4_[(cdc28)]	x	Cdc14_[net1]–Net1_[n]	Shou *et al.* (1999)
165	Visintin *et al.* (1998); Hypothesis	Cdc14_P-_Tub4_[(S360)]	x	Cdc14_[net1]–Net1_[n]	Shou *et al.* (1999)
166	Visintin *et al.* (1998); Hypothesis	Cdc14_P-_Tus1_[(cdc28)]	x	Cdc14_[net1]–Net1_[n]	Shou *et al.* (1999)
167	Visintin *et al.* (1998); Hypothesis	Cdc14_P-_Whi5_[(pho85)]	x	Cdc14_[net1]–Net1_[n]	Shou *et al.* (1999)
168	Visintin *et al.* (1998); Hypothesis	Cdc14_P-_Whi5_[(S154)]	x	Cdc14_[net1]–Net1_[n]	Shou *et al.* (1999)
169	Visintin *et al.* (1998); Hypothesis	Cdc14_P-_Whi5_[(S156)]	x	Cdc14_[net1]–Net1_[n]	Shou *et al.* (1999)
170	Visintin *et al.* (1998); Hypothesis	Cdc14_P-_Whi5_[(S161)]	x	Cdc14_[net1]–Net1_[n]	Shou *et al.* (1999)
171	Visintin *et al.* (1998); Hypothesis	Cdc14_P-_Whi5_[(S215)]	x	Cdc14_[net1]–Net1_[n]	Shou *et al.* (1999)
172	Visintin *et al.* (1998); Hypothesis	Cdc14_P-_Whi5_[(S262)]	x	Cdc14_[net1]–Net1_[n]	Shou *et al.* (1999)
173	Visintin *et al.* (1998); Hypothesis	Cdc14_P-_Whi5_[(S59)]	x	Cdc14_[net1]–Net1_[n]	Shou *et al.* (1999)
174	Visintin *et al.* (1998); Hypothesis	Cdc14_P-_Whi5_[(S62)]	x	Cdc14_[net1]–Net1_[n]	Shou *et al.* (1999)
175	Visintin *et al.* (1998); Hypothesis	Cdc14_P-_Whi5_[(S88)]	x	Cdc14_[net1]–Net1_[n]	Shou *et al.* (1999)
176	Visintin *et al.* (1998); Hypothesis	Cdc14_P-_Whi5_[(T143)]	x	Cdc14_[net1]–Net1_[n]	Shou *et al.* (1999)
177	Visintin *et al.* (1998); Hypothesis	Cdc14_P-_Whi5_[(T57)]	x	Cdc14_[net1]–Net1_[n]	Shou *et al.* (1999)
178	Mah *et al.* (2001)	Cdc15_P+_Dbf2_[(HM)]	!	<Cdc15Active>	Weiss (2012)
179	Mah *et al.* (2001)	Cdc15_P+_Dbf2_[(HM)]	!	<Dbf2Mob1Nud1>	Weiss (2012)
180	Rock *et al.* (2013)	Cdc15_P+_Nud1_[(T78)]	!	<Cdc15Active>	Weiss (2012)
181	Weiss (2012)	Cdc15_[tem1]_ppi_Tem1_[cdc15]	!	Nud1_[tem1]–Tem1_[nud1]	Weiss (2012)
182	Zich and Hardwick (2010)	Cdc20_[mad2]_ppi_Mad2_[cdc20]	!	<Mad1Mad2Mad2>	Biggins (2013)
183	Zich and Hardwick (2010)	Cdc20_[mad3]_ppi_Mad3_[cdc20]			
184	Nern and Arkowitz (1999)	Cdc24_[far1]_ppi_Far1_[cdc24]			
185	Zheng *et al.* (1994)	Cdc24_GEF_Cdc42_[(act)]	!	<Cdc42LocalizedActivation>	Woods *et al.* (2015); Hypothesis
186	Zheng *et al.* (1994)	Cdc24_GEF_Cdc42_[(act)]	K+	<Bem1Cdc24Cla4Cdc42>	Howell and Lew (2012)
187	Zheng *et al.* (1994)	Cdc24_GEF_Cdc42_[(act)]	K+	<Bem1Cdc24Ste20Cdc42>	Howell and Lew (2012)
188	Hypothesis	Cdc24PPT_P-_Cdc24_[(PAKsite)]			
189	Howell and Lew (2012)	Cdc24_[rsr1]_ppi_Rsr1_[cdc24]	!	Cdc24_[far1]–0	Enserink and Kolodner (2010)
190	Howell and Lew (2012)	Cdc24_[rsr1]_ppi_Rsr1_[cdc24]	!	Rsr1_[(act)]-{GTP}	Howell and Lew (2012)
191	Hadwiger *et al.* (1989)	Cdc28_[cks1]_ppi_Cks1_[cdc28]			
192	Ross *et al.* (2000)	Cdc28_[cyclin]_ppi_Clb1_[cdc28]	!	Cdc28_[Tloop(T169)]-{P}	Ross *et al.* (2000)
193	Ross *et al.* (2000)	Cdc28_[cyclin]_ppi_Clb2_[cdc28]	!	Cdc28_[Tloop(T169)]-{P}	Ross *et al.* (2000)
194	Ross *et al.* (2000)	Cdc28_[cyclin]_ppi_Clb3_[cdc28]	!	Cdc28_[Tloop(T169)]-{P}	Ross *et al.* (2000)
195	Ross *et al.* (2000)	Cdc28_[cyclin]_ppi_Clb4_[cdc28]	!	Cdc28_[Tloop(T169)]-{P}	Ross *et al.* (2000)
196	Ross *et al.* (2000)	Cdc28_[cyclin]_ppi_Clb5_[cdc28]	!	Cdc28_[Tloop(T169)]-{P}	Ross *et al.* (2000)
197	Ross *et al.* (2000)	Cdc28_[cyclin]_ppi_Clb6_[cdc28]	!	Cdc28_[Tloop(T169)]-{P}	Ross *et al.* (2000)
198	Ross *et al.* (2000)	Cdc28_[cyclin]_ppi_Cln1_[cdc28]	!	Cdc28_[Tloop(T169)]-{P}	Ross *et al.* (2000)
199	Ross *et al.* (2000)	Cdc28_[cyclin]_ppi_Cln2_[cdc28]	!	Cdc28_[Tloop(T169)]-{P}	Ross *et al.* (2000)
200	Ross *et al.* (2000)	Cdc28_[cyclin]_ppi_Cln3_[cdc28]	!	Cdc28_[Tloop(T169)]-{P}	Ross *et al.* (2000)
201	Enserink and Kolodner (2010)	Cdc28_[far1]_ppi-_Far1_[cdc28]	x	[Pheromone]	Peter and Herskowitz (1994); Hypothesis
202	Enserink and Kolodner (2010)	Cdc28_P+_Ace2_[NLS(cdc28)]	!	<Cdc28Clb12>	Enserink and Kolodner (2010)
203	Ostapenko *et al.* (2008)	Cdc28_P+_Acm1_[(S3)]	!	<Cdc28Cln123>	Ostapenko *et al.* (2008); Hypothesis
204	Ostapenko *et al.* (2008)	Cdc28_P+_Acm1_[(S31)]	!	<Cdc28Cln123>	Ostapenko *et al.* (2008); Hypothesis
205	Ostapenko *et al.* (2008)	Cdc28_P+_Acm1_[(S48)]	!	<Cdc28Cln123>	Ostapenko *et al.* (2008); Hypothesis
206	Ostapenko *et al.* (2008)	Cdc28_P+_Acm1_[(T161)]	!	<Cdc28Cln123>	Ostapenko *et al.* (2008); Hypothesis
207	Bi and Park (2012)	Cdc28_P+_Bem1_[(res1)]	!	<Cdc28Cln123>	Han *et al.* (2005); Hypothesis
208	Bi and Park (2012)	Cdc28_P+_Bem2_[(res1)]	!	<Cdc28Cln123>	Bi and Park (2012)
209	Bi and Park (2012)	Cdc28_P+_Bem3_[(res1)]	!	<Cdc28Cln123>	Bi and Park (2012)
210	Enserink and Kolodner (2010)	Cdc28_P+_Boi1_[(cdc28)]	!	<Cdc28Cln123>	McCusker *et al.* (2007)
211	Enserink and Kolodner (2010)	Cdc28_P+_Boi2_[(cdc28)]	!	<Cdc28Cln123>	McCusker *et al.* (2007)

Table A.4 – *Continued from previous page*

	Reference	Reaction	C	Statement	Reference
212	Bi and Park (2012)	Cdc28_P+_Cdc24_[(cdc28)]	!	<Cdc28Cln123>	Bi and Park (2012)
213	Rodriguez-Rodriguez *et al.* (2016)	Cdc28_P+_Cdc5_[(T238)]	!	<Cdc28Clb12>	Mortensen *et al.* (2005); Hypothesis
214	Rodriguez-Rodriguez *et al.* (2016)	Cdc28_P+_Cdc5_[(T242)]	!	<Cdc28Clb12>	Mortensen *et al.* (2005)
215	Elsasser *et al.* (1999)	Cdc28_P+_Cdc6_[(cdc28)]	!	<Cdc28Clb56>	Elsasser *et al.* (1999)
216	Weiss (2012)	Cdc28_P+_Cdh1_[(cdc28)]	!	<Cdc28Clb12>	Enserink and Kolodner (2010)
217	Teh *et al.* (2009)	Cdc28_P+_Chs2_[(S100)]	!	<Cdc28Clb12>	Teh *et al.* (2009)
218	Teh *et al.* (2009)	Cdc28_P+_Chs2_[(S14)]	!	<Cdc28Clb12>	Teh *et al.* (2009)
219	Teh *et al.* (2009)	Cdc28_P+_Chs2_[(S60)]	!	<Cdc28Clb12>	Teh *et al.* (2009)
220	Teh *et al.* (2009)	Cdc28_P+_Chs2_[(S69)]	!	<Cdc28Clb12>	Teh *et al.* (2009)
221	Jackson *et al.* (2006)	Cdc28_P+_Clb6_[(degron)]	!	<Cdc28Clb56>	Enserink and Kolodner (2010)
222	Enserink and Kolodner (2010)	Cdc28_P+_Cln1_[(cdc28)]	!	<Cdc28Cln123>	Enserink and Kolodner (2010)
223	Enserink and Kolodner (2010)	Cdc28_P+_Cln2_[(cdc28)]	!	<Cdc28Cln123>	Enserink and Kolodner (2010)
224	Yaglom *et al.* (1995)	Cdc28_P+_Cln3_[(cdc28)]	!	<Cdc28Cln123>	Landry *et al.* (2012)
225	Enserink and Kolodner (2010); SGD	Cdc28_P+_Dbf4_[(res1)]	!	<Cdc28Clb56>	Enserink and Kolodner (2010)
226	Enserink and Kolodner (2010)	Cdc28_P+_Far1_[(S87)]	!	<Cdc28Cln123>	Enserink and Kolodner (2010)
227	Enserink and Kolodner (2010)	Cdc28_P+_Fin1_[(cdc28)]	!	<Cdc28Clb56>	Loog and Morgan (2005); Hypothesis
228	Pic-Taylor *et al.* (2004)	Cdc28_P+_Fkh2_[(S683)]	!	<Cdc28Clb1256>	Pic-Taylor *et al.* (2004)
229	Pic-Taylor *et al.* (2004)	Cdc28_P+_Fkh2_[(T697)]	!	<Cdc28Clb1256>	Pic-Taylor *et al.* (2004)
230	Enserink and Kolodner (2010)	Cdc28_P+_Kar9_[(cdc28)]	!	<Cdc28Clb56>	Moore and Miller (2007); Hypothesis
231	Archambault *et al.* (2004); Hypothesis	Cdc28_P+_Lte1_[(cdc28)]	!	<Cdc28Clb12>	Archambault *et al.* (2004); Hypothesis
232	Enserink and Kolodner (2010)	Cdc28_P+_Mcm3_[NLS(cdc28)]	!	<Cdc28Clb12>	Liku *et al.* (2005)
233	Jaspersen *et al.* (2004)	Cdc28_P+_Mps1_[(T29)]	!	<Cdc28Cln123>	Jaspersen *et al.* (2004); Hypothesis
234	Reynolds *et al.* (2003)	Cdc28_P+_Ndd1_[(T319)]	!	<Cdc28Clb12>	Reynolds *et al.* (2003)
235	Weiss (2012)	Cdc28_P+_Net1_[(cdc28x6)]	!	<Cdc28Clb12>	Azzam *et al.* (2004)
236	Nguyen *et al.* (2001)	Cdc28_P+_Orc2_[(cdc28)]	!	<Cdc28Clb56>	Nguyen *et al.* (2001)
237	Nguyen *et al.* (2001)	Cdc28_P+_Orc6_[(cdc28)]	!	<Cdc28Clb56>	Nguyen *et al.* (2001)
238	Agarwal and Cohen-Fix (2002)	Cdc28_P+_Pds1_[(cdc28)]	!	<Cdc28Cln123>	Köivomägi *et al.* (2011)
239	Hypothesis	Cdc28PPT_P-_Cdc28_[(Y19)]			
240	Sopko *et al.* (2007); Hypothesis	Cdc28_P+_Rga1_[(res1)]	!	<Cdc28Cln123>	Sopko *et al.* (2007); Hypothesis
241	Bi and Park (2012)	Cdc28_P+_Rga2_[(res1)]	!	<Cdc28Cln123>	Enserink and Kolodner (2010)
242	Elserafy *et al.* (2014)	Cdc28_P+_Sfi1_[C(S801)]	!	<Cdc28Clb12>	Elserafy *et al.* (2014)
243	Elserafy *et al.* (2014)	Cdc28_P+_Sfi1_[C(S855)]	!	<Cdc28Clb12>	Elserafy *et al.* (2014)
244	Elserafy *et al.* (2014)	Cdc28_P+_Sfi1_[C(S882)]	!	<Cdc28Clb12>	Elserafy *et al.* (2014)
245	Elserafy *et al.* (2014)	Cdc28_P+_Sfi1_[C(S892)]	!	<Cdc28Clb12>	Elserafy *et al.* (2014)
246	Elserafy *et al.* (2014)	Cdc28_P+_Sfi1_[C(S923)]	!	<Cdc28Clb12>	Elserafy *et al.* (2014)
247	Elserafy *et al.* (2014)	Cdc28_P+_Sfi1_[C(T816)]	!	<Cdc28Clb12>	Elserafy *et al.* (2014)
248	Nash *et al.* (2001)	Cdc28_P+_Sic1_[(S69)]	!	<Cdc28Cln12>	Enserink and Kolodner (2010); Gap-filling step 2
249	Nash *et al.* (2001)	Cdc28_P+_Sic1_[(S76)]	!	<Cdc28Cln12>	Enserink and Kolodner (2010); Gap-filling step 2
250	Nash *et al.* (2001)	Cdc28_P+_Sic1_[(S80)]	!	<Cdc28Cln12>	Enserink and Kolodner (2010); Gap-filling step 2
251	Nash *et al.* (2001)	Cdc28_P+_Sic1_[(T2)]	!	<Cdc28Cln12>	Enserink and Kolodner (2010); Gap-filling step 2
252	Nash *et al.* (2001)	Cdc28_P+_Sic1_[(T33)]	!	<Cdc28Cln12>	Enserink and Kolodner (2010); Gap-filling step 2
253	Nash *et al.* (2001)	Cdc28_P+_Sic1_[(T45)]	!	<Cdc28Cln12>	Enserink and Kolodner (2010); Gap-filling step 2
254	Nash *et al.* (2001)	Cdc28_P+_Sic1_[(T5)]	!	<Cdc28Cln12>	Enserink and Kolodner (2010); Gap-filling step 2
255	Enserink and Kolodner (2010)	Cdc28_P+_Sld2_[(T84)]	!	<Cdc28Clb56>	Loog and Morgan (2005)
256	Tanaka *et al.* (2007)	Cdc28_P+_Sld3_[(S622)]	!	<Cdc28Clb56>	Tanaka *et al.* (2007)
257	Tanaka *et al.* (2007)	Cdc28_P+_Sld3_[(T600)]	!	<Cdc28Clb56>	Tanaka *et al.* (2007)
258	Robellet *et al.* (2015)	Cdc28_P+_Smc4_[(S109)]	!	<Cdc28Clb12>	Robellet *et al.* (2015)
259	Robellet *et al.* (2015)	Cdc28_P+_Smc4_[(S113)]	!	<Cdc28Clb12>	Robellet *et al.* (2015)
260	Robellet *et al.* (2015)	Cdc28_P+_Smc4_[(S117)]	!	<Cdc28Clb12>	Robellet *et al.* (2015)
261	Robellet *et al.* (2015)	Cdc28_P+_Smc4_[(S128)]	!	<Cdc28Clb12>	Robellet *et al.* (2015)
262	Robellet *et al.* (2015)	Cdc28_P+_Smc4_[(S4)]	!	<Cdc28Clb12>	Robellet *et al.* (2015)
263	Robellet *et al.* (2015)	Cdc28_P+_Smc4_[(T43)]	!	<Cdc28Clb12>	Robellet *et al.* (2015)
264	Robellet *et al.* (2015)	Cdc28_P+_Smc4_[(T60)]	!	<Cdc28Clb12>	Robellet *et al.* (2015)

Table A.4 – *Continued from previous page*

	Reference	Reaction	C	Statement	Reference
265	Enserink and Kolodner (2010)	Cdc28_P+_Spc110_[(S36)]	!	<Cdc28Clb1256>	Lin *et al.* (2014)
266	Enserink and Kolodner (2010)	Cdc28_P+_Spc110_[(S91)]	!	<Cdc28Clb1256>	Lin *et al.* (2014)
267	Jaspersen *et al.* (2004)	Cdc28_P+_Spc42_[(S4)]	!	<Cdc28Cln123>	Jaspersen *et al.* (2004)
268	Jaspersen *et al.* (2004)	Cdc28_P+_Spc42_[(T6)]	!	<Cdc28Cln123>	Jaspersen *et al.* (2004)
269	Truman *et al.* (2012)	Cdc28_P+_Ssa1_[(T36)]	!	<Cdc28Clb56>	Truman *et al.* (2012)
270	Costanzo *et al.* (2003)	Cdc28_P+_Stb1_[(cdc28)]	!	<Cdc28Cln123>	Costanzo *et al.* (2003)
271	Lee *et al.* (2005)	Cdc28_P+_Swe1_[Cdc28Sites(deg)]	!	<Cdc28Clb12>	Enserink and Kolodner (2010)
272	Lee *et al.* (2005)	Cdc28_P+_Swe1_[Cdc28Sites(deg)]	!	Hsl7_[swe1]–Swe1_[hsl7]	Howell and Lew (2012)
273	Haase and Wittenberg (2014)	Cdc28_P+_Swi4_[(cdc28)]	!	<Cdc28Clb12>	Haase and Wittenberg (2014); Hypothesis
274	Kõivomägi *et al.* (2011)	Cdc28_P+_Swi5_[NLS(cdc28)]	!	<Cdc28Clb12>	Kõivomägi *et al.* (2011)
275	Wagner *et al.* (2009); Hypothesis	Cdc28_P+_Swi6_[(S160)]	!	<Cdc28Cln123>	Wagner *et al.* (2009); Hypothesis
276	Wagner *et al.* (2009); Hypothesis	Cdc28_P+_Swi6_[(S228)]	!	<Cdc28Cln123>	Wagner *et al.* (2009); Hypothesis
277	Wagner *et al.* (2009); Hypothesis	Cdc28_P+_Swi6_[(S238)]	!	<Cdc28Cln123>	Wagner *et al.* (2009); Hypothesis
278	Wagner *et al.* (2009); Hypothesis	Cdc28_P+_Swi6_[(T179)]	!	<Cdc28Cln123>	Wagner *et al.* (2009); Hypothesis
279	Enserink and Kolodner (2010)	Cdc28_P+_Tgl4_[(cdc28)]	!	<Cdc28Clb56>	Enserink and Kolodner (2010)
280	Keck *et al.* (2011)	Cdc28_P+_Tub4_[(S360)]	!	<Cdc28Clb12>	Keck *et al.* (2011)
281	Kono *et al.* (2008)	Cdc28_P+_Tus1_[(cdc28)]	!	<Cdc28Cln123>	Kono *et al.* (2008); Hypothesis
282	Wagner *et al.* (2009)	Cdc28_P+_Whi5_[(S154)]	!	<Cdc28Cln123>	Enserink and Kolodner (2010)
283	Wagner *et al.* (2009)	Cdc28_P+_Whi5_[(S156)]	!	<Cdc28Cln123>	Enserink and Kolodner (2010)
284	Wagner *et al.* (2009)	Cdc28_P+_Whi5_[(S161)]	!	<Cdc28Cln123>	Enserink and Kolodner (2010)
285	Wagner *et al.* (2009)	Cdc28_P+_Whi5_[(S215)]	!	<Cdc28Cln123>	Enserink and Kolodner (2010)
286	Wagner *et al.* (2009)	Cdc28_P+_Whi5_[(S262)]	!	<Cdc28Cln123>	Enserink and Kolodner (2010)
287	Wagner *et al.* (2009)	Cdc28_P+_Whi5_[(S59)]	!	<Cdc28Cln123>	Enserink and Kolodner (2010)
288	Wagner *et al.* (2009)	Cdc28_P+_Whi5_[(S62)]	!	<Cdc28Cln123>	Enserink and Kolodner (2010)
289	Wagner *et al.* (2009)	Cdc28_P+_Whi5_[(S88)]	!	<Cdc28Cln123>	Enserink and Kolodner (2010)
290	Wagner *et al.* (2009)	Cdc28_P+_Whi5_[(T143)]	!	<Cdc28Cln123>	Enserink and Kolodner (2010)
291	Wagner *et al.* (2009)	Cdc28_P+_Whi5_[(T57)]	!	<Cdc28Cln123>	Enserink and Kolodner (2010)
292	Enserink and Kolodner (2010)	Cdc28_[sic1]_ppi_Sic1_[cdc28]			
293	Wang *et al.* (2004)	Cdc28_[whi3]_ppi_Whi3_[cdc28]	x	<ERReleaseSignal>	Yaglom *et al.* (1996); Hypothesis
294	Rüthnick and Schiebel (2016)	Cdc31_[kar1]_ppi_Kar1_[cdc31]			
295	Rüthnick and Schiebel (2016)	Cdc31_[sfi1]_ppi_Sfi1_[cdc31]			
296	Seol *et al.* (1999)	Cdc34_[scf]_ppi_Hrt1_[cdc34]			
297	Bertin *et al.* (2008)	Cdc3_[cdc10]_ppi_Cdc10_[cdc3]	!	Cdc10_[(cla4)]-{P}	Versele and Thorner (2004)
298	Bertin *et al.* (2008)	Cdc3_[cdc12]_ppi_Cdc12_[cdc3]	!	Cdc3_[(cla4)]-{P}	Versele and Thorner (2004)
299	Hypothesis	Cdc3PPT_P-_Cdc3_[(cla4)]			
300	Wu *et al.* (2010)	Cdc42_[exo70]_ppi_Exo70_[cdc42]	!	Cdc42_[(act)]-{GTP}	Wu *et al.* (2010)
301	Iwase *et al.* (2006); Hypothesis	Cdc42_[gic]_ppi_Gic1_[cdc42]	!	Cdc42_[(act)]-{GTP}	Iwase *et al.* (2006)
302	Iwase *et al.* (2006); Hypothesis	Cdc42_[gic]_ppi_Gic2_[cdc42]	!	Cdc42_[(act)]-{GTP}	Iwase *et al.* (2006)
303	Howell and Lew (2012)	Cdc42_[PAK]_ppi_Cla4_[cdc42]	!	Cdc42_[(act)]-{GTP}	Howell and Lew (2012)
304	Howell and Lew (2012)	Cdc42_[PAK]_ppi_Ste20_[cdc42]	!	Cdc42_[(act)]-{GTP}	Howell and Lew (2012)
305	Hoffman *et al.* (2000)	Cdc42_[rdi1]_ppi_Rdi1_[cdc42]			
306	Howell and Lew (2012)	Cdc42_[rsr1]_ppi_Rsr1_[cdc42]	!	Cdc42_[(act)]-{0}	Howell and Lew (2012)
307	Howell and Lew (2012)	Cdc42_[rsr1]_ppi_Rsr1_[cdc42]	!	Rsr1_[(act)]-{GTP}	Howell and Lew (2012)
308	Bi and Park (2012)	Cdc42_[sec3]_ppi_Sec3_[cdc42]	!	Cdc42_[(act)]-{GTP}	Wu *et al.* (2010); Hypothesis
309	Enserink and Kolodner (2010)	Cdc45_[sld3]_ppi_Sld3_[cdc45]	!	Mcm4_[sld3]–Sld3_[mcm4]	Yeeles *et al.* (2015)
310	Enserink and Kolodner (2010)	Cdc45_[sld3]_ppi_Sld3_[cdc45]	!	Mcm6_[sld3]–Sld3_[mcm6]	Yeeles *et al.* (2015)
311	Skowyra *et al.* (1997)	Cdc4_[scf]_ppi_Skp1_[Fprotein]			
312	Perkins *et al.* (2001)	Cdc4_Ub+_Cdc6_[(scf)]	!	Cdc6_[(cdc28)]-{P}	Elsasser *et al.* (1999)
313	Perkins *et al.* (2001)	Cdc4_Ub+_Cdc6_[(scf)]	!	<SCFCdc4>	Perkins *et al.* (2001)
314	Jackson *et al.* (2006)	Cdc4_Ub+_Clb6_[(scf)]	!	Clb6_[(degron)]-{P}	Jackson *et al.* (2006)
315	Jackson *et al.* (2006)	Cdc4_Ub+_Clb6_[(scf)]	!	<SCFCdc4>	Jackson *et al.* (2006)
316	Mendenhall and Hodge (1998)	Cdc4_Ub+_Cln1_[(scf)]	!	Cln1_[(cdc28)]-{P}	Mendenhall and Hodge (1998)
317	Mendenhall and Hodge (1998)	Cdc4_Ub+_Cln1_[(scf)]	!	<SCFCdc4>	Quilis and Igual (2017)

Table A.4 – *Continued from previous page*

	Reference	Reaction	C	Statement	Reference
318	Landry *et al.* (2012)	Cdc4_Ub+_Cln3_[(scf)]	!	Cln3_[(cdc28)]-{P}	Landry *et al.* (2012)
319	Landry *et al.* (2012)	Cdc4_Ub+_Cln3_[(scf)]	!	<SCFCdc4>	Landry *et al.* (2012)
320	Blondel *et al.* (2000)	Cdc4_Ub+_Far1_[(scf)]	!	Far1_[(S87)]-{P}	Gartner *et al.* (1998), Blondel *et al.* (2000)
321	Blondel *et al.* (2000)	Cdc4_Ub+_Far1_[(scf)]	!	<SCFCdc4>	Blondel *et al.* (2000)
322	Skowyra *et al.* (1997)	Cdc4_Ub+_Sic1_[(scf)]	!	<SCFCdc4>	Nash *et al.* (2001)
323	Skowyra *et al.* (1997)	Cdc4_Ub+_Sic1_[(scf)]	!	<Sic1x6P>	Nash *et al.* (2001)
324	Patton *et al.* (1998)	Cdc53_[scf]_ppi_Skp1_[cdc53]			
325	Koren *et al.* (2004)	Cdc55_[tpd3]_ppi_Tpd3_[regulatory]			
326	Song and Lee (2001)	Cdc5_[PBD]_ppi_Cdc11_[cdc5]			
327	Song and Lee (2001)	Cdc5_[PBD]_ppi_Cdc12_[cdc5]			
328	Lee *et al.* (2005)	Cdc5_[PBD]_ppi_Swe1_[cdc5]	K+	Swe1_[Cdc5Sites(HP)]-{P}	Enserink and Kolodner (2010)
329	Kim *et al.* (2012)	Cdc5_P+_Bfa1_[(cdc5)]	!	Cdc5_[(T242)]-{P}	Rodriguez-Rodriguez *et al.* (2016); Hypothesis
330	Kim *et al.* (2012)	Cdc5_P+_Bfa1_[(cdc5)]	x	Bfa1_[(kin4)]-{P}	Weiss (2012)
331	Darieva *et al.* (2006)	Cdc5_P+_Ndd1_[(S85)]	!	Cdc5_[(T242)]-{P}	Rodriguez-Rodriguez *et al.* (2016); Hypothesis
332	Shou *et al.* (2002)	Cdc5_P+_Net1_[(cdc5)]	!	Cdc5_[(T242)]-{P}	Rodriguez-Rodriguez *et al.* (2016)
333	Shou *et al.* (2002)	Cdc5_P+_Net1_[(cdc5)]	!	Net1_[(cdc28x6)]-{P}	Queralt *et al.* (2006)
334	Alexandru *et al.* (2001)	Cdc5_P+_Scc1_[(cdc5)]	!	Cdc5_[(T242)]-{P}	Rodriguez-Rodriguez *et al.* (2016); Hypothesis
335	Elserafy *et al.* (2014)	Cdc5_P+_Sfi1_[C(S826)]	!	Cdc5_[(T242)]-{P}	Rodriguez-Rodriguez *et al.* (2016); Hypothesis
336	Elserafy *et al.* (2014)	Cdc5_P+_Sfi1_[C(T866)]	!	Cdc5_[(T242)]-{P}	Rodriguez-Rodriguez *et al.* (2016); Hypothesis
337	Elserafy *et al.* (2014)	Cdc5_P+_Sfi1_[C(T876)]	!	Cdc5_[(T242)]-{P}	Rodriguez-Rodriguez *et al.* (2016); Hypothesis
338	Park *et al.* (2008)	Cdc5_P+_Slk19	!	Cdc5_[(T242)]-{P}	Rodriguez-Rodriguez *et al.* (2016); Hypothesis
339	Asano *et al.* (2005)	Cdc5_P+_Swe1_[Cdc5Sites(HP)]	!	Cdc5_[(T242)]-{P}	Rodriguez-Rodriguez *et al.* (2016); Hypothesis
340	Asano *et al.* (2005)	Cdc5_P+_Swe1_[Cdc5Sites(HP)]	!	Hsl7_[swe1]–Swe1_[hsl7]	Asano *et al.* (2005)
341	Asano *et al.* (2005)	Cdc5_P+_Swe1_[Cdc5Sites(HP)]	K+	Swe1_[Cdc28Sites(deg)]-{P}	Howell and Lew (2012)
342	Weiss (2012)	Cdc5_P+_Tus1_[(cdc5)]	!	Cdc5_[(T242)]-{P}	Rodriguez-Rodriguez *et al.* (2016); Hypothesis
343	Feng *et al.* (2000)	Cdc6_[orc1]_ppi_Orc1_[cdc6]	!	<ORCOrigin>	Speck *et al.* (2005)
344	Enserink and Kolodner (2010)	Cdc7_[dbf4]_ppi_Dbf4_[cdc7]			
345	Bell and Labib (2016)	Cdc7_P+_Mcm4_[(res1)]	!	Cdc7_[dbf4]–Dbf4_[cdc7]	Bell and Labib (2016)
346	Bell and Labib (2016)	Cdc7_P+_Mcm4_[(res1)]	!	[DNALicensed]	Bell and Labib (2016); Hypothesis
347	Bell and Labib (2016)	Cdc7_P+_Mcm6_[(res1)]	!	Cdc7_[dbf4]–Dbf4_[cdc7]	Bell and Labib (2016)
348	Bell and Labib (2016)	Cdc7_P+_Mcm6_[(res1)]	!	[DNALicensed]	Bell and Labib (2016); Hypothesis
349	Wu *et al.* (2012)	Cdt1_[C]_ppi_Mcm6_[C]	!	<Mcm27Complex>	Wu *et al.* (2012)
350	Bell and Labib (2016)	Cdt1_[orc6]_ppi_Orc6_[cdt1]	!	Cdc6_[orc1]–Orc1_[cdc6]	Bell and Labib (2016)
351	Bell and Labib (2016)	Cdt1_[orc6]_ppi_Orc6_[cdt1]	!	<Mcm27ComplexCdt1>	Bell and Labib (2016)
352	Macroscopic reaction	Cell_BIP_Cell_[(SPB)]	!	[MicrotubuleForces]	Scholey *et al.* (2016)
353	Macroscopic reaction	Cell_CYT_Cell	!	[Chs2Activity]	Enserink and Kolodner (2010)
354	Macroscopic reaction	Cell_DUP_Cell_[(SPB)]	!	[DuplicationPlaqueFormation]	Fu *et al.* (2015)
355	Macroscopic reaction	Cell_EM_Cell_[(bud)]	!	[BudNeck]	Howell and Lew (2012)
356	Macroscopic reaction	Cell_GROWTH_Cell_[(bud)]	!	[ActinCableMediatedExocytosis]	Bi and Park (2012); Hypothesis
357	Macroscopic reaction	Cell_GROWTH_Cell_[(bud)]	!	[ActinCables]	Pruyne *et al.* (2004)
358	Macroscopic reaction	Cell_GROWTH_Cell_[(bud)]	!	[GlucanSynthesis]	Bi and Park (2012)
359	Macroscopic reaction	Cell_LIC_Cell_[(DNA)]	!	[HelicaseLoading]	Bell and Labib (2016); Chen *et al.* (2007a)
360	Macroscopic reaction	Cell_POS_Cell_[(SPB)]	!	[AstralMTPositioning]	Markus *et al.* (2012); Fu *et al.* (2015)
361	Macroscopic reaction	Cell_POS_Cell_[(SPB)]	!	[MicrotubuleForces]	Scholey *et al.* (2016)
362	Macroscopic reaction	Cell_RepFinish_Cell_[(DNA)]	!	[dNTP]	Poli *et al.* (2012)
363	Macroscopic reaction	Cell_RepFinish_Cell_[(DNA)]	!	[Histones]	Norris *et al.* (1988)
364	Macroscopic reaction	Cell_Replnit_Cell_[(DNA)]	!	[OriginFiring]	Yeeles *et al.* (2015); Bell and Labib (2016); Douglas and Diffley (2016), Lööke *et al.* (2017)
365	Macroscopic reaction	Cell_SAT_Cell_[(SPB)]	!	[Bridge]	Rüthnick and Schiebel (2016)
366	Macroscopic reaction	Cell_SEG_Cell_[(DNA)]	x	[CohesinRing]	Marston (2014)
367	Macroscopic reaction	Cell_SEP_Cell_[(SPB)]	x	[Bridge]	Fu *et al.* (2015)
368	Macroscopic reaction	Cell_SPB_Cell_[(SPB)]	!	[PlaqueFormation]	Fu *et al.* (2015); Gap-filling step 2
369	Wang *et al.* (2001)	Chk1_P+_Pds1_[(chk1)]			

Table A.4 – *Continued from previous page*

	Reference	Reaction	C	Statement	Reference
370	Hypothesis	Chs2PPT_P-_Chs2_[(dbf2)]			
371	Hypothesis	Cin8_[mt]_ppi_Tub1_[motor]			
372	Hildebrandt *et al.* (2006)	Cin8_[stalk]_ppi_Cin8_[stalk]			
373	Versele and Thorner (2004)	Cla4_AP+_Cla4_[(ap)]	!	Cdc42_[PAK]–Cla4_[cdc42]	Rane and Minden (2014)
374	Wild *et al.* (2004)	Cla4_[lipid]_i_Pl_[pak]	!	Pl_[(4)]-{P}	Wild *et al.* (2004)
375	Perez *et al.* (2016)	Cla4_P+_Cdc10_[(cla4)]	!	<ActiveCla4>	Versele and Thorner (2004)
376	Perez *et al.* (2016)	Cla4_P+_Cdc10_[(cla4)]	!	Cla4_[lipid]–Pl_[pak]	Wild *et al.* (2004); Hypothesis
377	Bi and Park (2012)	Cla4_P+_Cdc24_[(PAKsite)]	!	<ActiveCla4>	Howell and Lew (2012); Hypothesis
378	Bi and Park (2012)	Cla4_P+_Cdc24_[(PAKsite)]	!	Cdc24_[far1]–0	Butty *et al.* (2002); Hypothesis
379	Perez *et al.* (2016)	Cla4_P+_Cdc3_[(cla4)]	!	<ActiveCla4>	Versele and Thorner (2004)
380	Perez *et al.* (2016)	Cla4_P+_Cdc3_[(cla4)]	!	Cla4_[lipid]–Pl_[pak]	Wild *et al.* (2004); Hypothesis
381	(Bertazzi *et al.* (2011)	Cla4_P+_Lte1_[(cla4)]			
382	Enserink and Kolodner (2010)	Cla4_P+_Swe1_[(cla4)]	!	<ActiveCla4>	Versele and Thorner (2004); Hypothesis
383	Enserink and Kolodner (2010)	Cla4_P+_Swe1_[(cla4)]	!	Hsl7_[swe1]–Swe1_[hsl7]	Enserink and Kolodner (2010)
384	Siegmund and Nasmyth (1996)	Clb2_[swi4]_ppi_Swi4_[cyclin]	!	Cdc28_[cyclin]–Clb2_[cdc28]	Haase and Wittenberg (2014)
385	Yaglom *et al.* (1996)	Cln3_[Jdomain]_ppi_Ydj1_[cln3]	!	<ActiveYdj1>	Cyr and Douglas (1994)
386	Garí *et al.* (2001)	Cln3mRNA_i_Whi3_[mrna]			
387	Elliott *et al.* (1999)	Cmd1_[spc110]_ppi_Spc110_[C]			
388	Winey and Bloom (2012)	Cmd1_[spc42]_ppi_Spc42			
389	Fu *et al.* (2015)	Cnm67_[cp]_ppi_Spc42_[cnm67]	!	Spc42@0_[C]–Spc42@1_[N]	Fu *et al.* (2015); Hypothesis
390	Fu *et al.* (2015)	Cnm67_[op]_ppi_Nud1_[cnm67]	!	Cnm67_[cp]–Spc42_[cnm67]	Fu *et al.* (2015); Hypothesis
391	Crabbé *et al.* (2010)	Ctf18_[rfc]_ppi_RFC_[ctf18]			
392	Legal *et al.* (2016)	Dad4_[coiledcoil]_ppi_Dam1_[N2]			
393	Legal *et al.* (2016)	Dam1_[Ca]_ppi_Tub1_[dam1]	x	<LowTensionDependentPhosphorylation>	Cheeseman *et al.* (2002)
394	Legal *et al.* (2016)	Dam1_[Ca]_ppi_Tub3_[dam1]	x	<LowTensionDependentPhosphorylation>	Cheeseman *et al.* (2002)
395	Legal *et al.* (2016)	Dam1_[Cb]_ppi_Tub2_[dam1]	x	<LowTensionDependentPhosphorylation>	Hypothesis
396	Legal *et al.* (2016)	Dam1_[coiledcoil]_ppi_Duo1_[coiledcoil]			
397	Legal *et al.* (2016)	Dam1_[N1]_ppi_Spc34_[N]			
398	Kim *et al.* (2017)	Dam1_[ndc80]_ppi_Ndc80_[dam1]	!	<Dam1Complex>	Lampert *et al.* (2010), Kim *et al.* (2017)
399	Kim *et al.* (2017)	Dam1_[ndc80]_ppi_Ndc80_[dam1]	!	<Ndc80Complex>	Lampert *et al.* (2010), Kim *et al.* (2017)
400	Kim *et al.* (2017)	Dam1_[ndc80]_ppi_Ndc80_[dam1]	x	<Dam1CTermPhos>	Kim *et al.* (2017)
401	Komarnitsky *et al.* (1998)	Dbf2_[n]_ppi_Mob1_[dbf2]			
402	Mohl *et al.* (2009)	Dbf2_P+_Cdc14_[(NLS)]	!	<Dbf2Active>	Mohl *et al.* (2009)
403	Oh *et al.* (2012)	Dbf2_P+_Chs2_[(dbf2)]	!	<Dbf2Active>	Oh *et al.* (2012)
404	Oh *et al.* (2012)	Dbf2_P+_Chs2_[(dbf2)]	x	[Chs2ERRetention]	Teh *et al.* (2009)
405	Meitinger *et al.* (2013)	Dbf2_P+_Hof1_[(dbf2)]	!	<Dbf2Active>	Mah *et al.* (2001); Hypothesis
406	Hypothesis	Dbf2PPT_P-_Dbf2_[(HM)]			
407	Hypothesis	Dbf4PPT_P-_Dbf4_[(rad53)]			
408	Hypothesis	Decay_DEG_Ace2mRNA			
409	Hypothesis	Decay_DEG_Acm1mRNA			
410	Hypothesis	Decay_DEG_Ase1mRNA			
411	Hypothesis	Decay_DEG_Cdc20mRNA			
412	Hypothesis	Decay_DEG_Cdc5mRNA			
413	Hypothesis	Decay_DEG_Cdc6mRNA			
414	Hypothesis	Decay_DEG_Cin8mRNA			
415	Hypothesis	Decay_DEG_Clb1mRNA			
416	Hypothesis	Decay_DEG_Clb2mRNA			
417	Hypothesis	Decay_DEG_Clb3mRNA			
418	Hypothesis	Decay_DEG_Clb4mRNA			
419	Hypothesis	Decay_DEG_Clb5mRNA			
420	Hypothesis	Decay_DEG_Clb6mRNA			
421	Hypothesis	Decay_DEG_Cln1mRNA			
422	Hypothesis	Decay_DEG_Cln2mRNA			

Table A.4 – *Continued from previous page*

	Reference	Reaction	C	Statement	Reference
423	Hypothesis	Decay_DEG_Cln3mRNA	K+	Cln3mRNA–Whi3_[mrna]	Holmes *et al.* (2013)
424	Hypothesis	Decay_DEG_Dbf4mRNA			
425	Hypothesis	Decay_DEG_Far1mRNA			
426	Hypothesis	Decay_DEG_Fkh1mRNA			
427	Hypothesis	Decay_DEG_Fkh2mRNA			
428	Hypothesis	Decay_DEG_Hcm1mRNA			
429	Hypothesis	Decay_DEG_Kip1mRNA			
430	Hypothesis	Decay_DEG_Mcm2mRNA			
431	Hypothesis	Decay_DEG_Mcm3mRNA			
432	Hypothesis	Decay_DEG_Mcm4mRNA			
433	Hypothesis	Decay_DEG_Mcm5mRNA			
434	Hypothesis	Decay_DEG_Mcm6mRNA			
435	Hypothesis	Decay_DEG_Mcm7mRNA			
436	Hypothesis	Decay_DEG_Mps1mRNA			
437	Hypothesis	Decay_DEG_Ndd1mRNA			
438	Hypothesis	Decay_DEG_Nrm1mRNA			
439	Hypothesis	Decay_DEG_Pcl1mRNA			
440	Hypothesis	Decay_DEG_Pcl2mRNA			
441	Hypothesis	Decay_DEG_Pcl9mRNA			
442	Hypothesis	Decay_DEG_Pds1mRNA			
443	Hypothesis	Decay_DEG_Rad53mRNA			
444	Hypothesis	Decay_DEG_Scc1mRNA			
445	Hypothesis	Decay_DEG_Sic1mRNA			
446	Hypothesis	Decay_DEG_Spc42mRNA			
447	Hypothesis	Decay_DEG_Swe1mRNA			
448	Hypothesis	Decay_DEG_Swi4mRNA			
449	Hypothesis	Decay_DEG_Swi5mRNA			
450	Hypothesis	Decay_DEG_Yhp1mRNA			
451	Hypothesis	Decay_DEG_Yox1mRNA			
452	Hernández-Ortega *et al.* (2013)	Dma1_Ub+_Pcl1_[(dma)]	!	Pcl1_[(deg)]-{P}	Hernández-Ortega *et al.* (2013)
453	Hernández-Ortega *et al.* (2013); Hypothesis	Dma1_Ub+_Pcl2_[(dma)]	!	Pcl2_[(deg)]-{P}	Hernández-Ortega *et al.* (2013); Hypothesis
454	Hernández-Ortega *et al.* (2013); Hypothesis; Gap-filling step 1	Dma1_Ub+_Pcl9_[(dma)]	!	Pcl9_[(deg)]-{P}	Hernández-Ortega *et al.* (2013); Hypothesis; Gap-filling step 1
455	Enserink and Kolodner (2010)	Dpb11_[BRCT1]_ppi_Sld2_[dpb11]	!	Dpb11_[BRCT2]–Sld3_[dpb11]	Yeeles *et al.* (2015)
456	Enserink and Kolodner (2010)	Dpb11_[BRCT1]_ppi_Sld2_[dpb11]	!	Sld2_[(T84)]-{P}	Enserink and Kolodner (2010), Bell and Labib (2016)
457	Enserink and Kolodner (2010)	Dpb11_[BRCT2]_ppi_Sld3_[dpb11]	!	<MCMCdc45Sld3>	Yeeles *et al.* (2015)
458	Enserink and Kolodner (2010)	Dpb11_[BRCT2]_ppi_Sld3_[dpb11]	!	<SldPP>	Bell and Labib (2016)
459	Tanaka *et al.* (2013)	Dpb11_[gins]_ppi_Psf1_[dpb11]			
460	Masumoto *et al.* (2000)	Dpb11_[pol]_ppi_Pol2_[dpb11]			
461	Hypothesis	Dun1PPT_P-_Dun1_[(T380)]			
462	Pardo *et al.* (2017)	Dun1_P+_Sml1_[(dun1)]	!	Dun1_[(T380)]-{P}	Pardo *et al.* (2017); Chen and Zhou (2009)
463	Legal *et al.* (2016)	Duo1_[Ca]_ppi_Tub1_[duo1]	!	Dam1_[coiledcoil]–Duo1_[coiledcoil]	Miranda *et al.* (2007)
464	Legal *et al.* (2016)	Duo1_[Ca]_ppi_Tub3_[duo1]	!	Dam1_[coiledcoil]–Duo1_[coiledcoil]	Miranda *et al.* (2007)
465	Legal *et al.* (2016)	Duo1_[Cb]_ppi_Tub2_[duo1]	!	Ndc80_[CH]–Tub2_[ndc80]	Legal *et al.* (2016); Hypothesis
466	Caydasi *et al.* (2010), Bertazzi *et al.* (2011)	Elm1_P+_Kin4_[AL(T209)]	x	[SpindlePositionCheckpoint]	Bertazzi *et al.* (2011); Hypothesis
467	Uhlmann *et al.* (1999)	Esp1_CUT_Scc1_[(esp1)]	!	Scc1_[(cdc5)]-{P}	Alexandru *et al.* (2001)
468	Uhlmann *et al.* (1999)	Esp1_CUT_Scc1_[(esp1)]	x	Pds1_[esp1]–Esp1_[pds1]	Ciosk *et al.* (1998)
469	Sullivan *et al.* (2001)	Esp1_CUT_Slk19	!	Slk19-{P}	Sullivan *et al.* (2001); Park *et al.* (2008)
470	He *et al.* (2007)	Exo70_[C]_i_PI	!	<PI45P2>	He *et al.* (2007)
471	Haase and Wittenberg (2014)	Fkh2_[DBD]_BIND_Ace2Gene_[promoter2]			
472	Haase and Wittenberg (2014)	Fkh2_[DBD]_BIND_Cdc20Gene_[promoter2]			
473	Haase and Wittenberg (2014)	Fkh2_[DBD]_BIND_Cdc5Gene_[promoter2]			
474	Haase and Wittenberg (2014)	Fkh2_[DBD]_BIND_Clb1Gene_[promoter2]			

Table A.4 – *Continued from previous page*

	Reference	Reaction	C	Statement	Reference
475	Haase and Wittenberg (2014)	Fkh2_[DBD]_BIND_Clb2Gene_[promoter2]			
476	Linke *et al.* (2017)	Fkh2_[DBD]_BIND_Clb3Gene_[promoter2]			
477	Haase and Wittenberg (2014)	Fkh2_[DBD]_BIND_Swi5Gene_[promoter2]			
478	Enserink and Kolodner (2010)	Fkh2_[mcm1]_ppi_Mcm1_[fkh2]			
479	Yelamanchi *et al.* (2014)	Fkh2_[ndd1]_ppi_Ndd1_[fkh2]	!	Fkh2_[(S683)]-{P}	Pic-Taylor *et al.* (2004); Gap-filling step 1
480	Yelamanchi *et al.* (2014)	Fkh2_[ndd1]_ppi_Ndd1_[fkh2]	!	Fkh2_[(T697)]-{P}	Pic-Taylor *et al.* (2004); Gap-filling step 1
481	Yelamanchi *et al.* (2014)	Fkh2_[ndd1]_ppi_Ndd1_[fkh2]	K+	<Ndd1Phosphorylation>	Reynolds *et al.* (2003), Darieva *et al.* (2006)
482	Yelamanchi *et al.* (2014)	Fkh2_[ndd1]_ppi_Ndd1_[fkh2]	x	Ndd1_[(rad53)]-{P}	Yelamanchi *et al.* (2014)
483	Qadota *et al.* (1996)	Fks1_[rho1]_ppi_Rho1_[synthase]	!	Rho1_[(act)]-{GTP}	Qadota *et al.* (1996)
484	Francisco *et al.* (1994)	Glc7_P-_Dam1_[(S20)]	K+	Glc7_[spc105]–Spc105_[rvsf]	Rosenberg *et al.* (2011); Hypothesis
485	Francisco *et al.* (1994)	Glc7_P-_Dam1_[(S257)]	K+	Glc7_[spc105]–Spc105_[rvsf]	Rosenberg *et al.* (2011); Hypothesis
486	Francisco *et al.* (1994)	Glc7_P-_Dam1_[(S265)]	K+	Glc7_[spc105]–Spc105_[rvsf]	Rosenberg *et al.* (2011); Hypothesis
487	Francisco *et al.* (1994)	Glc7_P-_Dam1_[(S292)]	K+	Glc7_[spc105]–Spc105_[rvsf]	Rosenberg *et al.* (2011); Hypothesis
488	Francisco *et al.* (1994)	Glc7_P-_Ndc80_[N(S100)]	K+	Glc7_[spc105]–Spc105_[rvsf]	Rosenberg *et al.* (2011); Hypothesis
489	Francisco *et al.* (1994)	Glc7_P-_Sli15_[(S578)]	K+	Glc7_[spc105]–Spc105_[rvsf]	Rosenberg *et al.* (2011); Hypothesis
490	Biggins (2013)	Glc7_P-_Spc105_[(mps1)]	K+	Glc7_[spc105]–Spc105_[rvsf]	Rosenberg *et al.* (2011); Hypothesis
491	Francisco *et al.* (1994)	Glc7_P-_Spc34_[(T199)]	K+	Glc7_[spc105]–Spc105_[rvsf]	Rosenberg *et al.* (2011); Hypothesis
492	Rosenberg *et al.* (2011)	Glc7_[spc105]_ppi_Spc105_[rvsf]	K+	[TensionInitiation]	Rosenberg *et al.* (2011); Hypothesis
493	Mendenhall and Hodge (1998)	Grr1_[scf]_ppi_Skp1_[Fprotein]			
494	Mendenhall and Hodge (1998)	Grr1_Ub+_Cln1_[(scf)]	!	Cln1_[(cdc28)]-{P}	Mendenhall and Hodge (1998)
495	Mendenhall and Hodge (1998)	Grr1_Ub+_Cln1_[(scf)]	!	<SCFGrr1>	Quilis and Igual (2017)
496	Mendenhall and Hodge (1998)	Grr1_Ub+_Cln2_[(scf)]	!	Cln2_[(cdc28)]-{P}	Mendenhall and Hodge (1998)
497	Mendenhall and Hodge (1998)	Grr1_Ub+_Cln2_[(scf)]	!	<SCFGrr1>	Mendenhall and Hodge (1998)
498	Landry *et al.* (2012)	Grr1_Ub+_Cln3_[(scf)]	!	Cln3_[(cdc28)]-{P}	Landry *et al.* (2012)
499	Landry *et al.* (2012)	Grr1_Ub+_Cln3_[(scf)]	!	<SCFGrr1>	Landry *et al.* (2012)
500	Edenberg *et al.* (2015)	Grr1_Ub+_Ndd1	!	<SCFGrr1>	Edenberg *et al.* (2015)
501	Bi and Park (2012)	Gsc2_[rho1]_ppi_Rho1_[synthase]	!	Rho1_[(act)]-{GTP}	Bi and Park (2012)
502	Pramila *et al.* (2006)	Hcm1_[DBD]_BIND_Cin8Gene_[hcm1]			
503	Pramila *et al.* (2006)	Hcm1_[DBD]_BIND_Fkh1Gene_[hcm1]			
504	Pramila *et al.* (2006)	Hcm1_[DBD]_BIND_Fkh2Gene_[hcm1]			
505	Pramila *et al.* (2006)	Hcm1_[DBD]_BIND_Ndd1Gene_[hcm1]			
506	Pramila *et al.* (2006)	Hcm1_[DBD]_BIND_Yhp1Gene_[hcm1]			
507	Hypothesis	Hof1PPT_P-_Hof1_[(dbf2)]			
508	Enserink and Kolodner (2010)	Hos3_[whi5]_ppi_Whi5_[hdac]	K-	Whi5_[(pho85)]-{P}	Wagner *et al.* (2009); Gap-filling step 1
509	Enserink and Kolodner (2010)	Hos3_[whi5]_ppi_Whi5_[hdac]	x	<Whi5PhosCombinations>	Wagner *et al.* (2009)
510	Seol *et al.* (1999)	Hrt1_[scf]_ppi_Cdc53_[hrt1]			
511	Howell and Lew (2012)	Hsl1_[hsl7]_ppi_Hsl7_[hsl1]	!	Hsl1_[septin]–Cdc3_[hsl1]	Howell and Lew (2012)
512	Howell and Lew (2012)	Hsl1_[hsl7]_ppi_Hsl7_[hsl1]	K+	Hsl7_[(hsl1)]-{P}	Perez *et al.* (2016)
513	Howell and Lew (2012)	Hsl1_P+_Hsl7_[(hsl1)]			
514	Howell and Lew (2012)	Hsl1_[septin]_ppi_Cdc3_[hsl1]	!	[BudGrowth]	Howell and Lew (2012); Gap-filling step 2
515	Hypothesis	Hsl7PPT_P-_Hsl7_[(hsl1)]			
516	Howell and Lew (2012)	Hsl7_[swe1]_ppi_Swe1_[hsl7]	!	Hsl1_[hsl7]–Hsl7_[hsl1]	Howell and Lew (2012)
517	Nelson *et al.* (2003)	Hym1_[kic1]_ppi_Kic1_[hym1]			
518	Nelson *et al.* (2003); Hypothesis	Hym1_[sog2]_ppi_Sog2_[hym1]			
519	Stolz *et al.* (1998)	Inp51_P-_Pl_[(5)]			
520	Cheeseman *et al.* (2002)	Ipl1_P+_Dam1_[(S20)]	!	<AuroraBActive>	Nakajima *et al.* (2009); Hypothesis
521	Cheeseman *et al.* (2002)	Ipl1_P+_Dam1_[(S20)]	x	[TensionInitiation]	Liu *et al.* (2009)
522	Cheeseman *et al.* (2002)	Ipl1_P+_Dam1_[(S257)]	!	<AuroraBActive>	Nakajima *et al.* (2009); Hypothesis
523	Cheeseman *et al.* (2002)	Ipl1_P+_Dam1_[(S257)]	x	[TensionInitiation]	Liu *et al.* (2009)
524	Cheeseman *et al.* (2002)	Ipl1_P+_Dam1_[(S265)]	!	<AuroraBActive>	Nakajima *et al.* (2009); Hypothesis
525	Cheeseman *et al.* (2002)	Ipl1_P+_Dam1_[(S265)]	x	[TensionInitiation]	Liu *et al.* (2009)
526	Cheeseman *et al.* (2002)	Ipl1_P+_Dam1_[(S292)]	!	<AuroraBActive>	Nakajima *et al.* (2009); Hypothesis
527	Cheeseman *et al.* (2002)	Ipl1_P+_Dam1_[(S292)]	x	[TensionInitiation]	Liu *et al.* (2009)

Table A.4 – *Continued from previous page*

	Reference	Reaction	C	Statement	Reference
528	Cheeseman *et al.* (2002)	Ipl1_P+_Ndc80_[N(S100)]	!	<AuroraBActive>	Nakajima *et al.* (2009); Hypothesis
529	Cheeseman *et al.* (2002)	Ipl1_P+_Ndc80_[N(S100)]	x	[TensionInitiation]	Liu *et al.* (2009)
530	Cheeseman *et al.* (2002)	Ipl1_P+_Sli15_[(S578)]	!	<AuroraBActive>	Nakajima *et al.* (2009); Hypothesis
531	Cheeseman *et al.* (2002)	Ipl1_P+_Sli15_[(S578)]	x	[TensionInitiation]	Liu *et al.* (2009)
532	Cheeseman *et al.* (2002)	Ipl1_P+_Spc34_[(T199)]	!	<AuroraBActive>	Nakajima *et al.* (2009); Hypothesis
533	Cheeseman *et al.* (2002)	Ipl1_P+_Spc34_[(T199)]	x	[TensionInitiation]	Liu *et al.* (2009)
534	Kang *et al.* (2001)	Ipl1_[sli15]_ppi_Sli15_[Inbox]			
535	Marston (2014)	Irr1_[scc1]_ppi_Scc1_[irr1]	!	<CohesinLoading>	Marston (2014)
536	Yin *et al.* (2000)	Kar9_[myo2]_ppi_Myo2_[kar9]			
537	Weiss (2012)	Kic1_P+_Cbk1			
538	Weiss (2012)	Kic1_[tao3]_ppi_Tao3_[kic1]			
539	Bertazzi *et al.* (2011)	Kin4Kinase_P+_Kin4_[(HP)]	!	Lte1_[n]–Kin4_[lte1]	Bertazzi *et al.* (2011)
540	Maekawa *et al.* (2007)	Kin4_P+_Bfa1_[(kin4)]	!	Kin4_[AL(T209)]-{P}	Caydasi *et al.* (2010)
541	Maekawa *et al.* (2007)	Kin4_P+_Bfa1_[(kin4)]	!	Kin4_[(HP)]-{0}	Bertazzi *et al.* (2011)
542	Maekawa *et al.* (2007)	Kin4_P+_Bfa1_[(kin4)]	K-	Lte1_[n]–Kin4_[lte1]	Bertazzi *et al.* (2011)
543	Fridman *et al.* (2013)	Kip1_[mt]_ppi_Tub1_[motor]			
544	Glotzer (2009), Chee and Haase (2010); Hypothesis	Kip1_[stalk]_ppi_Kip1_[stalk]			
545	Wakayama *et al.* (2001)	Lcd1_[mec1]_ppi_Mec1_[lcd1]			
546	Rouse and Jackson (2002); Hypothesis	Lcd1_[rfa1]_ppi_Rfa1_[lcd1]			
547	Watanabe *et al.* (2001)	Lrg1_GAP_Rho1_[(act)]	!	<GlucanSynthesisComplex>	Watanabe *et al.* (2001)
548	Bertazzi *et al.* (2011)	Lte1_[n]_ppi_Kin4_[lte1]	!	Lte1_[(cla4)]-{P}	Bertazzi *et al.* (2011)
549	Hypothesis	Lte1PPT_P-_Lte1_[(cla4)]			
550	Biggins (2013)	Mad1_[KT]_ppi_Ndc80_[mad1]	!	Bub1_[spc105]–Spc105_[bub1]	Biggins (2013)
551	Biggins (2013)	Mad1_[KT]_ppi_Ndc80_[mad1]	!	Ndc80_[spc105]–Spc105_[ndc80]	Biggins (2013)
552	Zich and Hardwick (2010)	Mad1_[mad2]_ppi_Mad2_[mad1]			
553	Zich and Hardwick (2010)	Mad2_[mad2]_ppi_Mad2_[mad2]	!	<KinetochoreMad1Mad2>	Zich and Hardwick (2010)
554	Ostapenko *et al.* (2008); Hypothesis	Mbp1_[mcb]_BIND_Acm1Gene_[mcb]			
555	Enserink and Kolodner (2010)	Mbp1_[mcb]_BIND_Clb5Gene_[mcb]			
556	Enserink and Kolodner (2010)	Mbp1_[mcb]_BIND_Clb6Gene_[mcb]			
557	Haase and Wittenberg (2014)	Mbp1_[mcb]_BIND_Hcm1Gene_[mcb]			
558	MacIsaac *et al.* (2006)	Mbp1_[mcb]_BIND_Pds1Gene_[mcb]			
559	Zheng *et al.* (1993)	Mbp1_[mcb]_BIND_Rad53Gene_[mcb]			
560	MacIsaac *et al.* (2006)	Mbp1_[mcb]_BIND_Scc1Gene_[mcb]			
561	Donaldson and Kilmartin (1996); Hypothesis	Mbp1_[mcb]_BIND_Spc42Gene_[mcb]			
562	Enserink and Kolodner (2010)	Mbp1_[swi6]_ppi_Swi6_[mbp1]	K+	Stb1_[N]–Swi6_[stb1]	de Bruin *et al.* (2008)
563	Haase and Wittenberg (2014)	Mcm1_[DBD]_BIND_Ace2Gene_[promoter1]			
564	Haase and Wittenberg (2014)	Mcm1_[DBD]_BIND_Cdc20Gene_[promoter1]			
565	Haase and Wittenberg (2014)	Mcm1_[DBD]_BIND_Cdc5Gene_[promoter1]			
566	Haase and Wittenberg (2014)	Mcm1_[DBD]_BIND_Clb1Gene_[promoter1]			
567	Haase and Wittenberg (2014)	Mcm1_[DBD]_BIND_Clb2Gene_[promoter1]			
568	Linke *et al.* (2017)	Mcm1_[DBD]_BIND_Clb3Gene_[promoter1]			
569	Haase and Wittenberg (2014)	Mcm1_[DBD]_BIND_Swi5Gene_[promoter1]			
570	Pramila *et al.* (2002)	Mcm1_[ECB]_BIND_Cdc6Gene_[ECB]	K+	<Mcm1Bck2Transcription>	Bastajian *et al.* (2013)
571	Pramila *et al.* (2002)	Mcm1_[ECB]_BIND_Cln3Gene_[ECB]	K+	<Mcm1Bck2Transcription>	Bastajian *et al.* (2013)
572	Pramila *et al.* (2002)	Mcm1_[ECB]_BIND_Mcm2Gene_[ECB]	K+	<Mcm1Bck2Transcription>	Bastajian *et al.* (2013)
573	Pramila *et al.* (2002)	Mcm1_[ECB]_BIND_Mcm3Gene_[ECB]	K+	<Mcm1Bck2Transcription>	Bastajian *et al.* (2013)
574	Pramila *et al.* (2002)	Mcm1_[ECB]_BIND_Mcm4Gene_[ECB]	K+	<Mcm1Bck2Transcription>	Bastajian *et al.* (2013)
575	Pramila *et al.* (2002)	Mcm1_[ECB]_BIND_Mcm5Gene_[ECB]	K+	<Mcm1Bck2Transcription>	Bastajian *et al.* (2013)
576	Pramila *et al.* (2002)	Mcm1_[ECB]_BIND_Mcm6Gene_[ECB]	K+	<Mcm1Bck2Transcription>	Bastajian *et al.* (2013)
577	Pramila *et al.* (2002)	Mcm1_[ECB]_BIND_Mcm7Gene_[ECB]	K+	<Mcm1Bck2Transcription>	Bastajian *et al.* (2013)
578	Pramila *et al.* (2002)	Mcm1_[ECB]_BIND_Swi4Gene_[ECB]	K+	<Mcm1Bck2Transcription>	Bastajian *et al.* (2013)
579	Pramila *et al.* (2002)	Mcm1_[yhp1]_ppi_Yhp1_[mcm1]			

Table A.4 – *Continued from previous page*

	Reference	Reaction	C	Statement	Reference
580	Pramila *et al.* (2002)	Mcm1_[yox1]_ppi_Yox1_[mcm1]			
581	Douglas and Diffley (2016)	Mcm2_[mcm10]_ppi_Mcm10_[mcm2]			
582	Bell and Labib (2016)	Mcm2_[mcm6]_ppi_Mcm6_[mcm2]			
583	Bell and Labib (2016)	Mcm3_[mcm5]_ppi_Mcm5_[mcm3]			
584	Bell and Labib (2016)	Mcm4_[mcm7]_ppi_Mcm7_[mcm4]			
585	Hypothesis	Mcm4PPT_P-_Mcm4_[(res1)]			
586	Bell and Labib (2016)	Mcm4_[sld3]_ppi_Sld3_[mcm4]	!	Mcm4_[(res1)]-{P}	Bell and Labib (2016)
587	Bell and Labib (2016)	Mcm5_[mcm6]_ppi_Mcm6_[mcm5]			
588	Bell and Labib (2016)	Mcm6_[mcm4]_ppi_Mcm4_[mcm6]			
589	Hypothesis	Mcm6PPT_P-_Mcm6_[(res1)]			
590	Bell and Labib (2016)	Mcm6_[sld3]_ppi_Sld3_[mcm6]	!	Mcm6_[(res1)]-{P}	Bell and Labib (2016)
591	Bell and Labib (2016)	Mcm7_[mcm3]_ppi_Mcm3_[mcm7]	x	Mcm3_[NLS(cdc28)]-{P}	Liku *et al.* (2005)
592	Chen and Zhou (2009)	Mec1_[mrc1]_ppi_Mrc1_[cT2T3]	!	<DNARFCCtf18Pol2Mrc1>	García-Rodríguez *et al.* (2015); Hypothesis
593	Chen and Zhou (2009)	Mec1_[mrc1]_ppi_Mrc1_[cT2T3]	!	<RPAssDNALcd1Mec1>	Hegnauer *et al.* (2012); Hypothesis
594	Pardo *et al.* (2017)	Mec1_P+_Mrc1_[(mec1)]	!	Mec1_[mrc1]–Mrc1_[cT2T3]	Chen and Zhou (2009)
595	Alcasabas *et al.* (2001)	Mec1_P+_Rad53_[(SCD1sites)]	!	<Mec1Mrc1Rad53>	Chen and Zhou (2009)
596	Palou *et al.* (2015)	Mec1_P+_Swe1_[(S385)]	!	<RPAssDNALcd1Mec1>	Palou *et al.* (2015), Pardo *et al.* (2017); Hypothesis
597	Kaiser *et al.* (1998)	Met30_[scf]_ppi_Skp1_[Fprotein]			
598	Kaiser *et al.* (1998)	Met30_Ub+_Swe1_[(scf)]	!	<SCFCdcMet30>	Kaiser *et al.* (1998)
599	Kaiser *et al.* (1998)	Met30_Ub+_Swe1_[(scf)]	!	<Swe1DegPhosphorylation>	Enserink and Kolodner (2010)
600	Kaiser *et al.* (1998)	Met30_Ub+_Swe1_[(scf)]	x	Swe1_[(S385)]-{P}	Palou *et al.* (2015); Hypothesis
601	Philip and Levin (2001)	Mid2_[rom2]_ppi_Rom2_[cwi]			
602	Howell and Lew (2012)	Mih1_P-_Cdc28_[(Y19)]			
603	Rock *et al.* (2013)	Mob1_[nud1]_ppi_Nud1_[mob1]	!	Nud1_[(T78)]-{P}	Rock *et al.* (2013)
604	Enserink and Kolodner (2010)	Mpb1_[mcb]_BIND_Nrm1Gene_[mcb]			
605	Zich and Hardwick (2010); Biggins (2013)	Mps1_AP+_Mps1_[(APSite)]			
606	Biggins (2013)	Mps1_[ndc80]_ppi_Ndc80_[mps1]	x	[Biorientation]	Biggins (2013)
607	Zich and Hardwick (2010)	Mps1_P+_Ndc80_[(mps1)]	!	Mps1_[(APSite)]-{P}	Zich and Hardwick (2010)
608	Biggins (2013)	Mps1_P+_Spc105_[(mps1)]	!	Mps1_[ndc80]–Ndc80_[mps1]	Biggins (2013)
609	Biggins (2013)	Mps1_P+_Spc105_[(mps1)]	K+	Mps1_[(APSite)]-{P}	Biggins (2013)
610	Lin *et al.* (2014)	Mps1_P+_Spc110_[(S60)]			
611	Lin *et al.* (2014)	Mps1_P+_Spc110_[(T68)]			
612	Enserink and Kolodner (2010)	Mps1_P+_Spc42_[(mps1)]	K+	Mps1_[(APSite)]-{P}	Biggins (2013)
613	Chen and Zhou (2009)	Mrc1_[rad53]_ppi_Rad53_[FHA1]	!	Mrc1_[(mec1)]-{P}	Chen and Zhou (2009)
614	Lou *et al.* (2008)	Mrc1_[pol2]_ppi_Pol2_[mrc1]			
615	Hypothesis	Mrc1PPT_P-_Mrc1_[(mec1)]			
616	Chen and Zhou (2009)	Mrc1_[rad53]_ppi_Rad53_[FHA1]			
617	Gao *et al.* (2003)	Msb3_GAP_Sec4_[(act)]	!	<PolarisomeMsb3>	Bi and Park (2012)
618	Gao *et al.* (2003)	Msb4_GAP_Sec4_[(act)]	!	<PolarisomeMsb4>	Bi and Park (2012)
619	Bi and Park (2012)	Msb3_[spa2]_ppi_Spa2_[MSB]			
620	Bi and Park (2012)	Msb4_GAP_Sec4_[(act)]			
621	Bi and Park (2012)	Msb4_[spa2]_ppi_Spa2_[MSB]			
622	Audhya and Emr (2002)	Mss4_P+_PI_[(5)]	!	PI_[(4)]-{P}	Audhya and Emr (2002)
623	Nakajima *et al.* (2009)	Nbl1_[sli15]_ppi_Sli15_[N]			
624	Biggins (2013)	Ndc80_[CH]_ppi_Tub2_[ndc80]	!	<Ndc80Complex>	Biggins (2013)
625	Biggins (2013)	Ndc80_[CH]_ppi_Tub2_[ndc80]	!	Ndc80_[N]-{0}	Yamagishi *et al.* (2014)
626	Biggins (2013)	Ndc80_[CH]_ppi_Tub2_[ndc80]	!	<NuclearMTpolymerization>	Biggins (2013)
627	Biggins (2013)	Ndc80_[nuf2]_ppi_Nuf2_[ndc80]			
628	Biggins (2013); Hypothesis	Ndc80_[spc105]_ppi_Spc105_[ndc80]			
629	Biggins (2013)	Ndc80_[spc24]_ppi_Spc24_[ndc80]			
630	Kim *et al.* (2017)	Ndc80_[spc34]_ppi_Spc34_[ndc80]	!	<Dam1Complex>	Kim *et al.* (2017)
631	Kim *et al.* (2017)	Ndc80_[spc34]_ppi_Spc34_[ndc80]	!	<Ndc80Complex>	Kim *et al.* (2017)
632	Kim *et al.* (2017)	Ndc80_[spc34]_ppi_Spc34_[ndc80]	K-	Dam1_[(S292)]-{P}	Kim *et al.* (2017)

Table A.4 – *Continued from previous page*

	Reference	Reaction	C	Statement	Reference
633	Kim *et al.* (2017)	Ndc80_[spc34]_ppi_Spc34_[ndc80]	K-	Ndc80_[N(S100)]-{P}	Kim *et al.* (2017)
634	Hypothesis	Ndd1PPT_P-_Ndd1_[(rad53)]			
635	Hypothesis	Ndd1PPT_P-_Ndd1_[(S85)]			
636	Travesa *et al.* (2013)	Nrm1_[GTB]_ppi_Swi6_[nrm1]	!	Mbp1_[swi6]–Swi6_[mbp1]	Travesa *et al.* (2013)
637	Travesa *et al.* (2013)	Nrm1_[GTB]_ppi_Swi6_[nrm1]	x	Nrm1_[(rad53)]-{P}	Travesa *et al.* (2012)
638	Hypothesis	Nrm1PPT_P-_Nrm1_[(rad53)]			
639	Hypothesis	Nud1PPT_P-_Nud1_[(T78)]			
640	Gruneberg *et al.* (2000)	Nud1_[spc72]_ppi_Spc72_[nud1]	!	[DuplicationPlaque]	Fu *et al.* (2015); Hypothesis
641	Valerio-Santiago and Monje-Casas (2011)	Nud1_[tem1]_ppi_Tem1_[nud1]			
642	Müller *et al.* (2010)	Orc1_[DBD]_i_ORI_[origin]	!	<ORCComplex>	Bell and Labib (2016)
643	Sun *et al.* (2012)	Orc1_[orc4]_ppi_Orc4_[orc1]			
644	Sun *et al.* (2012)	Orc2_[orc3]_ppi_Orc3_[orc2]			
645	Sun *et al.* (2012)	Orc2_[orc5]_ppi_Orc5_[orc2]			
646	Sun *et al.* (2012)	Orc2_[orc6]_ppi_Orc6_[orc2]			
647	Sun *et al.* (2012)	Orc4_[orc5]_ppi_Orc5_[orc4]			
648	Measday *et al.* (1997)	Pcl1_[pho85]_ppi_Pho85_[cyclin]			
649	Measday *et al.* (1997)	Pcl2_[pho85]_ppi_Pho85_[cyclin]			
650	Measday *et al.* (1997)	Pcl9_[pho85]_ppi_Pho85_[cyclin]			
651	Ciosk *et al.* (1998)	Pds1_[esp1]_ppi_Esp1_[pds1]			
652	Hypothesis	Pds1PPT_P-_Pds1_[(chk1)]			
653	Bi and Park (2012)	Pea2_[spa2]_ppi_Spa2_[pea2]			
654	Jackson *et al.* (2006)	Pho85_P+_Clb6_[(degron)]	!	<Pho85Cyclin>	Hernández-Ortega *et al.* (2013); Hypothesis
655	Hernández-Ortega *et al.* (2013)	Pho85_P+_Pcl1_[(deg)]	!	<Pho85Cyclin>	Hernández-Ortega *et al.* (2013)
656	Hernández-Ortega *et al.* (2013)	Pho85_P+_Pcl2_[(deg)]	!	<Pho85Cyclin>	Hernández-Ortega *et al.* (2013); Hypothesis
657	Hernández-Ortega *et al.* (2013); Hypothesis	Pho85_P+_Pcl9_[(deg)]	!	<Pho85Cyclin>	Hernández-Ortega *et al.* (2013); Hypothesis
658	Nishizawa *et al.* (1998)	Pho85_P+_Sic1_[(S69)]	!	Pcl1_[pho85]–Pho85_[cyclin]	Nishizawa *et al.* (1998)
659	Nishizawa *et al.* (1998)	Pho85_P+_Sic1_[(S76)]	!	Pcl1_[pho85]–Pho85_[cyclin]	Nishizawa *et al.* (1998)
660	Nishizawa *et al.* (1998)	Pho85_P+_Sic1_[(S80)]	!	Pcl1_[pho85]–Pho85_[cyclin]	Nishizawa *et al.* (1998)
661	Nishizawa *et al.* (1998)	Pho85_P+_Sic1_[(T2)]	!	Pcl1_[pho85]–Pho85_[cyclin]	Nishizawa *et al.* (1998)
662	Nishizawa *et al.* (1998)	Pho85_P+_Sic1_[(T33)]	!	Pcl1_[pho85]–Pho85_[cyclin]	Nishizawa *et al.* (1998)
663	Nishizawa *et al.* (1998)	Pho85_P+_Sic1_[(T45)]	!	Pcl1_[pho85]–Pho85_[cyclin]	Nishizawa *et al.* (1998)
664	Nishizawa *et al.* (1998)	Pho85_P+_Sic1_[(T5)]	!	Pcl1_[pho85]–Pho85_[cyclin]	Nishizawa *et al.* (1998)
665	Truman *et al.* (2012)	Pho85_P+_Ssa1_[(T36)]	!	Pcl2_[pho85]–Pho85_[cyclin]	Truman *et al.* (2012)
666	Huang *et al.* (2009)	Pho85_P+_Whi5_[(pho85)]	!	<Pho85Pcl1Pcl9>	Huang *et al.* (2009)
667	Chilkova *et al.* (2007)	Pol2_[rfc]_ppi_RFC_[pol2]			
668	Simon *et al.* (2001)	PolII_TRSC_Ace2Gene	!	Fkh2_[DBD]–Ace2Gene_[promoter2]	Simon *et al.* (2001)
669	Simon *et al.* (2001)	PolII_TRSC_Ace2Gene	!	[Fkh2Ndd1Mcm1Delay20]	Simon *et al.* (2001); Gap-filling step 2
670	Simon *et al.* (2001)	PolII_TRSC_Ace2Gene	!	Mcm1_[DBD]–Ace2Gene_[promoter1]	Simon *et al.* (2001)
671	Ostapenko *et al.* (2008); Hypothesis	PolII_TRSC_Acm1Gene	!	[MBFDelay20]	Ostapenko *et al.* (2008); Hypothesis; Gap-filling step 2
672	Ostapenko *et al.* (2008); Hypothesis	PolII_TRSC_Acm1Gene	!	Mbp1_[mcb]–Acm1Gene_[mcb]	Ostapenko *et al.* (2008); Hypothesis
673	Juang *et al.* (1997)	PolII_TRSC_Ase1Gene			
674	Simon *et al.* (2001)	PolII_TRSC_Cdc20Gene	!	Fkh2_[DBD]–Cdc20Gene_[promoter2]	Simon *et al.* (2001)
675	Simon *et al.* (2001)	PolII_TRSC_Cdc20Gene	!	[Fkh2Ndd1Mcm1Delay20]	Simon *et al.* (2001); Gap-filling step 2
676	Simon *et al.* (2001)	PolII_TRSC_Cdc20Gene	!	Mcm1_[DBD]–Cdc20Gene_[promoter1]	Simon *et al.* (2001)
677	Haase and Wittenberg (2014)	PolII_TRSC_Cdc5Gene	!	Fkh2_[DBD]–Cdc5Gene_[promoter2]	Haase and Wittenberg (2014)
678	Haase and Wittenberg (2014)	PolII_TRSC_Cdc5Gene	!	[Fkh2Ndd1Mcm1Delay20]	Gap-filling step 2
679	Haase and Wittenberg (2014)	PolII_TRSC_Cdc5Gene	!	Mcm1_[DBD]–Cdc5Gene_[promoter1]	Haase and Wittenberg (2014)
680	Pramila *et al.* (2002)	PolII_TRSC_Cdc6Gene	!	[EquilibriumDelay20]	Gap-filling step 2
681	Pramila *et al.* (2002)	PolII_TRSC_Cdc6Gene	!	Mcm1_[ECB]–Cdc6Gene_[ECB]	Pramila *et al.* (2002)
682	Pramila *et al.* (2006)	PolII_TRSC_Cin8Gene	!	Hcm1_[DBD]–Cin8Gene_[hcm1]	Pramila *et al.* (2006)
683	Pramila *et al.* (2006)	PolII_TRSC_Cin8Gene	!	[Hcm1Delay20]	Pramila *et al.* (2006); Gap-filling step 2
684	Enserink and Kolodner (2010)	PolII_TRSC_Clb1Gene	!	Fkh2_[DBD]–Clb1Gene_[promoter2]	Haase and Wittenberg (2014)

Table A.4 – *Continued from previous page*

	Reference	Reaction	C	Statement	Reference
685	Enserink and Kolodner (2010)	PolII_TRSC_Clb1Gene	!	[Fkh2Ndd1Mcm1Delay20]	Gap-filling step 2
686	Enserink and Kolodner (2010)	PolII_TRSC_Clb1Gene	!	Mcm1_[DBD]–Clb1Gene_[promoter1]	Haase and Wittenberg (2014)
687	Simon *et al.* (2001)	PolII_TRSC_Clb2Gene	!	Fkh2_[DBD]–Clb2Gene_[promoter2]	Simon *et al.* (2001)
688	Simon *et al.* (2001)	PolII_TRSC_Clb2Gene	!	[Fkh2Ndd1Mcm1Delay20]	Simon *et al.* (2001); Gap-filling step 2
689	Simon *et al.* (2001)	PolII_TRSC_Clb2Gene	!	Mcm1_[DBD]–Clb2Gene_[promoter1]	Simon *et al.* (2001)
690	Linke *et al.* (2017)	PolII_TRSC_Clb3Gene	!	Fkh2_[DBD]–Clb3Gene_[promoter2]	Linke *et al.* (2017)
691	Linke *et al.* (2017)	PolII_TRSC_Clb3Gene	!	[Fkh2Ndd1Mcm1Delay20]	Linke *et al.* (2017); Gap-filling step 2
692	Linke *et al.* (2017)	PolII_TRSC_Clb3Gene	!	Mcm1_[DBD]–Clb3Gene_[promoter1]	Linke *et al.* (2017)
693	Spellman *et al.* (1998)	PolII_TRSC_Clb4Gene			
694	Enserink and Kolodner (2010)	PolII_TRSC_Clb5Gene	!	[MBFDelay20]	Enserink and Kolodner (2010)
695	Enserink and Kolodner (2010)	PolII_TRSC_Clb5Gene	!	Mbp1_[mcb]–Clb5Gene_[mcb]	Enserink and Kolodner (2010)
696	Enserink and Kolodner (2010)	PolII_TRSC_Clb6Gene	!	[MBFDelay20]	Enserink and Kolodner (2010)
697	Enserink and Kolodner (2010)	PolII_TRSC_Clb6Gene	!	Mbp1_[mcb]–Clb6Gene_[mcb]	Enserink and Kolodner (2010)
698	Nasmyth and Dirick (1991)	PolII_TRSC_Cln1Gene	!	[SBFDelay20]	Nasmyth and Dirick (1991); Gap-filling step 2
699	Nasmyth and Dirick (1991)	PolII_TRSC_Cln1Gene	!	Swi4_[scb]–Cln1Gene_[scb]	Nasmyth and Dirick (1991)
700	Nasmyth and Dirick (1991)	PolII_TRSC_Cln2Gene	!	[SBFDelay20]	Nasmyth and Dirick (1991); Gap-filling step 2
701	Nasmyth and Dirick (1991)	PolII_TRSC_Cln2Gene	!	Swi4_[scb]–Cln2Gene_[scb]	Nasmyth and Dirick (1991)
702	Pramila *et al.* (2002)	PolII_TRSC_Cln3Gene	!	[EquilibriumDelay20]	Gap-filling step 2
703	Pramila *et al.* (2002)	PolII_TRSC_Cln3Gene	!	Mcm1_[ECB]–Cln3Gene_[ECB]	Pramila *et al.* (2002)
704	Spellman *et al.* (1998)	PolII_TRSC_Dbf4Gene			
705	Haase and Wittenberg (2014)	PolII_TRSC_Far1Gene			
706	Pramila *et al.* (2006)	PolII_TRSC_Fkh1Gene	!	Hcm1_[DBD]–Fkh1Gene_[hcm1]	Pramila *et al.* (2006)
707	Pramila *et al.* (2006)	PolII_TRSC_Fkh1Gene	!	[Hcm1Delay20]	Pramila *et al.* (2006); Gap-filling step 2
708	Pramila *et al.* (2006)	PolII_TRSC_Fkh2Gene	!	Hcm1_[DBD]–Fkh2Gene_[hcm1]	Pramila *et al.* (2006)
709	Pramila *et al.* (2006)	PolII_TRSC_Fkh2Gene	!	[Hcm1Delay20]	Pramila *et al.* (2006); Gap-filling step 2
710	Horak *et al.* (2002)	PolII_TRSC_Hcm1Gene	!	<SBForMBFHCM1>	Horak *et al.* (2002); Bean *et al.* (2005); Hypothesis
711	Spellman *et al.* (1998)	PolII_TRSC_Kip1Gene			
712	Pramila *et al.* (2002)	PolII_TRSC_Mcm2Gene	!	[EquilibriumDelay20]	Gap-filling step 2
713	Pramila *et al.* (2002)	PolII_TRSC_Mcm2Gene	!	Mcm1_[ECB]–Mcm2Gene_[ECB]	Pramila *et al.* (2002)
714	Pramila *et al.* (2002)	PolII_TRSC_Mcm3Gene	!	[EquilibriumDelay20]	Gap-filling step 2
715	Pramila *et al.* (2002)	PolII_TRSC_Mcm3Gene	!	Mcm1_[ECB]–Mcm3Gene_[ECB]	Pramila *et al.* (2002)
716	Pramila *et al.* (2002)	PolII_TRSC_Mcm4Gene	!	[EquilibriumDelay20]	Gap-filling step 2
717	Pramila *et al.* (2002)	PolII_TRSC_Mcm4Gene	!	Mcm1_[ECB]–Mcm4Gene_[ECB]	Pramila *et al.* (2002)
718	Pramila *et al.* (2002)	PolII_TRSC_Mcm5Gene	!	[EquilibriumDelay20]	Gap-filling step 2
719	Pramila *et al.* (2002)	PolII_TRSC_Mcm5Gene	!	Mcm1_[ECB]–Mcm5Gene_[ECB]	Pramila *et al.* (2002)
720	Pramila *et al.* (2002)	PolII_TRSC_Mcm6Gene	!	[EquilibriumDelay20]	Gap-filling step 2
721	Pramila *et al.* (2002)	PolII_TRSC_Mcm6Gene	!	Mcm1_[ECB]–Mcm6Gene_[ECB]	Pramila *et al.* (2002)
722	Pramila *et al.* (2002)	PolII_TRSC_Mcm7Gene	!	[EquilibriumDelay20]	Gap-filling step 2
723	Pramila *et al.* (2002)	PolII_TRSC_Mcm7Gene	!	Mcm1_[ECB]–Mcm7Gene_[ECB]	Pramila *et al.* (2002)
724	Poch *et al.* (1994)	PolII_TRSC_Mps1Gene			
725	Pramila *et al.* (2006)	PolII_TRSC_Ndd1Gene	!	Hcm1_[DBD]–Ndd1Gene_[hcm1]	Pramila *et al.* (2006)
726	Pramila *et al.* (2006)	PolII_TRSC_Ndd1Gene	!	[Hcm1Delay20]	Pramila *et al.* (2006); Gap-filling step 2
727	Enserink and Kolodner (2010)	PolII_TRSC_Nrm1Gene	!	[MBFDelay20]	Enserink and Kolodner (2010)
728	Enserink and Kolodner (2010)	PolII_TRSC_Nrm1Gene	!	Mpb1_[mcb]–Nrm1Gene_[mcb]	Enserink and Kolodner (2010)
729	Cho *et al.* (1998); Hypothesis	PolII_TRSC_Pcl1Gene	!	[SBFDelay20]	Cho *et al.* (1998); Hypothesis; Gap-filling step 2
730	Cho *et al.* (1998); Hypothesis	PolII_TRSC_Pcl1Gene	!	Swi4_[scb]–Pcl1Gene_[scb]	Cho *et al.* (1998); Hypothesis
731	Cho *et al.* (1998); Hypothesis	PolII_TRSC_Pcl2Gene	!	[SBFDelay20]	Cho *et al.* (1998); Hypothesis; Gap-filling step 2
732	Cho *et al.* (1998); Hypothesis	PolII_TRSC_Pcl2Gene	!	Swi4_[scb]–Pcl2Gene_[scb]	Cho *et al.* (1998); Hypothesis
733	Cho *et al.* (1998); Hypothesis	PolII_TRSC_Pcl9Gene	!	<Pcl9Transcription>	Tennyson *et al.* (1998)
734	MacIsaac *et al.* (2006)	PolII_TRSC_Pds1Gene	!	[MBFDelay20]	MacIsaac *et al.* (2006); Gap-filling step 2
735	MacIsaac *et al.* (2006)	PolII_TRSC_Pds1Gene	!	Mbp1_[mcb]–Pds1Gene_[mcb]	MacIsaac *et al.* (2006)
736	Zheng *et al.* (1993)	PolII_TRSC_Rad53Gene	K+	[MBFDelay20]	Zheng *et al.* (1993); Gap-filling step 2
737	Zheng *et al.* (1993)	PolII_TRSC_Rad53Gene	K+	Mbp1_[mcb]–Rad53Gene_[mcb]	Zheng *et al.* (1993)

Table A.4 – *Continued from previous page*

	Reference	Reaction	C	Statement	Reference
738	MacIsaac *et al.* (2006)	PolII_TRSC_Scc1Gene	!	[MBFDelay20]	MacIsaac *et al.* (2006); Gap-filling step 2
739	MacIsaac *et al.* (2006)	PolII_TRSC_Scc1Gene	!	Mbp1_[mcb]–Scc1Gene_[mcb]	MacIsaac *et al.* (2006)
740	Knapp *et al.* (1996)	PolII_TRSC_Sic1Gene	!	<Sic1Transcription>	Knapp *et al.* (1996)
741	Donaldson and Kilmartin (1996); Hypothesis	PolII_TRSC_Spc42Gene	!	[MBFDelay20]	Donaldson and Kilmartin (1996); Hypothesis; Gap-filling step 2
742	Donaldson and Kilmartin (1996); Hypothesis	PolII_TRSC_Spc42Gene	!	Mbp1_[mcb]–Spc42Gene_[mcb]	Donaldson and Kilmartin (1996); Hypothesis
743	Sia *et al.* (1996)	PolII_TRSC_Swe1Gene	!	[SBFDelay20]	Sia *et al.* (1996); Gap-filling step 2
744	Sia *et al.* (1996)	PolII_TRSC_Swe1Gene	!	Swi4_[scb]–Swe1Gene_[scb]	Sia *et al.* (1996)
745	Pramila *et al.* (2002)	PolII_TRSC_Swi4Gene	!	[EquilibriumDelay20]	Pramila *et al.* (2002); Gap-filling step 2
746	Pramila *et al.* (2002)	PolII_TRSC_Swi4Gene	!	Mcm1_[ECB]–Swi4Gene_[ECB]	Pramila *et al.* (2002)
747	Simon *et al.* (2001)	PolII_TRSC_Swi5Gene	!	Fkh2_[DBD]–Swi5Gene_[promoter2]	Simon *et al.* (2001)
748	Simon *et al.* (2001)	PolII_TRSC_Swi5Gene	!	[Fkh2Ndd1Mcm1Delay20]	Simon *et al.* (2001); Gap-filling step 2
749	Simon *et al.* (2001)	PolII_TRSC_Swi5Gene	!	Mcm1_[DBD]–Swi5Gene_[promoter1]	Simon *et al.* (2001)
750	Pramila *et al.* (2006)	PolII_TRSC_Yhp1Gene	!	Hcm1_[DBD]–Yhp1Gene_[hcm1]	Pramila *et al.* (2006)
751	Pramila *et al.* (2006)	PolII_TRSC_Yhp1Gene	!	[Hcm1Delay20]	Pramila *et al.* (2006); Gap-filling step 2
752	Haase and Wittenberg (2014)	PolII_TRSC_Yox1Gene	!	[SBFDelay20]	Haase and Wittenberg (2014); SGD
753	Haase and Wittenberg (2014)	PolII_TRSC_Yox1Gene	!	Swi4_[scb]–Yox1Gene_[scb]	
754	Kemmler *et al.* (2009)	PP2A_P-_Ndc80_[(mps1)]			
755	Chan and Amon (2009); Hypothesis	Pph21_P-_Kin4_[AL(T209)]	!	<PP2ARts1Pph21>	Chan and Amon (2009)
756	Bertazzi *et al.* (2011)	Pph21_P-_Kin4_[(HP)]	!	<PP2ARts1Pph21>	Bertazzi *et al.* (2011)
757	Queralt *et al.* (2006)	Pph21_P-_Net1_[(cdc5)]	!	<PP2ACdc55Pph21>	Queralt *et al.* (2006)
758	Jiang and Broach (1999); Hypothesis	Pph21_[tpd3]_ppi_Tpd3_[pph]			
759	Jiang and Broach (1999); Hypothesis	Pph22_[tpd3]_ppi_Tpd3_[pph]			
759	Chan and Amon (2009); Hypothesis	Pph22_P-_Kin4_[AL(T209)]	!	<PP2ARts1Pph22>	Chan and Amon (2009)
760	Bertazzi *et al.* (2011)	Pph22_P-_Kin4_[(HP)]	!	<PP2ARts1Pph22>	Bertazzi *et al.* (2011)
761	Queralt *et al.* (2006)	Pph22_P-_Net1_[(cdc5)]	!	<PP2ACdc55Pph22>	Queralt *et al.* (2006)
762	Enquist-Newman *et al.* (2008)	Proteasome_DEG_Acm1	!	Acm1_[(Dbox)]-{Ub}	Enquist-Newman *et al.* (2008)
763	Crasta *et al.* (2006)	Proteasome_DEG_Ase1	!	Ase1-{Ub}	Crasta *et al.* (2006)
764	Weiss (2012)	Proteasome_DEG_Cdc20	!	Cdc20-{Ub}	Weiss (2012)
765	Weiss (2012)	Proteasome_DEG_Cdc5	!	Cdc5-{Ub}	Weiss (2012)
766	Elsasser *et al.* (1999)	Proteasome_DEG_Cdc6	!	Cdc6_[(scf)]-{Ub}	Elsasser *et al.* (1999)
767	Crasta *et al.* (2006)	Proteasome_DEG_Cin8	!	Cin8_[(apc)]-{Ub}	Crasta *et al.* (2006)
768	Weiss (2012)	Proteasome_DEG_Clb1	!	Clb1_[(apc)]-{Ub}	Weiss (2012)
769	Wäsch and Cross (2002)	Proteasome_DEG_Clb2	!	Clb2_[(apc)]-{Ub}	Wäsch and Cross (2002)
770	Weiss (2012)	Proteasome_DEG_Clb3	!	Clb3_[(apc)]-{Ub}	Weiss (2012)
771	Weiss (2012)	Proteasome_DEG_Clb4	!	Clb4_[(apc)]-{Ub}	Weiss (2012)
772	Lu *et al.* (2014)	Proteasome_DEG_Clb5	!	Clb5_[(apc)]-{Ub}	Lu *et al.* (2014)
773	Enserink and Kolodner (2010)	Proteasome_DEG_Clb6	!	Clb6_[(scf)]-{Ub}	Enserink and Kolodner (2010)
774	Mendenhall and Hodge (1998)	Proteasome_DEG_Cln1	!	Cln1_[(scf)]-{Ub}	Mendenhall and Hodge (1998)
775	Mendenhall and Hodge (1998)	Proteasome_DEG_Cln2	!	Cln2_[(scf)]-{Ub}	Mendenhall and Hodge (1998)
776	Yaglom *et al.* (1995)	Proteasome_DEG_Cln3	!	Cln3_[(scf)]-{Ub}	Enserink and Kolodner (2010)
777	Lu *et al.* (2014)	Proteasome_DEG_Dbf4	!	Dbf4-{Ub}	Lu *et al.* (2014)
778	Blondel *et al.* (2000)	Proteasome_DEG_Far1	!	Far1_[(scf)]-{Ub}	Blondel *et al.* (2000)
779	Malo *et al.* (2016)	Proteasome_DEG_Fkh1	!	Fkh1_[(apc)]-{Ub}	Malo *et al.* (2016)
780	Malo *et al.* (2016); Hypothesis	Proteasome_DEG_Fkh2	!	Fkh2_[(apc)]-{Ub}	Malo *et al.* (2016), Hypothesis
781	Landry *et al.* (2014)	Proteasome_DEG_Hcm1			
782	Crasta *et al.* (2006)	Proteasome_DEG_Kip1	!	Kip1-{Ub}	Crasta *et al.* (2006)
783	Ostapenko *et al.* (2012)	Proteasome_DEG_Mps1	!	Mps1_[(apc)]-{Ub}	Ostapenko *et al.* (2012)
784	Haase and Wittenberg (2014)	Proteasome_DEG_Ndd1	!	Ndd1-{Ub}	Edenberg *et al.* (2015)
785	Ostapenko and Solomon (2011)	Proteasome_DEG_Nrm1	!	Nrm1_[(apc)]-{Ub}	Ostapenko and Solomon (2011)
786	Hernández-Ortega *et al.* (2013)	Proteasome_DEG_Pcl1	!	Pcl1_[(dma)]-{Ub}	Hernández-Ortega *et al.* (2013)
787	Hernández-Ortega *et al.* (2013); Hypothesis	Proteasome_DEG_Pcl2	!	Pcl2_[(dma)]-{Ub}	Hernández-Ortega *et al.* (2013); Hypothesis
788	Hernández-Ortega *et al.* (2013); Hypothesis	Proteasome_DEG_Pcl9	!	Pcl9_[(dma)]-{Ub}	Hernández-Ortega *et al.* (2013); Hypothesis; Gap-filling step 1

Table A.4 – *Continued from previous page*

	Reference	Reaction	C	Statement	Reference
789	Hilioti *et al.* (2001)	Proteasome_DEG_Pds1	!	Pds1-{Ub}	Hilioti *et al.* (2001)
790	Hypothesis	Proteasome_DEG_Rad53			
791	Uhlmann *et al.* (1999)	Proteasome_DEG_Scc1	!	Scc1_[(esp1)]-{Truncated}	Uhlmann *et al.* (1999)
792	Enserink and Kolodner (2010)	Proteasome_DEG_Sic1	!	Sic1_[(scf)]-{Ub}	Enserink and Kolodner (2010)
793	Hypothesis	Proteasome_DEG_Spc42	x	<Spc42Crystal>	Bullitt *et al.* (1997); Hypothesis
794	Howell and Lew (2012)	Proteasome_DEG_Swe1	!	Swe1_[(scf)]-{Ub}	Howell and Lew (2012)
795	Ostapenko and Solomon (2011)	Proteasome_DEG_Yhp1	!	Yhp1-{Ub}	Haase and Wittenberg (2014)
796	Haase and Wittenberg (2014)	Proteasome_DEG_Yox1	!	Yox1-{Ub}	Haase and Wittenberg (2014)
797	Cheng *et al.* (1999)	Ptc2_P-_Cdc28_[Tloop(T169)]			
798	Cheng *et al.* (1999)	Ptc3_P-_Cdc28_[Tloop(T169)]			
799	Chen *et al.* (2013)	Rad53_P+_Dbf4_[(rad53)]	!	Rad53_[(SCD1sites)]-{P}	Chen *et al.* (2007b); Hypothesis
800	Bashkirov *et al.* (2003), Chen *et al.* (2007b)	Rad53_P+_Dun1_[(T380)]	!	Rad53_[(SCD1sites)]-{P}	Chen *et al.* (2007b)
801	Yelamanchi *et al.* (2014)	Rad53_P+_Ndd1_[(rad53)]	!	Rad53_[(SCD1sites)]-{P}	Chen *et al.* (2007b); Hypothesis
802	Travesa *et al.* (2012)	Rad53_P+_Nrm1_[(rad53)]	!	Rad53_[(SCD1sites)]-{P}	Chen *et al.* (2007b); Hypothesis
803	Hypothesis	Rad53PPT_P-_Rad53_[(SCD1sites)]			
804	Lopez-Mosqueda *et al.* (2010)	Rad53_P+_Sld3_[(rad53)]	!	Rad53_[(SCD1sites)]-{P}	Chen *et al.* (2007b); Hypothesis
805	Brill and Bastin-Shanower (1998)	Rfa1_[C]_i_ssDNA_[rfa1]	!	<RPA>	Iftode *et al.* (1999); Hypothesis
806	Brill and Bastin-Shanower (1998)	Rfa1_[C]_i_ssDNA_[rfa1]	!	[ssDNA]	Iftode *et al.* (1999)
807	Hypothesis	Rfa1_[rfa2]_ppi_Rfa2_[rfa1]			
808	Hegnauer *et al.* (2012)	Rfa1_[sgs1]_ppi_Sgs1_[rfa1]	!	<RPAssDNA>	Hegnauer *et al.* (2012)
809	Philipova *et al.* (1996); Brill and Bastin-Shanower (1998)	Rfa2_[D]_i_ssDNA_[rfa2]	!	<RPA>	Iftode *et al.* (1999); Hypothesis
810	Philipova *et al.* (1996); Brill and Bastin-Shanower (1998)	Rfa2_[D]_i_ssDNA_[rfa2]	!	[ssDNA]	Iftode *et al.* (1999)
811	Hypothesis	Rfa2_[rfa3]_ppi_Rfa3_[rfa2]			
812	Chilkova *et al.* (2007); Hypothesis	RFC_[dna]_i_ssDNA_[rfc]	!	[ssdsDNAjunctions]	Chilkova *et al.* (2007); Hypothesis
813	Bi and Park (2012)	Rga1_GAP_Cdc42_[(act)]	!	Rga1_[(res1)]-{0}	Sopko *et al.* (2007); Hypothesis
814	Bi and Park (2012)	Rga2_GAP_Cdc42_[(act)]	!	Rga2_[(res1)]-{0}	Howell and Lew (2012); Hypothesis
815	Abe *et al.* (2003); Hypothesis	Rho1_[rom2]_ppi_Rom2_[rho1]	!	<Exocytosis>	Abe *et al.* (2003), Roumanie *et al.* (2005), He *et al.* (2007); Hypothesis
816	Guo *et al.* (2001)	Rho1_[sec3]_ppi_Sec3_[N]			
817	SGD	Ribo_TRSL_Ace2mRNA			
818	SGD	Ribo_TRSL_Acm1mRNA			
819	SGD	Ribo_TRSL_Ase1mRNA			
820	SGD	Ribo_TRSL_Cdc20mRNA			
821	SGD	Ribo_TRSL_Cdc5mRNA			
822	SGD	Ribo_TRSL_Cdc6mRNA			
823	SGD	Ribo_TRSL_Cin8mRNA			
824	SGD	Ribo_TRSL_Clb1mRNA			
825	SGD	Ribo_TRSL_Clb2mRNA			
826	SGD	Ribo_TRSL_Clb3mRNA			
827	SGD	Ribo_TRSL_Clb4mRNA			
828	SGD	Ribo_TRSL_Clb5mRNA			
829	SGD	Ribo_TRSL_Clb6mRNA			
830	SGD	Ribo_TRSL_Cln1mRNA			
831	SGD	Ribo_TRSL_Cln2mRNA			
832	SGD	Ribo_TRSL_Cln3mRNA	!	[NutrientAvailabilityCheck]	Barbet *et al.* (1996)
833	SGD	Ribo_TRSL_Dbf4mRNA			
834	SGD	Ribo_TRSL_Far1mRNA			
835	SGD	Ribo_TRSL_Fkh1mRNA			
836	SGD	Ribo_TRSL_Fkh2mRNA			
837	SGD	Ribo_TRSL_Hcm1mRNA			
838	SGD	Ribo_TRSL_Kip1mRNA			

Table A.4 – *Continued from previous page*

	Reference	Reaction	C	Statement	Reference
839	SGD	Ribo_TRSL_Mcm2mRNA			
840	SGD	Ribo_TRSL_Mcm3mRNA			
841	SGD	Ribo_TRSL_Mcm4mRNA			
842	SGD	Ribo_TRSL_Mcm5mRNA			
843	SGD	Ribo_TRSL_Mcm6mRNA			
844	SGD	Ribo_TRSL_Mcm7mRNA			
845	SGD	Ribo_TRSL_Mps1mRNA			
846	SGD	Ribo_TRSL_Ndd1mRNA			
847	SGD	Ribo_TRSL_Nrm1mRNA			
848	SGD	Ribo_TRSL_Pcl1mRNA			
849	SGD	Ribo_TRSL_Pcl2mRNA			
850	SGD	Ribo_TRSL_Pcl9mRNA			
851	SGD	Ribo_TRSL_Pds1mRNA			
852	SGD	Ribo_TRSL_Rad53mRNA			
853	SGD	Ribo_TRSL_Scc1mRNA			
854	SGD	Ribo_TRSL_Sic1mRNA			
855	SGD	Ribo_TRSL_Spc42mRNA			
856	SGD	Ribo_TRSL_Swe1mRNA			
857	SGD	Ribo_TRSL_Swi4mRNA			
858	SGD	Ribo_TRSL_Swi5mRNA			
859	SGD	Ribo_TRSL_Yhp1mRNA			
860	SGD	Ribo_TRSL_Yox1mRNA			
861	Zhao *et al.* (1998)	Rnr1_[sml1]_ppi_Sml1_[rnr1]	x	Sml1_[(dun1)]-{P}	Pardo *et al.* (2017)
862	Philip and Levin (2001)	Rom2_[cwi]_ppi_Slg1_[cytoplasmic]			
863	Ozaki *et al.* (1996)	Rom2_GEF_Rho1_[(act)]	!	<Rho1MembraneTargeting>	Philip and Levin (2001), Abe *et al.* (2003)
864	Audhya and Emr (2002)	Rom2_[PH]_i_PI	!	<PI45P2>	Audhya and Emr (2002)
865	Takahata *et al.* (2009); Hypothesis	Rpd3_[whi5]_ppi_Whi5_[hdac]	K-	Whi5_[(pho85)]-{P}	Wagner *et al.* (2009); Gap-filling step 1
866	Takahata *et al.* (2009); Hypothesis	Rpd3_[whi5]_ppi_Whi5_[hdac]	x	<Whi5PhosCombinations>	Wagner *et al.* (2009)
867	Riedel *et al.* (2006); Peplowska *et al.* (2014)	Rts1_[sgo1]_ppi_Sgo1_[N]	!	Sgo1_[DBD]–Centromere_[sgo1]	Peplowska *et al.* (2014)
868	Jiang and Broach (1999)	Rts1_[tpd3]_ppi_Tpd3_[regulatory]			
869	Foti *et al.* (2001)	Sac1_P-_PI_[(4)]			
870	Fernius *et al.* (2013); Hypothesis	Scc1_[scc2]_ppi_Scc2_[scc1]			
871	Marston (2014)	Scc1_[smc1]_ppi_Smc1_[NBD]	!	<CohesinLoading>	Marston (2014)
872	Marston (2014)	Scc1_[smc3]_ppi_Smc3_[NBD]	!	<CohesinLoading>	Marston (2014)
873	Hinshaw *et al.* (2015)	Scc2_[N]_ppi_Scc4_[tpr]			
874	Hinshaw *et al.* (2015)	Scc4_[DBD]_i_Centromere_[CohesinLoading]			
875	Enserink and Kolodner (2010)	Sec2_GEF_Sec4_[(act)]			
876	He *et al.* (2007)	Sec3_[Nlipidbinding]_i_PI	!	<PI45P2>	He *et al.* (2007)
877	Rüthnick and Schiebel (2016)	Sfi1_[C]_ppi_Sfi1_[C]	x	<Cdc28Phosphorylation>	Elserafy *et al.* (2014)
878	Rüthnick and Schiebel (2016)	Sfi1_[C]_ppi_Sfi1_[C]	x	<Cdc5Phosphorylation>	Elserafy *et al.* (2014)
879	Rüthnick and Schiebel (2016)	Sfi1_[N]_ppi_Spc42_[cp]	!	[SatelliteAssembly]	Rüthnick and Schiebel (2016)
880	Rüthnick and Schiebel (2016)	Sfi1_[N]_ppi_Spc42_[cp]	!	<Spc42Phosphorylation>	Jaspersen *et al.* (2004); Hypothesis
881	Elserafy *et al.* (2014); Hypothesis	Sfi1PPT_P-_Sfi1_[C(S826)]			
882	Elserafy *et al.* (2014); Hypothesis	Sfi1PPT_P-_Sfi1_[C(T866)]			
883	Elserafy *et al.* (2014); Hypothesis	Sfi1PPT_P-_Sfi1_[C(T876)]			
884	Peplowska *et al.* (2014)	Sgo1_[DBD]_i_Centromere_[sgo1]			
885	Hypothesis	Sld3PPT_P-_Sld3_[(rad53)]			
886	Marston (2014)	Smc1_[smc3]_ppi_Smc3_[smc1]			
887	Peplowska *et al.* (2014)	Smc2_[sgo1]_ppi_Sgo1_[smc2]	!	Rts1_[sgo1]–Sgo1_[N]	Peplowska *et al.* (2014)
888	Marston (2014)	Smc2_[smc4]_ppi_Smc4_[smc2]			
889	Hypothesis	Sml1PPT_P-_Sml1_[(dun1)]			
890	Hypothesis	Spc110PPT_P-_Spc110_[(S60)]			
891	Hypothesis	Spc110PPT_P-_Spc110_[(T68)]			

Table A.4 – *Continued from previous page*

	Reference	Reaction	C	Statement	Reference
892	Biggins (2013)	Spc24_[spc25]_ppi_Spc25_[spc24]			
893	Elliott *et al.* (1999)	Spc29_[spc110]_ppi_Spc110_[spc29]	!	Cmd1_[spc110]–Spc110_[C]	Elliott *et al.* (1999); Hypothesis
894	Elliott *et al.* (1999)	Spc29_[spc110]_ppi_Spc110_[spc29]	!	Spc29_[spc42]–Spc42_[spc29]	Elliott *et al.* (1999); Hypothesis
895	Fu *et al.* (2015)	Spc29_[spc42]_ppi_Spc42_[spc29]	!	[DuplicationPlaque]	Fu *et al.* (2015)
896	Bullitt *et al.* (1997)	Spc42_[C]_ppi_Spc42_[N]	!	Sfi1_[N]–Spc42_[cp]	Fu *et al.* (2015)
897	Erlemann *et al.* (2012)	Spc72_[N]_ppi_Spc98_[spc72]	!	Nud1_[spc72]–Spc72_[nud1]	Fu *et al.* (2015)
898	Erlemann *et al.* (2012)	Spc72_[spc97]_ppi_Spc97_[spc72]	!	Nud1_[spc72]–Spc72_[nud1]	Fu *et al.* (2015)
899	Winey and Bloom (2012)	Spc97_[spc110]_ppi_Spc110_[spc97]	!	Spc29_[spc110]–Spc110_[spc29]	Lyon *et al.* (2016)
900	Winey and Bloom (2012)	Spc98_[spc110]_ppi_Spc110_[N]	!	<Spc110Phos>	Lin *et al.* (2014); Hypothesis
901	Winey and Bloom (2012)	Spc98_[spc110]_ppi_Spc110_[N]	!	Spc29_[spc110]–Spc110_[spc29]	Lyon *et al.* (2016)
902	Winey and Bloom (2012)	Spc98_[spc110]_ppi_Spc110_[N]	!	<yTubulinSmallComplex>	Winey and Bloom (2012)
903	Winey and Bloom (2012)	Spc97_[spc]_ppi_Spc98_[spc]			
904	Fu *et al.* (2015)	Spc97_[tub4]_ppi_Tub4_[spc]			
905	Winey and Bloom (2012)	Spc98_[spc110]_ppi_Spc110_[N]			
906	Fu *et al.* (2015)	Spc98_[tub4]_ppi_Tub4_[spc]			
907	Caplan *et al.* (1992)	Ssa1_[ydj1]_ppi_Ydj1_[ssa]			
908	Caplan *et al.* (1992)	Ssa2_[ydj1]_ppi_Ydj1_[ssa]			
909	Yoshida *et al.* (1994)	Sst4_P+_PI_[(4)]			
910	Costanzo *et al.* (2003)	Stb1_[N]_ppi_Swi6_[stb1]	K-	Stb1_[(cdc28)]-{P}	Costanzo *et al.* (2003)
911	Howell and Lew (2012)	Swe1_P+_Cdc28_[(Y19)]			
912	Hypothesis	Swe1PPT_P-_Swe1_[Cdc5Sites(HP)]			
913	Hypothesis	Swe1PPT_P-_Swe1_[(cla4)]			
914	Hypothesis	Swe1PPT_P-_Swe1_[(S385)]			
915	Bean *et al.* (2005); Hypothesis	Swi4_[scb]_BIND_Cln1Gene_[scb]	x	Swi4_[(cdc28)]-{P}	Koch *et al.* (1996); Hypothesis
916	Bean *et al.* (2005); Hypothesis	Swi4_[scb]_BIND_Cln2Gene_[scb]	x	Swi4_[(cdc28)]-{P}	Koch *et al.* (1996); Hypothesis
917	Horak *et al.* (2002)	Swi4_[scb]_BIND_Hcm1Gene_[scb]	x	Swi4_[(cdc28)]-{P}	Koch *et al.* (1996); Hypothesis
918	Bean *et al.* (2005); Hypothesis	Swi4_[scb]_BIND_Pcl1Gene_[scb]	x	Swi4_[(cdc28)]-{P}	Koch *et al.* (1996); Hypothesis
919	Bean *et al.* (2005); Hypothesis	Swi4_[scb]_BIND_Pcl2Gene_[scb]	x	Swi4_[(cdc28)]-{P}	Koch *et al.* (1996); Hypothesis
920	Sia *et al.* (1996); Hypothesis	Swi4_[scb]_BIND_Swe1Gene_[scb]	x	Swi4_[(cdc28)]-{P}	Koch *et al.* (1996); Hypothesis
921	Bean *et al.* (2005); Hypothesis	Swi4_[scb]_BIND_Yox1Gene_[scb]	x	Swi4_[(cdc28)]-{P}	Koch *et al.* (1996); Hypothesis
922	Enserink and Kolodner (2010)	Swi4_[swi6]_ppi_Swi6_[swi4]			
923	Tennyson *et al.* (1998)	Swi5_[PBD]_BIND_Pcl9Gene_[pcl9]	x	Swi5_[NLS(cdc28)]-{P}	Moll *et al.* (1991); Hypothesis
924	Haase and Wittenberg (2014)	Swi5_[PBD]_BIND_Sic1Gene_[sic1]	x	Swi5_[NLS(cdc28)]-{P}	Moll *et al.* (1991); Hypothesis
925	Travesa *et al.* (2013)	Swi6_[whi5]_ppi_Whi5_[swi6]	K+	Swi4_[swi6]–Swi6_[swi4]	Travesa *et al.* (2013); Hypothesis
926	Travesa *et al.* (2013)	Swi6_[whi5]_ppi_Whi5_[swi6]	x	<Whi5HyperPhosOrSwi6Phosphorylation>	Wagner *et al.* (2009)
927	Geymonat *et al.* (2009)	Tem1_GEF_Tem1_[(act)]			
928	Winey and Bloom (2012)	Tub1_[tub2]_ppi_Tub2_[tub]	x	[Nocodazole]	Erlemann *et al.* (2012)
929	Nogales *et al.* (1999)	Tub1_[tub4]_ppi_Tub4_[tub1]			
930	Winey and Bloom (2012)	Tub2_[tub]_ppi_Tub3_[tub2]	x	[Nocodazole]	Erlemann *et al.* (2012)
931	Nogales *et al.* (1999)	Tub3_[tub4]_ppi_Tub4_[tub3]			
932	Schmelzle *et al.* (2002)	Tus1_GEF_Rho1_[(act)]	!	Tus1_[(cdc28)]-{P}	Kono *et al.* (2008)
933	Schmelzle *et al.* (2002)	Tus1_GEF_Rho1_[(act)]	!	Tus1_[(cdc5)]-{P}	Yoshida *et al.* (2006)
934	Hypothesis	Tus1PPT_P-_Tus1_[(cdc5)]			

Table A.5. *Macroscopic reactions skeleton rules.* The skeleton rules of the macroscopic reactions created for the CC-CNW.

Reaction name	Skeleton rule
DNA licensing	$y%#$y%-{0} -> $y%#$y%-{LIC}
DNA replication initiation	$y%#$y%-{LIC} -> $y%#$y%-{replicating}
DNA replication termination	$y%#$y%-{replicating} -> $y%#$y%-{replicated}
DNA segregation	$y%#$y%-{replicated} -> $y%#$y%-{segregated}
SPB satellite initiation	$y%#$y%-{0} -> $y%#$y%-{SAT}
SPB duplication plaque initiation	$y%#$y%-{SAT} -> $y%#$y%-{DUP}
SPB duplication	$y%#$y%-{DUP} -> $y%#$y%-{SPB}
SPB separation initiation	$y%#$y%-{SPB} -> $y%#$y%-{separated}
SPB bipolar initiation	$y%#$y%-{separated} -> $y%#$y%-{bipolar}
SPB daughter positioning initiation	$y%#$y%-{bipolar} -> $y%#$y%-{daughter}
Bud emergence initiation	$y%#$y%-{0} -> $y%#$y%-{emerged}
Bud growth	$y%#$y%-{emerged} -> $y%#$y%-{growth}
Cytokinesis	$x%#$x%_[(bud)]-{growth} + $x%#$x%_[(SPB)]-{daughter} + $x%#$x%_[(DNA)]-{segregated} -> $x%#$x%_[(DNA)]-{0} + $x%#$x%_[(SPB)]-{0} + $x%#$x%_[(bud)]-{0}

A.2 Network motifs

A.2.1 *Transcriptional clusters*

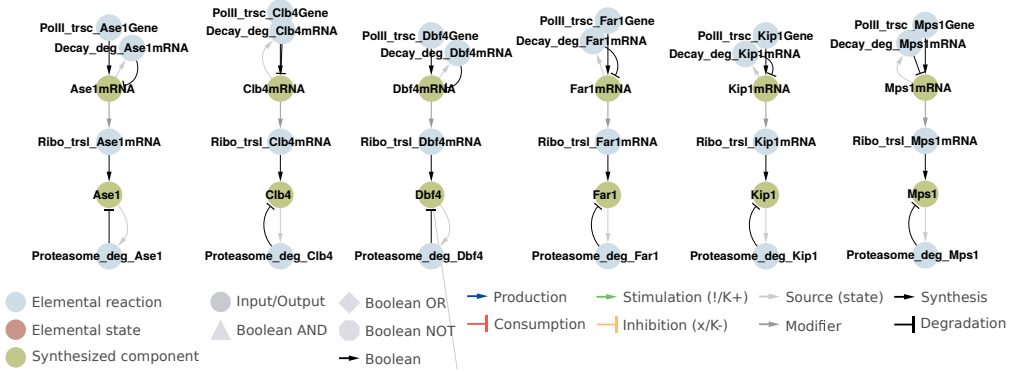

Figure A.1. *Unregulated genes.* These genes are transcribed in the CC-CNW but, with the exception of Far1, lack empirically verified transcriptional regulation.

A.2.2 *Unconnected states*

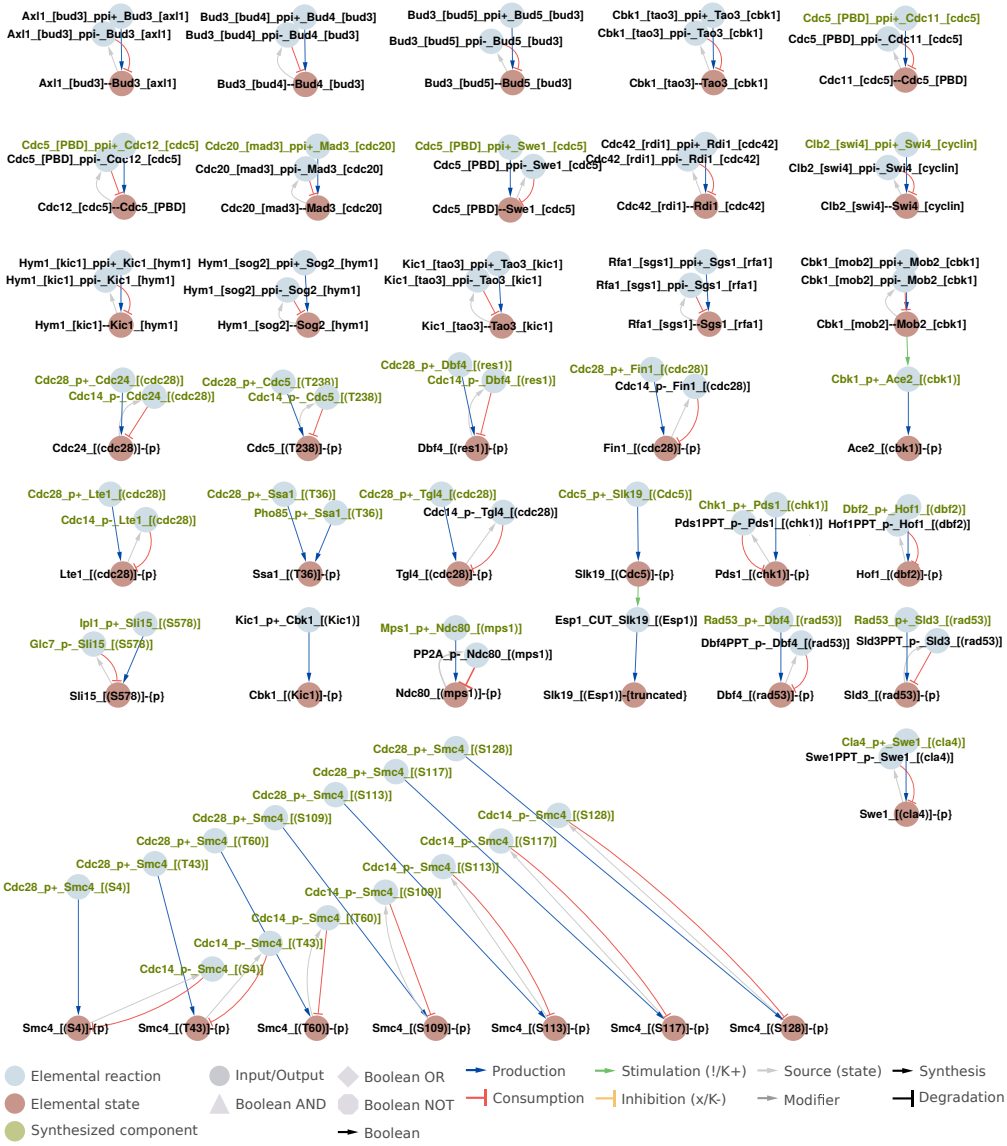

Figure A.2. *Unconnected states.* The states resulting from these reactions are not involved in any regulation, hence, they are physiologically irrelevant in the CC-CNW. However, in the future, these states could be connected to the CC-CNW, when their physiological relevance is discovered.

A.3 Kaizu model in rxncon language

This table lists the translation of the Kaizu model into elemental reactions in rxncon language. For reference, the original reaction numbers from Kaizu *et al.* (2010) are listed next to the translated reactions. In some cases, complexes were used in the original Kaizu model, but complex topology was not described. In these cases, elemental reactions were added and appended to the original reactions.

Table A.6. The translation of the Kaizu model (Kaizu *et al.*, 2010) into rxncon language. The reference to the original Kaizu model reactions referenced in the reference column. Reactions that were added are indicated.

	Reaction	Reference	Comment
1	Yox1_BIND_ECB_[YOX]	re1	
2	Nop7_BIND_ECB_[YOX]	re2	
3	PolII_TRSC_Swi4	re14	
4	PolII_TRSC_Cln3	re15	
5	PolII_TRSC_Cdc6	re16	
6	Fkh2_BIND_Mcm1Gene_[Fkh1Fkh2bs]	re20	
7	Cdc28_P+_Fkh2_[(S683)]	re21	
8	Cdc28_P+_Fkh2_[(T697)]	re21	
9	Fkh2_ppi_Ndd1	re22	
10	PolII_TRSC_Swi5	re31	
11	PolII_TRSC_Clb1	re32	
12	PolII_TRSC_Clb2	re32	
13	PolII_TRSC_Ace2	re33	
14	PolII_TRSC_Cdc20	re34	
15	Cdc28_P+_Ndd1_[(T319)]	re35	
16	Cdc5_ppi_Ndd1	re36	
17	PolII_TRSC_Spc110	re37	
18	Cdc28_P+_Swi5_[(S522)]	re39	
19	Cdc28_P+_Swi5_[(S646)]	re39	
20	Cdc28_P+_Swi5_[(S664)]	re39	
21	Cdc14_P-_Swi5_[(S522)]	re40	
22	Cdc14_P-_Swi5_[(S646)]	re40	
23	Cdc14_P-_Swi5_[(S664)]	re40	
24	Ssn3_P+_Swi5_[(8ST)]	re42	
25	Cdc4_Ub+_Swi5_[(rs5)]	re43	
26	Proteasome_DEG_Swi5	re45	
27	PolII_TRSC_Sic1	re46	
28	PolII_TRSC_Cts1	re47	
29	Fkh2_BIND_Ace2onlypromoter_[Fkh1Fkh2]	re48	
30	Ace2_BIND_Ace2onlypromoter_[Swi5Ace2]	re49	
31	Swi5_BIND_Ace2onlypromoter_[Swi5Ace2]	re50	
32	Cdc28_P+_Sic1_[(T5)]	re52	
33	Cdc28_P+_Sic1_[(T33)]	re52	
34	Cdc28_P+_Sic1_[(S76)]	re52	
35	Cdc28_P+_Sic1_[(T2)]	re52	
36	Cdc28_P+_Sic1_[(T45)]	re52	
37	Cdc28_P+_Sic1_[(S69)]	re52	
38	Cdc28_P+_Sic1_[(S80)]	re52	
39	Cdc28_P+_Sic1_[(S191)]	re52	
40	Cdc28_P+_Sic1_[(T173)]	re52	T173 modification declared as unknown; changed to P+
41	Ime2_P+_Sic1_[(T5)]	re52	
42	Ime2_P+_Sic1_[(T33)]	re52	
43	Ime2_P+_Sic1_[(S76)]	re52	
44	Ime2_P+_Sic1_[(T2)]	re52	
45	Ime2_P+_Sic1_[(T45)]	re52	
46	Ime2_P+_Sic1_[(S69)]	re52	
47	Ime2_P+_Sic1_[(S80)]	re52	
48	Ime2_P+_Sic1_[(S191)]	re52	
49	Ime2_P+_Sic1_[(T173)]	re52	T173 modification declared as unknown; changed to P+
50	Cdc14_P-_Sic1_[(T5)]	re53	
51	Cdc14_P-_Sic1_[(T33)]	re53	
52	Cdc14_P-_Sic1_[(S76)]	re53	
53	Cdc14_P-_Sic1_[(T2)]	re53	
54	Cdc14_P-_Sic1_[(T45)]	re53	
55	Cdc14_P-_Sic1_[(S69)]	re53	
56	Cdc14_P-_Sic1_[(S80)]	re53	
57	Cdc14_P-_Sic1_[(S191)]	re53	

Table A.6 – *Continued from previous page*

	Reaction	Reference	Comment
58	Cdc14_P-_Sic1_[(T173)]	re53	T173 modification declared as unknown; changed to P-
59	Cdc4_Ub+_Sic1_[(rs2)]	re54	
60	Proteasome_DEG_Sic1	re55	
61	Cdc28_P+_Ace2_[(T575)]	re56	
62	Cdc28_P+_Ace2_[(S701)]	re56	
63	Cdc28_P+_Ace2_[(S714)]	re56	
64	Ace2_AP-_Ace2_[(T575)]	re57	
65	Ace2_AP-_Ace2_[(S701)]	re57	
66	Ace2_AP-_Ace2_[(S714)]	re57	
67	PolII_TRSC_Egt2	re60	
68	Cbk1_ppi_Mob2	re61	
69	Cdc28_P+_Dbf2_[(S374)]	re62	
70	Cdc28_P+_Dbf2_[(T544)]	re62	
71	Cdc15_P+_Dbf2_[(S374)]	re62	
72	Cdc15_P+_Dbf2_[(T544)]	re62	
73	Dbf2_ppi_Mob1	re63	
74	Swi5_BIND_Hopromoters_[Swi5Ace2bs]	re65	
75	Pho85_P+_Swi5_[(8ST)]	re71	
76	Ash1_BIND_Hopromoters_[URS2]	re72	
77	Swi4_ppi_Swi6	re74	
78	Mbp1_ppi_Swi6	re75	
79	PolII_TRSC_Cln1	re77	
80	PolII_TRSC_Cln2	re78	
81	PolII_TRSC_Hogenes	re79	
82	Swi4_BIND_Hopromoters_[URS2]	re84	
83	Cdc28_P+_Swi4_[(rs1)]	re85	Declared as unknown; changed to P+
84	Stb1_ppi_Swi6	re87;re89;re123	Stb1 binding not declared in map; added (re89)
85	Cdc28_P+_Stb1_[(rs1)]	re88	
86	Swi6_ppi_Whi5	re89	
87	Cdc28_P+_Whi5_[(T41)]	re91	
88	Cdc28_P+_Whi5_[(S59)]	re91	
89	Cdc28_P+_Whi5_[(S62)]	re91	
90	Cdc28_P+_Whi5_[(S155)]	re91	
91	Cdc28_P+_Whi5_[(S157)]	re91	
92	Cdc28_P+_Whi5_[(S161)]	re91	
93	Cdc28_P+_Whi5_[(S262)]	re91	
94	PolII_TRSC_Nrm1	re93	
95	Nrm1_ppi_Swi6	re94	
96	Rad53_P+_Swi6_[(S547)]	re95	
97	Cdc28_P+_Swi6_[(S160)]	re97	
98	Fus3_P+_Far1_[(T306)]	re102	
99	Fus3_P+_Far1_[(T63)]	re102	
100	Cdc14_P-_Swi6_[(S160)]	re103	
101	Hrr25_P+_Swi6_[(rs3)]	re105	
102	PolII_TRSC_Fks2	re107	
103	Slt2_ppi_Swi4	re108	
104	Swi4_ppi_Swi6	re110	
105	PolII_TRSC_Pcl1	re111	
106	PolII_TRSC_Pcl2	re111	
107	Msa1_ppi_Swi6	re115; re116	Add domain name for mutually exclusive binding?
108	Msa2_ppi_Swi6	re115; re116	Add domain name for mutually exclusive binding?
109	Mbp1_ppi_Skn7	re118	
110	PolII_TRSC_Clb5	re119	
111	Slt2_P+_Swi4_[(rs2)]	re121	
112	Slt2_P+_Swi6_[(rs4)]	re122	
113	Mbp1_BIND_MCB	re124	
114	Mcm1_BIND_Mcm1Gene_[Mcm1bs]	re131	
115	Rom2_GEF_Rho1_[(rs1)]	re159	Residue name introduced
116	Tus1_GEF_Rho1_[(rs1)]	re159	Residue name introduced
117	Rho1_aGAP_Rho1_[(rs1)]	re162	Residue name introduced
118	PolII_TRSC_Exg1	re187	
119	Rga2_GEF_Cdc42_[(rs1)]	re215	Residue name introduced
120	Cdc42_ppi_Ste20	re216;re371	
121	Cdc28_P+_Ste20_[(rs1)]	re223	
122	Cdc28_P+_Dig1_[(rs1)]	re224	
123	Cdc28_P+_Dig2_[(rs1)]	re224	
124	Cdc28_P+_Far1_[(S87)]	re225	
125	Cdc4_Ub+_Far1_[(rs3)]	re226	
126	Proteasome_DEG_Far1	re227	
127	Cdc24_ppi_Far1	re228	
128	Cdc28_ppi_Far1	re233; re234	Same as re234; Cdc28 in different complexes
129	Proteasome_DEG_Cln3	re241	
130	Cdc28_P+_Cln3_[(S468)]	re242	
131	Cln3_ppi_Ydj1	re243	
132	Cln3_ppi_Ssa1_[br]	re246	
133	Cln3_ppi_Ssa2	re246	
134	Ribo_TRSL_Cln3	re248	

Table A.6 – *Continued from previous page*

	Reaction	Reference	Comment
135	Cdc28_ppi-_Whi3	re251	
136	Cdc28_ppi_Cln3	re252	
137	Cdc28_ppi_Whi3	re253	
138	mCLN3_i_Whi3	re254	
139	Cdc28_P+_Cln1_[(4T3S)]	re260	
140	Cdc28_P+_Cln2_[(4T3S)]	re260	
141	Proteasome_DEG_Cln1	re263	
142	Proteasome_DEG_Cln2	re263	
143	Cdc14_P-_Cln1_[(4T3S)]	re265	
144	Cdc14_P-_Cln2_[(4T3S)]	re265	
145	Grr1_ppi_Skp1	re267	
146	Cka1_P+_Cdc34_[(S207)]	re268	
147	Cka1_P+_Cdc34_[(S216)]	re268	
148	Cka1_P+_Cdc34_[(S130)]	re268	
149	Cka1_P+_Cdc34_[(S2167)]	re268	
150	Cka2_P+_Cdc34_[(S207)]	re268	
151	Cka2_P+_Cdc34_[(S216)]	re268	
152	Cka2_P+_Cdc34_[(S130)]	re268	
153	Cka2_P+_Cdc34_[(S2167)]	re268	
154	Cdc53_ppi_Skp1	re269	
155	Hrt1_ppi_Cdc53	re269	
156	Cdc34_ppi_Cdc53	re269	
157	Cdc34_ppi_Hrt1	re269	
158	Cdc4_ppi_Skp1	re271	
159	Cdc28_P+_Clb6_[(S6)]	re272	
160	Cdc28_P+_Clb6_[(T39)]	re272	
161	Cdc28_P+_Clb6_[(S147)]	re272	
162	Cdc34_Ub+_Cln3_[(rs2)]	re275	
163	Cln3_ppi-_Ydj1	re276	
164	Cdc28_ppi-_Cln3	re276	
165	Cdc34_Ub+_Cln1_[(rs1)]	re277	
166	Cdc34_Ub+_Cln2_[(rs1)]	re277	
167	Cdc28_ppi-_Cln1	re278	
168	Cdc28_ppi-_Cln2	re278	
169	Cdc34_Ub+_Clb6_[(rs4)]	re279	
170	Cdc28_ppi-_Clb6	re280	
171	Proteasome_DEG_Clb6	re281	
172	Cka1_P+_Sic1_[(S201)]	re282	
173	Cka2_P+_Sic1_[(S201)]	re282	
174	Cdc28_ppi_Sic1	re283;re291	
175	Hog1_P+_Sic1_[(T173)]	re284	
176	Cdc28_P+_Cdc6_[(T7)]	re285	
177	Cdc28_P+_Cdc6_[(T23)]	re285	
178	Cdc28_P+_Cdc6_[(T39)]	re285	
179	Cdc28_P+_Cdc6_[(S43)]	re285	
180	Ime2_P+_Cdc6_[(T7)]	re285	
181	Ime2_P+_Cdc6_[(T23)]	re285	
182	Ime2_P+_Cdc6_[(T39)]	re285	
183	Ime2_P+_Cdc6_[(S43)]	re285	
184	Cdc14_P-_Cdc6_[(T7)]	re286	
185	Cdc14_P-_Cdc6_[(T23)]	re286	
186	Cdc14_P-_Cdc6_[(T39)]	re286	
187	Cdc14_P-_Cdc6_[(S43)]	re286	
188	Cdc4_Ub+_Cdc6_[(rs1)]	re287	Residue name introduced
189	Proteasome_DEG_Cdc6	re288	
190	Cdc28_ppi_Cdc6	re289;re290	
191	Cdc6_ppi_Clb3	re292	
192	Cdc6_ppi_Clb4	re292	
193	Cak1_P+_Cdc28_[(T169)]	re295	
194	Ime2_P+_Cdh1_[(rs1)]	re297	
195	Cdc28_ppi_Clb6	re298	
196	Cdc28_ppi_Clb5	re299	
197	Cdc28_ppi_Clb1	re300	
198	Cdc28_ppi_Clb2	re300	
199	Cdc28_ppi_Cln1	re301	
200	Cdc28_ppi_Cln2	re301	
201	Cdc28_ppi_Cks1	re302	
202	Dia2_ppi_Skp1	re313	
203	Cdc42_ppi_Rdi1	re366	
204	Cdc24_GEF_Cdc42_[(rs1)]	re369	Residue name introduced
205	Bem1_ppi_Cdc42	re371;re376	
206	Cdc24_ppi_Cdc42	re372	
207	Bud5_GEF_Rsr1_[(rs1)]	re373	Residue name introduced
208	Bud2_GAP_Rsr1_[(rs1)]	re375	Residue name introduced
209	Cdc24_ppi_Cdc42	re377	
210	Cdc24_ppi_Rsr1	re377	
211	Bem1_ppi-_Cdc42	re380	

Table A.6 – *Continued from previous page*

	Reaction	Reference	Comment
212	Cdc24_ppi-_Rsr1	re380	
213	Cdc24_ppi-_Cdc42	re380	
214	Cdc28_P+_Cdc24_[(rs1)]	re382	Residue name introduced
215	Pho85_P+_Cdc24_[(rs1)]	re382	Residue name introduced
216	Cla4_P+_Cdc24_[(rs1)]	re384	Residue name introduced
217	Cdc42_ppi_Cla4	re385	
218	Bud4_ppi_Bud5	re389	
219	Bud5_ppi_Bud8	re390	
220	Bud5_ppi_Bud9	re390	
221	PolII_TRSC_Axl1Gene	re391	
222	PolII_TRSC_Bud4Gene	re392	
223	Bni1_ppi_Cdc42	re393	
224	Met30_ppi_Skp1	re395	
225	Pph21_P-_Mih1_[(rs1)]	re396	
226	Pph22_P-_Mih1_[(rs1)]	re396	
227	Yck1_P+_Mih1_[(rs1)]	re397	
228	Yck2_P+_Mih1_[(rs1)]	re397	
229	Cka1_P+_Mih1_[(rs1)]	re397	
230	Cka2_P+_Mih1_[(rs1)]	re397	
231	Swe1_P+_Cdc28_[(Y19)]	re399	
232	Mih1_P-_Cdc28_[(Y19)]	re400; re401	
233	Swe1_P+_Cdc28_[(Y19)]	re402	
234	Cdc28_P+_Swe1_[(rs1)]	re403	
235	Pph21_P-_Swe1_[(rs1)]	re404	
236	Pph22_P-_Swe1_[(rs1)]	re404	
237	Cdc14_P-_Swe1_[(rs1)]	re404	
238	Hsl7_ppi_Swe1	re407	
239	Cdc5_P+_Swe1_[(rs1)]	re408	
240	Hsl7_ppi-_Swe1	re409	
241	Met30_Ub+_Swe1_[(rs2)]	re411	Residue name introduced
242	Proteasome_DEG_Swe1	re412	
243	Hsl1_ppi_Hsl7	re413	
244	Hsl1_P+_Hsl7_[(rs1)]	re414	
245	Cla4_P+_Swe1_[(12TS)]	re415	
246	Cdh1_Ub+_Hsl1_[(KEN775)]	re416	
247	Cdh1_Ub+_Hsl1_[(RAAL828)]	re417	
248	Proteasome_DEG_Hsl1	re418; re419	
249	Hsl1_AP+_Hsl1_[(rs1)]	re420	
250	Mck1_P+_Hsl1_[(rs1)]	re420	
251	Cna1_P-_Hsl1_[(rs1)]	re421	
252	Cna2_P-_Hsl1_[(rs1)]	re421	
253	Hog1_P+_Hsl1_[(S1220)]	re422	
254	Cdc4_Ub+_Cdc4_[(rs1)]	re423	Residue name introduced
255	Proteasome_DEG_Cdc4	re424	
256	Grr1_Ub+_Grr1_[(rs1)]	re425	Residue name introduced
257	Proteasome_DEG_Grr1	re426	
258	PolII_TRSC_Met30	re429	
259	Cla4_P+_Cdc3_[(rs1)]	re431	
260	Cla4_P+_Cdc10_[(S256)]	re432	
261	Cla4_P+_Cdc10_[(S312)]	re432	
262	Cla4_P+_Shs1_[(rs1)]	re433	
263	Gin4_P+_Shs1_[(rs1)]	re433	
264	Pph21_P-_Shs1_[(rs1)]	re434	
265	Pph22_P-_Shs1_[(rs1)]	re434	
266	Elm1_P+_Gin4_[(13TS)]	re435	
267	Ras2_aGEF_Ras2_[(rs1)]	re436	Residue name introduced
268	Ras2_aGAP_Ras2_[(rs1)]	re437	Residue name introduced
269	Lte1_ppi_Ras2	re438	
270	Cla4_P+_Lte1_[(rs1)]	re439	
271	Cdc14_P-_Lte1_[(rs1)]	re440	
272	Cla4_P+_Myo3_[(S357)]	re441	
273	Ste20_P+_Myo3_[(S357)]	re441	
274	Gin4_AP+_Gin4_[(rs2)]	re442	
275	Elm1_P+_Snf1_[(T210)]	re443	
276	Elm1_P+_Hsl1_[(T273)]	re444	
277	Ppm1_Met+_Pph21_[(L369)]	re445	
278	Ppm1_Met+_Pph22_[(L369)]	re445	
279	Pph21_AP+_Pph21_[(T364)]	re446	Low confidence
280	Pph21_AP+_Pph21_[(Y367)]	re446	Low confidence
281	Pph22_AP+_Pph22_[(T364)]	re446	Low confidence
282	Pph22_AP+_Pph22_[(Y367)]	re446	Low confidence
283	Rts1_ppi_Tpd3	re447	
284	Pph21_ppi_Tpd3	re447	
285	Pph22_ppi_Tpd3	re447	
286	Cdc55_ppi_Tpd3	re448	
287	Sap155_[br]_ppi_Sit4	re458	
288	Sap185_[br]_ppi_Sit4	re458	

Table A.6 – *Continued from previous page*

	Reaction	Reference	Comment
289	Sap190_ppi_Sit4	re458	
290	Cdc28_ppi_Clb3	re460	
291	Cdc28_ppi_Clb4	re460	
292	Pph21_ppi_Ypa2	re462	
293	Pph22_ppi_Ypa2	re462	
294	Sit4_ppi_Ypa1_[br]	re463	
295	Pph3_ppi_Ypa1	re464	
296	Cdc20_Ub+_Clb5_[(RRAL56)]	re470	
297	Proteasome_DEG_Clb5	re473	
298	Cdc28_ppi-_Clb5	re474	
299	Cdc20_Ub+_Clb1_[(RLAL25)]	re475	
300	Cdc20_Ub+_Clb2_[(RLAL25)]	re475	
301	Cdh1_Ub+_Clb1_[(KEN85)]	re476	
302	Cdh1_Ub+_Clb2_[(KEN85)]	re476	
303	Cdh1_Ub+_Clb1_[(KEN100)]	re476	
304	Cdh1_Ub+_Clb2_[(KEN100)]	re476	
305	Cdc28_ppi-_Clb1	re477;re478	
306	Cdc28_ppi-_Clb2	re477;re478	
307	Proteasome_DEG_Clb1	re479;re480	
308	Proteasome_DEG_Clb2	re479;re480	
309	Cdc28_P+_Cdc5_[(T242)]	re481	
310	Cdh1_Ub+_Cdc5_[(KEN35)]	re482	
311	Proteasome_DEG_Cdc5	re483	
312	Cdc20_Ub+_Pds1_[(RLPL85)]	re484	
313	Proteasome_DEG_Pds1	re485	
314	Cdc20_Ub+_Kip1_[(rs1)]	re487	
315	Proteasome_DEG_Kip1	re488	
316	Cdc28_P+_Cdh1_[(11ST)]	re489	
317	Cdc14_P-_Cdh1_[(11ST)]	re490	
318	Cdc28_P+_Cdc15_[(T448)]	re491	
319	Cdc28_P+_Cdc15_[(S578)]	re491	
320	Cdc28_P+_Cdc15_[(S309)]	re491	
321	Cdc28_P+_Cdc15_[(S562)]	re491	
322	Cdc28_P+_Cdc15_[(S574)]	re491	
323	Cdc28_P+_Cdc15_[(S590)]	re491	
324	Cdc28_P+_Cdc15_[(S946)]	re491	
325	Cdc14_P-_Cdc15_[(T448)]	re492	
326	Cdc14_P-_Cdc15_[(S578)]	re492	
327	Cdc14_P-_Cdc15_[(S309)]	re492	
328	Cdc14_P-_Cdc15_[(S562)]	re492	
329	Cdc14_P-_Cdc15_[(S574)]	re492	
330	Cdc14_P-_Cdc15_[(S590)]	re492	
331	Cdc14_P-_Cdc15_[(S946)]	re492	
332	Cdh1_Ub+_Ase1_[(RQLF)]	re493	
333	Proteasome_DEG_Ase1	re494	
334	Cdc20_Ub+_Dbf4_[(rs1)]	re497	
335	Proteasome_DEG_Dbf4	re498	
336	Cdc14_P-_Swi5_[(S522)]	re499	
337	Cdc14_P-_Swi5_[(S646)]	re499	
338	Cdc14_P-_Swi5_[(S664)]	re499	
339	Cdh1_Ub+_Cin8_[(KEN970)]	re502	
340	Proteasome_DEG_Cin8	re503	
341	Ras2_GEF_Tem1_[(rs1)]	re507	Residue name introduced
342	Cdc5_P+_Bfa1_[(11ST)]	re508	
343	Cdc5_P+_Bub2_[(rs1)]	re508	
344	Cdc14_P-_Bfa1_[(11ST)]	re509	
345	Cdc14_P-_Bub2_[(rs1)]	re509	
346	Bfa1_GAP_Tem1_[(rs1)]	re513	Residue name introduced
347	Chk1_P+_Pds1_[(6ST)]	re514	
348	Amn1_ppi_Tem1	re515	
349	Amn1_aUb+_Amn1_[(rs1)]	re516	
350	Proteasome_DEG_Amn1	re517	
351	Cdc28_P+_Cdc16_[(S44)]	re519	
352	Cdc28_P+_Cdc16_[(S59)]	re519	
353	Cdc28_P+_Cdc16_[(S95)]	re519	
354	Cdc28_P+_Cdc16_[(T406)]	re519	
355	Cdc28_P+_Cdc16_[(T115)]	re519	
356	Cdc28_P+_Cdc16_[(S103)]	re519	
357	Cdc28_P+_Cdc23_[(S59)]	re519	
358	Cdc28_P+_Cdc27_[(S267)]	re519	
359	Cdc28_P+_Cdc27_[(T304)]	re519	
360	Cdc28_P+_Cdc27_[(S328)]	re519	
361	Cdc28_P+_Cdc27_[(T397)]	re519	
362	Cdc28_P+_Cdc27_[(T351)]	re519	
363	Cdc20_ppi_Doc1	re520	
364	Cdh1_Ub+_Cdc20_[(KEN586)]	re521	
365	Cdc20_ppi-_Doc1	re522	

Table A.6 – *Continued from previous page*

	Reaction	Reference	Comment
366	Proteasome_DEG_Cdc20	re523	
367	Cdh1_ppi_Doc1	re524	
368	Esp1_ppi-_Pds1	re526	
369	Esp1_CUT_Rec8	re527	
370	Cdc28_P+_Acm1_[(S102)]	re531	
371	Cdc28_P+_Acm1_[(S3)]	re531	
372	Cdc28_P+_Acm1_[(S31)]	re531	
373	Cdc28_P+_Acm1_[(S48)]	re531	
374	Cdc28_P+_Acm1_[(T161)]	re531	
375	Acm1_ppi_Bmh1	re532	
376	Acm1_ppi_Bmh2	re532	
377	Acm1_ppi_Cdh1	re532	
378	Cdh1_Ub+_Acm1_[(KEN98)]	re533	
379	Cdc20_Ub+_Acm1_[(RTIL8)]	re534	
380	Proteasome_DEG_Acm1	re535;re536	
381	Cdc14_P-_Acm1_[(S102)]	re537	
382	Cdc14_P-_Acm1_[(S3)]	re537	
383	Cdc14_P-_Acm1_[(S31)]	re537	
384	Cdc14_P-_Acm1_[(S48)]	re537	
385	Cdc14_P-_Acm1_[(T161)]	re537	
386	Cdc20_Ub+_Mps1_[(REVL356)]	re538	
387	Proteasome_DEG_Mps1	re539	
388	Mps1_P+_Mad1_[(rs1)]	re540	
389	Mps1_P+_Mob1_[(rs1)]	re541	
390	Mps1_AP+_Mps1_[(T29)]	re542	In comment: Cdc28 dependent phosphorylation
391	Cdc28_P+_Spc42_[(S4)]	re543	
392	Cdc28_P+_Spc42_[(T6)]	re543	
393	Mps1_P+_Spc42_[(rs3)]	re544	
394	Mad1_ppi_Mad2	re545	
395	Cdc20_ppi_Mad2	re548	
396	Bub3_ppi_Mad2	re551	
397	Bub3_ppi_Mad3	re551	
398	Cdc5_P+_Mad3_[(S222)]	re552	
399	Cdc5_P+_Mad3_[(S268)]	re552	
400	Cdc5_P+_Mad3_[(S380)]	re552	
401	Cdc5_P+_Mad3_[(S466)]	re552	
402	Cdc5_P+_Mad3_[(S564)]	re552	
403	Ipl1_P+_Mad3_[(S337)]	re554	
404	Ipl1_P+_Mad3_[(S303)]	re554	
405	Bub1_P+_Bub3_[(rs1)]	re555	
406	Bub1_ppi_Bub3	re556	
407	Bub3_ppi_Mad1	re556	
408	Mad1_ppi_Nup53	re558	
409	Mps1_P+_Mad1_[(rs1)]	re560	
410	Mps1_P+_Nup53_[(rs1)]	re560	
411	Rna1_GEF_Gsp1_[(rs1)]	re561	Residue name introduced
412	Gsp1_aGAP_Gsp1_[(rs1)]	re562	Residue name introduced
413	Proteasome_DEG_Pds1	re564;re485	
414	Cdh1_Ub+_Pds1_[(KEN8)]	re565	
415	Cdc5_P+_Scc1_[(S175)]	re570	
416	Cdc5_P+_Scc1_[(S263)]	re570	
417	Esp1_CUT_Scc1	re571	
418	Cdc28_P+_Pds1_[(T304)]	re572	
419	Cdc28_P+_Pds1_[(S277)]	re572	
420	Cdc28_P+_Pds1_[(S292)]	re572	
421	Cdc28_P+_Pds1_[(T27)]	re574	
422	Cdc28_P+_Pds1_[(S71)]	re574	
423	Cdc14_P-_Pds1_[(T27)]	re575	
424	Cdc14_P-_Pds1_[(S71)]	re575	
425	Rad53_P+_Scc1_[(S273)]	re576	
426	Rad53_P+_Scc1_[(S367)]	re576	
427	Rad53_P+_Scc1_[(S112)]	re576	
428	Eco1_Ac+_Smc3_[(K112)]	re580	
429	Eco1_Ac+_Smc3_[(K113)]	re580	
430	Mps1_P+_Spc110_[(S60)]	re581	
431	Mps1_P+_Spc110_[(T64)]	re581	
432	Mps1_P+_Spc110_[(T68)]	re581	
433	Mps1_P+_Spc110_[(S36)]	re581	
434	Mps1_P+_Spc98_[(rs1)]	re582	
435	Mps1_P+_Dam1_[(S218)]	re583	
436	Mps1_P+_Dam1_[(S221)]	re583	
437	Cdc5_P+_Spc72_[(rs1)]	re584	
438	Cdc5_P+_Nud1_[(rs2)]	re586	
439	Cdc28_P+_Nud1_[(rs1)]	re588	
440	Cdc5_P+_Stu2_[(rs1)]	re589	
441	Cdc28_P+_Stu2_[(rs2)]	re590	
442	Cdc28_P+_Kar9_[(S496)]	re591	

Table A.6 – *Continued from previous page*

	Reaction	Reference	Comment
443	Cdc28_P+_Kar9_[(S197)]	re592	
444	Kin4_P+_Bfa1_[(S150)]	re593	
445	Kin4_P+_Bfa1_[(S180)]	re593	
446	Net1_ppi-_Sir2	re594	
447	Cdc14_ppi-_Net1	re594	
448	Dbf2_P+_Cdc14_[(rs1)]	re595	
449	Cdc5_P+_Cdc14_[(rs1)]	re595	
450	Slk19c_P+_Cdc14_[(rs1)]	re595	
451	Spo12_P+_Cdc14_[(rs1)]	re595	
452	Dbf2_P+_Net1_[(rs4)]	re595	
453	Cdc5_P+_Net1_[(rs4)]	re595	
454	Slk19c_P+_Net1_[(rs4)]	re595	
455	Spo12_P+_Net1_[(rs4)]	re595	
456	Pph21_P-_Cdc14_[(rs1)]	re596	
457	Pph22_P-_Cdc14_[(rs1)]	re596	
458	Pph21_P-_Net1_[(rs4)]	re596	
459	Pph22_P-_Net1_[(rs4)]	re596	
460	Cdc14_P-_Cdc14_[(rs1)]	re596	
461	Cdc14_P-_Net1_[(rs4)]	re596	
462	Cdc28_P+_Net1_[(S116)]	re600	
463	Cdc28_P+_Net1_[(S252)]	re600	
464	Cdc28_P+_Net1_[(T212)]	re600	
465	Cdc14_P-_Net1_[(S116)]	re601	
466	Cdc14_P-_Net1_[(S252)]	re601	
467	Cdc14_P-_Net1_[(T212)]	re601	
468	Fob1_P+_Spo12_[(S118)]	re602	
469	Fob1_P+_Spo12_[(S125)]	re602	
470	Fob1_ppi-_Spo12	re603	
471	Cdc14_P-_Fob1_[(S118)]	re604	
472	Cdc14_P-_Fob1_[(S125)]	re604	
473	Cdh1_Ub+_Spo12_[(rs3)]	re605	
474	Proteasome_DEG_Spo12	re606	
475	Proteasome_DEG_Scc1	re607	
476	Cdc5_P+_Slk19_[(rs1)]	re608	
477	Esp1_CUT_Slk19	re609	
478	Cdc28_P+_Slk19_[(rs2)]	re610	
479	Proteasome_DEG_Rec8	re611	
480	Cdh1_AP-_Cdh1_[(11ST)]	re616	
481	Cdh1_Ub+_Fin1_[(RRSL7)]	re617	
482	Proteasome_DEG_Fin1	re618	
483	Cdc28_P+_Fin1_[(S36)]	re619	
484	Cdc28_P+_Fin1_[(S54)]	re619	
485	Cdc28_P+_Fin1_[(T68)]	re619	
486	Cdc28_P+_Fin1_[(S117)]	re619	
487	Cdc28_P+_Fin1_[(S148)]	re619	
488	Cdc14_P-_Fin1_[(S36)]	re620	
489	Cdc14_P-_Fin1_[(S54)]	re620	
490	Cdc14_P-_Fin1_[(T68)]	re620	
491	Cdc14_P-_Fin1_[(S117)]	re620	
492	Cdc14_P-_Fin1_[(S148)]	re620	
493	Glc7_P-_Fin1_[(S36)]	re620	
494	Glc7_P-_Fin1_[(S54)]	re620	
495	Glc7_P-_Fin1_[(T68)]	re620	
496	Glc7_P-_Fin1_[(S117)]	re620	
497	Glc7_P-_Fin1_[(S148)]	re620	
498	Ipl1_P+_Ase1_[(T524)]	re622	
499	Ipl1_P+_Ase1_[(T680)]	re622	
500	Ipl1_P+_Ase1_[(T733)]	re622	
501	Ipl1_P+_Ase1_[(S809)]	re622	
502	Glc7_P-_Ase1_[(S337)]	re622	
503	Glc7_P-_Ase1_[(T524)]	re623	
504	Glc7_P-_Ase1_[(T680)]	re623	
505	Glc7_P-_Ase1_[(T733)]	re623	
506	Glc7_P-_Ase1_[(S809)]	re623	
507	Ipl1_P+_Dam1_[(S265)]	re624	
508	Ipl1_P+_Dam1_[(S257)]	re624	
509	Ipl1_P+_Dam1_[(S292)]	re624	
510	Glc7_P-_Dam1_[(S265)]	re625	
511	Glc7_P-_Dam1_[(S257)]	re625	
512	Glc7_P-_Dam1_[(S292)]	re625	
513	Ipl1_P+_Spc34_[(T199)]	re626	
514	Dam1_aMet+_Dam1_[(K233)]	re627	
515	Ipl1_P+_Cbf2_[(rs1)]	re632	
516	Cdc28_P+_Bir1_[(9ST)]	re633	
517	Cdc28_P+_Tus1_[(10ST)]	re634	
518	Cdc14_P-_Tus1_[(10ST)]	re635	
519	Cdc28_P+_Ste5_[(8ST)]	re636	

Table A.6 – *Continued from previous page*

	Reaction	Reference	Comment
520	Cdc28_P+_Rga2_[(rs1)]	re639	
521	Pho85_P+_Rga2_[(rs1)]	re639	
522	Fus3_P+_Bni1_[(rs1)]	re641	
523	Bni1_AP-_Bni1_[(rs1)]	re642	
524	Bni1_ppi_Rho1	re643	
525	Cdc28_P+_Boi1_[(rs1)]	re644	
526	Cdc28_P+_Boi2_[(rs1)]	re644	
527	Cdc14_P-_Sli15_[(S335)]	re647	
528	Cdc14_P-_Sli15_[(S373)]	re647	
529	Cdc14_P-_Sli15_[(S427)]	re647	
530	Cdc14_P-_Sli15_[(S437)]	re647	
531	Cdc14_P-_Sli15_[(S462)]	re647	
532	Cdc14_P-_Sli15_[(T474)]	re647	
533	Cdc28_P+_Sli15_[(S335)]	re648	
534	Cdc28_P+_Sli15_[(S373)]	re648	
535	Cdc28_P+_Sli15_[(S427)]	re648	
536	Cdc28_P+_Sli15_[(S437)]	re648	
537	Cdc28_P+_Sli15_[(S462)]	re648	
538	Cdc28_P+_Sli15_[(T474)]	re648	
539	Ipl1_P+_Sli15_[(S560)]	re650	
540	Bir1_ppi_Cbf2	re654	
541	Glc7_P-_Cbf2_[(rs1)]	re656	
542	Ipl1_P+_Hht1_[(S10)]	re658	
543	Ipl1_P+_Hht2_[(S10)]	re658	
544	Glc7_P-_Hht1_[(S10)]	re659	
545	Glc7_P-_Hht2_[(S10)]	re659	
546	Rtt109_Ac+_Hht1_[(K14)]	re660	
547	Rtt109_Ac+_Hht2_[(K14)]	re660	
548	Gcn5_Ac+_Hht1_[(K14)]	re660	
549	Gcn5_Ac+_Hht2_[(K14)]	re660	
550	Htb1_Met+_Hht1_[(K4)]	re661	
551	Htb1_Met+_Hht2_[(K4)]	re661	
552	Htb2_Met+_Hht1_[(K4)]	re661	
553	Htb2_Met+_Hht2_[(K4)]	re661	
554	Bre1_Ub+_Hht1_[(K123)]	re662	
555	Bre1_Ub+_Hht2_[(K123)]	re662	
556	Ubp10_Ub-_Hht1_[(K123)]	re663	
557	Ubp10_Ub-_Hht2_[(K123)]	re663	
558	Mec1_P+_Rad9_[(T390)]	re682	
559	Mec1_P+_Rad9_[(T398)]	re682	
560	Mec1_P+_Rad9_[(T410)]	re682	
561	Mec1_P+_Rad9_[(T427)]	re682	
562	Mec1_P+_Rad9_[(S434)]	re682	
563	Mec1_P+_Rad9_[(T457)]	re682	
564	Mec1_P+_Rad9_[(T603)]	re682	
565	Mec1_P+_Chk1_[(T333)]	re683	
566	Mec1_P+_Chk1_[(T356)]	re683	
567	Mec1_P+_Chk1_[(T382)]	re683	
568	Rad9_P+_Chk1_[(T333)]	re683	Low confidence
569	Rad9_P+_Chk1_[(T356)]	re683	Low confidence
570	Rad9_P+_Chk1_[(T382)]	re683	Low confidence
571	Rad9_P+_Rad53_[(T5)]	re684	
572	Rad9_P+_Rad53_[(S473)]	re684	
573	Rad9_P+_Rad53_[(T8)]	re684	
574	Rad9_P+_Rad53_[(T12)]	re684	
575	Rad9_P+_Rad53_[(T15)]	re684	
576	Rad9_P+_Rad53_[(S480)]	re684	
577	Rad9_P+_Rad53_[(S485)]	re684	
578	Rad9_P+_Rad53_[(S489)]	re684	
579	Rad9_P+_Rad53_[(T354)]	re684	
580	Rad53_AP+_Rad53_[(T5)]	re684	
581	Rad53_AP+_Rad53_[(S473)]	re684	
582	Rad53_AP+_Rad53_[(T8)]	re684	
583	Rad53_AP+_Rad53_[(T12)]	re684	
584	Rad53_AP+_Rad53_[(T15)]	re684	
585	Rad53_AP+_Rad53_[(S480)]	re684	
586	Rad53_AP+_Rad53_[(S485)]	re684	
587	Rad53_AP+_Rad53_[(S489)]	re684	
588	Rad53_AP+_Rad53_[(T354)]	re684	
589	Ddc1_P+_Rad53_[(T5)]	re684	
590	Ddc1_P+_Rad53_[(S473)]	re684	
591	Ddc1_P+_Rad53_[(T8)]	re684	
592	Ddc1_P+_Rad53_[(T12)]	re684	
593	Ddc1_P+_Rad53_[(T15)]	re684	
594	Ddc1_P+_Rad53_[(S480)]	re684	
595	Ddc1_P+_Rad53_[(S485)]	re684	
596	Ddc1_P+_Rad53_[(S489)]	re684	

Table A.6 – *Continued from previous page*

	Reaction	Reference	Comment
597	Ddc1_P+_Rad53_[(T354)]	re684	
598	Rad53_P+_Dun1_[(T380)]	re688	
599	Dun1_AP+_Dun1_[(T380)]	re688	
600	Dun1_P+_Sml1_[(S56)]	re689	
601	Dun1_P+_Sml1_[(S58)]	re689	
602	Dun1_P+_Sml1_[(S60)]	re689	
603	Proteasome_DEG_Sml1	re690	
604	Rnr1_ppi_Sml1	re691	
605	Dun1_P+_Crt1_[(rs1)]	re692	
606	Crt1_BIND_Xbox	re693	
607	Crt1_ppi_Cyc8	re693	
608	Cyc8_ppi_Tup1	re693	
609	PolII_TRSC_Rnr1	re694	
610	PolII_TRSC_Crt1	re694	
611	Mec1_P+_Ddc1_[(rs1)]	re696	
612	Mec1_P+_Rfa1_[(S178)]	re697	
613	Mec1_P+_Rfa2_[(S120)]	re698	
614	Ime2_P+_Rfa2_[(S27)]	re699	
615	Mec1_P+_Rtt107_[(rs1)]	re700	
616	Mec1_P+_Htb1_[(S129)]	re702	
617	Mec1_P+_Htb1_[(S122)]	re702	
618	Mec1_P+_Htb2_[(S129)]	re702	
619	Mec1_P+_Htb2_[(S122)]	re702	
620	Sir2_Ac-_Hht1_[(K14)]	re703	
621	Sir2_Ac-_Hht2_[(K14)]	re703	
622	Rpd3_Ac-_Hht1_[(K14)]	re703	
623	Rpd3_Ac-_Hht2_[(K14)]	re703	
624	Hda1_Ac-_Hht1_[(K14)]	re703	
625	Hda1_Ac-_Hht2_[(K14)]	re703	
626	Rtt109_Ac+_Hht1_[(K56)]	re704	
627	Rtt109_Ac+_Hht2_[(K56)]	re704	
628	Gcn5_Ac+_Hht1_[(K56)]	re704	
629	Gcn5_Ac+_Hht2_[(K56)]	re704	
630	Hda1_Ac-_Hht1_[(K56)]	re705	
631	Hda1_Ac-_Hht2_[(K56)]	re705	
632	Rpd3_Ac-_Hht1_[(K56)]	re705	
633	Rpd3_Ac-_Hht2_[(K56)]	re705	
634	Ipl1_ppi_Sli15	re707	
635	Rad53_AP-_Rad53_[(T5)]	re708	
636	Rad53_AP-_Rad53_[(S473)]	re708	
637	Rad53_AP-_Rad53_[(T8)]	re708	
638	Rad53_AP-_Rad53_[(T12)]	re708	
639	Rad53_AP-_Rad53_[(T15)]	re708	
640	Rad53_AP-_Rad53_[(S480)]	re708	
641	Rad53_AP-_Rad53_[(S485)]	re708	
642	Rad53_AP-_Rad53_[(S489)]	re708	
643	Rad53_AP-_Rad53_[(T354)]	re708	
644	Asf1_ppi_Rad53	re709	
645	Asf1_ppi_Rtt109	re712	
646	Rtt109_ppi_Vps75	re714	
647	Cdc5_P+_Cdh1_[(S125)]	re715	
648	Cdc5_P+_Cdh1_[(S259)]	re715	
649	Esa1_Ac+_Hhf1_[(K12)]	re716	
650	Esa1_Ac+_Hhf1_[(K8)]	re716	
651	Esa1_Ac+_Hhf1_[(K5)]	re716	
652	Esa1_Ac+_Hhf2_[(K12)]	re716	
653	Esa1_Ac+_Hhf2_[(K8)]	re716	
654	Esa1_Ac+_Hhf2_[(K5)]	re716	
655	Gcn5_Ac+_Hhf1_[(K12)]	re716	
656	Gcn5_Ac+_Hhf1_[(K8)]	re716	
657	Gcn5_Ac+_Hhf1_[(K5)]	re716	
658	Gcn5_Ac+_Hhf2_[(K12)]	re716	
659	Gcn5_Ac+_Hhf2_[(K8)]	re716	
660	Gcn5_Ac+_Hhf2_[(K5)]	re716	
661	Rpd3_Ac-_Hhf1_[(K12)]	re717	
662	Rpd3_Ac-_Hhf1_[(K8)]	re717	
663	Rpd3_Ac-_Hhf1_[(K5)]	re717	
664	Rpd3_Ac-_Hhf2_[(K12)]	re717	
665	Rpd3_Ac-_Hhf2_[(K8)]	re717	
666	Rpd3_Ac-_Hhf2_[(K5)]	re717	
667	Hht1_aMet+_Hht1_[(K36)]	re718	
668	Hht2_aMet+_Hht2_[(K36)]	re718	
669	Hht1_aMet+_Hht1_[(K79)]	re719	
670	Hht2_aMet+_Hht2_[(K79)]	re719	
671	Gcn5_Ac+_Hhf1_[(K16)]	re720	
672	Gcn5_Ac+_Hhf2_[(K16)]	re720	
673	Sir2_Ac-_Hhf1_[(K16)]	re721	

Table A.6 – *Continued from previous page*

	Reaction	Reference	Comment
674	Sir2_Ac-_Hhf2_[(K16)]	re721	
675	Cdc5_P+_Rec8_[(11ST)]	re722	
676	Pph21_P-_Rec8_[(11ST)]	re723	
677	Pph22_P-_Rec8_[(11ST)]	re723	
678	Rts1_ppi_Sgo1	re725	
679	Sir3_ppi_Sir4	re727	
680	Sir2_ppi_Sir4	re727	
681	Hht1_ppi_Sir3	re728	
682	Hht2_ppi_Sir3	re728	
683	Hhf1_ppi_Sir3	re730	
684	Hhf2_ppi_Sir3	re730	
685	Cdc7_ppi_Dbf4	re731	
686	Cdc7_AP+_Cdc7_[(T281)]	re732	
687	Orc6_AP+_Orc6_[(S106)]	re733	
688	Orc6_AP+_Orc6_[(S116)]	re733	
689	Orc6_AP+_Orc6_[(S123)]	re733	
690	Orc6_AP+_Orc6_[(T146)]	re733	
691	Orc2_AP+_Orc2_[(S16)]	re734	
692	Orc2_AP+_Orc2_[(T24)]	re734	
693	Orc2_AP+_Orc2_[(T70)]	re734	
694	Orc2_AP+_Orc2_[(T174)]	re734	
695	Orc2_AP+_Orc2_[(S188)]	re734	
696	Orc2_AP+_Orc2_[(S206)]	re734	
697	Cdc28_P+_Mcm3_[(S761)]	re735	
698	Cdc28_P+_Mcm3_[(S765)]	re735	
699	Cdc28_P+_Mcm3_[(S781)]	re735	
700	Cdc28_P+_Mcm3_[(T786)]	re735	
701	Cdc28_P+_Mcm3_[(S845)]	re735	
702	Cdc28_P+_Sld2_[(S100)]	re737	
703	Cdc28_P+_Sld2_[(S128)]	re737	
704	Cdc28_P+_Sld2_[(T167)]	re737	
705	Cdc28_P+_Sld2_[(S172)]	re737	
706	Cdc28_P+_Sld2_[(S208)]	re737	
707	Cdc28_P+_Sld2_[(T241)]	re737	
708	Dpb11_ppi_Sld2	re738	
709	Clb5_ppi_Orc6	re739	
710	Cdc7_P+_Mcm2_[(rs1)]	re740	
711	PolII_TRSC_Amn1	re742	
712	PolII_TRSC_Hhf2	re743	
713	PolII_TRSC_Hht2	re744	
714	PolII_TRSC_Mcm3	re745	
715	Mcm1_BIND_PRE	re746	
716	PolII_TRSC_Far1	re747	
717	PolII_TRSC_CDC5	re749	
718	PolII_TRSC_HTB2	re750	
719	PolII_TRSC_BMH1	re751	
720	PolII_TRSC_ASH1	re752	
721	PolII_TRSC_CIN8	re754	
722	PolII_TRSC_DUN1	re757	
723	PolII_TRSC_SPC34	re758	
724	PolII_TRSC_NUD1	re759	
725	PolII_TRSC_SSA1	re763	
726	PolII_TRSC_SSA2	re763	
727	PolII_TRSC_PDS1	re764	
728	PolII_TRSC_YDJ1	re767	
729	PolII_TRSC_YOX1	re770	
730	PolII_TRSC_NDD1	re771	
731	PolII_TRSC_FKH2	re772	
732	PolII_TRSC_MSA1	re773	
733	PolII_TRSC_SWE1	re774	
734	PolII_TRSC_SAP185	re776	
735	Esa1_Ac+_Htb1_[(K11)]	re781	
736	Esa1_Ac+_Htb1_[(K16)]	re781	
737	Esa1_Ac+_Htb2_[(K11)]	re781	
738	Esa1_Ac+_Htb2_[(K16)]	re781	
739	Rpd3_Ac-_Htb1_[(K11)]	re782	
740	Rpd3_Ac-_Htb1_[(K16)]	re782	
741	Rpd3_Ac-_Htb2_[(K11)]	re782	
742	Rpd3_Ac-_Htb2_[(K16)]	re782	
743	Hda1_Ac-_Htb1_[(K11)]	re782	
744	Hda1_Ac-_Htb1_[(K16)]	re782	
745	Hda1_Ac-_Htb2_[(K11)]	re782	
746	Hda1_Ac-_Htb2_[(K16)]	re782	
747	Sko1_BIND-_CreGene	re787	
748	Cyc8_ppi-_Sko1	re787	
749	Cdc14_P-_Whi5_[(T41)]	re819	
750	Cdc14_P-_Whi5_[(S59)]	re819	

Table A.6 – *Continued from previous page*

	Reaction	Reference	Comment
751	Cdc14_P-_Whi5_[(S62)]	re819	
752	Cdc14_P-_Whi5_[(S155)]	re819	
753	Cdc14_P-_Whi5_[(S157)]	re819	
754	Cdc14_P-_Whi5_[(S161)]	re819	
755	Cdc14_P-_Whi5_[(S262)]	re819	
756	Cdc14_P-_Stb1_[(rs1)]	re820	
757	Cdc14_P-_Cln3_[(S468)]	re821	
758	Cdc14_P-_Cln1_[(4T3S)]	re822	
759	Cdc14_P-_Cln2_[(4T3S)]	re822	
760	Cdc14_P-_Ste5_[(8ST)]	re823	
761	Cdc14_P-_Ste20_[(rs1)]	re824	
762	Cdc14_P-_Rga2_[(rs1)]	re825	
763	Cdc14_P-_Boi1_[(rs1)]	re826	
764	Cdc14_P-_Boi2_[(rs1)]	re827	
765	Cdc14_P-_Dig1_[(rs1)]	re827	
766	Cdc14_P-_Dig2_[(rs1)]	re828	
767	Cdc14_P-_Cdc24_[(rs1)]	re829	
768	Cdc14_P-_Spc42_[(S4)]	re829	
769	Cdc14_P-_Spc42_[(T6)]	re830	
770	Cdc14_P-_Ace2_[(T575)]	re830	
771	Cdc14_P-_Ace2_[(S701)]	re830	
772	Cdc14_P-_Ace2_[(S714)]	re831	
773	Cdc14_P-_Dbf2_[(S374)]	re831	
774	Cdc14_P-_Dbf2_[(T544)]	re832	
775	Cdc14_P-_Fkh2_[(S683)]	re832	
776	Cdc14_P-_Fkh2_[(T697)]	re833	
777	Cdc14_P-_Ndd1_[(T319)]	re834	
778	Cdc14_P-_Sld2_[(S100)]	re834	
779	Cdc14_P-_Sld2_[(S128)]	re834	
780	Cdc14_P-_Sld2_[(T167)]	re834	
781	Cdc14_P-_Sld2_[(S172)]	re834	
782	Cdc14_P-_Sld2_[(S208)]	re834	
783	Cdc14_P-_Sld2_[(T241)]	re834	
784	Cdc14_P-_Mcm3_[(S761)]	re835	
785	Cdc14_P-_Mcm3_[(S765)]	re835	
786	Cdc14_P-_Mcm3_[(S781)]	re835	
787	Cdc14_P-_Mcm3_[(T786)]	re835	
788	Cdc14_P-_Mcm3_[(S845)]	re835	
789	Cdc14_P-_Bir1_[(9ST)]	re837	
790	Cdc14_P-_Cdc5_[(T242)]	re838	
791	Cdc14_P-_Slk19_[(rs2)]	re839	
792	Cdc14_P-_Cdc16_[(S44)]	re840	
793	Cdc14_P-_Cdc16_[(S59)]	re840	
794	Cdc14_P-_Cdc16_[(S95)]	re840	
795	Cdc14_P-_Cdc16_[(S103)]	re840	
796	Cdc14_P-_Cdc16_[(T115)]	re840	
797	Cdc14_P-_Cdc16_[(T406)]	re840	
798	Cdc14_P-_Cdc23_[(S59)]	re840	
799	Cdc14_P-_Cdc27_[(S267)]	re840	
800	Cdc14_P-_Cdc27_[(T304)]	re840	
801	Cdc14_P-_Cdc27_[(S328)]	re840	
802	Cdc14_P-_Cdc27_[(T351)]	re840	
803	Cdc14_P-_Cdc27_[(T397)]	re840	
804	Cdc14_P-_Pds1_[(T304)]	re841	
805	Cdc14_P-_Pds1_[(S277)]	re841	
806	Cdc14_P-_Pds1_[(S292)]	re841	
807	Cdc14_P-_Stu2_[(rs2)]	re842	
808	Cdc14_P-_Nud1_[(rs1)]	re843	
809	Cdc14_P-_Kar9_[(S197)]	re844	
810	Cdc14_P-_Kar9_[(S496)]	re845	
811	PolII_TRSC_BNI1	re849	
812	PolII_TRSC_SHS1	re851	
813	PolII_TRSC_CDC6	re852	
814	PolII_TRSC_PCL2	re853	
815	PolII_TRSC_PIL1	re854	
816	PolII_TRSC_KIN4	re856	
817	PolII_TRSC_HOF1	re857	
818	PolII_TRSC_YHP1	re858	
819	PolII_TRSC_MOB1	re859	
820	PolII_TRSC_SPO12	re860	
821	PolII_TRSC_DBF2	re861	
822	PolII_TRSC_MSG5	re862	
823	PolII_TRSC_BEM1	re863	
824	PolII_TRSC_RGA2	re864	
825	PolII_TRSC_RNA1	re865	
826	PolII_TRSC_FKH1	re870	
827	PolII_TRSC_HSL1	re871	

Table A.6 – *Continued from previous page*

	Reaction	Reference	Comment
828	PolII_TRSC_ACM1	re872	
829	PolII_TRSC_RFA2	re876	
830	PolII_TRSC_CLB6	re877	
831	PolII_TRSC_IRR1	re878	
832	PolII_TRSC_GIC1	re879	
833	PolII_TRSC_GIC2	re880	
834	PolII_TRSC_CLA4	re881	
835	PolII_TRSC_GIN4	re882	
836	PolII_TRSC_CDC46	re883	
837	PolII_TRSC_MCM7	re884	
838	Ribo_TRSL_Hsl1mRNA	re885	
839	Ribo_TRSL_Acm1mRNA	re886	
840	Ribo_TRSL_Gin4mRNA	re887	
841	Ribo_TRSL_Cla4mRNA	re888	
842	Ribo_TRSL_Gic1mRNA	re889	
843	Ribo_TRSL_Gic2mRNA	re889	
844	Ribo_TRSL_Irr1mRNA	re890	
845	Ribo_TRSL_Clb6mRNA	re891	
846	Ribo_TRSL_Rfa2mRNA	re892	
847	Ribo_TRSL_Fkh1mRNA	re894	
848	Ribo_TRSL_Msg5mRNA	re899	
849	Ribo_TRSL_Bem1mRNA	re900	
850	Ribo_TRSL_Rga2mRNA	re901	
851	Ribo_TRSL_Rna1mRNA	re902	
852	Ribo_TRSL_Bni1mRNA	re903	
853	Ribo_TRSL_Shs1mRNA	re904	
854	Ribo_TRSL_Cdc6mRNA	re905	
855	Ribo_TRSL_Pcl1mRNA	re906	
856	Ribo_TRSL_Pcl2mRNA	re906	
857	Ribo_TRSL_Pil1mRNA	re907	
858	Ribo_TRSL_Kin4mRNA	re908	
859	Ribo_TRSL_Hof1mRNA	re909	
860	Ribo_TRSL_Nop7mRNA	re910	
861	Ribo_TRSL_Mob1mRNA	re911	
862	Ribo_TRSL_Spo12mRNA	re912	
863	Ribo_TRSL_Dbf2mRNA	re913	
864	Ribo_TRSL_Cdc5mRNA	re914	
865	Ribo_TRSL_Rnr1mRNA	re915	
866	Ribo_TRSL_Amn1mRNA	re916	
867	Ribo_TRSL_Sic1mRNA	re917	
868	Ribo_TRSL_Crt1mRNA	re918	
869	Ribo_TRSL_Ash1mRNA	re919	
870	Ribo_TRSL_Ace2mRNA	re920	
871	Ribo_TRSL_Swi5mRNA	re921	
872	Ribo_TRSL_Cdc20mRNA	re922	
873	Ribo_TRSL_Crz1mRNA	re923	
874	Ribo_TRSL_Clb1mRNA	re924	
875	Ribo_TRSL_Clb2mRNA	re924	
876	Ribo_TRSL_Fus3mRNA	re925	
877	Ribo_TRSL_Spc34mRNA	re930	
878	Ribo_TRSL_Far1mRNA	re931	
879	Ribo_TRSL_Cin8mRNA	re932	
880	Ribo_TRSL_Spc110mRNA	re933	
881	Ribo_TRSL_Axl1mRNA	re934	
882	Ribo_TRSL_Bud4mRNA	re935	
883	Ribo_TRSL_Pds1mRNA	re936	
884	Ribo_TRSL_Dun1mRNA	re937	
885	Ribo_TRSL_Cln1mRNA	re938	
886	Ribo_TRSL_Cln2mRNA	re938	
887	Ribo_TRSL_Nrm1mRNA	re939	
888	Ribo_TRSL_Clb5mRNA	re941	
889	Ribo_TRSL_Pcl1mRNA	re942	
890	Ribo_TRSL_Pcl2mRNA	re942	
891	Ribo_TRSL_Bmh1mRNA	re943	
892	Ribo_TRSL_Bmh2mRNA	re943	
893	Ribo_TRSL_Ssa1brmRNA	re944	
894	Ribo_TRSL_Ssa2mRNA	re944	
895	Ribo_TRSL_Mcm7mRNA	re945	
896	Ribo_TRSL_Cdc46mRNA	re946	
897	Ribo_TRSL_Yox1mRNA	re947	
898	Ribo_TRSL_Hht1mRNA	re948	
899	Ribo_TRSL_Hht2mRNA	re948	
900	Ribo_TRSL_Hhf1mRNA	re949	
901	Ribo_TRSL_Hhf2mRNA	re949	
902	Ribo_TRSL_Htb1mRNA	re950	
903	Ribo_TRSL_Htb2mRNA	re950	
904	Ribo_TRSL_Cln3mRNA	re951	

Table A.6 – *Continued from previous page*

	Reaction	Reference	Comment
905	Ribo_TRSL_Ydj1mRNA	re952	
906	Ribo_TRSL_Sap185mRNA	re954	
907	Ribo_TRSL_Mcm3mRNA	re956	
908	Ribo_TRSL_Ndd1mRNA	re957	Original produces phosphorylated Ndd1
909	Ribo_TRSL_Swi4mRNA	re958	
910	Ribo_TRSL_Msa1mRNA	re961	
911	Ribo_TRSL_Msa2mRNA	re961	
912	Ribo_TRSL_Nud1mRNA	re962	
913	Ribo_TRSL_Swe1mRNA	re963	
914	Ribo_TRSL_Cdc6mRNA	re964	
915	Mcm1_BIND_ECB_[Mcm1bs]	Added	
916	Swi4_BIND_SCB_[SCB]	Added	
917	Hcm1_BIND_Hcm1bs_[Hcm1bs]	Added	
918	Ssn3_ppi_Ssn8	Added	
919	Pho80_ppi_Pho85	Added	
920	Pcl1_ppi_Pho85	Added	
921	Pcl2_ppi_Pho85	Added	
922	Rlm1_BIND_Rlm1Gene_[Rlm1bs]	Added	
923	Cna1_ppi_Cnb1	Added	
924	Cna2_ppi_Cnb1	Added	
925	Yap1_BIND_YRE	Added	
926	Ckb1_ppi_Ckb1	Added	
927	Cka1_ppi_Ckb1	Added	
928	Cka2_ppi_Ckb1	Added	
929	Far1_ppi_Ste4	Added	Low confidence
930	Bud3_ppi_Bud4	Added	
931	Axl2_ppi_Bud3	Added	
932	Axl1_ppi_Axl2	Added	
933	Cdc10GEF_GEF_Cdc10_[(rs1)]	Added	
934	Bfa1_ppi_Bub2	Added	
935	Esp1_ppi_Pds1	Added	
936	Rec8Kinase_P+_Rec8_[(S314)]	Added	
937	Rec8Kinase_P+_Rec8_[(S521)]	Added	
938	Rec8Kinase_P+_Rec8_[(S522)]	Added	
939	Cdc14_ppi_Net1	Added	
940	Net1_ppi_Sir2	Added	
941	Fob1_ppi_Spo12	Added	
942	Bre1_ppi_Rad6	Added	
943	Lcd1_ppi_Mec1	Added	
944	Lcd1Kinase_P+_Lcd1_[(rs1)]	Added	
945	Rtt109Acetylase_Ac+_Rtt109_[(K290)]	Added	
946	Bcy1_ppi_Tpk1	Added	
947	Snf1Kinase_P+_Snf1_[(T210)]	Added	
948	Sko1_BIND_CreGene	Added	
949	Cyc8_ppi_Sko1	Added	
950	Apc1_ppi_Apc2	Added	
951	Apc2_ppi_Apc11	Added	
952	Apc2_ppi_Doc1	Added	
953	Cdc16_ppi_Cdc23	Added	
954	Apc5_ppi_Cdc23	Added	
955	Cdc16_ppi_Cdc27	Added	
956	Apc1_ppi_Apc4	Added	
957	Apc1_ppi_Apc5	Added	
958	Cdc16_ppi_Apc9	Added	
959	Cdc16_ppi_Cdc26	Added	
960	Apc1_ppi_Mnd2	Added	
961	Cdc16_ppi_Swm1	Added	
962	Bud8_ppi_Rax2	Added	
963	Bud9_ppi_Rax2	Added	
964	Rax1_ppi_Rax2	Added	
965	Smc1_ppi_Smc3	Added	
966	Scc1_ppi_Smc1	Added	
967	Smc1_ppi_Smc1	Added	
968	Smc3_ppi_Smc3	Added	
969	Scc1_ppi_Irr1	Added	

Acknowledgements

Finally, I would like to acknowledge the people who have contributed, academically and non-academically, to the completion of the presented work and support during this time. I would like to express my sincere gratitude to my supervisor Marcus Krantz, who lay the foundation of the rxncon approach, for all his support and many insights that nurtured this study, for his *gästvänlighet* and incredible knowledge about baker's yeast that made the cell cycle study so accessible. I had the pleasure to work on the rxncon project with my current and former colleagues Magdalena Rother, Sebastian Thieme and Jesper Romers, who further developed the rxncon toolbox and ideas. I thank Edda Klipp for co-supervision and useful insights that helped to advance this study. I am grateful to Tatsuya Akutsu for our collaboration, and for welcoming me to his group at Kyoto University for an academic exchange. I thank Angela Relógio and Rukeia El-Athman for our collaboration, and for introducing me to the circadian clock.

I enjoyed the hospitable atmosphere in the TBP group very much. Especially, I would like to thank Katja Tummer and Jens Hahn, for enduring so many puns and willingly proofread the manuscript, for the scientific and non-scientifi discussions in our office, and for being who you are. I thank Max Schelker for sustaining the coffee infrastructure in the TBP group. I thank Wolfgang Giese, Judith Wodke, Stefan Forgó, Roman Rainer, and Timo Lubitz for their support and encouragement.

Furthermore, I thank Ivo Maintz who maintained the computational infrastructure and knows a solution to every problem. I would like to thank Sabine Wagnitz for the smooth bureaucratic handling of all kinds of issues. I greatly acknowledge the BMBF for funding, and the Schleiermacher doctoral program for additional support.

I thank the board game team including Martin Seeger and Joachim Schmitz for the magical gatherings and the times we tried to become cadets to defend our spaceship. I thank the members of the Taekwondo group for making kicking and punching so enjoyable.

I thank Lisa, Hilde, David and Annika for keeping in touch with me at long distance. I thank Silvia for our long friendship, for her support, and the adventures we shared. I thank Andreas for always being at my side. Finally, I would like to thank my family. Especially, I want to express my deepest gratitude to Betty and Flo. You are the best sisters I could ever wish for.

Eidesstattliche Erklärung

Ich erkläre an Eides statt, dass ich die vorliegende Arbeit selbständig und nur unter Verwendung der angegebenen Literatur und Hilfsmittel erstellt habe.

Ulrike Münzner
Berlin, 25. August 2017